Universitat Autònoma de Barcelona

Carborane derivatives with electron rich moieties. Synthesis, properties and electronic communication.

RADU-ADRIAN POPESCU

TESI DOCTORAL
Programa de Doctorat en Química

Directora: Prof. Clara Viñas Teixidor

Departament de Química
Facultat de Ciències

2012

ICMAB

GOBIERNO DE ESPAÑA
MINISTERIO DE ECONOMÍA Y COMPETITIVIDAD

CSIC

Memòria presentada per aspirar al Grau de Doctor per

Radu-Adrian Popescu

Vist i plau

Prof. Clara Viñas Teixidor

Bellaterra, 16 de novembre de 2012

La Professora CLARA VIÑAS i TEIXIDOR, Professora d'Investigació del C*onsejo Superior de Investigaciones Científicas* a l'*Institut de Ciència de Materials de Barcelona*

CERTIFICA

Que en RADU-ADRIAN POPESCU, llicenciat en Enginyeria Química, ha realitzat sota la meva direcció la Tesí Doctoral que porta per títol "*Carborane derivatives with electron rich moieties. Synthesis, properties and electronic communication*" i que recull aquesta memòria per optar al títol de Doctor en Química per la Universitat Autònoma de Barcelona.

I, perquè consti i tingui els efectes corresponents, signa aquest certificat a Bellaterra, a 16 de novembre de 2012.

Prof. CLARA VIÑAS i TEIXIDOR
ICMAB (CSIC)

Campus de la Universitat Autònoma de Barcelona
08193 Bellaterra, Catalunya, Espanya
Telf.: +34 935 801 853
Fax.: +34 935 805 729

Aquest treball de recerca ha estat finançat per la *Comisión Interministerial de Ciencia y Tecnología*, CICYT, mitjançant el projecte CTQ2010-16237 (subprograma BQU) i per la *Generalitat de Catalunya* amb el projecte 2009/SGR/00279. Alhora, s'ha pogut realitzar gràcies a una beca per la Formació de Personal Universitari (FPU) concedida pel *Miniesterio de Ciencia e Innovación*, des del juliol del 2008 al juliol del 2012.

Aquest treball d'investigació, amb la data de defensa del 18 de gener de 2013 , té com a membres del tribunal a:

- Prof. Miquel Solà, *Catedràtic* de la Universitat de Girona (president).

- Dr. Juli Real, *Professor Titular d'Universitat* de la Universitat Autònoma de Barcelona (secretari).

- Prof. Evamarie Hey-Hawkins, *Chair of Organometallic Chemistry and Photochemistry at the University of Leipzig,* Alemanya (vocal).

Com a membres suplents:

- Prof. Joan Suades Ortuño, *Catedràtic* de la Universitat Autònoma de Barcelona.

- Dra. Marisa Romero García, *Professora Titular de Química* de la Universitat de Girona.

ACKNOWLEDGEMENTS

I'm in debt to many people for the accomplishment of this PhD thesis. The thesis would have been impossible without the unconditional scientific and private support of my PhD director, Prof. Clara Viñas, who put her trust in me and help me the come to Barcelona. I want to thank her for all the knowledge that I recieved from her and for her guidance and dedication. The same debt I owe to Prof. Francesc Teixidor, how contributed to my arrival at ICMAB, and having always the office door open for any consult. His scientific guidance was very valuable to my research, as well the private advices.

I would also want to give my gratitude to Dr. José Giner and Dr. Rosario Núñez for their support and advices. To Dr. José Giner I'm also very grateful for his private support.

To Prof. Reijo Sillanpää for the University of Jyväskylä (Finland), I wish to thank for the X-ray analysis and the structural characterization.

I will like to thank to Dr. Lluis Escriche from Universitat Autònoma de Barcelona for accepting to be my PhD tutor.

I am thankful to both Prof. Carles Miravitlles, the former Director of ICMAB, and to Prof. Xavier Obradors, the actual Director of ICMAB for accepting me in the institute and allowing me to use the installations and apparatus. My gratitude for all the administrative and support staff from the ICMAB, without whom, the good working of the institute would be impossible.

I wish also to give my thanks to Anna Fernández for all the patience and dedication in doing the NMR and MS analysis and to Jordi Cortés for his dedication to a work that cannot be seen easily, but that makes the laboratories to work perfectly. Also, I thank to Elena Marchante for the electrochemical analysis.

I wish to thank to Dr. Pau Farràs and Dr. Emilio Juárez-Pérez for their friendship and the useful discussions about the computational chemistry, and not only. To Dr. Florencia Di Salvo and Dr. Arántzazu González I wish to thank for all that I learned from them and for their friendship and useful advices.

My colleagues were an indispensable source of collaboration, friendship and knowledge, and without them, the years of PhD would have been monotones. I'm feeling?? privileged to have seen every day at work, both friends, always available to help on the personal plane, and colleagues, always available to help on the professional plane. Ana C., Albert and Ari know best the moments when they were vital, and I'm forever indebted to them for this. I wish to thank to David for this friendship, amiability and availability to help in any moment I needed. Màrius Tarrés is the "coloured voice" in our group and together with Victor, José, Mireia and Jordi B. made the atmosphere in the office and in the laboratory more entertaining. To Adnana, Marius Lupu, Ana-Daniela, Ivy, Elena O. and Justo, I wish to thank for their collaboration and good companionship in the laboratory.

I wish to remind other persons that I had the pleasure to meet and work with, and from which I surely learned something: Patricia, Mònica, Greg, Yolanda, Bea, Chelo, Paula, Chris, Will, Noe, Yan and Damien.

All my gratitude to Dr. Cristi Matei and Dr. Dana Berger from Faculty of Applied Chemistry and Materials Science from Polytechnic University of Bucharest for the good recommendations that I received from them in order to come to Barcelona and for introducing me to Prof. Clara Viñas. I also want to thank to Prof. Ana Maria S. Oancea from Faculty of Applied Chemistry and Materials Science from Polytechnic

University of Bucharest for her confidence and for introducing me in the world of research, and for guidance during all the years of University courses.

As usually, the family is left at the end, but this doesn't mean that is the least. I wish to thank them for their love and support, without them everything would have been impossible. To Ana, the words are incapable to describe what I owe to her.

ORGANITZACIÓ DEL MANUSCRIT

D'acord amb la normativa vigent i prèvia acceptació de la comissió de Doctorat de la Universitat Autònoma de Barcelona, aquesta Memòria es presenta com a recull de publicacions. Els treballs inclosos en aquesta memòria són:

Addendum I: Articles publicats i presentats a la Comissió de Doctorat de la Universitat Autònoma de Barcelona al juliol de 2012:

1.- "*Influential Role of Ethereal Solvent on Organolithium Compounds: The Case of Carboranyllithium*". Adrian-Radu Popescu, Ana Daniela Musteti, Albert Ferrer-Ugalde, Clara Viñas, Rosario Núñez, and Francesc Teixidor, *Chemistry – A European Journal*, **2012**, *18*, 3174-3184.

2.- "*Chelation of a proton by oxidized diphosphines.*" Adrian-Radu Popescu, Isabel Rojo, Francesc Teixidor, Reijo Sillanpää, Mikko M. Hänninen, Clara Viñas, *Journal of Organometallic Chemistry*, Accepted, DOI: 10.1016/j.jorganchem.2012.06.023.

3. – "*Uncommon Coordination Behaviour of P(S) and P(Se) Units when Bonded to Carboranyl Clusters: Experimental and Computational Studies on the Oxidation of Carboranyl Phosphine Ligands.*" Adrian-Radu Popescu, Anna Laromaine, Francesc Teixidor, Reijo Sillanpää, Raikko Kivekäs, Joan Ignasi Llambias, and Clara Viñas. *Chemistry – A European Journal*, **2011**, *17*, 4429-4443.

Numbering of the compounds

Section 1

(1)

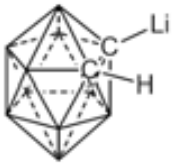

(2)

(3)

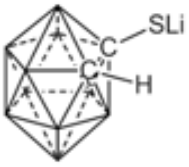

(4)

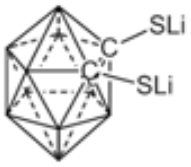

(5)

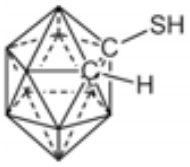

(6)

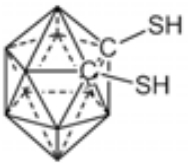

(7)

Section 2

R = Ph R' = H	**(8)**	R = Ph R' = Me	**(10)**	R = Ph R' = Ph	**(11)**	R = Ph R' = SBz	**(12)**
R = ^{i}Pr R' = H	**(13)**	R = ^{i}Pr R' = Me	**(15)**	R = ^{i}Pr R' = Ph	**(16)**	R = Cy R' = Me	**(17)**

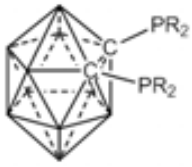

R = Ph **(9)**
R = ^{i}Pr **(14)**

E = O R = Ph R' = Me	**(18)**	E = O R = Ph R' = Ph	**(19)**	E = O R = Ph R' = SBz	**(20)**	E = O R = ^{i}Pr R' = Me	**(21)**	E = O R = ^{i}Pr R' = Ph	**(22)**
E = O R = Cy R' = Ph	**(23)**	E = S R = Ph R' = H	**(24)**	E = S R = Ph R' = Ph	**(25)**	E = S R = Ph R' = PPh_2	**(26)**	E = S R = ^{i}Pr R' = H	**(27)**
E = S R = ^{i}Pr R' = $P^{i}Pr_2$	**(28)**	E = Se R = Ph R' = H	**(29)**	E = Se R = Ph R' = Me	**(30)**	E = Se R = Ph R' = Ph	**(31)**	E = Se R = Ph R' = PPh_2	**(32)**

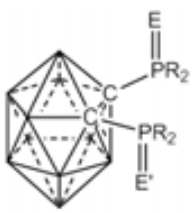

E = E' = O R = Ph	**(34)**	E = E' = O R = ^{i}Pr	**(35)**
E = E' = S R = Ph	**(36)**	E = O E' = S R = Ph	**(37)**

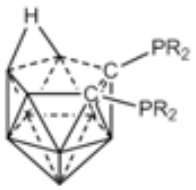

R = Ph **(38)**
R = ^{i}Pr **(39)**

R = Ph **(40)**	
R = ^{i}Pr **(41)**	

R = Ph **(43)**	
R = ^{i}Pr **(44)**	

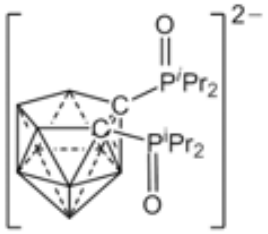

(42)

(45)

(46)

Section 3

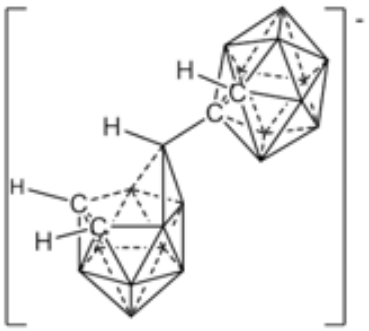

(47)

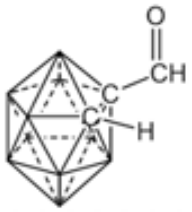

(48)

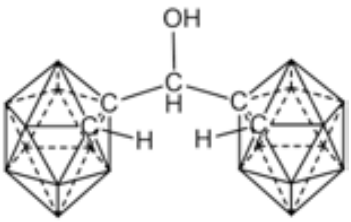

(49)

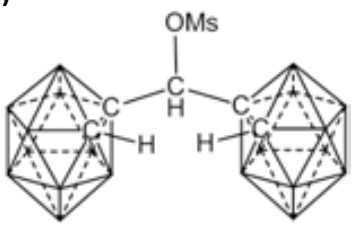

(50)

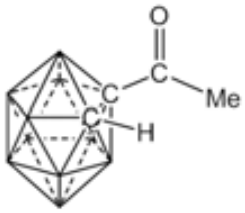

(51)

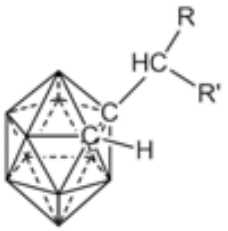

R = R′ = -C_6H_5 **(52)**	R = R′ = -C_6H_5 **(53)**	R = R′= -α-$C_{10}H_7$ **(54)**
R=R′= -*9*-$C_{13}H_9$ **(55)**	R=R′= -*9*-$C_{14}H_9$ **(56)**	R = R′ = -*p*-$C_6H_4CH_3$ **(57)**
R = -*p*-$C_6H_4CH_3$ R′ = -*o*-$C_6H_4CH_3$ **(58)**	R =R′= -*p*-C_6H_4Cl **(59)**	R = -H R′ = -*m*-$C_6H_4NO_2$ **(60)**
R = R′ = -*2*-C_4H_3NH **(61)**	R = R′ = -*2*-C_8H_5NH **(62)**	
R = R′ = -*3*- C_8H_5NH **(63)**	R = R′ = -*3*-$C_{12}H_7NH$ **(64)**	

Section 4

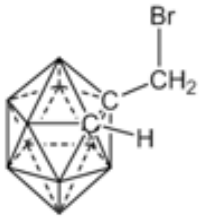

(65)

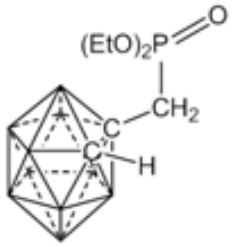

(66)

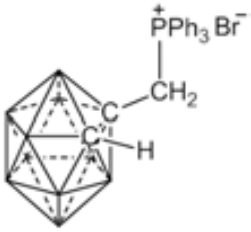

(67)

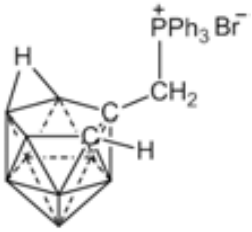

(68)

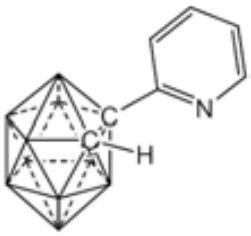

(69)

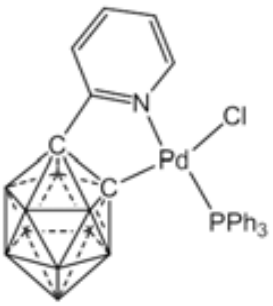

(70)

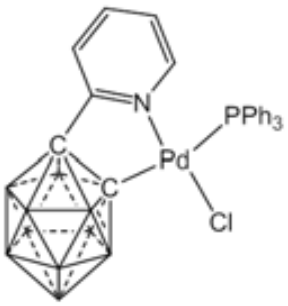

(71)

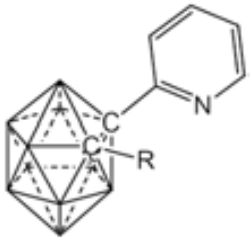

R = PPh_2	**(72)**	R = $^{i}PPr_2$	**(73)**	R = PCy_2	**(74)**
R = $SPPh_2$	**(75)**	R = $SePPh_2$	**(76)**	R = BCy_2	**(77)**

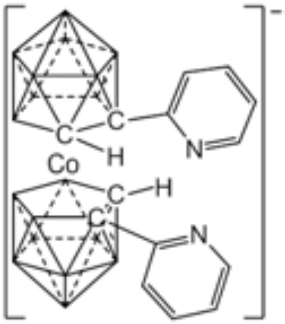

(78)

Abbreviations

δ - NMR chemical shift

σ_d – diamagnetic contribution to the shielding constant

σ_p – paramagnetic contribution to the shielding constant

σ^*_{AB} – sigma antibondig orbital for the bond between atom A and atom B

ρ - electron density

$\nabla^2\rho$ - Laplacian of the electron density

τ^*_{ABC} – tricentre antibonding orbital

AN – acceptor number

aq. - aqueous

BCP – bond critical point

BINAP - 2,2'-bis(diphenylphosphino)-1,1'-binaphthyl

BNCT – Boron Neutron Capture Therapy

*n*Bu – *normal*-butyl

^{t}Bu – *tert*-butyl

*s*Bu – *sec*-butyl

Bz - benzyl

C(A) – core basins for the ELF for atom A

C_C – carbon atom from the carborane cluster.

cod- cyclooctadiene

COSY – correlation spectroscopy

CSD – Cambridge Structural Database

CTC – cluster total charge

Cy – cyclohexyl

d_6-acetone – deuterated acetone

DFT – Density Functional Theory

DME – dimethoxyethane

DMF – Dimethyl Formamide

DMSO – Dimethyl Sulfoxide

DN – donor number

ELF – Electron Localization Function

eq. - chemical equivalent

ESI-MS – Electrospray Ionization-Mass Spectroscopy

Et – ethyl

FLP – Frustrated Lewis Pairs

FTIR – Fourier Transform Infrared Spectroscopy

IEFPCM - Integral Equation Formalism Polarizable Continuum Model

HF – Hartree-Fock Theory

HOMO – Highest Occupied Molecular Orbital

lp – electron lone pair

LUMO – Lowest Unoccupied Molecular Orbital

Me - methyl

NBO – Natural Bond Orbitals

NHO – Natural Hybrid Orbitals

NLO – non-linear optics.

NMR – nuclear magnetic resonance

NPA – natural population analysis

Ph – phenyl

PMDTA - *N*,*N*,*N*',*N*',*N*''-pentamethyl-diethylenetriamine

^{i}Pr – *iso*-propyl

Py - pyridyl

QTAIM - Quantum Theory of Atoms in Molecules

TBA – tetrabutyl amine

TD-DFT – Time-Dependent Density Ffunctional Theory

THF - tetrahydrofurane

tht – tetrahydrothiophene

UV - ultraviolet

V(A) – monosynaptic valence basins for the ELF for atom A

V(A,H) – disynaptic protonated basin for the ELF between atom A and H.

V(A,B,C) – trisynaptic valence basins for the ELF for the three-centre bonds between atoms A, B and C

Table of Contents

“Why, anybody can have a brain. That`s a very mediocre commodity. Every pusillanimous creature that crawls on the Earth or slinks through slimy seas has a brain. Back where I come from, we have universities, seats of great learning, where men go to become great thinkers. And when they come out, they think deep thoughts and with no more brains than you have. But they have one thing you haven`t got: a diploma.”

The Wonderful Wizard of Oz

L. Frank Baum

I. INTRODUCTION

1. Overview

The *closo*-1,2-dicarbadodecaborane or trivially *ortho*-carborane, 1,2-$C_2B_{10}H_{12}$, (Figure 1.1.) was the first carborane discovered and characterized, although it was not the first carborane reported in the literature. Nowadays, a half of century ago after its discovery, is the most widely used member of its genre. In a recent monograph on carboranes the number of derivatives of this compound is set to thousands and their applications are extended over a wide range from the supramolecular chemistry of polymers and dendrimers, to catalysis, medicine, molecular imagining and radiotherapy, ionic liquids, liquid crystals, NLO materials, electroactive systems, and other.[1]

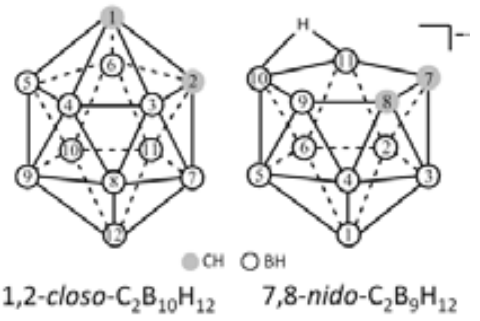

Figure 1.1. Numbering scheme of *ortho*-carborane (1,2-*closo*-$C_2B_{10}H_{12}$) and *nido*-carborane (7,8-*nido*-$C_2B_9H_{12}$).

The proprieties of the carboranes were recently reviewed,[2] but some aspects that are of interest for this work are detailed. Structurally, the dicarba-*closo*-dodecaboranes adopt regular icosahedral geometry in which the carbon and boron vertices are hexacoordinated. Besides the above mentioned, *ortho* isomer, there are other two isomers: *meta*-carborane, 1,7-*closo*-$C_2B_{10}H_{12}$, and *para*-carborane, 1,12-*closo*-$C_2B_{10}H_{12}$, respectively. This other two isomers are obtained by rearrangement of the *ortho*-carborane, under inert atmosphere at 500°C for *meta* isomer and over 600°C for the *para* isomer.

The *ortho*-carborane derivatives can be achieved by direct substitution on the cluster (all the B and C vertices can be substituted) or by the reaction of substituted acetylenes with decaborane, $B_{10}H_{14}$ (only C-substituted derivatives are obtained).

The charge distribution on the cluster atoms makes the *o*-carborane suitable for different types of reaction. The difference in electronegativity between the C and B atoms, makes the negative charge to be located on the C atoms. The B atoms in the proximity of the C atoms are more positive and the ones located further are more negative.[3] Consequently, the protons at the cluster carbon atoms are relatively acidic, having the experimental equilibrium acidity constants, pK_a, of 23.3 (Streitwieser's scale) and 19 (polarographic scale)[3a] and so, being easily removed by a strong base, yielding the conjugated base of *o*-carborane, which then can be reacted with an electrophile to yield new C_C-derivatives. The B atoms that are more negative (B4, B5, B7-B12) can be involved in electrophilic substitution reactions, whereas B3 and B6 (which are the less negative B vertices) can be attacked by nucleophiles. Therefore, the carboranes are unstable in alkaline media, where they are susceptible of nucleophilic attack by Lewis bases and undergo partial degradation, yielding the corresponding *nido* derivative.

The C-substituted *o*-carborane derivatives covers all the elements form the main group of the Periodic Table, starting with the metalation by Li and Mg and going through transition metal groups and elements from Groups 13 to 17. We were interested in this work, as the title of the thesis suggests, in elements that are rich in electrons, and can induce interesting properties to the carborane derivative, especially in the field of organometallic chemistry. For that, in the following, a brief review on carborane derivatives with electron reach moieties will be presented. As another part of this work was centred on the "confined space" multicage derivatives of carborane, as short survey on the literature on the so-called "star shape" derivatives will be presented.

2. Carborane with phosphorus moieties: Carboranylphosphines

2.1. *Closo*-carboranylphosphines

2.1.1. General aspects on the synthesis of *closo*-carboranylphosphines

The interest in carborane-phosphine compounds started almost half of century ago, when 1,2-$(PPh_2)_2$-1,2-*closo*-$C_2B_{10}H_{10}$, was synthesized for the first time,[4] in a simple reaction between dilithiocarborane and diphenylchlorophosphine. Besides the investigation of the properties of these phosphines as ligands for organometallic chemistry, just some years after their discovery the first patent was produced in United States, back in the 1960s.[5] Treating the cyclic bis-chloro compound [1,2-PCl-1,2-*closo*-$C_2B_{10}H_{10}]_2$ with sodium azide afforded the cyclic bis-azide, [1,2-PN_3-1,2-*closo*-$C_2B_{10}H_{10}]_2$ (Scheme 2.1.a). This compound was a good candidate to the first reported reaction between a phosphorus (III) azide and a phosphine, to form a phosphineimino compound, [1,2-(PN)PPh_3-1,2-*closo*-$C_2B_{10}H_{10}]_2$ (Scheme 2.1b). Based on this, Alexander and Schroeder, extended the use of this cyclic bis-azide in the reaction with *p*-$[(C_6H_5)_2P]_2$-C_6H_4, to form a trimmer which was the object of the patent, for its potential use as binder in the preparation of high temperature stable composites. In order to increase its thermal stability, investigation on the synthesis of these types of compounds with halogenated carboranes was also done, but the diazide obtained were explosive on impact, friction and heating, and no further studies can be found in the literature.

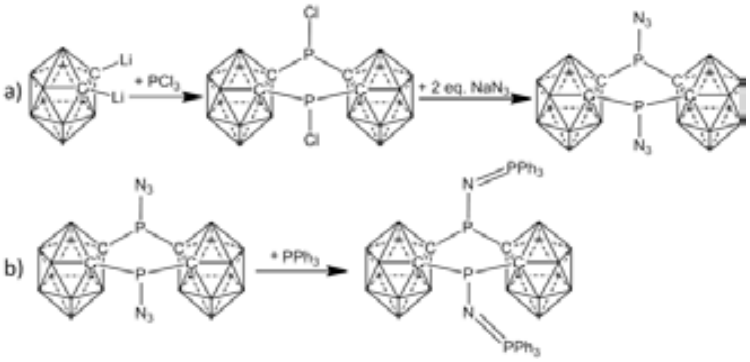

Scheme 2.1. Synthesis of: a) [1,2-PN_3-1,2-*closo*-$C_2B_{10}H_{10}]_2$ and b) [1,2-(PN)PPh_3-1,2-*closo*-$C_2B_{10}H_{10}]_2$.

Parallel with the research done in the 1960s in United States, the Russian scientists also were interested in the chemistry of the carboranyl-phosphines, the first monophosphine, namely, 1-P(*n*-$C_6H_{13})_2$-2-Ph-1,2-*closo*-$C_2B_{10}H_{10}$, being synthesized in 1965, from the reaction of the lithiated phenyl-o-carborane with chlorodi(*n*-hexyl)phosphine[6] as well as the 1,1-PCl-(2-Ph-1,2-*closo*-$C_2B_{10}H_{10})_2$, from the reaction with PCl_3.

Bis(dimethylamino)-*o*-carboranylphosphines were also synthesized upon reaction of lithiated carboranes with $ClP[N(CH_3)_2]_2$, which can be transformed almost quantitatively into o-carboranyldichlorophosphines upon reaction with dry HCl in benzene solution. The carborane moiety induces a rare property to these chlorophosphines, which makes then stable at air, contrary to the alkyl- or aryldichlorophosphines. Even more, the *o*-carboranyldichlorophosphines are inert against the reaction with sulfur to a temperature up to 200°C, although, they react energetically, with chlorine, in bezene, with formation of *o*-carboranyltetrachlorophosphines.[7]

The tertiary chlorophosphines derivates from carboranes can be reduced to secondary phosphines by reaction with $LiAlH_4$, although specific conditions have to be applied in order to maintain the C-P bonds.[8,9] Thus, using excess of $LiAlH_4$ and 50 equivalents of water, the C-P bond is cleaved,

whereas the equimolar amounts of $LiAlH_4$ and ether or 10 equivalents of water yield the secondary phosphine.

The bis(halophosphanyl)dicarba-*closo*-dodecaborane compounds were recently employed[10] as starting materials for facile synthesis of 1,2-diphosphetanes. As presented in Scheme 2.2., the reduction of a diastereomeric mixture of different halophosphines with magnesium or zinc gave 1,2-diphosphetanes in which the substituents have a *trans* arrangement.

Scheme 2.2. Synthesis of carborane based 1,2-diphosphethanes.

If the synthesis of homodisubstituted phosphine derivatives of *o*-carborane, is in principle a simple task, by employing one equivalent of carborane, two equivalents of buthylithium and two equivalents of appropriate halophosphine; the synthesis of the monosubstituted phosphine derivatives or heterodisubstituted phosphine derivatives of *o*-carborane is not so trivial. It has been postulated[11] that the equilibrium shown in Scheme 2.3., dominates the formation of mono-, and disubstituted derivates of *o*-carborane. In a reaction aimed at producing monosubstituted 1-R-1,2-*closo*-$C_2B_{10}H_{11}$, the formation of the disubstituted species 1,2-R_2-1,2-*closo*-$C_2B_{10}H_{10}$ implies to leave unreacted 1,2-*closo*-$C_2B_{10}H_{12}$ in the reaction mixture. This is undesirable because the three compounds mono-, di- and unreacted, commonly share very similar solubility properties causing difficulties in their separation. [12] This was a bottle-neck in the development of new derivatives of carborane, on which we turned our attention in this work and, as will be seen in the Results and Discussion (Section 1), we showed that the choice of the appropriate solvent for the reaction is an important factor when synthesizing monoderivatives of *o*-carborane. But even so, in some application further purification of the *o*-carboranylmonophosphine, by column chromatography from hexanes have to be done.[13] Another important factor, which must be taken into consideration when synthesizing heterodisubstituted phosphine derivatives of *o*-carborane, is the cleavage of the C-P bond when reacted with buthylithium.[14] To overcome this, low temperatures are mandatory,[15] or, if the one of the moiety is not a phosphine, just synthesizing first the monoderivative, and later synthesizing the phosphine (Scheme 2.4.a).[14] Another route to heterodisubstituted of *o*-carboranes, is first the synthesis of the monoderivative of o-carborane from $B_{10}H_{14}$ and suitable alkynes derivatives, followed by the reaction of the lithiated monosubstituted derivative with the chlorophosphine (Scheme 2.4.b).[16]

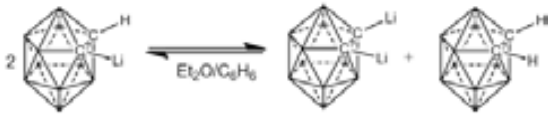

Scheme 2.3. The equilibrium between the species involved in the reaction of 1,2-$C_2B_{10}H_{12}$ with *n*BuLi.

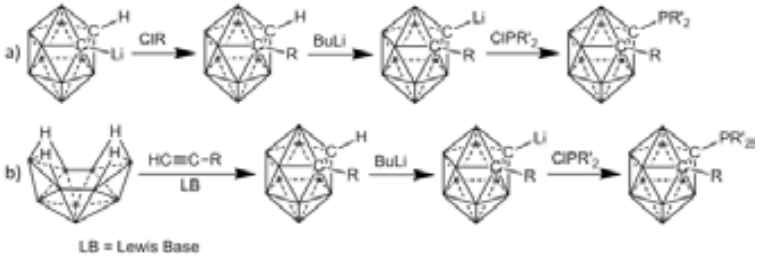

Scheme 2.4. Synthesis of heterodisubstituted carboranylphosphines: a) from *o*-carborane and b) from decaborane.

2.1.2. *Closo*-carboranylphosphines with tetracoordinate phosphorus

The disclosure of the structure of $^{t}Bu_3PI_2$ where significant iodine – iodine interactions and four-coordinate phosphorus center[17] were observed, stimulated the interest of the researchers in the area, and our group was interested in investigation of this type of interactions for carboranyl phoshpines.[18] As DuMont *et al.* suggested, the above mentioned compound could be interpreted either as a iodophosphonium salt or as a iodine charge transfer complex. Our group first studied this type of interactions for 1-Me-2-P^{i}Pr$_2$-1,2-*closo*-$C_2B_{10}H_{10}$.[18a] By titration of this phosphine with different amounts of I_2 in $CHCl_3$ it was observed that for 1:1 ratio, a charge transfer "spoke" adduct is formed, whereas increasing the amount of I_2 after 2 equivalents, the cationic tetra-coordinated phosphorus specie, [1-Me-2-IP^{i}Pr$_2$-1,2-*closo*-$C_2B_{10}H_{10}$]$^{+}$ is obtained. The (1-Me-2-P^{i}Pr$_2$-1,2-*closo*-$C_2B_{10}H_{10}$)I_2 adduct was very interesting structurally because it presents one of the shortest I-I distance found for these type of adducts. Very interesting though is the different behavior found for a similar phosphine, where the ^{i}Pr groups are substituted for Ph moieties. In this case, no evidence of formation of [1-Me-2-IPPh$_2$-1,2-*closo*-$C_2B_{10}H_{10}$]$^{+}$ was found with increasing the I_2 ratio. In change, an adduct that accommodates two carboranyl-phosphines is formed, (1-Me-2-PPh$_2$-1,2-*closo*-$C_2B_{10}H_{10}$)$_2I_2$ (Figure 2.1.). This adduct is unique,[18b] having the shortest I-I distance (2.7753Å) found ever for a R_3PI_2 adduct, and is comparable with distances found in R_2SI_2 adducts, being just slightly longer than that found for I_2 in solid state at 110K (2.7156Å).[19]

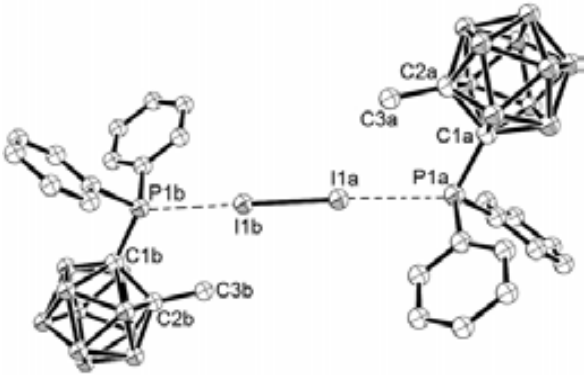

Figure 2.1. Crystal structure of [1-Me-2-PPh$_2$-1,2-*closo*-$C_2B_{10}H_{10}$]$_2$·I_2 (H atoms are omitted for clarity).

Scheme 2.5. Synthesis of phosphonium salts starting from carboranylphosphines.

Also, tetracoordinated phosphorus derivatives, as phosphonium salts, were synthesized by methylation of 1-PPh$_2$-1,2-*closo*-$C_2B_{10}H_{11}$ with MeI.[20] This phosphonium salt was further reacted with CsF in ethanol to yield *nido*-carborane phosphonium zwitterions (Scheme 2.5.).

2.1.3. *Closo*-carboranylphosphines with P(V) moieties

The first derivatives of carborane which contains pentavalent phosphorus were synthesized by the hydrolysis of the carboranyl-dichloride derivatives, obtaining phosphonous acid derivatives,[7] but P(V) derivatives can also be achieved by the direct reaction of lithiated carborane with phosphoryl chloride,[21] by the reaction of the carboranylphosphonites with chloral[22] or during the Arbuzov rearrangement in organophsophorus derivatives of carboranes.[23] The oxidation of carboranyl-

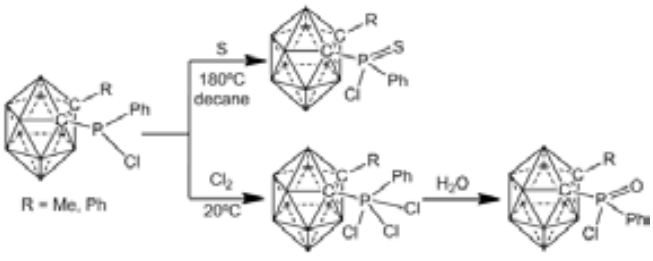

Scheme 2.6. Synthesis of oxidised carboranylphosphines.

phosphines was first reported to take place in the reaction of carboranylchlorophospines with sulfur, in decane, at 180°C (Scheme 2.6.), whereas the derivative with oxygen was achieved by first the oxidation of carboranylchlorophosphines with chlorine, followed by hydrolysis of the carboranyl-trichlorophosphorane (Scheme 2.6.).[8] Though, the carboranylphosphine oxides were prepared by oxidation of carboranyl-phosphines with Jones reagent or sodium dichromate(VI).[24] All these reactions involve monophosphines, but when the oxidation with S was tried for carboranyldiphosphines, like 1,2-$(PHPh)_2$-1,2-*closo*-$C_2B_{10}H_{10}$[25] or 1,2-$(PClPh)_2$-1,2-*closo*-$C_2B_{10}H_{10}$,[26] only the cyclic anhydride of dithiodiphosphinic acid derivate from carborane, was obtained (Scheme 2.7).

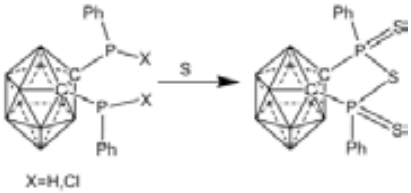

Scheme 2.7. Synthesis of carborane based dithiophosphonic acid anhydrides.

Although, other oxidized carboranylmonophosphine derivatives were reported,[27] no systematic study could be found in the literature on the oxidation of the carboranylphosphines. This was the motivation of another topic of this thesis in which we made a comprehensive study of the oxidation of *closo*-carboranylmonophsphines and *closo*-carboranyldiphosphines with O, S and Se.

2.1.4. Metal complexes of *closo*-carboranylphosphines

Practically concomitant with the synthesis of the first carboranyl-phosphines, the interest of the researchers was directed toward the synthesis of their metal complexes, first with nickel and its congeners.[28]

Hill *et al.* studied a series of carboranyl-diphosphine ligands like 1-PPh_2-2-P(R)R'-1,2-*closo*-$C_2B_{10}H_{10}$ (R=R'=Ph, NMe_2, F; R=NMe_2, R'=F) and 1-$P(NMe_2)_2$-2-P(R)R'-1,2-*closo*-$C_2B_{10}H_{10}$ (R=R'=C_6F_5; R=NMe_2, R'=F) as *cis* chelating ligands toward Pt in order to establish the *cis* and *trans* influence of these ligands.[29] It was found by ^1H, ^{19}F and ^{31}P-NMR that the predicted order of *trans* influence is: PPh_2 > $P(C_6F_5)_2$ > $P(NMe_2)_2$ > P(F)NMe_2 > PF_2, whereas the *cis* influence decrease in order: $P(C_6F_5)_2$ > P(F)NMe_2 > PPh_2 > $P(NMe_2)_2$. During this research, Hill *et al.* were unable to characterize well the compound [*cis*-$PtCl_2$(1-PPh_2-2-PF_2-1,2-*closo*-$C_2B_{10}H_{10}$)] due to its low solubility. Muir *et al.*, studding the electronic effects of phosphine substituents on metal-ligand bonding, were interested in the crystallographic determination of this compound.[30] They tried the recrystalization of this phosphine from benzene, chloroform, dichloromethane and acetone. During these attempts they produced a new compound, in which the cleavage of C_c-PF_2 bond was produced, as observed by X-ray diffraction (Figure 2.2.).[30] Kalinin *et al*.[31] also determinate that under special conditions, intermolecular metallation with Pd or Pt of *o*-carboranylphosphines can occur. From the *trans*-[MCl_2(1-PPh_2-1,2-*closo*-$C_2B_{10}H_{11}$)$_2$] (M=Pd, Pt) by heating in toluene, the *exo*-cyclic compounds [MCl(1-PPh_2-1,2-*closo*-$C_2B_{10}H_{11}$)(1-PPh_2-1,2-*closo*-$C_2B_{10}H_{10}$)] (M=Pd, Pt) can be obtained. The palladium complex [PdCl(1-PPh_2-1,2-*closo*-$C_2B_{10}H_{11}$)(1-PPh_2-1,2-*closo*-$C_2B_{10}H_{10}$)] dissociates readily in solution yielding the dimmeric chlorine-bridged complex [PdCl(1-PPh_2-1,2-*closo*-$C_2B_{10}H_{10}$)]$_2$.

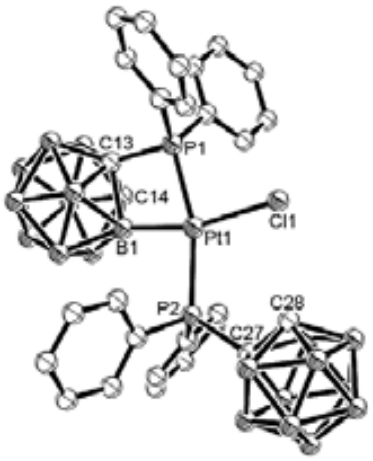

Figure 2.2. Crystal structure of [PtCl(1-PPh_2-1,2-*closo*-$C_2B_{10}H_{10}$)(1-PPh_2-1,2-*closo*-$C_2B_{10}H_{11}$)] (H atoms are omitted for clarity).

A series of Pd and Pt complexes with *closo*-

carboranyldiphosphines were systematic investigated by our group from synthetic and crystallographic point of view.[32]

Complexes with Pd and Pt were also prepared with mixed heterodisubstituted derivatives of carborane, having on one C_C atom a phosphine moiety and on the other C_C atom an organosilicon, organogermanium or organotin group.[15,33] So, with 1-PR_2-2-$YXMe_2$-1,2-*closo*-$C_2B_{10}H_{10}$ (R = Me, OEt, Ph; Y=Si, Ge, Sn and X = H, Cl) mononuclear or binuclear complexes where obtained, depending on the X moiety (Scheme 2.8.).

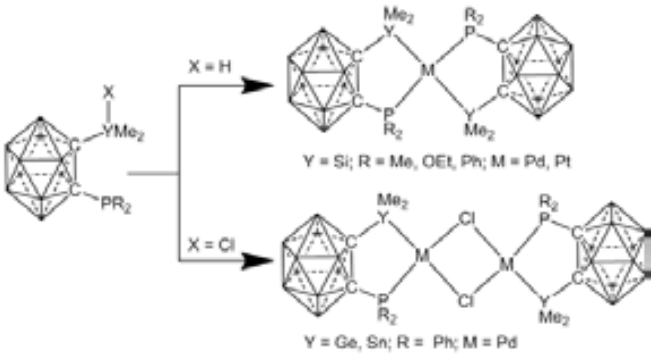

Scheme 2.8. Synthesis of Pd(II) and Pt(II) complexes with heteredisubstituted carboranylphosphines.

Metal complexes with Co are difficult to obtain, and special care is to be taken when working with this compounds, as hydroxylic solvents decompose them easily. Nevertheless, tetrahedral blue complexes like $[CoX_2\{(1,2\text{-}(PPh_2)_2\text{-}1,2\text{-}closo\text{-}C_2B_{10}H_{10}\}]$ (X=Cl, NCS) and square pyramidal green complexes like $[CoX\{1,2\text{-}(PPh_2)_2\text{-}1,2\text{-}closo\text{-}C_2B_{10}H_{10}\}_2]^+$ (X=Br, I, NCS) were synthesized.[34]

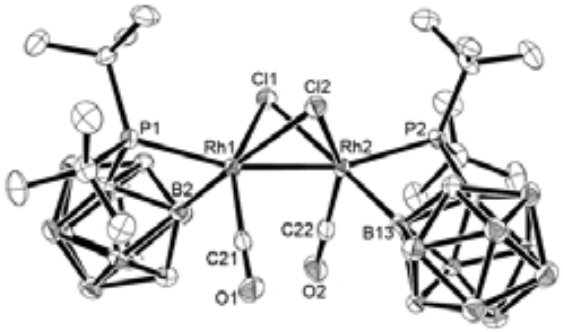

Figure 2.3. Crystal structure of $[Rh(Cl)(CO)(1\text{-}P^tBu_2\text{-}1,2\text{-}closo\text{-}C_2B_{10}H_{10})]_2$ (H atoms are omitted for clarity).

The iridium (I) was studied for its possibility to undergo B-σ-carboranyl bonds by oxidative addition of terminal boron-hydrogen bonds.[35] Hawthorne and Hoel showed, by deuteration studies, that by reacting $[IrCl(C_8H_{12})]_2$ with 1-PMe_2-1,2-*closo*-1,2-$C_2B_{10}H_{11}$ in cyclohexane a B-σ-carboranyl iridium complex is formed.[36] When 1-propenyl-2-(diphenylphosphino)-*ortho*-carborane is reacted with rhodium complexes, the resulting complex is a dimmer in which the B-metalation does not occur.[37] Just recently, Pringle *et al*.[38] showed that rhodium can also form B-carboranyl complexes, and they determinate the crystal structure of an unusual dirhodium (II) complex (Figure 2.3.).

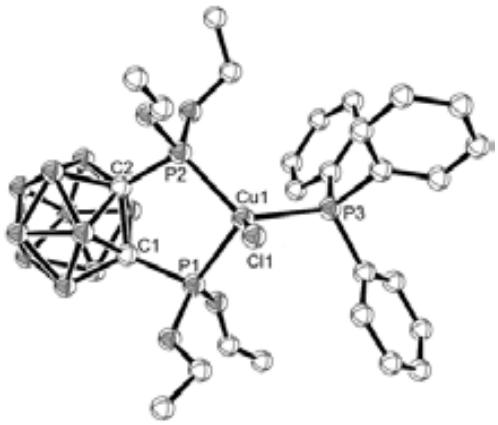

Figure 2.4. Crystal structure of $[Cu(Cl)(PPh_3)\{1,2\text{-}(P^nPr_2)_2\text{-}1,2\text{-}closo\text{-}C_2B_{10}H_{10}\}]$ (H atoms are omitted for clarity).

Kang *et al.*[16] prepared complexes of Ir and Rh with N,P- chelate carboranyl phosphines and showed that this ligand can be easily displaced by CO and PPh_3 ligands. On the other hand, when S,P-chelate carboranylphosphines are used,[39] the iridium and rhodium complexes integrate the carboranyl ligand in its complexes with CO and PEt_3 ligands.

The reaction of copper(I) halides with the tertiaty phosphine, 1-PPh_2-1,2-*closo*-$C_2B_{10}H_{11}$, in different molar ratios produces complexes $[CuX(1\text{-}PPh_2\text{-}1,2\text{-}closo\text{-}C_2B_{10}H_{11})]$, $[CuX(1\text{-}PPh_2\text{-}1,2\text{-}closo\text{-}$

$C_2B_{10}H_{11})_2$] (X=Cl, Br, I) and [CuX_2(1-PPh_2-1,2-*closo*-$C_2B_{10}H_{11})_3$] (X = Cl, Br).[40] With chelating ligands as 1,2-$(PR_2)_2$-1,2-*closo*-$C_2B_{10}H_{10}$ (R = Et, OEt, *i*Pr), the trigonal copper (I) complex [$CuCl(PPh_3)_2$] forms the distorted tetrahedral complex [$CuCl(PPh_3)${1,2-$(PR_2)_2$-1,2-*closo*-$C_2B_{10}H_{10}$}], where a PPh_3 ligand is displaced by the carboranyldiphosphine (Figure 2.4.).[41] On the other hand, if the chelating ligand 1,2-$(PPh_2)_2$-1,2-*closo*-$C_2B_{10}H_{10}$ is reacted with copper (I) halides, the halogen-bridged dimmers [CuX{1,2-$(PPh_2)_2$-1,2-*closo*-$C_2B_{10}H_{10}$}]$_2$ (X = Cl, Br, I) are obtained.[42] The same type of halogen-bridged dimmers are obtained in reaction of CuCl with 1,2-$(PClP^tBu_2)_2$-1,2-*closo*-$C_2B_{10}H_{10}$,[43] whereas with the secondary phosphine 1,2-$(PHPh)_2$-1,2-*closo*-$C_2B_{10}H_{10}$, tetrahedral complexes are formed, where the fourth coordination is occupied by a solvent molecule.

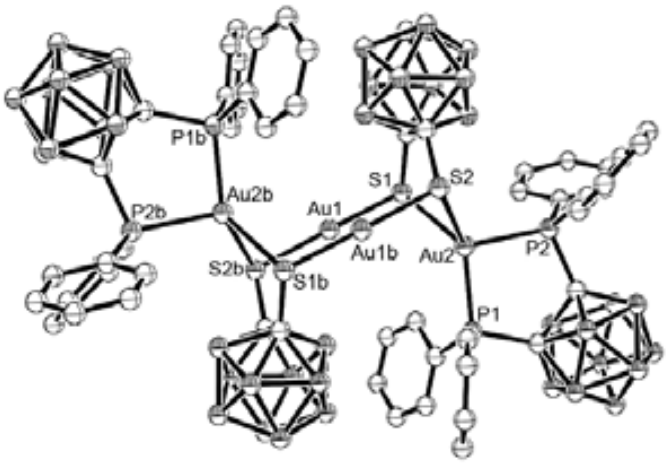

Figure 2.5. Crystal structure of carboranylphosphine based tetranuclear Au complex (H atoms are omitted for clarity).

The chemistry of gold (I) with carboranyl-phosphine ligands offers a variety of complexes were the number of ligands and metal atoms can be tuned by reaction stoichiometry.[44] By treating [AuX(tht)] (X= Cl, C_6F_5; tht=tetrahydrothiophene) with 1,2-$(PPh_2)_2$-1,2-*closo*-$C_2B_{10}H_{10}$ in 2:1 or 1:1 ratio, the dinuclear complexes [$(AuX)_2${1,2-$(PPh_2)_2$-1,2-*closo*-$C_2B_{10}H_{10}$}] and the mononuclear complexes [AuX{1,2-$(PPh_2)_2$-1,2-*closo*-$C_2B_{10}H_{10}$}], respectively, can be obtained. Also, by using the complex [Au(tht)L][ClO_4] (L = PPh_3, PPh_2(4-Me-C_6H_4), P(4-OMe-C_6H_4), PPh_2Me, CH_2PPh_3, CH_2PPh_2Me, $SPPh_3$, $AsPh_3$, C_5H_4NSH, $(PPh_2)_2CH_2$, $(PPh_2)_2NH$, $(PPh_2CH_2)_2$) in reaction with 1,2-$(PPh_2)_2$-1,2-*closo*-$C_2B_{10}H_{10}$ a plethora of mononuclear compounds of the type [AuL{1,2-$(PPh_2)_2$-1,2-*closo*-$C_2B_{10}H_{10}$}][ClO_4] can be obtained. The special chelation properties of carborane derivatives toward gold (I) is evidenced in the synthesis of tetranuclear [Au_4(1,2-S_2-1,2-*closo*-$C_2B_{10}H_{10})_2${1,2-$(PPh_2)_2$-1,2-*closo*-$C_2B_{10}H_{10}$}$_2$] (Figure 2.5.).[44c] The formation of this complex is unexpected since analogous ligands like the ditiolate $(CH_2)_3S_2^{2-}$ and bis(diphenylphosphino)methane (dppm) produce with gold (I) the dinuclear complex [Au_2{μ-$S(CH_2)_3S$}(μ-dppm)]. This fact could be attributed to the presence of rigid carborane backbones which promote chelation. The silver (I) chemistry with carboranyl-phosphines is similar with the one of gold (I).[45]

Studies on the coordination chemistry of [$Cr(CO)_4$], [$Mo(CO)_4$] and [$W(CO)_4$] with bidentate carboranyl-diphsophines can be found in the literature.[46] In general, the bidentate ligand replace two carbonyl moieties yielding [$M(CO)_4${1,2-$(PR_2)_2$-1,2-closo-$C_2B_{10}H_{10}$)}] complexes. The achievement of these compounds involve very energetic condition, although the [(nbd)$Mo(CO)_4$] seems to react with 1,2-$(PXPh)_2$-1,2-*closo*-1,2-$C_2B_{10}H_{10}$ (X=H, Cl) or 1,2-$[P(OR)_2]_2$-1,2-*closo*-1,2-$C_2B_{10}H_{10}$ (R = 4-t-buthylphenyl or menthyl) at room temperature to yield [$Mo(CO)_4${1,2-$(PXPh)_2$-1,2-*closo*-$C_2B_{10}H_{10}$}] and [$Mo(CO)_4${1,2-$[P(OR)_2]_2$-1,2-*closo*-$C_2B_{10}H_{10}$}], respectively.[46c-e] Also, heterobimetallic trinuclear clusters of the type [$M_2M'S_4${1,2-$(PPh_2)_2$-1,2-*closo*-$C_2B_{10}H_{10}$}] (M=Cu, Ag and M' = Mo, W) have been prepared.[47]

2.1.5. Complexes with oxidized *closo*-carboranylphosphines

Complexes with P(V) carboranylphosphines are rather rare. Even so, some complexes with oxidized carboranylmonophosphines in the presence of a thiolate were prepared.[27a,48] Other oxidized

carboranylmonophosphine as is the anionic [1-$SPPh_2$-1,2-*closo*-$C_2B_{10}H_{10}$]$^-$ acts as a C,S chelate and forms air and moisture stable five members ring complexes with Rh and Ir.[48] The analogous [1-$SPPh_2$-2-S-1,2-*closo*-$C_2B_{10}H_{10}$]$^-$ react different with Ir(I) and Rh(I) complexes With Rh(I), it coordinates through the S atoms to form six member ring complexes, whereas, with Ir(I), the ligand acts as tridentate as it is shown in Scheme 2.9.

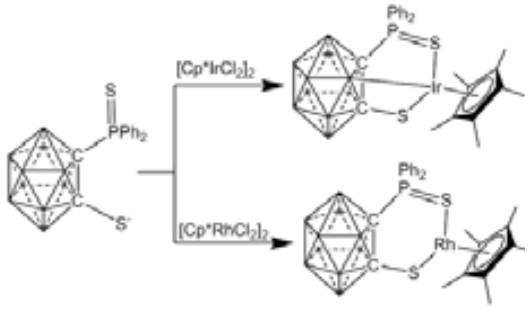

Scheme 2.9. Synthesis of metallic complexes of oxidised carboranylphosphines.

Other metal complexes with P(V) derivatives of carboranylphosphines were prepared with oxophilic Group 4 metals (Zr, Hf, Ti). The oxidized P atoms is bonded to a N^{i}Pr$_2$ group and an indenylide or fluoronyl groups. During the complexation reaction the C_C metalation takes place and the ligand acts as bidentate.[49]

We also investigated in this thesis the potential of the carboranylphosphine chalcogenides to be used as hybrid hemilabile ligands as it is presented in the Results and Discussion (Section 2).

2.2. *Nido*-carboranylphosphines

2.2.1. General aspects on the synthesis of *nido*-carboranylphosphines

Early pioneering work by Hawthorne and co-workers[50] demonstrated that *closo*-carboranes could be partially degraded to the corresponding *nido* monoanions, by strong bases such as potassium hydroxide in methanol or ethanol. Other reagents have been found to effect partial degradation, e.g. tertiary amines,[51] hydrazine,[52] ammonia,[53] piperidine,[54] fluoride anions[55] and iminophosphorane derivatives.[56]

The *closo*-carboranes are usually very stable compounds with respect to chemical attack by acids and oxidizing agents, fact that allowed the synthesis of a very large number of derivatives that retain the *closo* nature of the cluster.

The synthesis of *nido*-carboranylphosphines resisted a lot of time to the researchers, taking into consideration that the first *closo*-carboranylphosphines were synthesized in 1963,[4] whereas the first *nido*-carboranylphosphines were reported in 1993.[57] The main reason for this drawback was the poor stability of the C_c-P bond in nucleophilic conditions. Our group was the first to find that the synthesis of the *nido* carboranylphosphines can be achieved, essentially, in two ways: a) by reaction of *closo*-carboranylphosphines with transition metals in nucleophilic solvents (Scheme 2.10.), or b) by direct degradation of the *closo*-carboranylphosphines with the proper nuclephilic agent, which have the strength to deboronate the carborane cluster but in the same time is gentle with the C_c-P bond (Scheme 2.11.).[58]

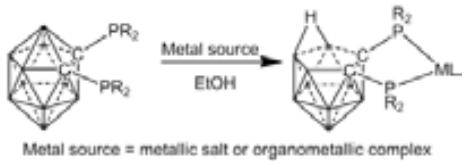

Scheme 2.10. Synthesis of organometallic complexes of *nido*-carboranylphosphines from *closo*-carboranylphosphines.

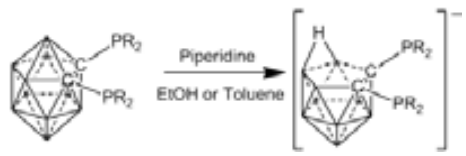

Scheme 2.11. Synthesis of *nido*-carboranylphosphines from *closo*-carboranylphosphines by direct degradation.

2.2.1.1. Degradation by complexation

The first metals which, we observed, that induce the cluster deboronation were the metallic ions of the d^{10} type[57] although other types of metals can produce *nido* compounds (Table 2.1.). The deboronation by complexation, though, was achieved only when the carborane-based ligand acts as bidentate as in carboranyldiphosphines, or carboranylmonophosphine-thioethers as it happens with carboranyldithioethers.[59] The main parameter that dictates if the *closo*-carboranyldiphosphines will form *nido* derivatives upon complexation is the solvent. The alcohols, in general, and especially methanol or ethanol, are the solvents which favor the degradation, whereas, less nucleophilic solvents or aprotic solvents, like dichloromethane, chloroform or toluene, retain the *closo* nature of the carborane cluster as reported in the section 2.1.4..

The phenomenon of degradation by complexation can be explained if electronic and steric effects are considered. As the phosphorus (III) atoms posses a lone pair of electrons, it gives electronic

Metal	Type	Metal sources	Solvent	Ref.
Cu(I)	d^{10}	$[CuCl(PPh_3)_2]$	EtOH	[57], [59c]
Ag(I)	d^{10}	$[Ag(NO_3)(PPh_3)]$ $AgNO_3$ $[Ag(ClO_4)(PPh_3)]$ $[Ag(ClO_4)(PPh_2Me)]$	EtOH THF	[59b], [70]
Au(I)	d^{10}	$[AuCl(PPh_3)]$ $[AuCl(PPh_2Me)]$ $[AuCl(PPh_2(4\text{-}Me\text{-}C_6H_4))]$ $[AuCl(P(4\text{-}Me\text{-}C_6H_4)_3)]$ $[AuCl(AsPh_3)]$ $[AuPh_3(tht)](ClO_4)$ [(AuBr)2(PPh3)4]	EtOH	[59b], [69], [71], [63], [79]
Hg(II)	d^{10}	$[Hg(NO_3)_2(PPh_3)]$ $Hg(NO_3)_2{\cdot}H_2O$ $[HgCl_2(PPh_3)]$ $HgCl_2$	EtOH MeCN	[45d], [45f], [59b]
Pd(II)	d^8	$[PdCl_2(PPh_3)_2]$ $[PdCl_2(BZN)_2]$ $[PdCl_2(PPh_2Me)_2]$ $PdCl_2$	EtOH MeCN PhCN	[82], [83], [84a]
Ni(II)	d^8	$NiCl_2{\cdot}2H_2O$ $NiCl_2{\cdot}6H_2O$ $NiBr_2{\cdot}6H_2O$ $[NiCl_2(PPh_3)_2]$	EtOH CH_2Cl_2 (solvothermal)	[83], [84b], [85]
Pt(II)	d^8	$[PtCl_2(PPh_3)_2]$	EtOH	[83]
Rh(I)	d^8	$[RhCl(CO)(PPh_3)_2]$ $[RhCl(PPh_3)_3]$	EtOH	[59b]
Au(III)	d^8	$AuCl_3{\cdot}nH_2O$ $[AuCl_3(tht)]$	EtOH	[59b], [72]
Ru(II)	d^6	$[RuClH(CO)(PPh_3)_3]$	EtOH	[59b]
Rh(III)	d^6	$RhCl_3.xH_2O$	EtOH	[59b]
Ir(III)	d^6	$[(Cp^*IrCl_2)]_2$	EtOH	[78]

Table 2.1. Metals which lead to the conversion of *closo*-carboranylphsphines to *nido*-carboranylphosphines.

density to the cluster. When the phosphorus atoms coordinate to the metal, a two way electron flux takes place: on one hand, the σ-donation of the lone pair of electrons from the phosphorus atom to the metal; and on the other hand, the π back-bonding from the metal to the P atom.

The phosphorus atom is enriched in electronic density and favors the electronic donation to the cluster through the C_C atom. It is worth mentioning that *closo*-C_2B_{10} cluster acts as a stronger electron withdrawing group than a phenyl moiety.[60] In this process, similar to a reduction, the B(3) and B(6) atoms are the most affected due to their direct bonding to the C_C atoms. When the cluster receive charge density, the charge is mainly dissipated toward the B(9), B(12), which leave the B(3) and B(6) atoms poor in electrons, and so, susceptible to nucleophilic attack.[3b,c]

Although this method of degradation is mainly general for any carboranyldiphosphine with any metallic complex or metal salt, in ethanol, independently of the metal or its coordination environment; there are some exceptions, which can be explained if the steric factors are taken into consideration. These is the case of the reaction of 1,2-$(PPh_2)_2$-1,2-*closo*-$C_2B_{10}H_{10}$, with $[RhCl(PPh_3)_3]$ (Wlikinson's catalyst) in ethanol, which yield $[RhCl(PPh_3)(1,2\text{-}(PPh_2)_2\text{-}1,2\text{-}closo\text{-}C_2B_{10}H_{10})]$, instead of the expected, $[Rh(PPh_3)_2(7,8\text{-}(PPh_2)_2\text{-}7,8\text{-}nido\text{-}C_2B_9H_{10})]$.[59b] The *nido* complex is sterically unavailable, due to the fact that the presence of two PPh_3 moieties in the cis positions, in a square planar environment, where the other two positions are occupied by the *nido*-carboranyldiphosphine, creates great steric hindrance, which elevates so much the stabilization energy of the molecule that its formation is impossible. Instead, the *closo* derivative is preferred by the displacement of two PPh_3 moieties by the neutral *closo*-carboranydiphosphine, being required the presence of a Cl moiety to both compensate the positive charge and to release the steric tension. A study performed with different monodentate phosphine ligands, which request different steric demands, confirms the impossibility of the coordination of two PPh_3 moieties, whereas, other moieties, less voluminous, like PMe_2Ph or $P(OEt)_2$, can be accommodated to form the $[Rh(PMe_2Ph)_2(7,8\text{-}PPh_2\text{-}7,8\text{-}nido\text{-}C_2B_9H_{10})]$ or $[Rh(POEt)_2(7,8\text{-}PPh_2\text{-}7,8\text{-}nido\text{-}C_2B_9H_{10})]$ derivatives.[61]

2.2.1.2. Direct degradation

As described above, the usual established procedures for degradation of carboranes were inefficient in the case of carboranylphosphines. The direct degradation of the *closo*-carboranyldiphosphine derivatives, using the well established procedure[62] with KOH in ethanol, was unsuccesfull because the $C_{cluster}$-P bond in the *closo* species is very susceptible to nucleophiles producing C_C-P cleavage and yielding the $[7,8\text{-}nido\text{-}C_2B_9H_{10}]^-$ anion. In contrast, the degradation process with piperidine in toluene[63] in a 1:4 molar ratio of *closo*-carboranylmonophosphines to piperidine at 20 °C did not give the desired *nido* species, and the starting *closo* compounds were recovered. Since our group discovered the degradation by complexation we were also interested to develop a method for the direct degradation, opening in this way the possibility for new, unprecedented and interesting anionic phosphine ligands.

In 1983, Allcock *et al.*[64] were the first to report the degradation of a carborane derivative with a C_c-P bond, namely carboranylphosphazenes. The *nido*-carboranylphosphazenes were obtained from the *closo* derivatives in the reaction with 75 equivalents of piperidine in refluxing benzene. Aimed by these results our group investigated the degradation of carboranylphosphines with piperidine using toluene or ethanol as solvents.[59] Appropriate synthetic procedures to yield cluster partial degradation with C_C-P bond retention by using toluene with a ratio of 1:50 (carborane : piperidine) or in ethanol with a ratio of 1:10 (carborane : piperidine) have been described (Table 2.2).[59] The explanation of why the partial

Substance	Non-reacted (%)		Degraded, with C_c-P cleavage (%)		Degraded, without C_c-P cleavage (%)	
	A	B	A	B	A	B
1-PEt_2-2-Me-$C_2B_{10}H_{10}$	38	28	2	2	60	72
1-P^iPr_2-2-Me-$C_2B_{10}H_{10}$	73	50	0	0	27	50
1-$P(OEt)_2$-2-Me-$C_2B_{10}H_{10}$	0	0	20	40	80	60
1-PPh_2-2-Me-$C_2B_{10}H_{10}$	0	0	1	10	99	90
1-PPh_2-$C_2B_{10}H_{11}$	0	0	7	27	93	73
2,2'-PPh(1-Me-$C_2B_{10}H_{10})_2$	50	50	0	0	50	50
1,2-$(PEt_2)_2$-$C_2B_{10}H_{10}$	0	0	66	66	33	34
1,2-$(P^iPr_2)_2$-$C_2B_{10}H_{10}$	8	90	3	2	70*	8
1,2-$[(POEt)_2]_2$-$C_2B_{10}H_{10}$	23	0	7	80	64*	20
1,2-$(PPh_2)_2$-$C_2B_{10}H_{10}$	0	0	1	1	99	99
$(PPh$-$C_2B_{10}H_{10})_2$	0	0	0	1	100	99

A – (*closo*-carboranylphosphine:piperidine=1:50) in toluene, 24 h

B – (*closo*-carboranylphosphine:piperidine=1:10) in ethanol, 16 h

* the difference until 100% is cluster decomposition

Table 2.2. Comparison of degradation conditions for carboranyl-phosphines.

degradation reaction of *closo*-carboranylmonophosphines with piperidine in ethanol is successful is based on the fact that piperidine is a secondary amine, a possible nucleophile and a base, that establishes an acid/base equilibrium with ethanol. Piperidinium ethoxide is present in a minor amount in the reaction medium, much less than is required for a quick degradation but sufficient enough amount to slowly and smoothly produce $B(OEt)_3$. The low $[EtO]^-$ concentration produces mild conditions that prevent the C_C-P hydrolysis.

2.2.2. Oxidation of *nido*-carboranylphosphines

Our group was the first to inquire on the oxidation process of the *nido*-carboranylphsphines. The oxidation of the *nido*-carboranylphosphines can be easily forced by reaction with hydrogen peroxide in acetone, although it can also be achieved by the prolonged contact between a solution of *nido*-carboranylphosphines in acetone and air.[65] The oxidized *nido*-carboranyldiphosphines can also be obtained by the prolonged reaction of *closo*-carboranyldiphosphines with hydrogen peroxide in THF, where, given the necessary chemical and geometrical arrangements to produce proton chelation, the proton can also induce conversion of the *closo* specie to *nido* (Scheme 2.12.).[66]

Scheme 2.12. Oxidation of carboranyl-phosphines with hydrogen peroxide.

Although some work was done on the oxidation of the *nido*-carboranylphosphine, no further studies were done to understand the oxidation process and to assess the strength of the P=O···H^+···O=P bonds. As can be seen in Results and Discussion (Section 2), another objective of this work was the study of this process.

Derivatives of the *nido*-carboranylmonophosphines with tetravalent phosphorus were also obtained, by the prolonged reaction of the *closo*-carboranylmonophosphines adducts with iodine in ethanol.[67] As showed previously, the *closo*-carboranylmonophosphines form different adducts with iodine in chloroform or toluene, depending on the moiety bonded to phosphorus. The compounds that have alkyl moieties form either the "spoke" adduct, (carboranyl)R_2P-I-I or the ionic [(carboranyl)R_2PI]$^+$I$^-$ species, whereas the ones that have aryls moieties, produce the encapsulated (carboranyl)R_2P···I-I···PR_2(carboranyl) motif. These differences account for the formation of the *nido* species. The derivatives with alkyls moieties do yield the *nido* derivatives upon prolonged time in ethanol, whereas the ones with aryls moieties do not produce the *nido* derivatives (Scheme 2.13.).

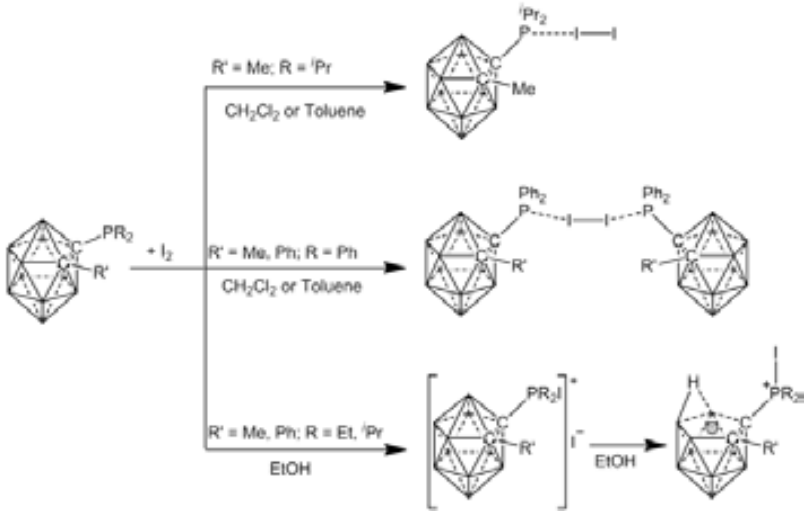

Scheme 2.13. Reaction of carboranyl-phosphines with iodine.

Another type of *nido* derivatives with tetravalent phosphorus were also obtained from *closo* derivatives by HCl promoted cleavage of the C_C-C_C bond.[68] It was observed that the addition of HCl to 1-P^{t}Bu$_2$-2-PEt$_2$-1,2-*colso*-$C_2B_{10}H_{10}$ give rapid and quantitatively, a zwitterionic *nido* 12-vertex specie, which can be reconverted to the trivalent phosphorus *closo* species by reaction with triethylamine.

2.2.3. Metal complexes with *nido*-carboranylphosphines

The discovery of the complexation induced degradation of *closo*-carboranylphosphines and the direct degradation and subsequent complexation opened the door to the research in this field yielding organometallic complexes with very interesting properties. Is difficult to make a systematic of the metal complexes found in the literature since not for all the metals these types of complexes has been studied. Our group focused mainly on the most employed metals in catalysis that are Pd, Rh and Ru, and the group of Professor Laguna on the Au and Ag complexes, although less investigation can be found in the literature for other metals.

The copper (I) complex incorporating the anionic [7,8-(PPh$_2$)$_2$-7,8-*nido*-$C_2B_9H_{10}$]$^-$ ligand was the first type of this complex synthesized directly from the 1,2-(PPh$_2$)$_2$-1,2-*closo*-$C_2B_{10}H_{10}$ compound in reaction with [CuCl(PPh$_3$)$_2$] in ethanol.[57] This complex was found to be extremely stable, and the reactive location is the fourth metal coordination site. Thus, the acetone adduct is obtained upon dissolution in acetone, or the chloro

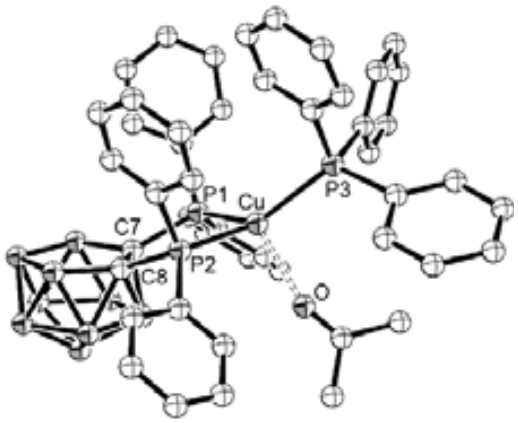

Figure 2.6. Crystal structure of [Cu(PPh$_3$){7,8-(PPh$_2$)$_2$-7,8-$C_2B_9H_{10}$}]·Me$_2$CO (H atoms are omitted for clarity).

complex is obtained upon treatment with NMe_4Cl. In any case the chelating carboranylphosphine ligand is maintained together with a PPh_3 moiety, the X-ray structure of the acetone adduct (Figure 2.6.) revealing the copper ion in a distorted tetrahedral environment. The same reaction carried out with 1-PPh_2-2-SBz-1,2-*closo*-$C_2B_{10}H_{10}$ yields [Cu(7-PPh_2-8-SBz-7,8-*nido*-$C_2B_9H_{10}$)] and the ligand acts as bidentate. Interestingly, the reaction of [AuCl(PPh_3)] with [7-PPh_2-8-SBz-7,8-*nido*-$C_2B_9H_{10}$]$^-$ yields [Au(7-PPh_2-8-SBz-7,8-*nido*-$C_2B_9H_{10}$)(PPh_3)] but the ligand acts as monodentate, the Au atom being bonded only to the phosphorus moiety (Figure 2.7.).[59c]

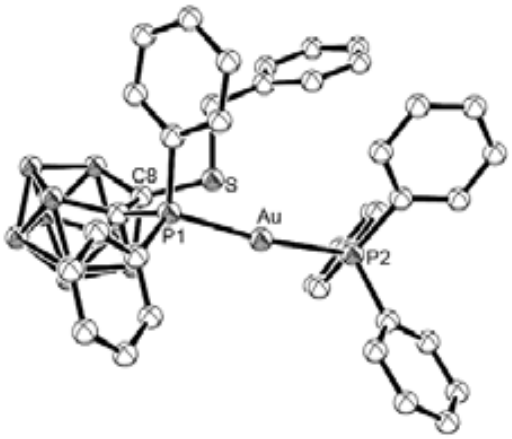

Figure 2.7. Crystal structure of [Au(PPh_3){7-PPh_2-8-SCH_2Ph-7,8-$C_2B_9H_{10}$}] (H atoms are omitted for clarity).

The carboranyldiphosphines act as chelating ligands for Au(I) and Ag(I) and trigonal compounds were two coordination sites are occupied by the carboranyl-diphosphine and the third by other ligands can be obtained. The strong chelating ability of *nido*-carboranyldiphosphines is evidenced when other chelating ligands as bis(diphenylthio-phosphoryl)methane (dppsm), 1,10-phenanthroline (phen), 1,2-bis(diphenyl-phosphino)ethane (dppe) or 1,3-bis(di-phenylphosphino)propane (dppp) are employed in the reactions. Both for Au(I) and Ag(I) the *nido*-carboranyldiphosphines act as chelating ligands, whereas the other chelating ligands employed act different depending on the metal. In the case of Au(I) they act as bridge forming dinuclear complexes where each Au atom is chelated by *nido*-carboranyldiphosphine ligand,[69] whereas for Ag(I), mononuclear complexes are obtained where the metal accommodates the other chelating ligand,[70] changing the metal environment form trigonal to tetrahedral. The versatility of these ligands can be further observed for a Au(I) dinuclear complex. If the trigonal complex [Au(PPh_3)(7,8-(PPh_2)$_2$-7,8-*nido*-$C_2B_9H_{10}$][71] is reacted with NaH, the apical hidrogen atom from the C_2B_3 open face is lost, and subsequent reaction with [Au(PPh_3)(tht)]ClO_4 gives [Au_2{PPh_2)$_2C_2B_9H_9$}-(PPh_3)$_2$]. In this compound one $AuPPh_3^+$ fragment has a *exo-nido* coordination to the phosphorus atoms, and the other has an η^5-coordination to the open C_2B_3 face.

The Au(III) complexes were also prepared by the reaction of 1,2-PR_2-1,2-*closo*-$C_2B_{10}H_{10}$ (R=^{i}Pr, Ph) with $HAuCl_4$ in ethanol, yielding *cis* square-planar complexes [$AuCl_2$(7,8-PR_2-7,8-*nido*-$C_2B_9H_{10}$)].[59b,72]

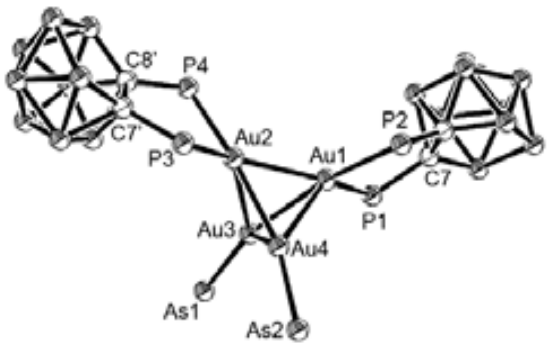

Figure 2.8. Crystal structure of [Au_4-{7,8-(PPh_2)$_2$-7,8-*nido*-$C_2B_9H_{10}$}$_2$($AsPh_3$)$_2$] (H atoms and the Ph groups are omitted for clarity).

The *nido*-carboranylphosphine ligands are also attractive in coordination chemistry of gold because they can stabilize new and unexpected products, which cannot be reached employing other ligands. This is the case of the of the tetranuclear gold clusters co-stabilized by arsane ligands. The reaction of 1,2-(PPh_2)$_2$-1,2-*closo*-1,2-$C_2B_{10}H_{10}$ with [AuCl($AsPh_3$)] in a 1:2 ratio, yielded the unexpected [Au_4-{7,8-(PPh_2)$_2$-7,8-*nido*-$C_2B_9H_{10}$}$_2$($AsPh_3$)$_2$] (Figure 2.8).[73]

In the reaction of $Me_4N[7,8\text{-}PPh_2\text{-}7,8\text{-}nido\text{-}C_2B_9H_{10}]$ with $[Rh_2\text{-}(\mu\text{-}Cl)_2(cod)_2]$ the displacement of the diolefinic ligand from the starting Rh complex takes place, yielding $[Rh\{7,8\text{-}PPh_2\text{-}7,8\text{-}nido\text{-}C_2B_9H_{10}\}(cod)]$.[61] This product turned to be a versatile starting compound for the synthesis of a plethora of Rh complexes incorporating the anionic $[7,8\text{-}PPh_2\text{-}7,8\text{-}nido\text{-}C_2B_9H_{10}]^-$ ligand (Scheme 2.14) first by replacing the diolefinic ligand by CO and second by P-donor or N-donor ligands. It has not been possible to prepare the complex analogous to Wilkinson's catalyst by direct substitution of Cl^- and PPh_3 by the anionic diphosphine $[7,8\text{-}(PPh_2)_2\text{-}7,8\text{-}nido\text{-}C_2B_9H_{10}]^-$. The steric hindrance may not allow the formation of $[Rh\{7,8\text{-}(PPh_2)_2\text{-}7,8\text{-}nido\text{-}C_2B_9H_{10}\}(PPh_3)_2]$, although the analogous *exo*-dithiocarborane complexes are well-known.[74] The *nido*-carboranylmonophosphines yielded with Rh(I) very interesting results that are very important from the catalytically point of view. When $[RhCl(PPh_3)_3]$ was reacted with $[7\text{-}PR_2\text{-}8\text{-}R'\text{-}7,8\text{-}nido\text{-}C_2B_9H_{10}]^-$ (R= Ph, R'= H, Me, Ph; R = Et, R'= Me, Ph; R= iPr, R'= Me)[75] the square-planar Rh(I) derivatives were obtained, where the carboranylmonophosphine acts as a bidentate ligands, with one coordination through the PPh_2 moiety and the other through a B-H group (Scheme 2.15.). When the starting rhodium complex was changed from Wilkinson's catalyist to the olefinic, $[Rh_2\text{-}(\mu\text{-}Cl)_2(cod)_2]$ complex, the carboranyl-monophosphines $[7\text{-}PR_2\text{-}8\text{-}R'\text{-}7,8\text{-}nido\text{-}C_2B_9H_{10}]^-$ (R= Ph, R' = H, Me) turned to be a tridentate ligand.[76]

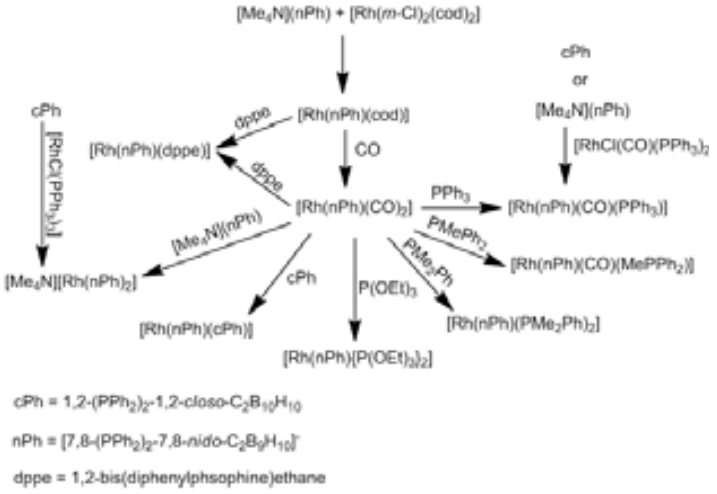

Scheme 2.14. Synthesis of Rh(I) complexes with *nido*-carboranyl-phsphine ligands.

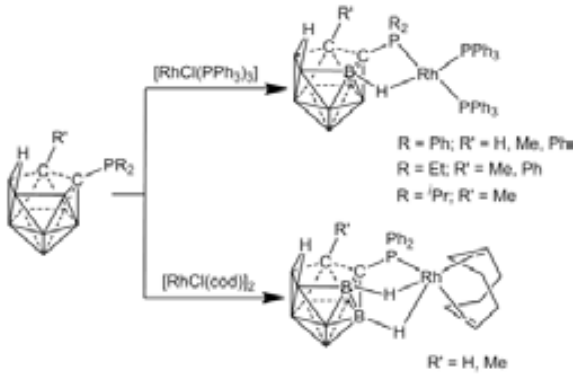

Scheme 2.15. Reaction of *nido*-carboranylphosphines with Rh(I) complexes.

Recently, Rh(III) and Ir(III) complexes were prepared starting from the heterodisubstituted derivative, $1\text{-}PPh_2\text{-}2LiS\text{-}1,2\text{-}closo\text{-}C_2B_{10}H_{10}$.[13] The reaction of this ligand with $[Cp^*MCl(\mu\text{-}Cl)]_2$ (M= Rh, Ir) in methanol in presence of AgOTf yield the 16-electron *closo* derivative, $[M(Cp^*)(1\text{-}PPh_2\text{-}2\text{-}S\text{-}1,2\text{-}closo\text{-}C_2B_{10}H_{10}][OTf]$, which can be converted to the zwitterionic *nido* specie by reaction with pyrazine in methanol. Surprisingly, during the degradation process a methoxy group is inserted in the B(3) position. The carboranylmonophosphine, $1\text{-}PPh_2\text{-}1,2\text{-}closo\text{-}C_2B_{10}H_{11}$, was proved to be an attractive ligand for the synthesis of different complexes of Rh(III) and Ir(III), only by changing slightly the reaction conditions (Scheme 2.16.).[77] Treating $1\text{-}PPh_2\text{-}1,2\text{-}closo\text{-}C_2B_{10}H_{11}$ with dimmeric complex $[Cp^*IrCl(\mu\text{-}Cl)]_2$ under a dihydrogen atmosphere, the metal–hydride complex $[Cp^*Ir(H)(7\text{-}PPh_2\text{-}7,8\text{-}C_2B_9H_{11})]$ was obtained, where the carboranylmonophosphine acts as a bidentate ligand through the PPh_2 moiety and a B-H group.

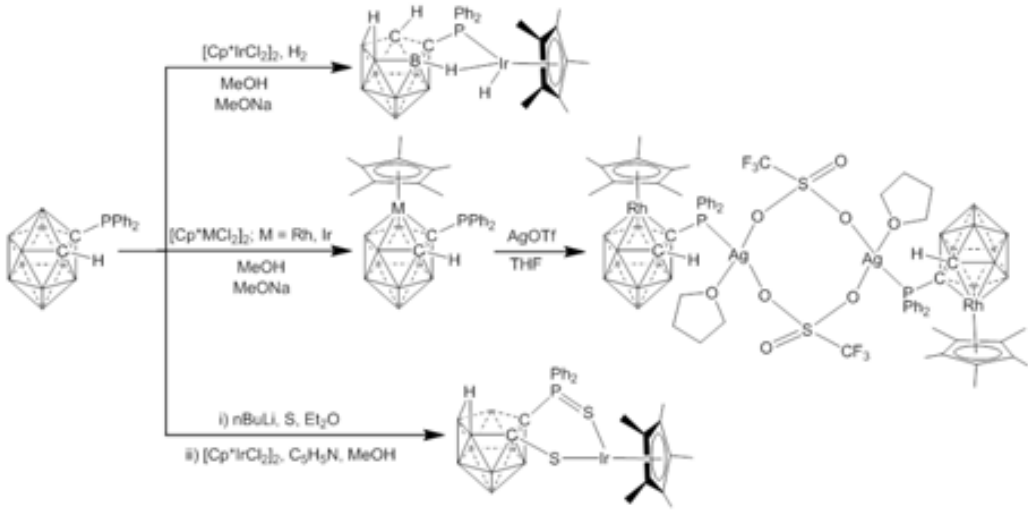

Scheme 2.16. Complexes with Rh(III) and Ir(III) with *nido*-carboranylphosphines.

Interestingly, if the dihydrogen atmosphere is removed, an boron vertex is substituted by the metal, yielding the half-dicarbollide metalocene, [1-PPh_2-3-(η^5-Cp*)-3,1,2-$MC_2B_9H_{10}$], in which the PPh_2 moiety is innocent towards coordination. The addition of AgOTf over this metallocene produce the coordination of the PPh_2 to the Ag(I). Employing the same conditions as above and changing the base from sodium methoxide to pyridine and adding two equivalents of elemental sulfur to the reaction mixture, afforded the complex [Cp*Ir{7-(S)PPh_2-8-S-7,8-*ndio*-$C_2B_9H_{10}$}], in which the P(III) centre was oxidized to P(V) and the second carbon atom from the carborane was functionalized with a thiol moiety. The metal is coordinated in this compound by the two sulfur centers, which are not chemically equivalent. The η^5-bonding ability of the carboranylmonophosphines described above was also observed before for Rh and Ru.[78]

The reaction of [7-PPh_2-8-Me-*nido*-7,8-$C_2B_9H_{10}$]$^-$ with $RuCl_3 \cdot nH_2O$ in a 2:1 ratio in ethanol yielded in very low yield a specie that have two carborane cages, namely, [Ru(7-PPh_2-8-Me-*nido*-7,8-$C_2B_9H_{10}$)$_2$].[79] The low yield was attributed to the consumption of the phosphine ligand during the reduction of the Ru(III) to Ru(II). In order to overcome the low yield of the previous synthesis, the [$RuCl_2(DMSO)_4$] was used as source of Ru(II). A series of the compounds of type [RuCl(7-PR_2-8-Me-*nido*-7,8-$C_2B_9H_{10}$)(PPh_3)$_2$] (R = Et, Ph) [RuX(7-PPh_2-8-R'-*nido*-7,8-$C_2B_9H_{10}$)(PPh_3)$_2$] (X=Cl, H and R' = H, Ph) and [RuX(7-PPh_2-8-Me-*nido*-7,8-$C_2B_9H_{10}$)(L)(PPh_3)] (L = EtOH, tht, CO) were prepared[80] and a modulation of the B(11)-H→Ru and B(2)-H→Ru resonances was observed.

The first complex of Pd that incorporates a *nido*- arboranylphosphine was reported by our group some years ago, though the clomplex was obtained from *closo*-carboranylphosphines.[81] Later, we reported complexes of Pd synthesized directly from *nido*-carboranylmonophosphines, for which we

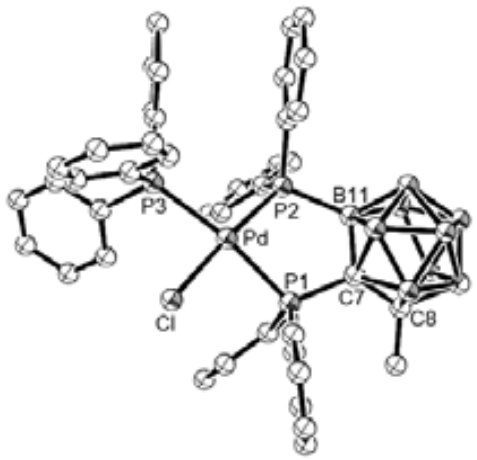

Figure 2.9. Crystal structure of [PdCl(7-PPh_2-8-Me-11-PPh_2-7,8-*nido*-$C_2B_9H_9$)(PPh_3)] (H atoms are omitted for clarity).

observed that the reaction of $[NMe_4][7\text{-}PPh_2\text{-}8\text{-}R\text{-}7,8\text{-}nido\text{-}C_2B_9H_{10}]$ (R = H, Me, Ph) with *cis*-$[PdCl_2(PPh_3)_2]$ in degassed ethanol lead to the formation of an unexpected product, where a B-H vertex is activated and the H is substituted by a PPh_2 moiety, forming the first example of a chelating $R_2P\text{-}C\text{-}B\text{-}PR_2$ diphosphine.[82] The crystal structure (Figure 2.9.) of $[PdCl(7\text{-}PPh_2\text{-}8\text{-}Me\text{-}11\text{-}PPh_2\text{-}7,8\text{-}nido\text{-}C_2B_9H_9)(PPh_3)]$ revealed the bidentate nature of the carborane cage and the formation of B(11)-P bond.

Group 10 complexes containing $[7,8\text{-}(PPh_2)_2\text{-}7,8\text{-}nido\text{-}C_2B_9H_{10}]^-$ with similar formula $[MCl(7,8\text{-}(PPh_2)_2\text{-}7,8\text{-}nido\text{-}C_2B_9H_{10})(PPh_3)]$ (M = Ni, Pd, Pt) were synthesized starting from the $1,2\text{-}(PPh_2)_2\text{-}1,2\text{-}closo\text{-}C_2B_{10}H_{10}$ in ethanol with $[MCl_2(PPh_3)_2]$ as metal source.[83] When the starting source of the metal was changed to correspondent chloride, namely $PdCl_2$ or $NiCl_2{\cdot}6H_2O$, binuclear species were obtained, with the formula $[M_2(\mu\text{-}Cl)_2\{7,8\text{-}(PPh_2)_2\text{-}7,8\text{-}nido\text{-}C_2B_9H_{10}\}_2]$ (M = Pd, Ni).[84] Complexes with the same stoichiometry, where Pd bonded to $[7,8\text{-}(PR_2)_2\text{-}7,8\text{-}nido\text{-}C_2B_9H_{10}]^-$ (R= ^{i}Pr, OEt) forms also chloro bridges, were also reported by us before.[81] The metal induced degradation of *closo*-carboranylphosphines in nucleophilic solvents was presented above, but it is worth mentioning that complexes of *nido*-carboranylphosphines with nickel were recently obtained directly from the *closo*-carboranyl-phosphines with metallic salts in less nucleophilic solvents as dichloromethane (CH_2Cl_2), but under solvothermal conditions.[85] Also, binuclear Pd and Pt *nido* complexes are obtained from the decomposition of *closo* complexes in toluene or dichloromethane at room temperature for several weeks.[86]

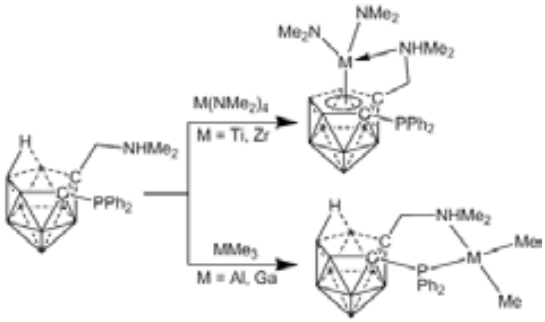

Scheme 2.17. Sythesis of Group 4 and Group 13 metal complexes with *nido*-carboranylphosphines.

Different metal complexes were obtained in the reaction of zwitterionic $[7\text{-}NHMe_2(CH_2)\text{-}8\text{-}PPh_2\text{-}7,8\text{-}nido\text{-}C_2B_9H_{10}]$ with Group 4 (Ti, Zr) and Group 13 (Al, Ga) metallic complexes[87] in toluene (Scheme 2.17.). The Ti and Zr give π,σ-complexes coordinated to the carborane derivative, being π-bound to the C_2B_3 open face and the N-donor moiety being coordinated to the metal in a strain-free manner. The PPh_2 moiety plays no role in the coordination. On the other hand, Al and Ga yield σ,σ-complexes, where the metal is coordinated to both P-donor and N-donor moieties.

2.3. Applications of carboranylphosphines and P-containing boron compounds

The phosphines are notorious ligands in coordination chemistry and present a special interest in catalysis.[88] As it could not be otherwise, the metal complexes with carboranylphosphines were also studied for their potential use as catalysts for different reactions. Phosphorus-substituted at the C_C atoms of carboranes were found useful ligands for metal complexes which catalyze 12 different synthetic processes as: hydrogenation, hydroformylation, hydrosilylation, carbonylation, amination, alkylation and sulfonylation, Kharasch reaction, polymerization, ring-opening metathesis polymerization, cyclopropanation, cross-coupling with Grignard reagents, and finally, Sonogashira coupling with hydride transfer.[88c] Although the report of the use in different catalytic processes is found in the literature, still a large number of carboranylphosphines has yet to be tested for their catalytic activity. The *closo*- and *nido*- structures and the wide range of possibility of coordination of the metals to the carborane cluster offers a broad spectrum of customization of the ligands and permit the synthesis of "on demand" tailored metal complexes.

Another future application of the carboranylphosphines is based on the exploitation of the photoluminescence properties of *nido*-carboranylphosphines ligands when bound within trigonal-planar Au complexes.[89] These complexes are long known but their actual application in OLEDs is still to be tested.

Phosphorus-containing boron compounds are also interesting in medicine, where they found especially application for the treatment of bone cancer due to their capability of targeting calcium-rich tumor tissue.[90] Besides their use for cancer treatment in BNCT, carboranyl phosphonates are known as highly bioactive compounds, showing high anticholinesterase activity and bactericidal activity.

3. Carborane derivatives with nitrogen moieties

Derivatives of carborane with C_C-N bonds, which could be directly synthesized from *o*-carborane, are rare and were generally achieved by reaction with nitrosyl chloride to generate C-nitroso compounds,[91] which are used to generate hydroxyl-amines.[52e] Various compounds with direct C_C-N bonds were synthesized and their application was directed towards biomedical applications.[92]

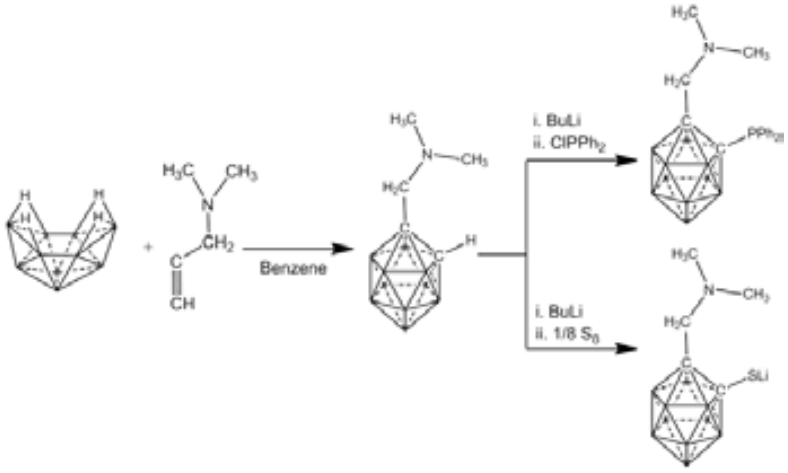

Scheme 3.1. Synthesis of N,P- and N,S-chelating dimethylamino-carborane derivatives.

Interest to the organometallic chemistry was directed towards other compounds, which have the N atom not directly bonded to the C_C, but with another C atom as spacer. These compounds were synthesized either from decaborane, $B_{10}H_{14}$ or from C-metalated-*o*-carborane. One of the first reported compounds was *o*-carboranylamine, [1-$(CH_2)N(CH_3)_2$-$C_2B_{10}H_{11}$], which was synthesized from $B_{10}H_{14}$.[93] Although it was obtained with an yield of 50%, it was used as platform for the synthesis of different *o*-carboranylaminophosphine[16, 94] or *o*-carboranylaminothiolate[95] ligands (Scheme 3.1.).

Carboranylpyridine derivatives were also described in the literature[96] and its preliminary study as ligand was reported in the literature,[97] despite its low synthesis yield.[98] As the pyridine ligand is very interesting from the coordination point of view we turned our attention on this compounds in this work

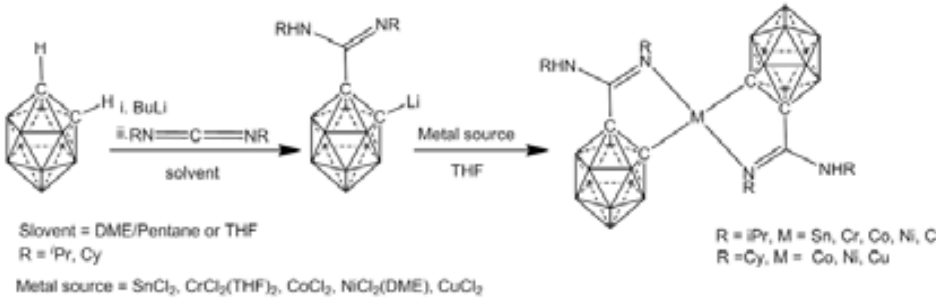

Scheme 3.2. Synthesis of carboranylamidinates and its organometallic complexes.

and developed a very efficient way of synthesis, which, as can be seen in the Results and Discussion (Section 4), permits the synthesis of new and unprecedented ligands.

Also, picolyl-carborane derivatives were prepared, where the ligands act as C,N- and N, S-chelating ligands. Also, half-sandwich complexes with Ir, Rh and Ru were prepared from this derivatives.[99] The Ir complex was proved to exhibit activity towards polymerization of ethylene. Just recently, carboranylamidinates were reported via the reaction of C-lithiated *o*-carborane with N,N'-dialkylcarbo-diimides[100a] and were proved to be good ligands for different main group (Li, Sn) and transition metals (Co, Ni, Cu, Cr) (Scheme 3.2.).[100]

4. "Space confined" polycarborane derivatives

The "space confined" carborane derivatives are the compounds which present different number of carborane cages bonded to one or two atoms very close one to each other, with the scope to obtain an elevated number of boron atoms per molecular unit.

Though few examples exist in the literature, the synthesis of these compounds is done in the reaction of C-metalated carborane derivatives with halides. The derivative of methyl-*o*-carborane which has two carborane cages was synthesized from C-lithiated carborane, either with diphenylboron chloride or with chloro-diphenylphosphine (Scheme 4.1.).[60b,101] With Group 14 (Si, Ge, Sn) halides, two-cage derivatives were obtained (Scheme 4.2.).[102]

Bis(phosphino)- and bis(arsino)carborane derivatives are easily generated from lithiated derivatives or their -CH_2MgX counterparts.[4,6,8,103] Bis(amino)carborane derivatives was obtained by the reaction of lithiated derivatives with nitrosyl chloride.[104] Tris-carborane derivatives with elements from Group 15, were reported by the reaction of lithiated carborane with trichlorides.[6,105] Also, the related tris(*o*-carboranylmethyl)-phosphine is similarly prepared.[106] In the reaction of chlorobis(carboranylmethyl)phosphine, $ClP(1\text{-}CH_2\text{-}1,2\text{-}C_2B_{10}H_{11})_2$, with 1-Me-2-Li-1,2-$C_2B_{10}H_{10}$ the five-cage specie was isolated as a minor product and was characterized by X-ray diffraction (Figure 4.1.).[107]

With chalcogens (S, Se and Te), various derivatives were synthesized by the reaction of lithiated carborane to yield carborane derivatives where two carborane cages are liked by chalcogens bridges (Scheme 4.3.).[108] The reaction of disulphide

Scheme 4.1. Synthesis of two-cage derivatives of carborane with boron and phosphorus.

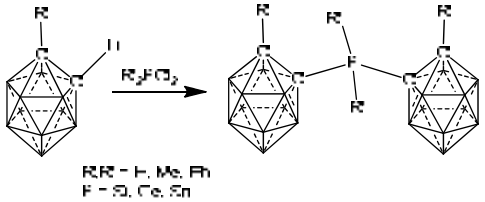

Scheme 4.2. Synthesis of two-cage derivatives of carborane with Group 14 metals.

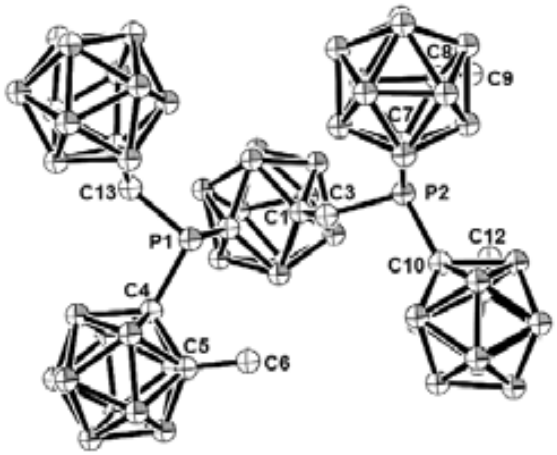

Figure 4.1. Five-cage phosphorus derivative of carborane

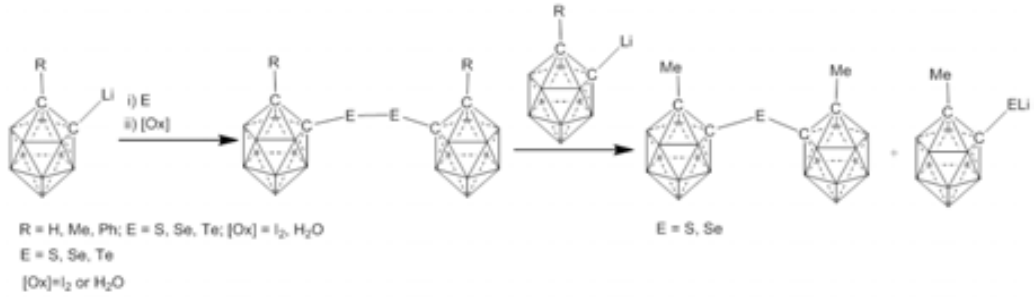

Scheme 4.3. Synthesis of two-cage derivatives of of carborane with chalcogens.

or diselenide derivatives with C-lithiated carborane, yield the two-cage thioether derivative and the two-cage selenide derivative, respectively (Scheme 4.3.).[109] The two-cage thioether derivative can be also obtained from the reaction of bromosulfenyl specie with monolithiated carborane.[108a]

Derivatives where the C atom is the central atom were not found in the literature, though the carbon atom is the most customizable one. For that we proposed in this work to study the possibility of synthesizing "star-shape" molecules like the ones presented above, but with the carbon atom as centre.

5. Objectives and justification of the thesis

It is clear from the brief review presented above that the chemistry of the carborane derivatives with electron rich moieties is still a hot topic. Though the derivatives with phosphorus moieties were the most studied synthetically and some of their properties were exploited, still work has to be done to understand their electronic properties that may ultimate lead to a rationalized design of new derivatives.

As the title of the thesis reveal, the main objective of this work is to synthesize and study new derivatives of *o*-carborane with electron rich moieties. The most applied reaction for the synthesis of new derivatives of *o*-carborane is the direct reaction of the lithiated salts of carborane with electrophiles. The synthesis of C_C-monosubstituted derivatives is important in several applications. For that, the first specific objective of this work was to get at the bottom of this reaction, tiring to understand both experimentally and computationally how it works, in order to control the monolithiation.

As presented above, though the carboranylphosphines are known for more than 50 years ago, no systematic and comprehensive investigation on their oxidation reactions were found in the literature as well as investigations on the electronic properties of these phosphines. For that the second specific objective was the study of the oxidation of carboranylphsophines with hydrogen proxide, sulphur and selenium and the study of their properties as ligands. Once the synthetic study on the carboranylphsophines and their oxides and chalcogenides was completed we proceded with the computational study of the carboranylphosphines and their oxides and chalcogenides.

Though the carboranylformadehyde is long known in the literature, studies on its reactivity are rare. For that, the fourth objective was to understand the reactivity carboranylformaldehyde as platform for new derivatives. For that we plan to study: i) the nucleophilic addition to the carbonyl group with lithated carborane in order to synthesize "confined space" multi-cage compounds; ii) the electrophilic substitution reactions with aromatic substrates in order to obtain derivatives with luminescent properties; and iii) the Wittig and Horner-Wadaworth-Emmons reaction using carboranylformaldehyde and carborane containing phosphonates and phsophonium salts.

The fourth specific objective was the study of carboranylpyridine as platform for new derivatives, for which we studied: i) the metalation reaction of carboranylpyridine; ii) synthesis of

carboranylpyridine-phosphine hybrid ligands; iii) synthesis of carboranylpyridine-borane derivative and iv) synthesis of cobalta(bisdicarbollide)-pyridine derivative.

References

[1] Grimes, R. N. *Carboranes*. 2nd Ed. Elsevier. **2011**.

[2] Scholz, M.; Hey-Hawkins, E. *Chem. Rev.*, **2011**, *111*, 7035.

[3] a) Hermansson, K.; Wójcik, M.; Sjöberg, S. *Inorg. Chem.*, **1999**, *38*, 6039. b) F. Teixidor, G. Barberà, A. Vaca, R. Kivekäs, R. Sillanpää, J. Oliva, C. Viñas, *J. Am. Chem. Soc.*, **2005**, *127*, 10158. c) Puga, A. V.; Teixidor, F.; SillanpäÄ, R.; Kivekäs, R.; Arca, M.; Barberà, G.; Viñas, C. *Chem. Eur. J.*, **2009**, *15*, 9755. d) Oliva, J. M.; Schleyer, P. v.R.; Aullon, G.; Burgos, J. I.; Fernandez-Barbero, A.; Alkorta, I. *Phys. Chem. Chem. Phys.*, **2010**, *12*, 5101.

[4] Alexander, R. P.; Schroeder, H. *Inorg. Chem.*, **1963,** *2*, 1107.

[5] Alexander, R. P.; Schroeder, H. *U.S. Patent*, **1963**, *Ser. No. 323*, 394.

[6] Zakharkin, L. I.; Bregadze, V. I.; Okhlobystin, O. Yu. *J. Organomet. Chem.*, **1965**, *4*, 211.

[7] Zakharkin, L. I.; Kazantsev, A. V.; Zhubekova, M. N. *Izv. Akad. Nauk SSSR, Ser. Khim.*, **1969**, *9*, 2056; *Bull. Acad. Sci. USSR, Div. Chem.*, **1969**, *18*, 1910.

[8] Kazantsev, A. V.; Zhubekova, M. N.; Zakharkin, L. I. *Zh. Obshch. Khim.,* **1971**, *41*, 2027.

[9] Balema, V. P.; Pink, M.; Sieler, J.; Hey-Hawkins, E.; Hennig, L. *Polyhedron*, **1998**, *17*, 2087.

[10] Kreienbrink, A.; Sárosi, M. B., Rys, E. G.; Lönnecke, P.; Hey-Hawkins, E. *Angew. Chem. Int. Ed.*, **2011**, *50*, 4701.

[11] Zakharkin, L. I.; Grebennikov, A. V.; Kazantzev, A. V. *Izv. Akad. Nauk SSSR, Ser. Khim*, **1967**, 2077; *Bull. Acad. Sci. USSR, Div. Chem. Sci.,* **1967**, *16*, 1994.

[12] Viñas, C.; Benakki, R.; Teixidor, F.; Casabo, J. *Inorg. Chem.*, **1995**, 34, 3844.

[13] Huo, X.K.; Su, G.; Jin, G.X. *Dalton Trans.*, **2010**, 1954.

[14] Teixidor, F.; Viñas, C.; Benakki, R.; Kivekäs, R.; Sillanpää, R. *Inorg. Chem.*, **1997**, 36, 1719.

[15] Lee, Y.J.; Bae, J.-Y.; Kim, S.J.; Ko, J.; Choi, M.-G.; Kang, S.O. *Organometallics*, **2000**, *19*, 5546.

[16] Lee, H.-S.; Bae, J.-Y.; Ko, J.; Kang, Y. S.; Kim, H. S.; Kim, S.-J.; Chung, J.-H.; Kang, S. O. *J. Organomet. Chem.*, **2000**, *614–615*, 83.

[17] DuMont, W. W.; Bätcher, M.; Pohl, S.; Saak, W. *Angew. Chem. Int. Ed.*, **1987**, *26*, 912.

[18] a) Teixidor, F.; Núñez, R.; Viñas, C.; Sillanpää, R.; Kivekäs, R. *Angew. Chem. Int Ed.*, **2000**, *39*, 4290. b) Núñez, R.; Farràs, P.; Teixidor, F.; Viñas, C.; Sillanpää, R.; Kivekäs, R. *Angew. Chem. Int Ed.*, **2006**, *45*, 1270.

[19] Bolhuis, F.; van Koster, P. B.; Migchelsen, T.; *Acta Crystallogr.*, **1967**, *23*, 90.

[20] Ioppolo, J. A.; Clegg, J. K.; Rendina, L. M. *Dalton Trans.* **2007**, 1982.

[21] Zakharkin, L. I.; Zhubekova, M. N.; Kazantsev, A. V. *Zh. Obshch. Khim.*, **1971**, *41*, 588.

[22] Godovikov, N. N.; Degtyarev, A. N.; Bregadze, V. I.; Kabachnik, M. I. *Izv. Akad. Nauk SSSR, Ser. Khim.*, **1975**, *12*, 2797.

[23] Degtyarev, A. N.; Godovikov, N. N.; Bregadze, V. I.; Kabachnik, M. I. *Izv. Akad. Nauk SSSR, Ser. Khim.*, **1973**, *10*, 2369; *Bull. Acad. Sci. USSR, Div. Chem.*, **1973**, *22*, 2314.

[24] Zakharkin, L. I.; Zhubekova, M. N.; Kazantsev, A. V. *Zh. Obshch. Khim.*, **1972**, *42*, 1024.

[25] Balema, P. V.; Pink, M.; Sieler, J.; Hey-Hawkins, E.; Hennig, L. *Polyhedron*, **1998**, *17*, 2087.

[26] Balema, P. V.; Blaurock, S.; Hey-Hawkins, E. *Polyhedron*, **1999**, *18*, 545.

[27] a) Lee, J. D.; Kim, B. Y.; Lee, C. M.; Lee, Y. J.; Ko, J. J.; Kang, S. O. *B. Kor. Chem. Soc.*, **2004**, *25*, 1012. b) Wang, H.; Chan, H. S.; Xie, Z. *Organometallics*, **2006**, *25*, 2569. c) Dou, J.; Zhang, D.; Li, D.; Wang, D. *Eur. J. Inorg. Chem.*, **2007**, 53. d) Wang, H.; Shen, H.; Chan, H. S.; Xie, Z. *Organometallics*, **2008**, *27*, 3964.

[28] a) Smith, H. D. *J. Am. Chem. Soc.*, **1965**, *87*, 1817. b) Röhrscheid, F.; Holm, R. H. *J. Organomet. Chem.*, **1965**, *4*, 335. c) Zakharkin, L. I.; Zhigareva, G. G. *Rus. Chem. Bull.*, **1965**, *14*, 905. d) Zakharkin, L. I.; Zhigareva, G. G. *Zh. Obshch. Khim.*, **1967**, *37*, 1791.

[29] Hill, W. E.; Rackley, B. G.; Silva-Trivino, L. M. *Inorg. Chim. Acta*, **1983**, *75*, 51.

[30] Manojlovic-Muir, L.; Muir, K. W.; Solomun, T. *J. Chem. Soc., Dalton Trans.*, **1980**, 317.

[31] a) Kalinin, V. N.; Usatov, A. V.; Zakharkin, L. I. *J. Organomet. Chem.*, **1983**, *254*, 127. b) Ryabov, A. D.; Eliseev, A. V.; Sergeyenko, E. S.; Usatov, A. V.; Zakharkin, L. I.; Kalinin, V. N. *Polyhedron*, **1989**, *12*, 1485. c) Ryabov, A. D.; Usatov, A. V.; Kalinin, V. N.; Zakharkin. L. I. *Izv. Akad. Nauk. SSSR Ser. Khim.*, **1986**, *12*, 2790.

[32] a) Paavola, S.; Kivekäs, R.; Teixidor, F.; Viñas, C. *J. Organomet. Chem.*, **2000**, *606*, 183. b) Paavola, S.; Teixidor, F.; Viñas, C.; Kivekäs, R. *J. Organomet. Chem.*, **2002**, *645*, 39. c) Paavola, S.; Teixidor, F.; Viñas, C.; Kivekäs, R. *J. Organomet. Chem.*, **2002**, *657*, 187. d) Sundberg, M. R.; Paavola, S.; Viñas, C.; Teixidor, F.; Uggla, R.; Kivekäs, R. *Inorg. Cheim. Acta*, **2005**, *358*, 2107.

[33] a) Lee, T.; Kim, S.; Kong, M. S.; Kang, S. O.; Ko, J. *B. Kor. Chem. Soc.*, **2002**, *23*, 845. b) Lee, Y.; Lee, J; Kim, S. Keum, S.; Ko, J.; Suh, I.; Cheong, M.; Kang, S. O. *Organometallics*, **2003**, *23*, 203.

[34] Hill, W. E.; Levason, W.; McAuliffe, C. A. *Inorg. Chem.*, **1974**, *13*, 244.

[35] Hoel, E. L.; Hawthorne, M. F. *J. Am. Chem. Soc.*, **1973**, *95*, 2712.

[36] Hoel, E. L.; Hawthorne, M. F. *J. Am. Chem. Soc.*, **1975**, *97*, 6388.

[37] Kalinin, V. N.; Usatov, A. V.; Kobel'kova, N. I.; Zakharkin, L. I. *Zh. Obshch. Khim.*, **1985**, *55*, 1874.

[38] Fey, N.; Haddow, M. F.; Mistry, R.; Norman, N. C.; Orpen, A. G.; Reynolds, T. J.; Pringle, P. G. *Organometallics*, **2012**, *31*, 2907.

[39] a) Lee, H. S.; Bae, J. Y.; Ko, J.; Kang, Y. S.; Kim, H. S.; Kang, S. O. *Chem. Lett.*, **2000**, *29*, 602. b) Lee, H. S.; Bae, J. Y.; Kim, D. H.; Kim, H. S.; Kim, S. J.; Cho, S.; Ko, J.; Kang, S. O. *Organometallics*, **2002**, *21*, 210.

[40] Contreras, J. G.; Silva-Triviño, L. M.; Solis, M. E. *Inorg. Chim. Acta*, **1988**, *142*, 51.

[41] Kivekäs, R.; Sillanpää, R.; Teixidor, F.; Viñas, C.; Abad, M. M. *Acta Chem. Scand.*, **1996**, *50*, 499.

[42] Zhang, D.; Dou, J.; Gong, S.; Li, D.; Wang, D. *Appl. Organomet. Chem.*, **2006**, *20*, 632.

[43] Sterzik, A.; Rys, E.; Blaurock, S.; Hey-Hawkins, E. *Polyhedron*, **2001**, *20*, 3007.

[44] a) Al-Baker, S.; Hill, W. E.; McAuliffe, C. A. *J. Soc. Chem. Dalton Trans.*, **1985**, 1387. b) Crespo, O.; Gimeno, M. C.; Laguna, A.; Jones, P. G. *J. Chem. Soc. Dalton Trans.*, **1992**, 1601. c) Crespo, O.; Gimeno, M. C.; Jones, P. G.; Laguna, A. *J. Chem. Soc. Chem. Commun.*, **1993**, 1696. d) Crespo, O.; Gimeno, M. C.; Jones, P. G.; Laguna, A. *Inorg. Chem.*, **1994**, *33*, 6128.

[45] a) Bembenek, E.; Crespo, O.; Gimeno, M. C.; Jones, P. G.; Laguna, A. *Chem. Ber.*, **1994**, *127*, 835. b) McWhannell, M. A.; Rosair, G. M.; Welch, A. J. *Acta Cristallogr. C*, **1998**, *54*, 13. c) Yang, L.; Zhu, C.; Li, D. *Acta Crystallogr. E*, **2011**, *67*, m2. d) Kong, L.; Zhang, D.; Su, F.; Li, D.; Dou, J. *B. Kor. Chem. Soc.*, **2011**, *32*, 2249. e) Yang, L.; Zhu, C.; Zhang, D.; Li, D., Wang, D.; Dou, J. *Polyhedron*, **2011**, *30*, 1469. f) Kong, L.; Zhang, D.; Su, F.; Lu, J.; Li, D.; Dou, J. *Inorg. Chim. Acta*, **2011**, *370*, 1.

[46] a) Zakharkin, L. I.; Kazantsev, A. V.; Meiramov, M. G. *Zh. Obshch. Khim.*, **1984**, *54*, 1536. b) Park, Y.; Kim, S.; Ko, J.; Kang, S. O. *B. Kor. Chem. Soc.*, **1997**, *18*, 1061. c) Balema, V. P.; Somoza Jr, F.; Hey-Hawkins, E. *Eur. J. Inor. Chem.*, **1998**, 651. d) Balema, V. P.; Blaurock, S.; Hey-Hawkins, E. *Z. Anorg. Allg. Chem.*, **1999**, *625*, 1237. e) Bauer, S.; Tschirschwitz, S.; Lönnecke, P.; Frank, R.; Kirchner, B.; Clarke, M. L.; Hey-Hawkins, E. *Eur. J. Inorg. Chem.*, **2009**, 2776.

[47] a) Dou, J.; Zhang, D.; Li, D.; Wang, D. *Inorg. Chem. Commun.*, **2006**, *9*, 1099. b) Dou, J.; Zhang, D.; Zhu, Y.; Li, D.; Wang, D. *Polyhedron*, **2007**, *26*, 4216. c) Dou, J.; Zhang, D.; Zhu, Y.; Li, D.; Wang, D. *Inorg. Chim. Acta*, **2007**, *360*, 3387.

[48] a) Yao, Z.-J.; Jin, G.-X. *Organometallics*, **2011**, *30*, 5365. b) Hu, P.; Yao, Z.-J.; Wang, J.-Q.; Jin, G.-X. *Organometallics*, **2011**, 30, 4935.

[49] a) Wang, H.; Chan, H.-S.; Xie, Z. *Organometallics*, **2006**, *25*, 2569. b) Wang, H.; Shen, H.; Chan, H.-S.; Xie, Z. *Organometallics*, **2008**, *27*, 3964.

[50] a) Wiesboeck, R. A.; Hawthorne, M.F. *J. Am. Chem. Soc.*, **1964**, *86*, 1642. b) Garrett, P. M.; Tebbe, F. N.; Hawthorne, M. F. *J. Am. Chem. Soc.*, **1964**, *86*, 5016. c) Hawthorne, M. F.; Young, D. C.; Garrett, P. M.; Owen, D. A.; Schwerin, S. G.; Tebbe, F. N.; Wegner, P. A. *J. Am. Chem. Soc.*, **1968**, *90*, 862.

[51] a) Yoshizaki, T.; Shiro, M.; Nakagawa, Y.; Watanabe H. *Inorg. Chem.*, **1969**, *8*, 698. b) Zakharkin, L.I.; Kalinin, V.N. *Dokl. Akad. Nauk SSSR*, **1965**, *163*, 110.

[52] a) Grafstein, D.; Bobinski, J.; Dvorak, S.; Smith, H.; Schwartz, N.; Cohen, M.S.; Fein, M.M. *Inorg. Chem.*, 1963, *2*, 1120. b) Stanko, V.I.; Brattsev, V.A. *J. Gen. Chem. USSR*, **1967**, *37*, 486. c) Stanko, V.I.; Brattsev, V.A. *Zh. Obshch. Khim.*, **1968**, *38*, 662; *J. Gen. Chem. USSR*, **1968**, *38*, 4636. d) Stanko, V.I.; Brattsev, V.A. *Zh. Obshch. Khim.*, **1965**, *35*, 1691; *J. Gen. Chem. USSR*, **1965**, *35*, 1693. e) Zakharkin, L.I.; Kalinin, V.N. *Dokl. Akad. Nauk. SSSR*, **1965**, *164*, 577.

[53] Zakharkin, L.I.; Grebennikov, A.V. *Izv. Akad. Nauk. SSSR Ser. Khim*, **1966**, 2091; *Bull. Acad. Sci. USSR*, **1966**, 1952.

[54] a) Zakharkin, L.I.; Kalinin, V.N., *Tetrahedron Lett.*, **1965**, 407. b) Hawthorne, M.F.; Wegner, P.A.; Stafford, R.C. *Inorg. Chem.*, **1965**, *4*, 1675.

[55] a) Tomita, H.; Luu, H.; Onak, T. *Inorg. Chem.*, **1991**, *30*, 812. b) Fox, M. A.; Gill, W. R.; Herbertson, P. L.; MacBride, J. A. H.; Wade, K. *Polyhedron*, **1996**, *15*, 565.

[56] Davidson, M. G.; Fox, M. A.; Hibbert, T. G.; Howard, J. A. K.; Mackinnon, A.; Neretin, I. S.; Wade, K. *Chem. Commun.*, **1999**, 1649.

[57] Teixidor, F.; Viñas, C.; Abad, M. M.; Lopez, M.; Casabó, J. *Organometallics*, **1993**, *12*, 3766.

[58] Teixidor, F.; Viñas, C.; Abad, M. M.; Nuñez, R.; Kivekäs, R.; Sillanpää, R. *J. Organomet. Chem.*, **1995**, *503*, 193.

[59] a) Teixidor, F.; Viñas, C.; Sillanpää, R.; Kivekäs, R.; Casabó, J. *Inorg, Chem.*, **1994**, *33*, 2645. b) Teixidor, F.; Viñas, C.; Abad, M. M.; Kivekäs, R.; Sillanpää, R. *J. Organomet. Chem.* **1996**, *509*, 139; c) Teixidor, F.; Benakki, R.; Viñas, C.; Kivekäs, R.; Sillanpää, R. *Inorg. Chem.*, **1999**, *25*, 5916.

[60] a) Bregadze, V.I. *Chem. Rev.*, **1992**, *92*, 209. b) Núñez, R.; Viñas, C.; Teixidor, F.; Sillanpää, R.; Kivekäs R. *J. Organomet. Chem.*, **1999**, *592*, 22.

[61] Teixidor, F.; Viñas, C.; Abad, M. M.; Whitaker, C.; Rius, J. *Organometallics*, **1996**, *15*, 3154.

[62] a) Weisboeck, R.A. ; Hawthorne, M.F. *J. Am. Chem. Soc.*, **1964**, *86*, 1642. b) Garret, P.M.; Tebbe, F.N.; Hawthorne, M.F. *J. Am. Chem. Soc.*, **1964**, *86*, 5016. c) Hawthorne, M.F.; Young, D.C.; Garret, P.M.; Owen, D.A.; Schwerin, S.G.; Tebbe, F.N.; Wegner, P.M. *J. Am. Chem. Soc.*, **1968**, *90*, 862.

[63] a) Zakharkin, L. I.; Kalinin, U. N. *Tetrahedron Lett.*, **1965**, 407. b) Zakharkin, L. I.; Kirillova, V. S. *IzV. Akad. Nauk SSSR, Ser. Khim.*, **1975**, 2596.

[64] Allcock, H. R.; Scopelianos, A. G.; Whittle, R. R.; Tollefson, N. M. *J. Am. Chem. Soc.*, **1983**, *105*, 1316.

[65] Teixidor, F.; Núñez, R.; Viñas, C.; Sillanpää, R.; Kivekäs, R. *Inorg. Chem.*, **2001**, *40*, 2587.

[66] Viñas, C.; Núñez, R.; Rojo, I.; Teixidor, F.; Kivekäs, R.; Sillanpää, R. *Inorg. Chem.*, **2001**, *40*, 3259.

[67] Núñez, R.; Teixidor, F.; Kivekäs. R.; Sillanpää, R.; Viñas, C. *Dalton Trans.*, **2008**, 1471.

[68] Charmant, J. P. H.; Haddow, M. F.; Mistry, R.; Norman, N. C.; Orpen, A. G.; Pringle, P. G. *Dalton. Trans.*, **2008**, 1409.

[69] Crespo, O.; Gimeno, M. C.; Jones, P. G.; Laguna, A. *Inorg. Chem.*, **1996**, *5*, 1361.

[70] Crespo, O.; Gimeno, M. C.; Jones, P. G.; Laguna, A. *J. Chem. Soc., Dalton Trans.*, **1996**, 4583.

[71] Crespo, O.; Gimeno, M. C.; Jones, P. G.; Laguna, A. *Acta Crystallogr. C*, **2000**, *56*, 46 .

[72] Jones, P. G.; Villacampa, M. D.; Crespo, O.; Gimeno, M. C.; Laguna, A. *Acta Crystallogr. C*, **1997**, *53*, 570.

[73] Crespo, O.; Gimeno, M. C.; Jones, P. G.; Laguna, A.; Villacampa, M. D. *Angew. Chem. Int. Ed.*, **1997**, *36*, 993.

[74] Teixidor, F.; Rius, J.; Miravitlles, C.; Viñas, C.; Escriche, Ll.; Sánchez, E.; Casabó, J. *Inorg. Chim. Acta* **1990**, *176*, 61.

[75] Viñas, C.; Flores, M. A.; Núñez, R.; Teixidor, F.; Kivekäs, R.; Sillanpää, R. *Organometallics*, **1998**, *17*, 2278.

[76] Núñez, R.; Teixidor, F.; Kivekäs, R.; Sillanpää, R. *Organometallics*, **1998**, *17*, 2376.

[77] Huo, X. K.; Su, G.; Jin, G. X. *Chem. Eur. J.* **2010**, *16*, 12017.

[78] McWhannell, M. A.; Rosair, G. M.; Welch, A. J.; Teixidor, F.; Viñas, C. *J. Organomet. Chem.* **1999**, *573*, 165.

[79] Viñas, C.; Núñez, R.; Flores, M. A.; Teixidor, F.; Kivekas, R.; Sillanpää, R. *Organometallics*, **1995,** *14*, 3952.

[80] Viñas, C.; Núñez, R.; Teixidor, F.; Kivekäs, R.; Sillanpää, R. *Organometallics,* **1996**, *15*, 3850.

[81]Viñas, C.; Abad, M. M.; Teixidor, F.; Sillanpää, R.; Kivekäs, R. *J. Organomet. Chem.*, **1998**, *555*, 17.

[82] Viñas, C.; Núñez, R.; Teixidor, F.; Sillanpää, R.; Kivekäs, R. *Organometallics*, **1999**, *18*, 4712.

[83] Zhang, D.; Dou, J., Li, D.; Wang, D. *Inorg. Chim. Acta* **2006**, *359*, 4243.
[84] a) Dou, J. M.; Zhang, D. P.; Li, D. C.; Wang, D. Q. *Polyhedron* **2007**, *26*, 719. b) Dou, J.; Zhang, D.; Li, D.; Wang, D. *J. Organomet. Chem.* **2006**, *691*, 5673.
[85] Kong, L.; Zhang, D.; Li, D.; Dou, J. *J. Clust. Sci.* **2011**, *22*, 97.
[86] Maulana, I.; Lönnecke, P.; Hey-Hawkins, E. *Inorg. Chem.*, **2009**, *48*, 8638.
[87] Lee, J. D.; Kim, H. Y.; Han, W. S.; Kang, S. O. *Organometallics*, **2010**, *29*, 2348.
[88] a) *Applied Homogenous Catalysis with Organometallic Complexes* Vols. 1 & 2 (Cornils, B., Herrmann, W.A., Eds.), Wiley-VCH, Weinheim, **2002**. b) *Phosphorus Compounds. Advanced Tools in Catalysis and Materials Science*. (Peruzzini, M.; Gonsalvi, L.; Eds.) in *Catalysis By Metal Complexes*, vol. 37, Springer, **2011**. c) Bauer, S.; Hey-Hawkins, E. *Phosphorus-Substituted Carboranes in Catalysis*. in *Boron Science. New Technologies and Applications.* Hosmane, N. S. (Ed.). CRC Press, **2012**.
[89] Jelliss, P. *Photoluminescence from Boron-Based Polyhedral Clusters*. in *Boron Science. New Technologies and Applications.* Hosmane, N. S. (Ed.). CRC Press, **2012.**
[90] Stadlauer, S.; Hey-Hawkins, E. *Bioconjugates of carboranyl Phosphonates*. in *Boron Science. New Technologies and Applications.* Hosmane, N. S. (Ed.). CRC Press, **2012.**
[91] Zakharkin, L. I.; Kazantsev, A. V. *Zh. Obshch. Khim.*, **1966**, *36*, 958. b) Kauffman, J. M.; Green, J.; Cohen, M. S.; Fein, M. M.; Cottrill, E. L.; *J. Am. Chem. Soc.,* **1964**, *86*, 4210. c) Fox, M. A.; MacBride, J. A. H.; Peace, R. J.; Clegg, W.; Elsegood, M. R. J.; Wade, K. *Polyhedron*, **2009**, *28*, 789.
[92] Valliant, J. F.; Guenther, K. J.; King, A. S.; Morel, P.; Schaffer, P.; Sogbein, O. O.; Stephenson, K. A. *Coord. Chem. Rev.*, **2002**, *232*, 173.
[93] Heying, T.L.; Ager Jr., J.W.; Clark, S.L.; Mangold, D.J.; Goldstein, H.L.; Hilman, M.; Polak, R.J.; Szymanski, J.W. *Inorg. Chem.*, **1963**, *2*, 1089-1092.
[94] Lee, J.-D.; Kim, S.-J.; Yoo, D.; Ko, J.; Cho, S.; Kang, S. O. *Organometallics*, **2000**, *19*, 1695.
[95] Chung, S.-W.; Ko, J.; Park, K.; Cho, S.; Kang, S. O. *Collect. Czech. Chem. Commun.*, **1999**, *64*, 883.
[96] a) Coult, R.; Fox, M. A.; Gill, W. R.; Herbertson, P. L.; MacBride, J. A. H.; Wade, K. *J. Organomet. Chem.*, **1993**, *462*, 19. b) Gill, W. R.; Herbertson, P. L.; MacBride, J. A. H.; Wade, K. *J. Organomet. Chem.*, **1996**, *507*, 249. c) Alekseyeva, E. S.; Batsanov, A. S.; Boyd, L. A.; Fox, M. A.; Hibbert, T. G.; Howard, J. A. K. ; MacBride, J. A. H.; Mackinnon, A.; Wade, K. *Dalton Trans.*, **2003**, 475.
[97] Teixidor, F.; Laromaine, A.; Kivekäs, R.; Sillanpää, R.; Viñas, C.; Vespalec, R.; Horáková, H. *Dalton Trans.*, **2008**, 345.
[98] Bould, J.; Laromaine, A.; Bullen, N. J.; Viñas, C.; Thornton-Pett, M.; Sillanpää, R.; Kivekäs, R.; Kennedy, J. D.; Teixidor, F. *Dalton Trans.*, **2008**, 1552.
[99] Wang, X.; Jin, G.-X. *Chem. Eur. J.*, **2005**, *11*, 5758.
[100] a) Dröse, P.; Hrib , C. G.; Edelmann, F. T. *J. Am. Chem. Soc.*, **2010**, *132*, 15540. b) Yao, Z.-J.; Jin, G.-X. *Organometallics*, **2012**, *31*, 1767.
[101] Brown, D. A.; Colquhoun, H. M.; Daniels, J. A.; MacBride, J. A. H.; Stephenson, I. R.; Wade, K. *J. Mater. Chem.*, **1992**, *2*, 793.
[102] Grimes, R. N. *Carboranes*. 2nd Ed. Elsevier. **2011**, p383, and the references therein.
[103] a) Zakharkin, L. I.; Bregadze, V. I.; Okhlobystin, O. Yu. *Izv. Akad. Nauk. SSSR, Ser. Khim.*, **1964**, 1449. b) Zaborowski, R.; Cohn, K. *Inorg. Chem.*, **1969**, *8*, 678. c) King, A. S.; Ferguson, G.; Britten, J. F.; Valliant, J. F. *Inorg. Chem..*, **2004**, *43*, 3507.
[104] Fox, M. A.; MacBride, J.A. H.; Peace, R. J.; Clegg, W.; Elsegood, M. R.J.; Wade K. *Polyhedron*, **2009**, *28*, 789.
[105] Bregadze, V. I.; Godovikov, N. N.; Degtyarev, A. N.; Kabachnik, M. I. *J. Organomet. Chem.*, **1976**, *112*, C25. b) Zakharkin, L. I.; Pisareva, I. V. *Izv. Akad. Nauk. SSSR, Ser. Khim.*, **1978**, 1226.
[106] Zakharkin, L. I.; Kalinin, V. N.; Podvisotskaya, L. S. *Izv. Akad. Nauk. SSSR, Ser. Khim.*, **1968**, 664.
[107] Furmanova, N. G.; Yanovskii, A. I.; Struchkov, Yu. T.; Bregadze, V. I.; Godovikov, N. N.; Degtyarev, A. N.; Kabachnik, M. I. *Izv. Akad. Nauk. SSSR, Ser. Khim.*, **1979**, 2346.
[108] a) Canales, S.; Crespo, O.; Gimeno, M. C.; Jones, P. G.; Laguna, A.; Romero, P. *Dalton Trans.*, **2003**, 4525. b) Zakharkin, L. I.; Krainova, N. Yu.; Zhigareva, G. G.; Pisareva, I. V. *Izv. Akad. Nauk. SSSR, Ser. Khim.*, **1982**, 1650. c) Zakharkin, L. I.; Pisareva, I. V. *Izv. Akad. Nauk. SSSR, Ser. Khim.*, **1984**, 472. d) Zakharkin, L. I.; Pisareva, I. V. *Izv. Akad. Nauk. SSSR, Ser. Khim.*, **1987**, 877. e) Heberhold, M.; Milius, W.; Jin, G.-X.; Kremnitz, W.; Wrackmeyer,

B.; *Anorg, Z. Allg. Chem.*, **2006**, *632*, 2031. f) Batsanov, A. S.; Clegg, W.; Copley, R. C.B.; Fox, M. A.; Gill, W. R.; Grimditch, R. S.; Hibbert, T. G.; Howard, J. A.K.; MacBride, J.A. H.; Wade K. *Polyhedron*, **2006**, *25*, 300.
[109] a) Laromaine, A.; Teixidor, F.; Kivekäs, R.; Sillanpää, R.; Benakki, R.; Grüner, B.; Viñas, C. *Dalton Trans.*, **2005**, 1785. b) Laromaine, A.; Teixidor, F.; Kivekäs, R.; Sillanpää, R.; Arca, M.; Lippolis, V.; Crespo, E.; Viñas, C. *Dalton Trans.*, **2006**, 5240.

II. RESULTS AND DISCUSSION

1. Study of the reaction of *o*-carborane with buthylithium. Influence of the ethereal solvents

Almost all the compounds synthesized in this work are achieved direct from *o*-carborane. The modification of the C vertexes of the *o*-carborane is done in two steps. First a deprotonating agent as organolithium compounds, alkali-metal amides or alkali-metal hydrides is added, followed by the addition of a suitable electrophile (carbon dioxide, chalcogens, halogens, halides, epoxides, aldehydes). Although the substitution at the both carbon atoms is always achieved, the monosubstitution is not so trivial, being almost always accompanied by the disubstituted derivative. For that we wanted to get as more as possible to the core of this reaction and to understand how it works.

Almost fifty years ago, Zakharkin et al.[1] showed that, upon the addition of one equivalent of buthylitium over one equivalent of *o*-carborane, 1,2-$C_2B_{10}H_{12}$ (**1**), in ether-benzene, equilibrium is established between the unreacted *o*-carborane, the monolithiated and the dilithiated species (Scheme 1.1.). This is undesirable because the three compounds mono-, di- and unreacted, commonly share very similar solubility properties causing difficulties in their separation. As an alternative, to obtain pure monoderivatives, Hawthorne et al.[2] proposed the protection of one C_C-positions in *o*-carborane with -$Si(Me)_3CMe_3$ (TBDMS) group; effecting the desired reaction in the other C_C site; and subsequently cleaving the original C_C-Si bond with *n*-Bu_4NF. The drawback of this method comes from the bulkiness of the silane group, that difficult the substitution to the other carbon atom. Our group reported later[3] that the monolithiation can be successfully achieved in dimethoxyethane due to the stabilization of the monolithiated species by Li^+ coordination of the solvent but not further research was done to understand the influence of the ethereal solvents on the reaction. Therefore we have done further research to understand: i) the influence of the solvent in the reaction, ii) to determine if the equilibrium shown in Scheme 1.1. is decisive for the high yield preparation of monosubstituted derivatives, 1-R-1,2-$C_2B_{10}H_{11}$, or alternatively there are other factors to be taken into account, and iii) to learn why such uncommon equilibrium takes place.

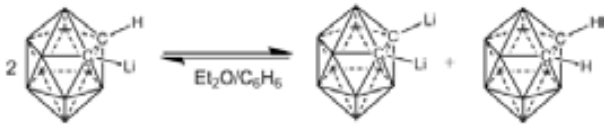

Scheme 1.1. The equilibrium between the species involved in the reaction of 1,2-$C_2B_{10}H_{12}$ with *n*-BuLi.

Our qualitative interpretation regarding the disproportionation of 1-Li-1,2-$C_2B_{10}H_{11}$ is that the C_C-Li bond has a very strong covalent character, otherwise the build-up of negative charges that would result if the bond had a large ionic character would not favor such process. Therefore a coordinating solvent rarely could be innocent in such a process, either a) it can fully solvate the Li^+, pulling out the resulting solvated ion far from the influence of [2-H-1,2-$C_2B_{10}H_{10}$]$^-$ thus reducing the chances of having a second negative charge on the cluster, or alternatively; b) the solvent can partially solvate the Li^+ in which case it may stabilize the co-existence of two Li^+ on the same carborane. The strategy we had used earlier[3] when using a chelating solvent, DME, was aimed to produce monosubstitution due to physical hindrance with a destabilized disubstituted 1,2-[$Li(DME)_x$]$_2$-1,2-$C_2B_{10}H_{10}$. However we could not establish exactly which the role of the solvent was.

To experimentally get information about the questions raised above, we decided to restrict this investigation to only one type of solvents, ethereal solvents, and to three different types of reagents S_8, $ClPPh_2$[4] and $BrCH_2CHCH_2$, which give us the opportunity to study the lithiated intermediates and the post-reaction influence of the Li^+.

1.1. *Reaction of carboranyllithium with sulfur*

The reaction of **1** with one equivalent of *n*-BuLi and 1/8 equivalents of S_8 (Scheme 1.2.) was carried out in three different ethereal solvents: diethyl ether (Et_2O), tetrahydrofurane (THF) and 1,2-dimethoxyethane (DME). To get the maximum information on the etheral solvent influence, the reactions with carboranyllithium have been conducted over a range of temperatures between -80°C and 0°C, in steps of 20°C. The concentration dependence of the reaction was also studied, thus two different concentrations, one of 0.07 mol·L^{-1} (that is 100 mg of *o*-carborane per 10 mL of solvent) and a second of 0.23 mol·L^{-1}(that is 100 mg of *o*-carborane per 3 mL of solvent) have been utilized.

In a typical experiment under nitrogen, *o*-carborane was dissolved in the studied ethereal solvent and the solution was cooled to the targeted temperature for half an hour using a cooling bath. Then, one equivalent of *n*-BuLi (1.6M in hexane) was added drop-wise using a syringe. The mixture was left for 2 hours under mixing in the cooling bath. Next, one equivalent of sulfur was added. The resulting solution was left to stand for another 2 hours under the same conditions. Then the cooling bath was removed and the reaction mixture was stirred for additional 30 minutes until the room temperature was reached. The solvent was evaporated and diethyl ether was added. The solution was cooled using an ice-bath (0°C) and aqueous hydrochloric acid (0.1M, 5mL) was added. After removal of the cooling bath the mixture was left to reach room temperature. Finally, the organic phase was separated and evaporated to dryness. The percentages in terms of molar fraction of the compounds separated in the reaction of carboranyllithium with sulfur are presented in Table 1.1. The reactions in DME were carried out starting at -60°C due to the melting point of the solvent. To assure the reproducibility of the experimental data the reactions were double or triple checked.

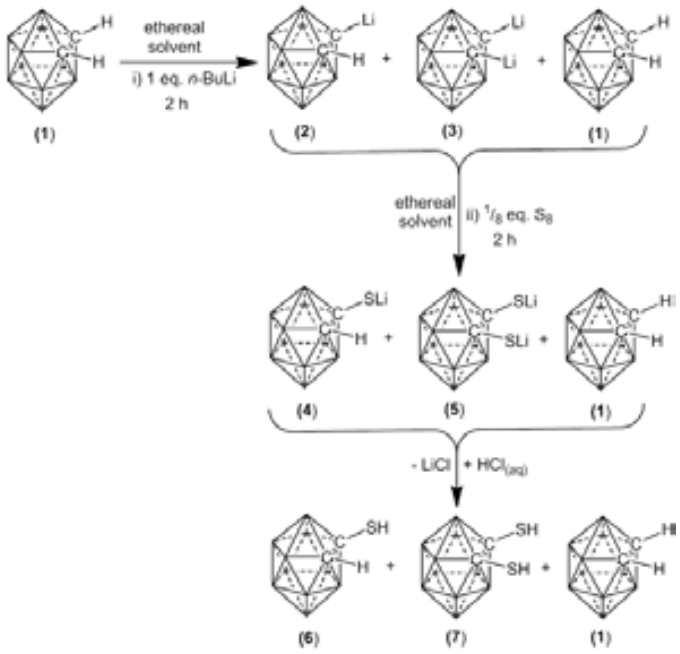

Scheme 1.2. Reaction of carboranyllithium with sulfur.

As shown in Table 1.1, in both THF and DME in almost all conditions, over 90% of 1-SH-1,2-$C_2B_{10}H_{11}$, **6**, was obtained, reaching up to 98%. The exception was with DME at -60°C at which temperature DME is solid (mp -58°C). When the solvent was Et_2O significantly lower yields of **6** were obtained, while the ratio of 1,2-$(SH)_2$-1,2-$C_2B_{10}H_{10}$, **7**, increased. The latter eventually exceeded **6** at 0°C. To notice is that the reaction was not completed under these conditions, and upon addition of water all the lithiated species present in the reaction medium were protonated yielding, in addition, pristine 1,2-$C_2B_{10}H_{12}$.

Remarkably, the reaction of Li[$C_2B_{10}H_{11}$], **2**, with sulfur in THF is within experimental error independent of the temperature or concentration. This implies that the two steps (Scheme 1.2.): i) the reaction of **1** with *n*BuLi and ii) the nucleophilic attack of the carboranyl on sulfur, are both temperature independent. The temperature independence of the first of the two steps was confirmed by theoretical

T [ºC]	*[Carb]* [mol·L^{-1}][a]	THF			Et_2O			DME		
		mono [%]	di [%]	o-car-borane[b] [%]	mono [%]	di [%]	o-car-borane[b] [%]	mono [%]	di [%]	o-car-borane[b] [%]
-80	0,07	91	4	5	56	6	39	-	-	-
-80	0,23	95	0	5	57	9	34	-	-	-
-60	0,07	96	0	4	74	3	23	85	0	14
-60	0,23	98	0	2	53	0	47	81	2	17
-40	0,07	97	0	3	71	16	13	92	1	7
-40	0,23	93	0	7	72	4	24	95	1	4
-20	0,07	97	0	3	80	9	11	95	1	4
-20	0,23	95	0	5	74	12	14	95	1	4
0	0,07	95	0	5	49	13	37	91	1	8
0	0.23	98	0	2	26	38	36	92	3	5

[a] [Carb] = *o*-carborane concentration. [b] Unreacted *o*-carborane

Table 1.1. Molar fraction of 1-SH-1,2-$C_2B_{10}H_{11}$ in ethereal solvents.

calculations (Figure 1.1.). This result implies that the kinetics of the global reaction depends on the rate of the second step, that is, the reaction between the electrophile and the carboranyllithium. Thus the mechanism of the reaction between the lithiated species and the electrophile is the relevant one to produce the targeted compound. As different yields and compounds are obtained in different solvents, it is clear that the reactivity of the reagents greatly depends on the interactions with the solvent.

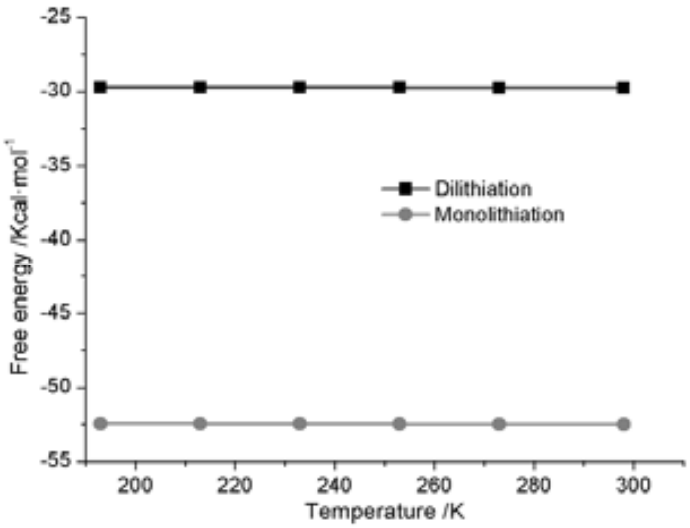

Figure 1.1. Variation of the free energy of the reaction with the temperature in the reaction of 1,2-$C_2B_{10}H_{12}$ with *n*-BuLi.

Sulfur reacts with **2** in THF and DME to yield almost exclusively **4**, which is hydrolyzed with HCl to produce **6**. This is not true in Et_2O, in which the proportion of **5** is even superior to the one for **4**. Therefore, in what concerns the mechanism of the reaction between the electrophile and the lithiated carborane, one has to take into consideration the solvation of all involved species.

1.2. *Reaction of carboranyllithium with chlorodiphenylphosphine*

The reaction of *o*-carborane with one equivalent of *n*-BuLi and one equivalent of $ClPPh_2$ in precisely the same conditions as for the reaction with sulfur described above produced lower yields of the monosubstituted species in any of the three solvents. Even more, the percentage of unreacted *o*-carborane is high, indicating that the reaction was quenched before being finished (Table 1.2). The highest yields and the highest ratio of monosubstituted *o*-carborane, however, are obtained in Et_2O. This result is opposite to the reaction of Li[1,2-$C_2B_{10}H_{11}$] with sulfur, for which, Et_2O was the worst solvent.

T [ºC]	*[Carb]* [mol·L^{-1}][a]	THF			Et_2O			DME		
		mono [%]	di [%]	o-car-borane[b] [%]	mono [%]	di [%]	o-car-borane[b] [%]	mono [%]	di [%]	o-car-borane[b] [%]
-80	0,07	40	11	49	34	4	62	-	-	-
-80	0,23	16	9	75	28	8	64	-	-	-
-60	0,07	23	6	71	79	8	13	12	21	67
-60	0,23	16	8	76	81	5	14	55	3	42
-40	0,07	16	7	77	55	8	37	28	7	65
-40	0,23	20	6	74	57	6	37	54	10	36
-20	0,07	30	5	65	53	1	46	26	7	67
-20	0,23	26	2	72	41	3	56	57	2	41
0	0,07	5	3	92	57	5	38	35	4	61
0	0.23	15	5	80	60	8	32	32	3	65

[a] [Carb] = *o*-carborane concentration. [b] Unreacted *o*-carborane

Table 1.2. Molar fraction of 1-PPh_2-1,2-$C_2B_{10}H_{11}$ in ethereal solvents.

The diethyl ether could then be a suitable solvent for the preparation of 1-PPh_2-1,2-$C_2B_{10}H_{11}$ (**8**). To this aim, and as a complementary task away from the conditions described above and for comparison purposes, we performed the reaction of Li[1,2-$C_2B_{10}H_{11}$] with $ClPPh_2$ at room temperature, and after two hours 1-PPh_2-1,2-$C_2B_{10}H_{11}$ was obtained with a yield over 90%.

In the reaction of Li[1,2-$C_2B_{10}H_{11}$] with $ClPPh_2$ two main compounds are produced (Scheme 1.3.): 1-PPh_2-1,2-$C_2B_{10}H_{11}$ and LiCl whereas in the reaction with sulfur only one compound is obtained, namely 1-SLi-1,2-$C_2B_{10}H_{11}$. Thus, the mechanism of the reaction of Li[1,2-$C_2B_{10}H_{11}$] with $ClPPh_2$ is different from that of the reaction with sulfur. The experimental evidence that different yields and compounds are obtained in the studied solvents, lead to the conclusion that the reactivity of the reagents and the coupling reaction mechanism between carboranyl-lithium and the electrophile greatly depend on the interactions with the solvent and the solvation of all involved species.

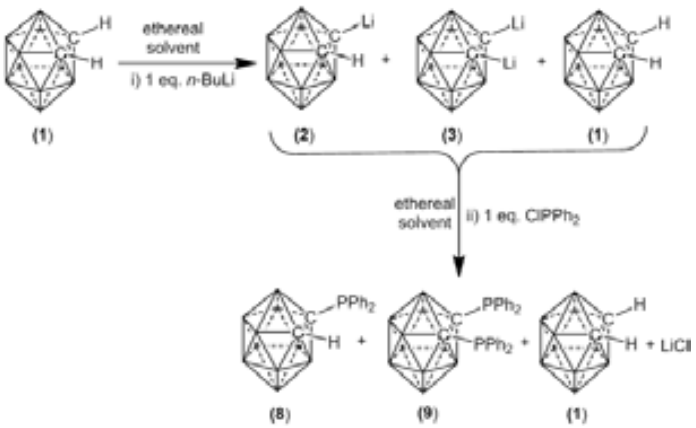

Scheme 1.3. Reaction of carboranyllithium with $ClPPh_2$.

1.3. *Solvation capacity of the ethereal solvents*

To account for the influence of the solvent both in the yield and compounds of the reaction, it is necessary to take into consideration the solvation of Li^+ and also the solvation of the anion. The solvation of the cation and the anion should depend on inherent solvating properties of the solvents. Table 1.3. contains the donor (DN) and acceptor number (AN) for the three solvents.[5] The magnitude of the donor number refers to the ability of a solvent to solvate cations and the magnitude of the acceptor number

refers to the ability of a solvent to solvate anions. The three ethers have comparable donor numbers but with respect to the acceptor number, both THF and DME have ANs that are at least twice the AN value for diethyl ether. Thus, solvation of the carboranyl moiety should be lower in Et_2O than in THF or DME and therefore the carboranyl in Et_2O should behave as a stronger nucleophile than in donor solvents with greater AN.

	AN	DN
Et_2O	3,9	19,2
THF	8,0	20,0
DME	10,2	24

Table 1.3. Acceptor number (AN) and Donicities (DN) for selected solvents in [kcal·mol^{-1}].

It has been proven that the solvent effects dramatically influence the aggregation state and the reactivity of alkyllithium, lithium dialkylamides, and other organolithium compounds.[6] However, the solvation of organolithium compounds is a complex issue, and no single existing solvation model is appropriate for all such compounds. Although molecular dynamics may ultimately provide best method to determine average equilibrium solvation numbers,[7] a number of recent studies have modeled the thermodynamics of ethereal solvation of organolithiums by locating explicit solvates.[8]

In order to see the solvation of the monolithiated species in different solvents, we also calculated the solvation free energies for Li[1,2-$C_2B_{10}H_{11}$] by the microsolvation model and by the Integral Equation Formalism Polarizable Continuum Model (IEFPCM).[9] The continuum model is most appropriate for systems in which the molecules of interest do not form a complex with the solvent molecules or for organolithium compounds in hydrocarbon solvents, such as hexane or benzene. Conventionally, to study the solvation of lithiated species in solvents that could form solvated complexes with Li^+, it is, in general, more favorable using the microsolvation model. As can be observed in Table 1.4., the values obtained with the continuum model indeed overestimate the solvation energy, and in particular, the solvation in DME seems less favored. These results are due to the steric effects of coordinating ether ligands that are important in reproducing the aggregation state of organolithium compounds, and may not be adequately represented by continuum solvent models. On the contrary, when solvation of the explicit solvent molecules is considered as in the microsolvation method, the effect of DME is two times greater than these of THF or diethyl ether, the latter being the lower. These results however do not take into consideration the second solvation sphere because the bulk solvent effects are not adequately represented by microsolvation. For the microsolvation, the model structures [1-Li(Solvent)$_n$-1,2-$C_2B_{10}H_{11}$] (Solvent = THF, n = 3; Solvent = Et_2O, n = 2; Solvent = DME, n = 1), were chosen after discrimination on the bases of computational studies presented further. These results are in agreement with the qualitative description about the donor and acceptor numbers.

	IEFPCM	Microsolvation
THF	-39,57	-3,29
Et_2O	-32,76	-2,87
DME	-13,85	-7,87

Table 1.4. Free energies of solvation in the three solvents for Li[1,2-$C_2B_{10}H_{11}$] [kcal·mol^{-1}].

1.4. *Ethereal solvents impact in the carboranyllithium self-reaction*

We have already shown that the readiness to react of carboranyllithium is smaller in Et_2O than in THF or DME. Having this in mind we checked the evolution of a sample of carboranyllithium in these solvents with time. The stability of the sample was monitored with multinuclear NMR analysis. The NMR experiments were run with a concentric NMR tube, the inner tube contained d_6-acetone that provided for the NMR lock signal.

The sensitivity of the electron distribution in carboranes to the presence of substituents has long been apparent and it is manifested in the ^{11}B-NMR spectra.[10] As can be observed from Figure 1.2., the $^{11}B\{^1H\}$-NMR spectra of the three species (1,2-$C_2B_{10}H_{12}$, Li[1,2-$C_2B_{10}H_{11}$] and $Li_2[C_2B_{10}H_{10}]$) involved in the equilibrium of Scheme 1.1., are clearly different.

For the monolithiated species, Li[1,2-$C_2B_{10}H_{11}$], however, the NMR analysis showed distinctive feature in the three ethereal solvents. The ^{7}Li-NMR spectra show a singlet in all the three solvents (Figure 1.3.), that shifts upfield form -0.40 ppm when using Et_2O as solvent, to -1.32 ppm in both THF and DME. These experimental values fully agree with acceptor and donor numbers of the studied ethereal solvents (Table 1.3.). Conversely, the $^{11}B\{^1H\}$-NMR spectra show different features in different solvents. In Et_2O, the $^{11}B\{^1H\}$-NMR spectrum (red) shows five resonances (Figure 1.4.), whereas in THF and DME, a four resonances pattern is presented. Besides this dominating pattern, in THF and DME a second set of peaks, with lower intensity spread in the interval +37.5 ppm to -20.5 ppm is also found. All peaks of the second pattern generate doublets in the ^{11}B-NMR spectra indicating that every boron is bonded to a *exo*-cluster hydrogen. Fox *et al.*[11] have reported a compound with the same pattern, formed after mixing 1,3-di-*tert*-pentylimidazol-2-ylidene with *o*-carborane. In this case, the heterocyclic carbene abstracted a proton from a C_C-H bond generating the $[C_2B_{10}H_{11}]^-$ anion; this in turn attacked a second molecule of *o*-carborane at B(3), forming a two clusters anion, $[C_4B_{20}H_{23}]^-$. Based on DFT calculations, it was there shown that the imidazolium salt of the discrete $[C_2B_{10}H_{11}]^-$ is less favorable by 13.3 kcal·mol^{-1} than the adduct result of the cluster CH···C(carbene)

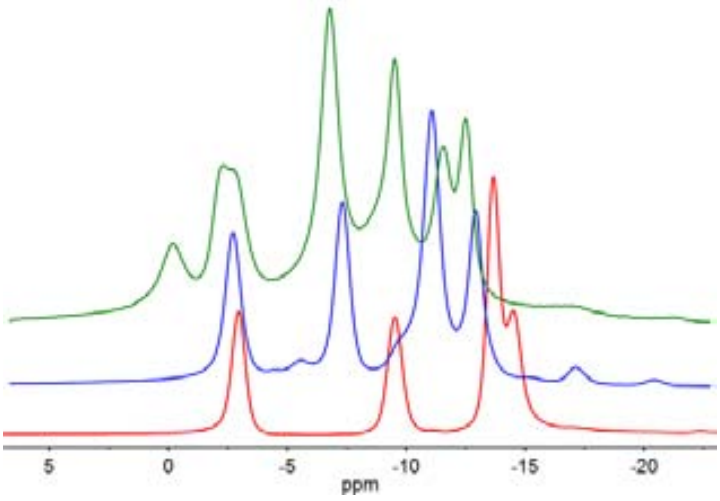

Figure 1.2. $^{11}B\{^1H\}$-NMR (in THF) spectra for 1,2-$C_2B_{10}H_{12}$ (red), Li[1,2-$C_2B_{10}H_{11}$] (blue) and Li_2[1,2-$C_2B_{10}H_{10}$] (green).

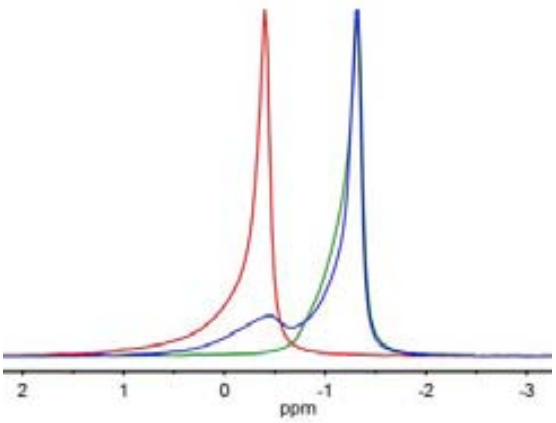

Figure 1.3. ^{7}Li-NMR spectra for Li[1,2-$C_2B_{10}H_{11}$] in Et_2O (red), THF (blue) and DME (green).

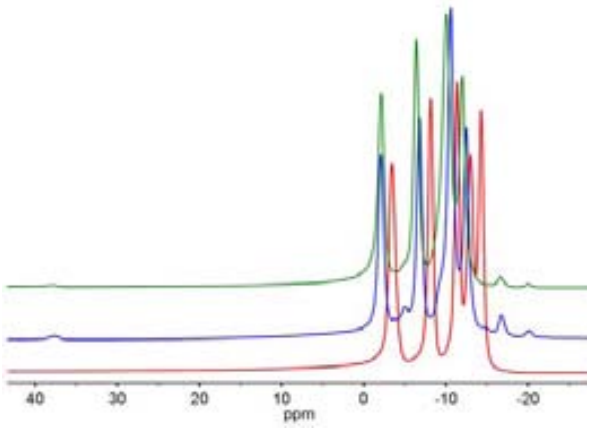

Figure 1.4. $^{11}B\{^1H\}$-NMR spectra for Li[1,2-$C_2B_{10}H_{11}$] in Et_2O (red), THF (blue) and DME (green).

interaction between the carbene and the $[C_2B_{10}H_{11}]^-$ anion. In our case, the *in situ* formed $[C_2B_{10}H_{11}]^-$ anion attacks another carborane molecule. However, the persistence of a large quantity of unreacted $[C_2B_{10}H_{11}]^-$ upon the monolithiation of the o-carborane in THF or DME indicates that in these solvents, 1-Li-1,2-$C_2B_{10}H_{11}$ is still present mainly as a contact ion pair between Li^+ and $[C_2B_{10}H_{11}]^-$. The alternative separated ion pair could not exist in solution due to the high reactivity of $[C_2B_{10}H_{11}]^-$, that would attack a second molecule of 1-Li-1,2-$C_2B_{10}H_{11}$ to produce $[LiC_4B_{20}H_{22}]^-$. To enhance further the nucleophilicity of the $Li^+[C_2B_{10}H_{11}]^-$ contact ion pairs, KBr or KI were added to the THF solution, and the mixture was refluxed overnight. The ^{11}B-NMR and $^{11}B\{^1H\}$-NMR analysis (Figure 1.5.) of the crude of the reaction has demonstrated that the equilibrium presented in Scheme 1.4. is shifted to the formation of $[LiC_4B_{20}H_{22}]^-$. Even more, if a solution of 1-Li-1,2-$C_2B_{10}H_{11}$ in THF is left for 60h at room temperature in the presence of carbon tetraiodide or iodoforme, $[LiC_4B_{20}H_{22}]^-$ is generated in high yield.

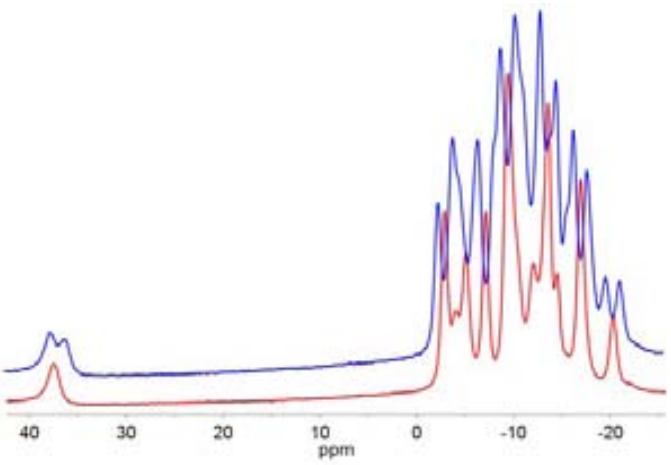

Figure 1.5. $^{11}B\{^1H\}$-NMR (red) and ^{11}B-NMR (blue) (in THF) for $[LiC_4B_{20}H_{22}]^-$

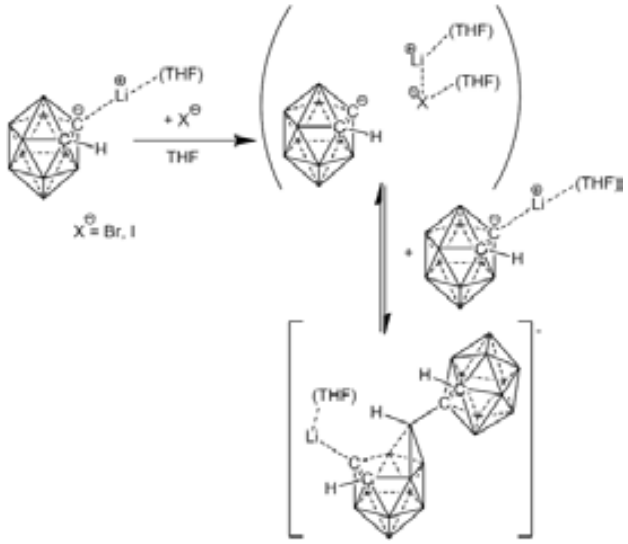

Scheme 1.4. Reaction of carboranyllithium with halides in THF.

The self-attack of the discrete carboranyl anion to a second molecule of 1-Li-2-Me-$C_2B_{10}H_{10}$, was also observed for methylcarborane in THF and DME. The $^{11}B\{^1H\}$ NMR spectrum of the lithiated methyl-carborane shows a main pattern of three signals in the region between -1.9 ppm and -8.9 ppm and a second pattern of six other signals of low intensity in the range +34 ppm to -19 ppm. In the ^{11}B NMR spectrum all these peaks were identified as doublets, indicating the presence of the same type of anion formed by two clusters, $[Li(CH_3)_2C_4B_{20}H_{20}]^-$.

These results evidence that the nucleophilicity of carboranyllithium salts, and most probably of other lithiated compounds, can be tuned by the adequate choice of the ether solvent utilized. This nucleophilicity can be further enhanced, on demand, by the synergy with potassium salts (KBr or KI), in a manner similar to the LiCl modulation of Grignard reagents successfully achieved by Knochel and co-workers, e.g. *i*-PrMgCl·LiCl and *s*-BuMgCl·LiCl.[12]

1.5. *Molecular approach to the nucleophilicity of carboranyllithium in ethereal solvents*

Understanding the reactivity of lithiated compounds modulated by the solvent is particularly difficult[13] because: 1) the solvent has a dual activity as reaction medium and as ligand, 2) lithium compounds may aggregate in solution, 3) lithium can have the coordination numbers from 1 to 12, 4) solvent exchanges take place extremely rapid, 5) competitive and cooperative (mixed) solvation processes occur when solvent mixtures are employed, 6) the limits of primary and secondary solvation shells are not well defined.

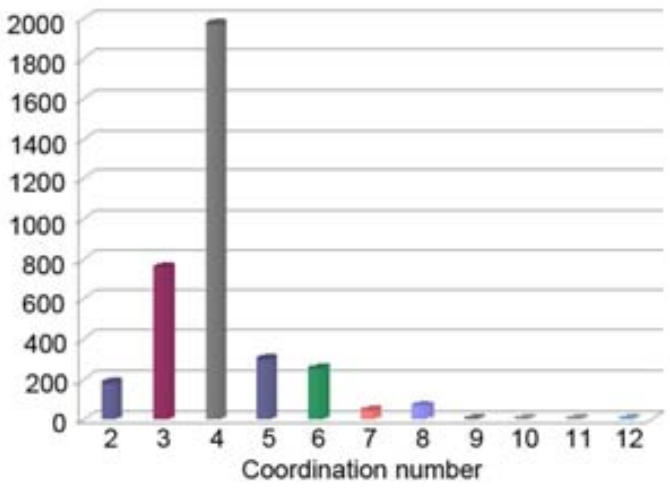

Scheme 1.6. Distribution of the number of crystal structures function of the coordination number for Li^+.

Although the coordination number of Li^+ is very wide, typically a Li^+ is surrounded by four coordinating entities as found either in solution or in solid state.[14] Also, a survey[15] of the Crystallographic Cambridge Database[16] reveal that the more preferred coordination number for lithium in crystal structures is four (Figure 1.6.). In the literature only two crystal structures with carborane moieties, containing C_C-Li bonds are found and Li^+ is tetracoordinated.[17] Therefore, as a first approach to study the nucelophilicity of carboranyllithium in ethereal solvents, we will take a coordination number of four.

Presumably, Li[1,2-$C_2B_{10}H_{11}$] is present in solution as a contact ion pair, ($Li^+[C_2B_{10}H_{11}]^-$) or solvent separated ion pairs, ($Li^+/[C_2B_{10}H_{11}]^-$). If Li[1,2-$C_2B_{10}H_{11}$] is in solution as contact ion pairs, it would be expected that Li was solvated with three solvent molecules. This might be the case for mono ethers like THF or Et_2O, but not for DME, in which the molecule has two oxygen atoms. For the latter there would be one or two DME molecules solvating the Li moiety. Therefore we optimized the structures with three THF, three Et_2O, and two DME molecules, respectively. The optimized structures are shown in Figure 1.7. Based on the distances Li-O and Li-C_C (Table 1.5.) of the optimized structures, we could discriminate between the structures the number of solvent molecules coordinated to Li. Based on the sum of vand der Waals radii between Li and O, the only structure that accommodates three solvent molecules is the one with THF (**I**). For Et_2O (**II**) the energy minimum was found for a structure with two ether molecules

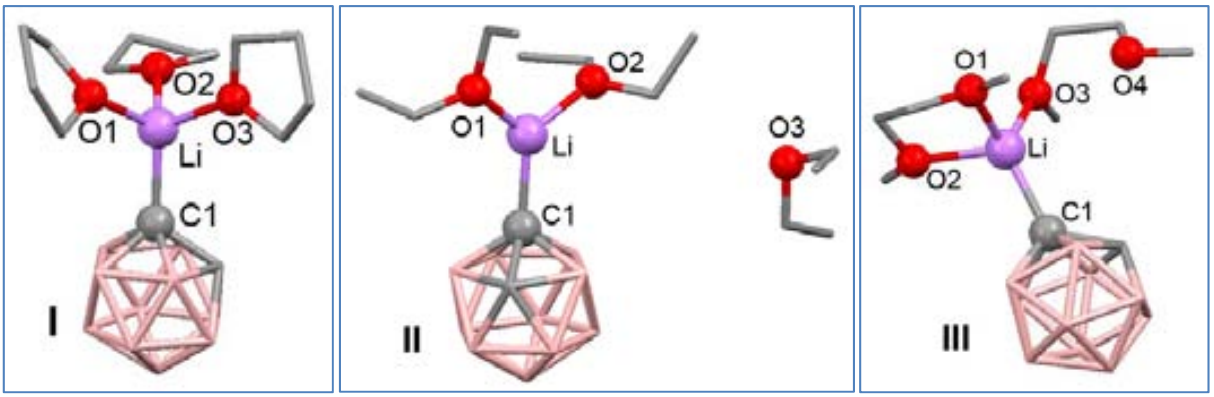

Figure 1.7. Optimized structures for Li[1,2-C2B10H11] with the explicit solvent molecules: **I** with THF, **II** with Et2O and **III** with DME (H atoms are omitted for clarity).

solvating the lithium. The other molecules are at a distance 1.5 times greater than the sum of the van der Waals radii between Li and O. For DME (**III**), there are three coordinating oxygen atoms whereas the fourth is at a distance a little bit farther than the sum of the van der Waals radii. These results prompted us to optimize 1-Li(Solvent)$_n$-1,2-$C_2B_{10}H_{11}$, for Li coordinated to two molecules of Et_2O and for Li coordinated to one molecule of DME, respectively (Figure 1.8.). In the case of Et_2O the Li-O distance for **IV** was found close to the one found in **II**, whereas in case of DME, the Li-O distance was found to be lower in **V** than in **III**. The C_C-Li distances decreased in the sense: **I** > **IV** > **V**, and are close to the experimental C_C-Li distances of 2.176(8) Å reported for 1-Li(PMDTA)-2-Me-1,2-$C_2B_{10}H_{10}$,[17a] and 2.088(2) Å reported for 1-Li(DME)-2-DIPC-1,2-$C_2B_{10}H_{10}$,[17b] respectively.

To support these computed structures with experimental evidence, the theoretical $^{11}B\{^1H\}$-NMR spectra for the optimized geometries were calculated and compared with the experimental NMR spectra for the carboranyl lithiated compounds in the ethereal solvents studied. As can be observed from Figure 1.9., the computed spectrum for **IV** (Figure 1.9.b) matches very well the experimental one. Although the calculated spectra for **I** (Figure 1.9.a) and **V** (Figure 1.9.c) have some similar points with the experimental ones, do not

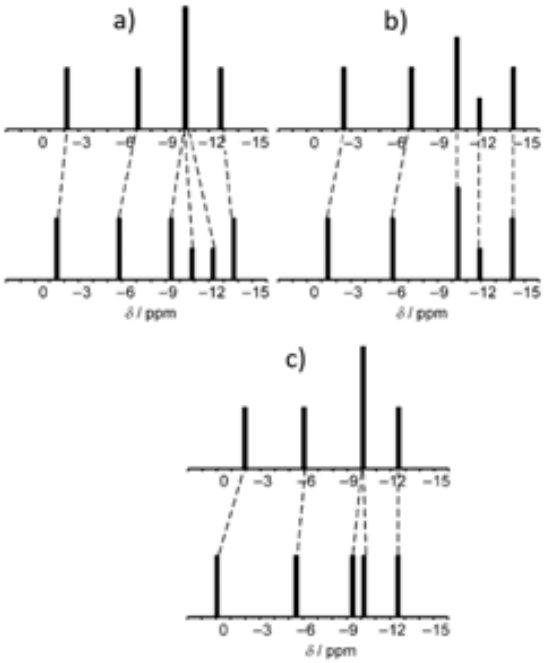

Figure 1.9. Experimental (upper trace) $^{11}B\{^1H\}$-NMR spectra for Li[1,2-$C_2B_{10}H_{11}$] in: a) THF , b) Et_2O, and c) DME and computed $^{11}B\{^1H\}$-NMR spectra (lower trace) for structures: a) **I**, b) **IV**, and c) **V**.

Structure	Distance (Å)	
I	C1-Li	2.133(7)
	O1-Li	2.022(5)
	O2-Li	2.026(4)
	O3-Li	2.016(1)
II	C1-Li	2.064(6)
	O1-Li	1.927(2)
	O2-Li	1.947(4)
	O3-Li	6.071(2)
III	C1-Li	2.092(7)
	O1-Li	2.065(3)
	O2-Li	2.059(1)
	O3-Li	2.011(6)
	O4-Li	3.418(6)
IV	C1-Li	2.059(4)
	O1-Li	1.956(9)
	O2-Li	1.924(3)
V	C1-Li	2.016(6)
	O1-Li	1.957(6)
	O2-Li	1.946(1)

Table 1.5. Selected bond distances for the carboranyllithium-ether adducts.

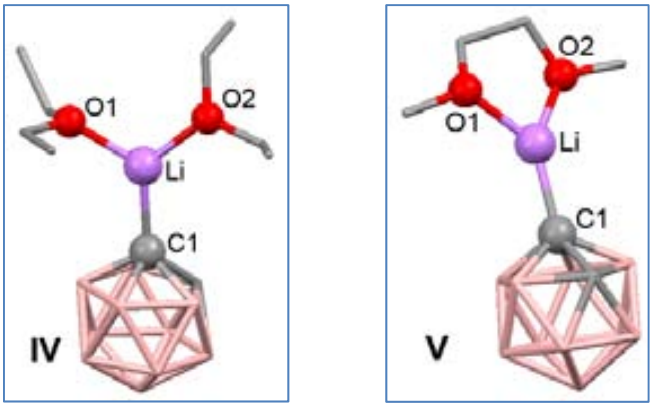

Figure 1.8. Optimized structures for Li[1,2-C2B10H11] after exclusion of uncoordinated solvent molecules: **IV** with Et2O and **V** with DME (H atoms are omitted for clarity).

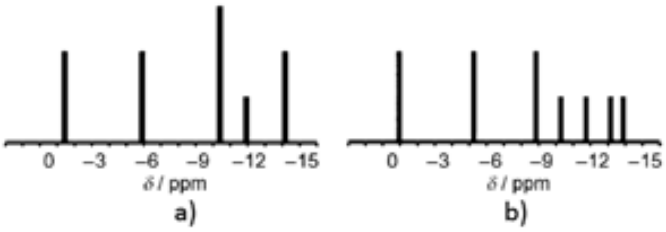

Figure 1.10. Computed $^{11}B\{^1H\}$-NMR spectra for a) [Li(Et_2O)$_2$][1,2-$C_2B_{10}H_{11}$] (**IV**) and b) [Li(Et_2O)$_3$][1,2-$C_2B_{10}H_{11}$] (**V**).

match as properly as for **IV**. The computed spectra display a six and five peaks pattern, respectively, contrarily to the experimental one, that have a four peak pattern.

As a proof of concept the $^{11}B\{^1H\}$-NMR computed spectrum for **II** was calculated and compared with the one for **IV** (Figure 1.10.). Despite having the same ether solvent, the matching with the experimental spectrum of $Li[1,2\text{-}C_2B_{10}H_{11}]$ in Et_2O is now poor for **II**, fact that supports the adequacy of the comparison method.

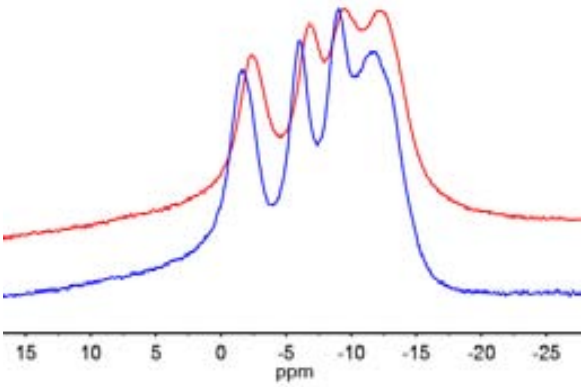

Figure 1.11. $^{11}B\{^1H\}$-NMR spectra for $Li[1,2\text{-}C_2B_{10}H_{11}]$ at -80°C in Et2O (red) and THF (blue).

To our view the good matching of **IV** computed and experimental $^{11}B\{^1H\}$-NMR spectra is not accidental. It agrees well with all experimental evidence given before. Diethyl ether is the oxy-solvent, of the three studied here, that has lower AN and thus is more prone than THF or DME to produce a contact ion pair between Li^+ and $[C_2B_{10}H_{11}]^-$. On the other hand THF and DME have larger DN and AN than Et_2O, and thus are more suitable to produce separate ion pairs. Of the three computed structures **IV**, **I** and **V**, only **IV** meets the experimental criteria discussed, to say a contact ion pair for the solvent studied; conversely, the structures **I** and **V** do not represent properly the separate ion pair concept, and is thus reasonable that the matching of the calculated and experimental spectra of these structures **I** and **V** is poor.

The low temperature $^{11}B\{^1H\}$-NMR spectra for $Li[1,2\text{-}C_2B_{10}H_{11}]$ in Et_2O and THF give somehow similar results. The five pick pattern observed at room temperature when using Et_2O as solvent disappear, and at -80°C, a four picks pattern is observed, as in case of THF (Figure 1.11.).

1.6. *Post-reaction Li^+ influence. Reaction of carboranyllithium with allylbromide*

The forward experimental and theoretical results have provided some insights on the factors that govern the formation of Li^+ contact or solvent separated ion-pair. For that, we wanted to extend our study to the reaction with $BrCH_2CHCH_2$ in three solvents Et_2O, THF and DME and to observed the effect of lithium as a polarizing ion. The choice of allylbromide ($BrCH_2CHCH_2$) is not random since unexpected results have been observed experimentally. It should, in principle, give the

Entry	Solvent	T (°C)	Yield of allyl derivative [%]		
			o-carborane	methyl-*o*-carborane	phenyl-*o*-carborane
1	THF	25	-	86	-
2	THF	40	-	80	-
3	THF	70	95	50	100
4	Et_2O	40	100	100	100
5	DME	40	-	66	-
6	DME	85	85	75	50
7	Et_2O:Toluene (1:2)	40	-	100	-
8	Et_2O:Toluene (1:2)	100	100	100	100
9	Toluene	110	Unknown mixture	-	Unknown mixture

Table 1.6. Molar fraction of the allyl derivative of *o*-carborane, methyl-*o*-carborane and phenyl-*o*-carborane in different reaction conditions.

same type of reaction as chlorodipheylphosphine ($ClPPh_2$), but due to the presence of the allyl moiety, it gives the allyl derivative of carborane or the propenyl derivative, depending on the solvent. To confirm the results obtained with Li[1,2-$C_2B_{10}H_{11}$], we have extended the study to other C_C-substituted carboranes, such as Li[2-R-1,2-$C_2B_{10}H_{10}$] R= Me, Ph. In all reactions the concentration of *o*-carborane was 0.30 mol·L^{-1}.

The general procedure for these reactions consists in mixing the corresponding carborane with 1 equivalent of *n*-BuLi at 0 °C, to produce the monolithium salt,[18] and subsequently add the stoichiometric amount of CH_2=CH-CH_2-Br. The reaction was also performed at different temperatures (Table 1.6.). Considering that the expected mechanism for the reaction with CH_2=CH-CH_2-Br should be basically similar to the reaction of carboranyl lithium with $ClPPh_2$, of the three solvents the best performing should be Et_2O and indeed this is the case. From data gathered from ^{1}H-NMR spectra (Table 1.6.), for all carboranes 1-R-1,2-$C_2B_{10}H_{11}$ (R= H, Me, Ph) the reaction in Et_2O led to the C_c-CH_2-CH=CH_2 substituted compound as unique product (Entry 4 in Table 1.6.). Nevertheless, when THF or DME were used as solvents a mixture of isomers was obtained, having either the fragments C_C-CH_2-CH=CH_2, allyl isomer, or the C_C-CH=CH-CH_3, propenyl isomer, respectively. The ratio of the propenyl versus the allyl isomer depends on the solvent and reaction temperatures, being the propenyl most favorable at higher temperatures. For example, in THF at 70 °C the ratio allyl/propenyl is 1:1, at 40 °C the ratio has decreased to 4/1, whereas at room temperature the ratio 7/1 was obtained according to the ^{1}H-NMR spectra. The importance of crowdedness near the reaction site, for the isomerisation process, can be well visualized comparing different carboranes, 1-R-1,2-$C_2B_{10}H_{11}$(R =H, Me, Ph). Interestingly, the degree of isomerization allyl/propenyl parallels the bulkiness of the R group. Thus, in the most favorable conditions, the percentage of isomerization is 15%, 50% and 60% for R =H, Me, and Ph, respectively.

To the best of our knowledge this isomerisation reaction has not previously been reported mediated by Li^+. This isomerization usually proceeds by acid, base, or organometallic complexes, giving in general, the thermodynamically stable compound.[19] Our view of the phenomenon relates again with the donor and acceptor numbers (DN, AN) characteristics of the solvent, and also to the formation of Li^+ contact ion pair. As for $ClPPh_2$, the substitution of the bromine atom in CH_2=CH-CH_2-Br by the anion [1-R-$C_2B_9H_{10}$]$^-$ most probably follows a S_N2 mechanism (Scheme 1.5.). Our interpretation of the isomerization is that one intermediate similar to this shown in Scheme 1.5. is formed in which the interactions of the anion [1-R-$C_2B_9H_{10}$]$^-$ and the cation Li^+ with CH_2=CH-CH_2-Br are very relevant. They depend largely on the degree of contact ion pair formed, that in its turn depends on the solvent. In Et_2O, the solvent with lowest AN (Table 1.3.), the carboranyl acts as a stronger nucleophile than in THF facilitating the interaction with the electrophile to quickly remove the bromine and give the pure allyl-carborane derivative. On the contrary, when THF or DME are used, due to a larger degree of solvent separated ion pair, the Li^+ is more prone to interact with the allyl system easing the isomerisation. The resulting cation interacts subsequently with the carboranyl fragment leading to the

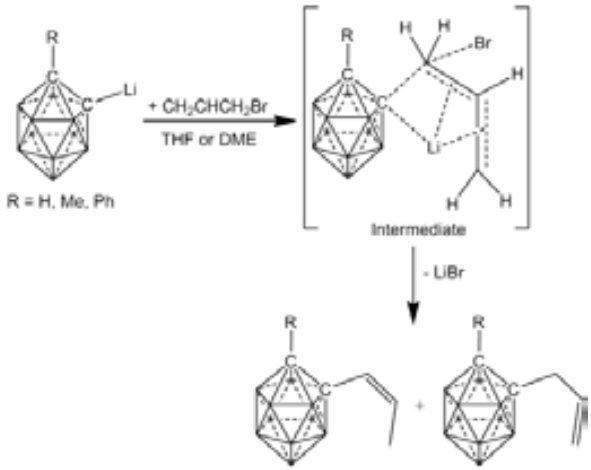

Scheme 1.5. Reaction of carboranyllithium with allyl bromide.

formation of the C_C-C bond. We consider that the isomerisation and the C_C-C bond formation occur sequentially in the reaction timescale, as the allyl did not isomerizes when placed in contact with Li^+, even in DME.

The disproportionation of $Li[1,2\text{-}C_2B_{10}H_{11}]$ into $Li_2[1,2\text{-}C_2B_{10}H_{10}]$ and $1,2\text{-}C_2B_{10}H_{12}$ in ethereal solvents is consequence of the formation of contact ion pair, and in less extent of separated ion pair. In the contact ion pair a large degree of covalent C_C-Li(solvated) bond can be assumed. All ethereal solvents, Et_2O, THF and DME, studied generate contact ion pair; however THF and DME tend to produce carboranyllithium ion pair with a slightly higher degree of separated ion pair than Et_2O. The different degree of contact or separated ion pair is significant to facilitate mono- or disubstitution but is strongly influenced by the reagent type. In reactions in which a halide is generated as with $ClPPh_2$, Et_2O appears to produce the largest degree of monosubstitution. In other situations, such as with S_8, or when no halide is generated, THF or DME facilitate the largest degree of monosubstitution, although the difference with Et_2O is small. It has been shown that upon the self reaction of $Li[1,2\text{-}C_2B_{10}H_{11}]$ to produce $[LiC_4B_{20}H_{22}]^-$, the nucleophilicity of the carboranyllithium can even be further enhanced, besides the ethereal solvent, by synergism with halide salts. The Li^+ mediated isomerization has also been demonstrated to be dependent on the ethereal solvent utilized. Et_2O tends to not induce isomerization on allyl substituents; conversely THF or DME produce isomerization. The results presented here most

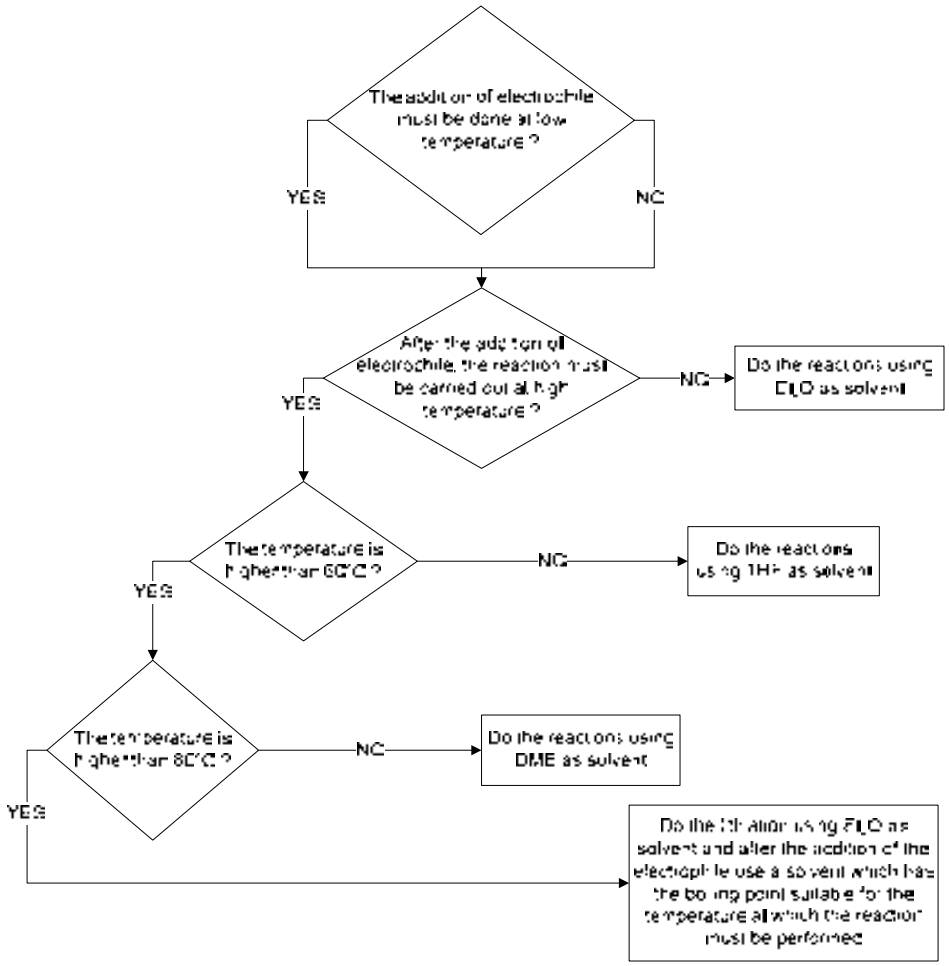

Figure 1.12. Reaction planning algorithm for discriminating between the ethereal solvents.

probably can be extended to other molecular types to interpret the Li^+ mediation in C-C or other C-X couplings. Based on these results, in Figure 1.12. is presented a general algorithm that serves for discrimination between the studied ethereal solvents when planning syntheses conditions.

[1] Zakharkin, L. I.; Grebennikov, A. V.; Kazantzev, A. V. *Izv. Akad. Nauk SSSR, Ser. Khim*, **1963**, 2077.
[2] Gomez, F. A.; Hawthorne, M. F. *J. Org. Chem.*, **1992**, *57*, 1384.
[3] Viñas, C.; Benakki, R.; Teixidor, F.; Casabo, J. *Inorg. Chem.*, **1995**, *34*, 3844.
[4] Musteti, A. D. *Oxy solvents influence on $C_{Cluster}$-monosubstituted derivatives of 1,2-dicarba-closo-dodecaborane synthesis with sulphur and chlorodiphenylphosphine*. Master Diseratation. Universitat Autònoma de Barcelona. **2009**.
[5] Gutmann, V. *Coord. Chem. Rev.*, **1976**, *18*, 225.
[6] a) Leroy, B.; Marko, I.E. *J. Org. Chem.*, **2002**, *67*, 8744. b) Katritzky, A.R.; Xu, Y.-J.; Jian, R. *J. Org. Chem.*, **2002,** *67*, 8234. c) Fraenkel, G.; Duncan, J.H.; Martin, K.; Wang, J.; *J. Am. Chem. Soc.*, **1999**, *121*, 10538. d) Streitwieser, A.; Juaristi, E.; Kim, Y.-J.; Pugh, J. *Org. Lett.*, **2000**, *2*, 3739. e) Hoffmann, D.; Collum, D. B. *J. Am. Chem. Soc.*, **1998**, *120*, 5810.
[7] a) Gérard, H.; de la Lande, A.; Maddalunu, J.; Parisel, O.; Tuckerman, M. E. *J. Phys. Chem. A,* **2006**, *110*, 4787. b) Declerck, R.; De Sterck, B.; Verstraelen, T.; Verniest, G.; Mangelinckx, S.; Jacobs, J.; De Kimpe, N.; Waroquier, M.; Van Speybroeck, V. *Chem. Eur. J.*, **2009**, *15*, 580.
[8] a) Pratt, L. M.; Ramachandran, B.; Xidos, J. D.; Cramer, C. J.; Truhlar, D. G. *J. Org. Chem.*, **2002**, *67*, 7607. b) Pratt, L. M.; Truhlar, D. G.; Cramer, C. J.; Kass, S. R.; Thompson, J. D.; Xidos, J. D. *J. Org. Chem.*, **2007**, *72*, 2962. c) Pratt, L. M.; Jones, D.; Sease, A.; Busch, D.; Faluade, E.; Nguyen, S. C.; Thanh, B. T. *Int. J. Quantum Chem.*, **2009**, *109*, 34. d) Dixon, D. D.; Tius, M. A.; Pratt, L. M. *J. Org. Chem.*, **2009**, *74*, 5881. e) Pratt, L. M.; Mogali, S.; Glinton, K. *J. Org. Chem.*, **2003**, *68*, 6484. f) Pratt, L. M.; Mu, R. *J. Org. Chem.*, **2004**, *69*, 7519. g) Pratt, L. M.; Mu, R.; Jones, D. R. *J. Org. Chem.*,**2005**, *70*, 101.
[9]Quantum-chemical calculations were performed with the Gaussian 03 commercial suite of programs at DFT level of theory with B3LYP hybrid functional adopting for all the atoms the 6-31G+(d,p) basis set
[10] Hermanek, S. *Chem. Rev.*, **1992**, *92*, 325; *Inorg. Chim. Acta*, **1999**, *289*, 20.
[11] Willans, C. E.; Kilner, C. A.; Fox, M. A. *Chem. Eur. J.*, **2010**, *16*, 10644.
[12] a) Piller, F. M.; Appukkuttan, P.; Gavryushin, A.; Helm, M.; Knochel, P. *Angew. Chem. Int. Ed.*, **2008**, *47*, 6802. b) Rohbogner, C. J.; Clososki, G. C.; Knochel, P. *Angew. Chem. Int. Ed.*, **2008**, *47*, 1503.
[13] Lucht, B. L.; Collum, D. B. *Acc. Chem. Res.***1999**, *32*, 1035.
[14] a) Izatt, R. M.; Bradshaw, J. S.; Dalley, N. K. *Chem. Rev.*, **1991**, *91*, 137. b) Weiss, E. *Angew. Chem. Int. Ed.*, **1993**, *32*, 1501. c) Gessner, V. H.; Däschlein, C.; Strohmann, C. *Chem. Eur. J.*, **2009,** *15*, 3320.
[15] Search performed on September 18th, 2012.
[16] a) For CSD see: Allen, F. H. *Acta Crystallogr. B*, **2002**, *58*, 380. b) For ConQuest program see: Bruno, I. J.; Cole, J. C.; Edgington, P. R.; Kessler, M.; Macrae, C. F.; Pearson, J.; Taylor, R. *Acta Crystallogr. B*, **2002**, *58*, 389.
[17] a) Clegg, W.; Brown, D. A.; Bryan, S. J.; Wade, K. *Polyhedron*, **1984**, *3*, 307. b) Dröse, P.; Hrib, C. G.; Edelamnn, F. T. *J. Am. Chem. Soc.*, **2010**, *132*, 15540.
[18] a) González-Campo, A.; Viñas, C.; Teixidor, F.; Núñez, R.; Kivekäs, R.; Sillanpää, R. *Macromolecules*, **2007**, *40*, 5644. b) González-Campo, A.; Juárez-Pérez, E. J.; Viñas, C.; Boury, B.; Kivekäs, R.; Sillanpää, R.; Núñez, R. *Macromolecules*, **2008**, *41*, 8458.
[19] a) Deryagina, E. N.; Korchevin, N. A. *Russ. Chem. Bull*., **1996**, *45*, 223. b) Wakamatsu, H.; Nishida, M.; Adachi, N.; Mori, M. *J. Org. Chem.*, **2000**, *65*, 3966.

2. Study on the oxidation of *closo*-carboranylphosphines

Since their discovery more than half a century ago, phosphines became notorious ligands. They can be tailored "on demand" by changing the moieties bonded to the phosphorus atom, altering in this way their steric and electronic properties in a systematic and predictable manner. Apart from the phosphines, their chalcogenides also present interest due to their key role in catalytic mechanisms.[1] Compounds as R_3PE, $[RP(E)(ESiMe_3)_2]$, $[\{RP(E)(\mu\text{-}E)\}_2]$ (E= S, Se and R= organic group), were found to be useful starting materials for metal chalcogenide nanoparticles,[2] molecular complexes with P-chalcogen ligands[3] and chalcogen-transfer reactions.[4] Several different sources of chalcogen have been used to obtain soluble chalcogen-containing compounds, although the simplest sources is elemental chalcogen (E = S, Se, Te).[5]

Our group is interested in the synthesis of carborane derivatives with electron rich moieties bonded *exo*-cluster, due to their potential in metal catalysis.[6] Although it is known the affinity of the phosphines towards chalcogens and the drawback that present the destruction of the transition metal catalysts through oxidation of the phosphorus containing ligands, we found a surprisingly lack of studies on these reactions, especially for the carborane derivatives. Previous to our study [7] in the Cambridge Crystallographic Database[8] only four crystal structures for carboranylphosphines oxides[9] and only one crystal structure for carboranylphosphine sulfide[10] were found, and there were no reported structures for a carboranyl moiety containing a phosphorus-selenium bond.[11] This motivated us to start a systematic and comprehensive investigation on the oxidation of carboranylphosphines and further to study their properties as ligands.

2.1. Oxidation of *closo*-carboranylmono- and *closo*-carboranyldiphosphines

2.1.1. Synthetic aspects on the oxidation of *closo*-carboranylmonophosphines

Our group showed some time ago, that in contrast to other common phosphines, *closo*-carboranylmonophosphines 1-PR_2-2-R'-1,2-*closo*-$C_2B_{10}H_{10}$ present high stability in the solid state and in solution, under air or in the presence of mild oxidizing agents, alcohols and some acids.[12] The basicity/nucleophilicity of the P atoms in *closo*-carboranyldi- and *closo*-carboranylmonophosphines is influenced by the strong electron-acceptor character of the *o*-carborane through the C_C atoms. This makes the carboranylphosphines resistant towards partial degradation, and confers a high chemical stability, making difficult the coordination of the P atoms to transition metal ions.[13]

The phosphines can be tuned in a predictable manner by changing the R moieties bonded to P atom. With this scope we studied the oxidation of different *closo*-carboranylmonophosphines with hydrogen peroxide (Scheme 2.1.). By changing the moieties directly bonded to phosphorus from aryl groups (e.g. Ph) to alkyls groups (e.g. ^{i}Pr, Cy) the time of the reaction was modified from 18 h to 1,5 h. When the other C_C atom from carborane is substituted by a methyl or a phenyl group no improvement in the reaction time is observed, whereas the presence of a high electron donating group like a thioether group definitely alter the

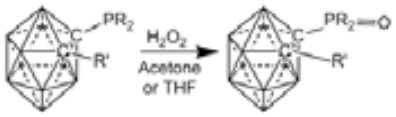

R= Ph, R'= Me (**10**); R= iPr, R'= Me (**11**); R= Cy, R'= Me (**12**).
R= Ph, R'= Ph (**13**); R= iPr, R'= Ph (**14**); R= Ph, R'= SBz (**15**).

Scheme 2.1. Reaction of carboranylmonophosphines with hydrogen peroxide.

reaction rate. In this way, changing the Me or Ph moieties from the second C_C atom, with SBz group, the time of the reaction decrease to 25 minutes.

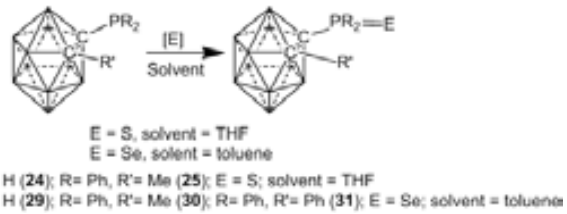

Scheme 2.2. Reaction of carboranylmonophosphines with chalcogens.

The rate of the reaction of carboranylmonophosphines with sulphur and selenium (Scheme 2.2.) are different of the one with hydrogen peroxide, the oxidation being completed after a longer time. With selenium the total oxidation is achieved after 1 day, whereas for sulphur several days are needed. In the literature, studies on the oxidation of phosphines with selenium are scarce. We used the commercial form of selenium, which is the vitreous black allotropic form. This form comprises an extremely complex and irregular structure of large polymeric rings having up to 1000 atoms per ring,[14] and so, a rationalization of reaction mechanism of the oxidation of the phosphines with Se is complicated. On the other hand, studies of the reaction of phosphines with sulphur can be found in the literature. The reactions of tertiary phosphines with sulphur are in general very fast, contrary to the reactions of carboranylmonophosphines.

The mechanism of the reaction of triphenylphosphine with sulphur was studied more than 60 years ago[15] and was also extended to other tricoordinate phosphorus compounds.[16] It is proposed as a process in steps, which begin by a nucleophilic displacement of sulphur on sulphur by the phosphorus atom of phosphine, opening the sulphur ring. The positive charge is retained by the P atom and the negative charge is displaced on the S atom (Scheme 2.3.). The stability of the orthorhombic α-form of sulphur, which consist in a eight member ring, is superior of other forms of sulphur[17] and consequently, the rate determining step in the oxidation reactions is the cleavage of the ring. After this step, there are other seven successive steps which follow the same nucleophilic displacement mechanism.

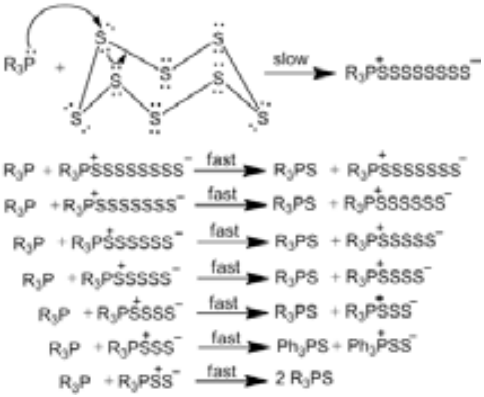

Scheme 2.3. Proposed mechanism of the reaction of phosphines with sulphur

This mechanism can be extrapolated to carboranylmono- and carboranyldiphosphines also, and the longer reaction times compared with triphenylphosphine can be rationalized in the terms of nucleophilicity of the P atoms. Taking into consideration the above described mechanism, the reaction time of carboranylphosphines oxidation with sulphur can be lowered if the stable eight member ring of sulphur is cleaved before reacting with the carboranylphosphine. In order to test this hypothesis, we added 10 equivalents of LiCl over a mixture of 1 equivalent of 1-PPh_2-1,2-*closo*-$C_2B_{10}H_{11}$ (**8**) and 4 equivalents of S_8 in THF. The reaction time was lowered from 2 days with no LiCl to 8 h in the presence of LiCl. This result indicates that the rate determining step is the cleavage of the S_8 ring. Even more, the enhancement of the reaction rate of the oxidation of carboranylphosphines with sulphur was also recently reported by others, using as additives bases as triethylamine.[18]

To further understand the different reactivity of carboranylmonophosphine, 1-PPh_2-1,2-*closo*-1,2-$C_2B_{10}H_{11}$ (**8**), respect to the triphenylphosphine, we undertook a computational study based on NBO analysis, that is reported in Section 2.2.2.

2.1.2. Synthetic aspects on the oxidation of *closo*-carboranyldiphosphines

Oxidation of carboranyldiphosphines follows the general trends observed for the carboranylmonophosphines. With hydrogen peroxide the reaction time also depends of the substituent of the P atom. So, the oxidation of 1,2-$(PPh_2)_2$-1,2-*closo*-$C_2B_{10}H_{10}$, **9**, with H_2O_2 in acetone takes 4 h, whereas, for 1,2-$(P^iPr_2)_2$-1,2-*closo*-$C_2B_{10}H_{10}$, **14**, the reaction is completed after 15 minutes (Scheme 2.4.). The reaction time is important since if it is prolonged the deboronation of the cluster starts, as will be presented further.

Scheme 2.4. Reaction of carboranyldiphosphines with hydrogen peroxide.

The importance of the substituents at the phosphorus atom can be further observed for the oxidation of carboranyldiphosphines with sulphur and selenium. When using sulphur, **9** produced three different species after purification by preparative thin layer chromatography (silica gel, CH_2Cl_2/hexane 8:2): 1-$SPPh_2$-2-PPh_2-1,2-*closo*-$C_2B_{10}H_{10}$ (**26**), 1,2-$(SPPh_2)_2$-1,2-*closo*-$C_2B_{10}H_{10}$ (**36**) and 1-$SPPh_2$-2-$OPPh_2$-1,2-*closo*-$C_2B_{10}H_{10}$ (**37**) (Scheme 2.5.a). Conversely, **14** produced the species 1-P^iPr_2-2-SP^iPr_2-1,2-*closo*-$C_2B_{10}H_{10}$ (**28**) with just one phosphorus atom oxidized after 4 h refluxing. One of the -P^iPr_2 bonds on the parent diphosphine was cleaved after 48 h at reflux yielding 1-SP^iPr_2-1,2-*closo*-$C_2B_{10}H_{11}$ (**27**) (Scheme 2.5.a).

Oxidation of **9** with elemental black selenium powder in refluxing toluene leads to a species with just one selenophosphoryl group while the second group in the molecule remains intact, 1-$SePPh_2$-2-PPh_2-1,2-*closo*-$C_2B_{10}H_{10}$ (**32**). Prolonged reflux of this mixture does not oxidize the remaining phosphine group. This differs to the oxidation with sulphur where two thiophosphoryl groups were produced. Conversely, selenium oxidation reaction of **14** splits a C_c-P bond yielding 1-SeP^iPr_2-1,2-*closo*-$C_2B_{10}H_{11}$ (**33**) (Scheme 2.5.b).

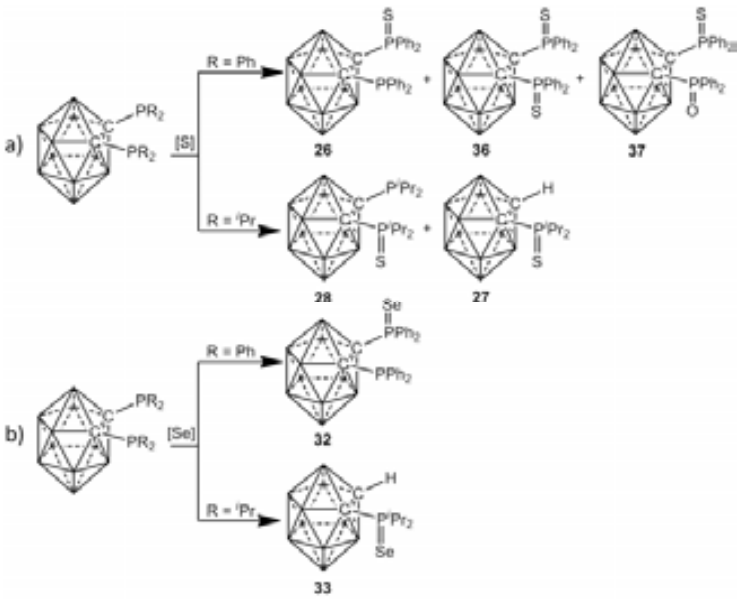

Scheme 2.5. Reaction of carboranyldiphosphines with sulphur and selenium.

2.1.3. Characterization and structural aspects on the oxidized *closo*-carboranylphosphines

All the compounds were characterized by multinuclear NMR spectroscopy (^1H, $^1H\{^{11}B\}$, ^{11}B, $^{11}B\{^1H\}$, $^{13}C\{^1H\}$, $^{31}P\{^1H\}$), infrared spectroscopy and, where possible by X-ray diffraction.

The FTIR spectra of the compounds offered the first information on the success of the oxidation reactions, showing the BH stretches in the range 2644-2550 cm^{-1} that offers information about the nature of the carborane cage, supporting the *closo* cluster structure. The strong and sharp absorptions in

the range 1214-1081, 690-652 or 697-687 cm^{-1} were the first information on the nature of the phosphine moiety, confirming the oxidation with O, S and Se, since these absorptions are characteristic of the P=O, P=S and P=Se stretches, respectively. Additionally, the IR spectrum of **27** showed a strong stretch absorption at 3029 cm^{-1} that confirms the presence of C_C-H bond, and so was the first clue that one C_C-P bond was cleaved upon the oxidation of **14** with sulphur.

The $^{11}B\{^1H\}$-NMR spectroscopy brought information both on the symmetry and the cluster structure of the oxidized species. The 2:4:4 or 2:2:6 pattern with the chemical shifts from +1.7 ppm to –12.0 ppm, fully supports a symmetric *closo* structure while the 1:1:8, 1:1:4:4, 1:1:5:3 or 1:1:2:4:2 pattern with the chemical shifts in the range +3.0 /–10.4 ppm, indicates, beside the *closo* nature of the cluster, also an unsymmetrical compounds that comes from the C_c asymmetric substitution. Only minor differences with regard to the starting carboranylphosphines have been observed in the $^{11}B\{^1H\}$-NMR spectra of the oxidized species (Figure 2.1). It is worth noticing, though, that the resonance corresponding to the antipodal boron atoms (B9 and B12) has been shifted to lower field with regard to the non-oxidized starting ones.

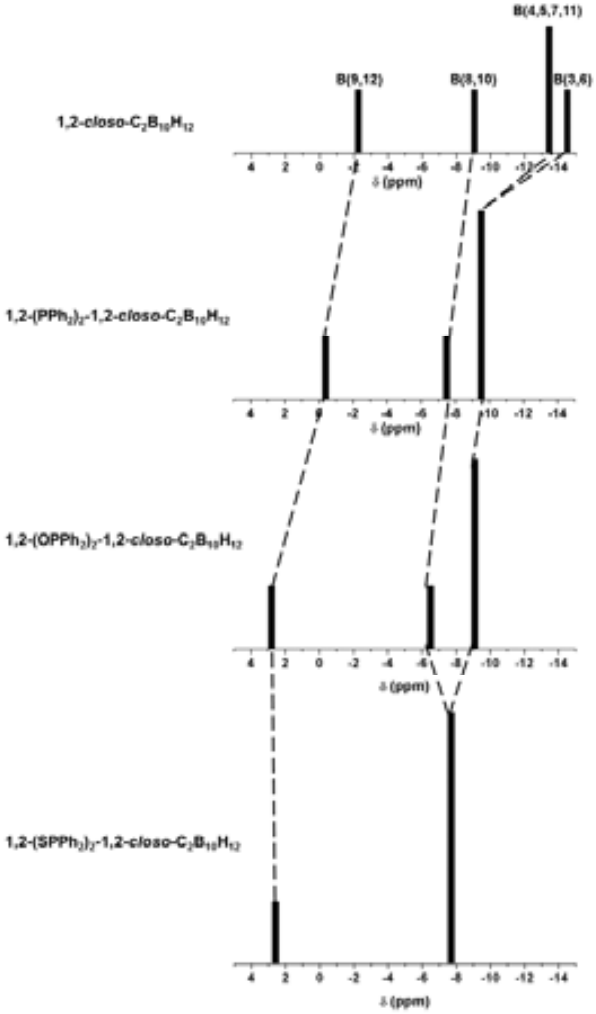

Figure 2.1. Stick representation of the $^{11}B\{^1H\}$-NMR chemical shifts for *o*-carborane, its phosphine derivative and oxygen and sulphur oxidized carboranyldiphosphine.

For all oxidized species the *closo* cluster structure has been preserved despite the oxidation state has changed from P(III) to P(V). Table 2.1. shows the $^{31}P\{^1H\}$-NMR chemical shift of oxidized compounds, where can be seen that all the oxidized carboranylphosphines appear at lower field than the resonance corresponding to the phosphine precursors. For the carboranylmonophosphine oxides it can be observed that $^{31}P\{^1H\}$-NMR chemical shifts are modulated by the substituent at the phosphorus atom, following the trend: Ph<Cy<^{i}Pr. If the same substituent is presented at the P atom, but the substituent at the other C_C atom is changed, then the deshielding of the $^{31}P\{^1H\}$-NMR chemical shift for the carboranylmonophosphine oxides follow the order: Ph<Me<SBz<PPh_2. Also, for carboranylmono- and carboranyldiphosphine chalcogenides, it can be observed that the deshielding capacity on the $^{31}P\{^1H\}$-NMR chemical shift follows the tendency S>Se>O.

P(III)-compounds	δ (ppm)	P(V)-compounds	δ (ppm)	Δ δ (ppm)
1-PPh_2-2-H-1,2-*closo*-$C_2B_{10}H_{10}$ (**8**)	25.83	1-$SPPh_2$-2-H-1,2-*closo*-$C_2B_{10}H_{10}$ (**24**)	52.19	+26.36
		1-$SePPh_2$-2-H-1,2-*closo*-$C_2B_{10}H_{10}$ (**29**)	52.21	+26.38
1-PPh_2-2-Me-1,2-*closo*-$C_2B_{10}H_{10}$ (**10**)	11.18	1-$OPPh_2$-2-Me-1,2-*closo*-$C_2B_{10}H_{10}$ (**18**)	19.28	+8.10
		1-$SPPh_2$-2-Me-1,2-*closo*-$C_2B_{10}H_{10}$ (**25**)	47.65	+36.85
		1-$SePPh_2$-2-Me-1,2-*closo*-$C_2B_{10}H_{10}$ (**30**)	45.10	+34.3
1-PPh_2-2-Ph-1,2-*closo*-$C_2B_{10}H_{10}$ (**11**)	12.66	1-$OPPh_2$-2-Ph-1,2-*closo*-$C_2B_{10}H_{10}$ (**19**)	19.65	+6.99
		1-$SePPh_2$-2-Ph-1,2-*closo*-$C_2B_{10}H_{10}$ (**31**)	45.06	+32.16
1-PPh_2-2-SBz-1,2-*closo*-$C_2B_{10}H_{10}$ (**12**)	11.17	1-$OPPh_2$-2-SBz-1,2-*closo*-$C_2B_{10}H_{10}$ (**20**)	21.87	+10.70
1,2-$(PPh_2)_2$-1,2-*closo*-$C_2B_{10}H_{10}$ (**9**)	8.22	1,2-$(OPPh_2)_2$-1,2-*closo*-$C_2B_{10}H_{10}$ (**34**)	23.67	+15.45
		1,2-$(SPPh_2)_2$-1,2-*closo*-$C_2B_{10}H_{10}$ (**36**)	48.65	+40.43
		1-$SPPh_2$-2-PPh_2-1,2-*closo*-$C_2B_{10}H_{10}$ (**26**)	49.16	+40.94
			12.77	+4.43
		1-$SPPh_2$-2-$OPPh_2$-1,2-*closo*-$C_2B_{10}H_{10}$ (**37**)	49.96	+41.74
			21.65	+13.43
		1-$SePPh_2$-2-PPh_2-1,2-*closo*-$C_2B_{10}H_{10}$ (**29**)	46.48	+38.26
			10.48	+2.26
1-P^iPr_2-2-H-1,2-*closo*-$C_2B_{10}H_{10}$ (**13**)	54.20	1-SP^iPr_2-2-H-1,2-*closo*-$C_2B_{10}H_{10}$ (**28**)	77.90	+23.74
		1-SeP^iPr_2-2-H-1,2-*closo*-$C_2B_{10}H_{10}$ (**33**)	83.67	+29.51
1-P^iPr_2-2-Me-1,2-*closo*-$C_2B_{10}H_{10}$ (**15**)	33.82	1-OP^iPr_2-2-Me-1,2-*closo*-$C_2B_{10}H_{10}$ (**21**)	58.18	+24.36
1-P^iPr_2-2-Ph-1,2-*closo*-$C_2B_{10}H_{10}$ (**16**)	38.50	1-OP^iPr_2-2-Ph-1,2-*closo*-$C_2B_{10}H_{10}$ (**22**)	53.27	+14.77
1,2-$(P^iPr_2)_2$-1,2-*closo*-$C_2B_{10}H_{10}$ (**14**)	32.79	1,2-$(OP^iPr_2)_2$-1,2-*closo*-$C_2B_{10}H_{10}$ (**35**)	59.08	+26.29
		1-SP^iPr_2-2-P^iPr_2-1,2-*closo*-$C_2B_{10}H_{10}$ (**28**)	78.0	+45.21
			35.5	+2.71
1-PCy_2-2-Me-1,2-*closo*-$C_2B_{10}H_{10}$ (**17**)	29.85	1-$OPCy_2$-2-Me-1,2-*closo*-$C_2B_{10}H_{10}$ (**23**)	48.84	+18.99

Table 2.1. $^{31}P\{^1H\}$-NMR chemical shifts for the *closo*-carboranylphosphines and their oxides and chalcogenides.

The $^{31}P\{^1H\}$-NMR spectroscopy has been an useful tool for corroborating the P oxidation state, the presence of a Se bonded to P and the asymmetry of the oxidized species. As an example, $^{31}P\{^1H\}$-NMR of **32** shows two doublets at δ = 46.48 ppm and 10.48 ppm with a coupling constant $^3J(P,P)$= 27 Hz (Figure 2.2.). The resonance at δ = 46.48 ppm suggests the formation of a P-Se bond whereas the signal at δ = 10.48 ppm corresponds to non-oxidized phosphorus. Evidence for the formation of the P-Se bond can be drawn from the $^{31}P\{^1H\}$ NMR spectra of the $SePR_2$(Carboranyl) compounds. Upon prolonged recording times, two satellite lines due to the $^1J(^{31}P,^{77}Se)$ become visible, indicating the presence of a P-

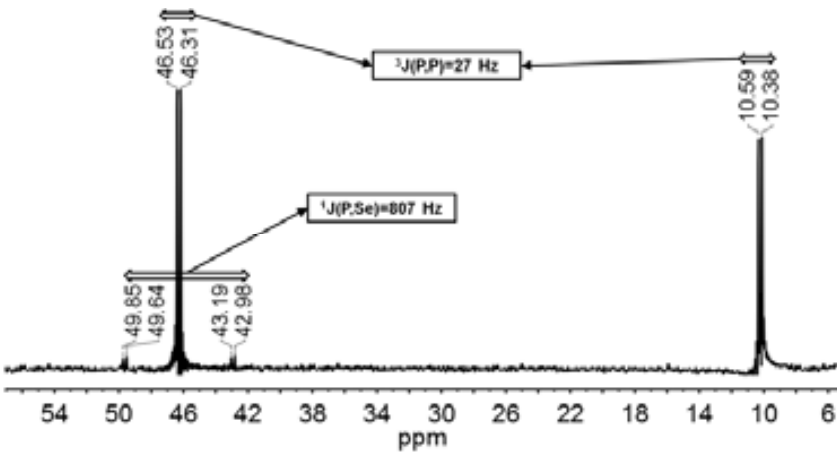

Figure 2.2. $^{31}P\{^1H\}$-NMR spectrum for 1-$SePPh_2$-2-PPh_2-1,2-$C_2B_{10}H_{10}$ showing P-P and P-Se spin coupling.

Se bond. The coupling constants $^{1}J(^{31}P,^{77}Se)$ can reach high values ranging from 200 to 1100 Hz. A large $^{1}J(^{31}P,^{77}Se)$ value indicates a strong electron withdrawing capacity of the substituents attached to the phosphorus atom,[19] an increased *s* character for the phosphorus lone pair[20] and a more positive P atom.[21] The ^{77}Se satellites, $^{1}J(^{31}P,^{77}Se)$= 807 Hz, that are centred at 46.48 ppm confirm the P-Se bond formation (Figure 2.2.). The $^{31}P\{^{1}H\}$ NMR resonances for **29**, **30**, **31** and **32** appear at higher frequency (52.21, 45.10, 46.48 and 45.06 ppm, respectively) than the $SePPh_3$ (δ= 35.8 ppm).[22] In addition, the coupling constant value $^{1}J(^{31}P,^{77}Se)$= 730 Hz for $SePPh_3$[23] is smaller than $^{1}J(^{31}P,^{77}Se)$= 797 Hz, $^{1}J(^{31}P,^{77}Se)$= 804 Hz, $^{1}J(^{31}P,^{77}Se)$= 812 Hz and $^{1}J(^{31}P,^{77}Se)$= 807 Hz for $SePPh_2$(Carboranyl) **29**, **30**, **31** and **32** respectively, indicating once again that a carboranyl group displays stronger electron-acceptor character than a phenyl group.[12] Some minor tuning due to the substituent at the second cluster carbon (H, **29**, Me, **30**, Ph, **31** or PPh_2, **32**) is produced.

The oxidation 1-PPh_2-2-SBz-1,2-*closo*-$C_2B_{10}H_{10}$ with hydrogen peroxide offered the possibility to observed the competitive oxidation of S/P, each connected to one of the adjacent C_C atoms. Our target was to demonstrate that the P atom at the C_c-PPh_2 vertex was most susceptible to oxidation with H_2O_2 than the S atom at the tioether C_C-SBz, and indeed this was the case, as proven by IR and $^{31}P\{^{1}H\}$ NMR spectroscopies.

For the carboranylmonophosphine oxides **18** and **23** the X-ray structure was obtained (Figure 2.3.). The structures were similar, diverging from one another in the six-member ring at the phosphorus atoms: a planar phenyl rings in **18** and the cyclohexyl rings with normal *chair* conformation in **23**. Slight differences in the P-C bonds originate from the aromatic and aliphatic carbons connected to phosphorus atoms. The P-O bond lengths were 1.476 and 1.486 Å for **18** and for **23.** Interestingly, if the P-O bonds are calculated using the covalent radii proposed by Pyykkö[24] the value for a P-O double bond is of 1.59 Å, whereas for the P-O triple bond the value is 1.47 Å, which fits better with the experimental results. The oxygen atom in each compound pointed to the methyl group, the C2-C1-P-C25 torsion angle values were –39.41(15)° for **18** and –40.1(2)° for **23**. These conformations arise from the existence of weak intramolecular H-bonds between a methyl hydrogen atom and the oxygen atom in each compound (H···O distances are 2.39 and 2.34 Å for **18** and **23**). In **18** there are also two short H···O distances of 2.51Å from phenyl hydrogen atoms to the oxygen atom indicating weak intramolecular H-bonds (the C-H···O angles are 108 and 109°) and in **23** there is also an intramolecular H···O contact (2.60 Å) (the C-H···O angle is 109°). Weak intermolecular H···O bonds controlled the crystal packing of **18** and **23** (the shortest intermolecular H···O distances were 2.76 and 2.45 Å respectively).

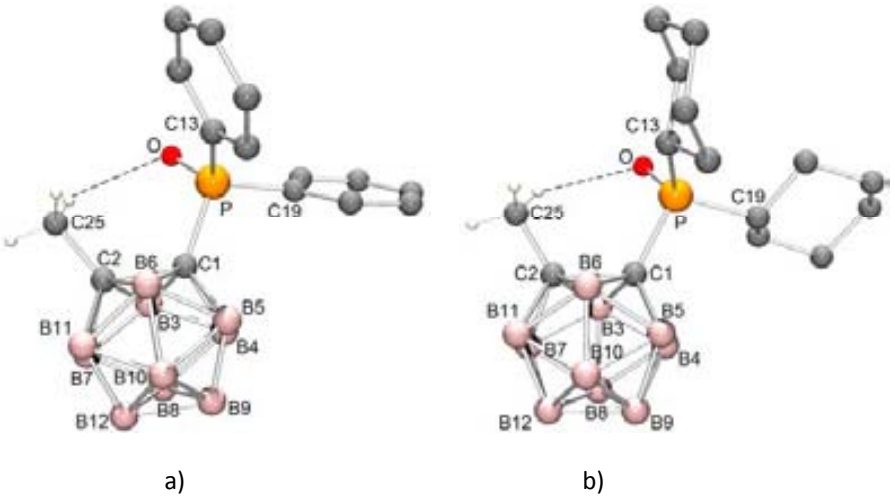

Figure 2.3. Molecular structure of a) **18** and b) **23**. (The hydrogen atoms are omitted for clarity, except those of the methyl group).

For the carboranyldiphosphine chalcogenides **26**, **37** and **32**, X-ray structure was also determinated.

The structural analysis of **26** confirmed that only one of the two phosphorus atoms bonded to the *closo* cage was oxidized by sulfur (Figure 2.4). The structure consists of well-separated entities with no short contacts between sulfur atoms from neighbouring molecules. Minor differences in the P-C and P-C_C distances between the two phosphorus atoms have been observed are due to their different oxidation states. The C1-C2 distance of 1.736 Å is close to the values 1.719 and 1.722 Å found for 1,2-(P^iPr_2)$_2$-1,2-*closo*-$C_2B_{10}H_{10}$[25] and 1,2-(PPh_2)$_2$-1,2-*closo*-$C_2B_{10}H_{10}$[26], respectively. Also P1-S distance of 1.942 Å is normal for P=S bonds[27] and is close to the P-S double bond value obtained from the covalent radii proposed by Pyykkö,[24] which is 1.96 Å. In **26** there are four S···H(Ph) contacts from the three ordered phenyl groups shorter than 3.0 Å, three of them (from H18, H20 and H26) are intramolecular (2.76-2.82 Å) and one (from H21) is intermolecular (2.88 Å). Also there is a S···H6B6 contact of 2.95 Å. All these structural features have an important effect on the reactivity of these compounds as discussed later.

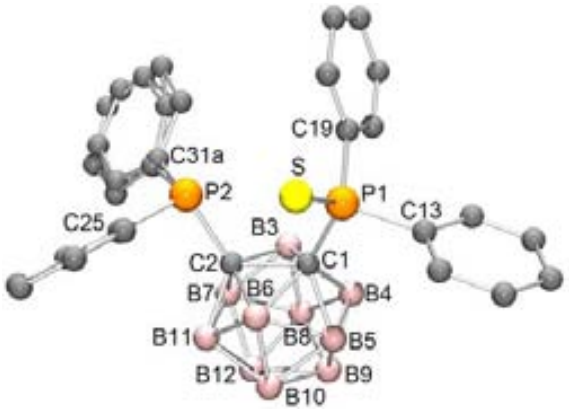

Figure 2.4. Molecular structure of **26**. (The hydrogen atoms are omitted for clarity).

The structural analysis of **37**·CH_2Cl_2 confirmed that both phosphorus atoms are oxidized, although unsymmetrically, where one phosphorus is oxidized by a single oxygen whereas the second by a sulfur. The positions of the oxygen and sulfur atoms are disordered such that they are bonded either to P1 or P2 in the crystal, but not to both at the same time (if O is at P1 then S at P2 and *vice versa*). Each P atom is bonded to a partially occupied oxygen (SOP = 0.5) and sulfur atom (SOP = 0.5) (Figure 2.5.). Spectral data supported that one of the P atoms is substituted by O and the other by S. The P-S bonds in this compound are shorter than the usual P-S double bonds that are around 1.95 Å[27], having the values of 1.913 and 1.908 Å. However, there is one remarkable difference between the P-C_C-C_C angles of **26** and **37**. In **26** (with only one oxidized phosphorus atom) P-C_C-C_C angles are 113.25 and 122.44°**,** but in **37** (with two oxidized phosphorus atoms) the P-C_C-C_C angles are 122.1 and 121.8°. Therefore the reason for the opening has to be due to steric interactions.

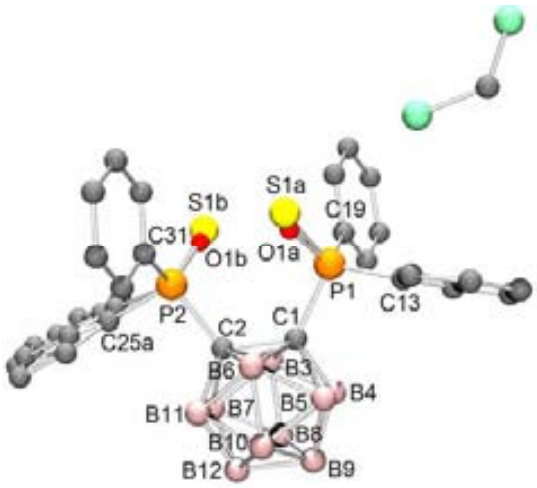

Figure 2.5. Molecular structure of **37**·CH_2Cl_2. (The hydrogen atoms are omitted for clarity).

Structural analysis of **32** confirmed that the 1-$SePPh_2$-2-PPh_2-1,2-*closo*-$C_2B_{10}H_{10}$ compound retained a *closo* architecture during selenization and only one of the phosphorus atoms was oxidized by

selenium. The compound is isostructural with **32**. The $SePPh_2$ substituent at C1 is ordered but one of the phenyl groups of the PPh_2 substituent bonded to C2 is disordered and adopts two orientations (Figure 2.6). There are slight differences in the corresponding P1-C1 and P2-C2 distances between the phosphorus atoms having different oxidation states, the P1-C1 distance being of 1.907 Å and the P2-C2 distance of 1.882 Å, respectively. Also the P-C_C-C_C angles are different with P1-C1-C2 being more opened, 122.54°, than the P2-C2-C1 angle, 113.44°, this is most likely due to the bulkier substituent at C1. The C1-C2 distance of 1.733 Å equals within experimental errors with the distances of 1.719 and 1.722 Å in the disubstituted *o*-carborane derivatives 1,2-(P^iPr_2)$_2$-1,2-*closo*-$C_2B_{10}H_{10}$[25] and 1,2-(PPh_2)$_2$-1,2-*closo*-$C_2B_{10}H_{10}$.[26] The Se-P1 distance of 2.0982 Å is also in the range for comparable Se-P bonds[28] and fits to the value of 2.09 obtained for the P-Se double bonds calculated form covalent radii proposed by Pyykkö.[24] In the structure of **32** there are four Se···H(Ph) bonds, from the three ordered phenyl groups, that are shorter than 3.0 Å, three of which are intramolecular (2.76-2.87 Å) and one (from H21) is intermolecular (2.96 Å). Also there is a Se···H6B6 contact of 3.04 Å. All these quite long contacts in **26** and **32** gave bond critical points in the QTAIM theoretical calculations, as it will be seen further (see Section 2.2.3.).

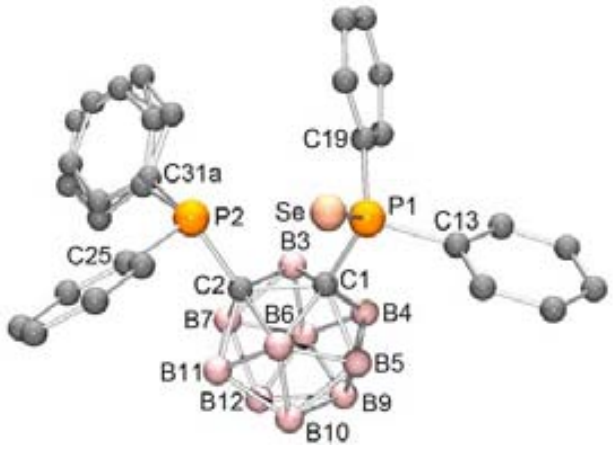

Figure 2.6. Molecular structure of **32**. (The hydrogen atoms are omitted for clarity).

2.1.4. Prolonged oxidation of carboranyldiphosphines with hydrogen peroxide: partial deboronation of carboranyldiphosphines oxides

Partial deboronation of *closo*-carboranyldiphosphines using the well-established procedure[29] with alkoxide did not produce the expected new *nido* species, instead it yielded 7,8-dicarba-*nido*-undecaborate(1-) by C_c-P bond cleavage. On the other hand, the reaction carried out in refluxing ethanol in the absence of alkoxide yielded the *closo*-carboranyldiphosphine unaltered, as it was also the case with piperidine-toluene[30] in 1:4 ratio (*closo*-carboranyldiphosphine:piperidine) at 20° C. Boron removal to yield the *nido* species while preserving the C_c-P bond was successfully obtained in a 99% yield by reaction of 1,2-(PR_2)$_2$-1,2-*closo*-$C_2B_{10}H_{10}$ (R=Ph, ^{i}Pr) with piperidine in ethanol in a ratio 1:10.[29c]

We later demonstrated that proton can induce partial deboronation, therefrom conversion of the *closo*-C_2B_{10} to the *nido*-$[C_2B_9]^-$ species given the necessary chemical and geometrical arrangements to produce proton chelation.[9a] For this purpose, an *o*-carborane adequately C_c-disubstituted with H^+ scavenger elements, such as oxygen was used. The 1,2-(OPR_2)$_2$-1,2-*closo*-

Scheme 2.6. Prolonged oxidation of 1,2-(PR_2)$_2$-1,2-*closo*-$C_2B_{10}H_{10}$ with H_2O_2 in acetone.

$C_2B_{10}H_{10}$ species (R=Ph, **34**, R=^{i}Pr, **35**) did fulfil these requirements as they are chelating agents and contain oxygen atoms. Hydrogen peroxide which had been used to produce *closo*-$[B_{12}(OH)_{12}]^{2-}$ was a suitable oxidizing agent,[31] and a source of H^+. Thus it was expected that upon oxidation of the phosphorus atoms, and the availability of protons, the *closo* cluster would progress to the anionic [7,8-$(OPR_2)_2$-7,8-*nido*-$C_2B_9H_{10}]^-$ (R= Ph, [**40**]$^-$, R= ^{i}Pr, [**41**]$^-$) liberating one boron atom and overall producing a neutral species. Indeed this is what happened. The reaction is schematically represented in Scheme 2.6.

The *nido* nature of the cluster was clearly demonstrated in the ^{1}H-NMR by the apical proton resonance at δ –2.10 and –2.58 ppm for compounds H[**40**] and H[**41**] respectively, and by the $^{11}B\{^1H\}$-NMR, 2:2:1:2:1:1 pattern (low field to high field) observed in the range δ –5.0/-33.9 typical for *nido*-$[C_2B_9]^-$ derivatives. The resonances were separated enough to permit their unambiguous assignment by means of $^{11}B\{^1H\}$ -$^{11}B\{^1H\}$ 2D-COSY NMR (Figure 2.7.). The peak at δ –29.1 ppm is easily assigned to B(10) since it appears as a doublet of doublets in the ^{11}B-NMR spectrum due to coupling with the H bridge as well as the *exo*-H. The peak at δ –31.8 ppm, which is at highest field, corresponds to B(1), the antipodal position to the open face. The spectrum also exhibits a singlet at δ –14.0 ppm that does not show any cross peak and correspond to B(3) which is adjacent to both cluster carbon atoms. With the resonances due to B(1), B(3) and B(10) thus established, analysis of the cross peaks easily allowed the assignment of the 2:2:1:2:1:1 pattern to B(9,11): B(5,6): B(3): B(2,4): B(10): B(1), respectively.

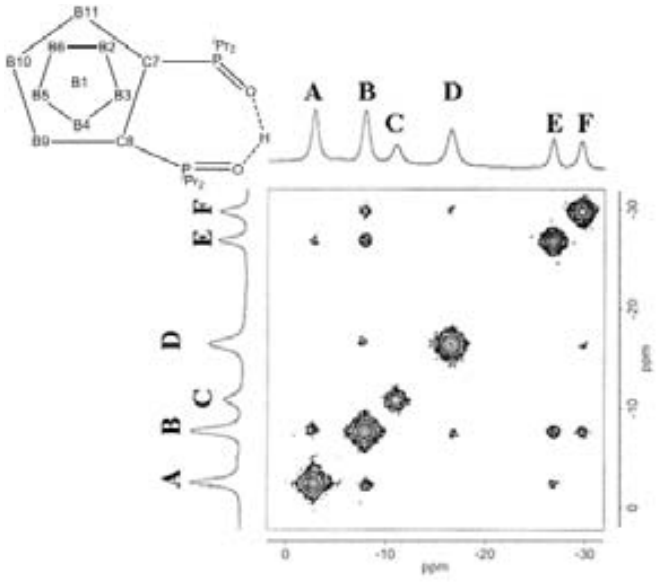

Figure 2.7. $^{11}B\{^1H\}$-$^{11}B\{^1H\}$ 2D-COSY NMR spectrum of H[**41**]. The resonance marked **A** corresponds to B(9, 11), **B** to B(5, 6), **C** to B(3), **D** to B(2, 4), **E** to B(10), **F** to B(1).

Although the negative charge of the *nido* cluster is maintained in the oxidized species, the phosphorus oxidation state has changed from P(III) to P(V). This is clearly reflected on the $^{31}P\{^1H\}$-NMR spectra (Table 2.5.) in which the chemical shifts for the oxidized species have shifted to lower field.

The ν(B-H) in the IR spectra at 2605, 2584, 2526 cm^{-1} for H[**40**] and at 2629-2526 cm^{-1} for H[**41**] are in agreement with a *nido* structure of the *o*-carboranyl fragment[32] and the vibration at 1184 and 1073 cm^{-1} respectively confirm the presence of P=O groups. This IR data could not be further supported by the observation of a resonance attributed to the chelated proton neither in the ^{1}H-NMR spectra of H[**40**] nor H[**41**] probably due to the rapid exchange with deuterium from the solvent. For this, we run the ^{2}H-NMR for H[**41**], and a small pick at 3.32 ppm was observed, that could be assigned to the D^+.

To ensure that H_2O_2 was the sole agent causing the *closo* to *nido* conversion, an alternative sequential process was developed, which is indicated in Scheme 2.7. Oxidation of $[NMe_4][7,8\text{-}(PPh_2)_2$-*nido*-7,8-$C_2B_9H_{10}]$,[9a] with H_2O_2 was performed in acetone at 0° C to yield after stirring for 4 h a white solid that corresponds to $[NMe_4][7,8\text{-}(OPPh_2)_2$-*nido*-7,8-$C_2B_9H_{10}]$, $[NMe_4]$[**40**]. As it is well known, phosphines react with perchloric acid in ethanol to give the corresponding phosphonium salts.[33]

Acidification of $[NMe_4][$**40**$]$ in CH_2Cl_2 with HCl gas produces a white solid corresponding to $[NMe_4]Cl$. Subsequent evaporation of the CH_2Cl_2, after filtration, yields H[**40**]. The ν(O-H) in the IR spectra at 3082 cm^{-1} and 3059 cm^{-1} confirmed the formation of the protonated zwitterionic species.

P(III) compounds	δ(^{31}P) (ppm)	Compounds P(V)	δ(^{31}P) (ppm)	Δδ (ppm)
$[NMe_4][7,8\text{-}(PPh_2)_2\text{-}7,8\text{-}nido\text{-}C_2B_9H_{10}]$ $[NMe_4][$**38**$]$	7.13	$[NMe_4][7,8\text{-}(OPPh_2)_2\text{-}7,8\text{-}nido\text{-}C_2B_9H_{10}]$ $[NMe_4][$**40**$]$	29.33	+22.20
		$H[7,8\text{-}(OPPh_2)_2\text{-}7,8\text{-}nido\text{-}C_2B_9H_{10}]$ H[**40**]	47.09	+39.96
$[NMe_4][7,8\text{-}(P^iPr_2)_2\text{-}7,8\text{-}nido\text{-}C_2B_9H_{10}]$ $[NMe_4][$**39**$]$	35.43	$Mg[7,8\text{-}(OP^iPr_2)_2\text{-}7,8\text{-}nido\text{-}C_2B_9H_{10}]_2$ Mg[**41**]$_2$	65.48	+30.05
		$H[7,8\text{-}(OP^iPr_2)_2\text{-}7,8\text{-}nido\text{-}C_2B_9H_{10}]$ H[**41**]	77.31	+46.27

Table 2.2. $^{31}P\{^1H\}$-NMR chemical shifts for the anionic carboranylphosphines and their oxides.

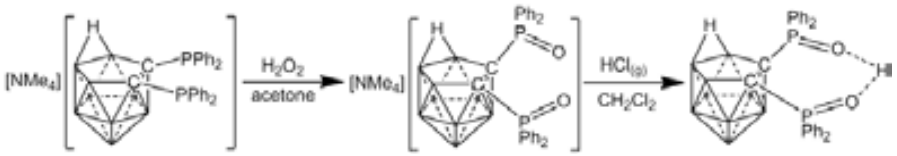

Scheme 2.7. Synthesis of $H[7,8\text{-}(OPPh_2)_2\text{-}7,8\text{-}nido\text{-}C_2B_9H_{10}]$ starting from $[NMe_4][7,8\text{-}(PPh_2)_2\text{-}7,8\text{-}C_2B_9H_{10}]$.

The partial deboronation of 1,2-$(PPh_2)_2$-1,2-*closo*-$C_2B_{10}H_{10}$ with hydrogen peroxide in THF at room temperature for 24 hours was carried out to identify the nature of the removed B^+ containing species. The H[**40**] species was isolated by filtration. The $^{11}B\{^1H\}$ spectrum of the remaining aqueous solution shows a resonance at δ +19.3 ppm corresponding to a boron atom with no B-H bond. According to the literature, the chemical shift for $B(OH)_3$ appears at δ +19.3 ppm,[34] confirming that the removed B^+ stays in solution as $B(OH)_3$. Even more, after 15 min of reaction of 1,2-$(P^iPr_2)_2$-1,2-*closo*-$C_2B_{10}H_{10}$ with H_2O_2, the *closo* phosphine, 1,2-$(OP^iPr_2)_2$-1,2-*closo*-$C_2B_{10}H_{10}$, **35**, was separated in order to obtain crystals suitable for X-ray diffraction. It seems that the reaction was quenched just a moment after the deboronation process started because, serendipitously, together with the structure of compound **35** (Figure 2.8.), we obtain the co-crystal of $B(OH)_3$, fact that supports our hypothesis.

In order to see the lability of the chelated proton, an excess of a saturated solution of $MgCl_2$ was added over a solution of H[**41**] in ethanol. After stirring, the solution was evaporated and extracted 3 times with ethyl acetate. After the evaporation of the organic phase, the NMR spectra of the compound changed. First, the $^{31}P\{^1H\}$-NMR chemical shift moves from +77.26 ppm in H[**41**] to +65,48 ppm. The $^{11}B\{^1H\}$-NMR shows changes form a six peaks pattern (2:2:1:2:1:1) to a five peaks pattern (2:2:3:1:1). Even more, the chemical shift range from -6.2 ppm to -31.8 ppm for H[**41**], is wider, spreading from -2.92 ppm to -35.34 ppm, for Mg[**41**]$_2$. The crystal structure determination (Figure 2.11.) confirmed the cation exchange, the actual formula of the compound being $[Mg(\mathbf{41})_2(H_2O)]\cdot 2CH_3CN$.

Similar changes in the NMR spectra were also observed changing the proton in H[**40**] by $[NMe_4]^+$. The $^{31}P\{^1H\}$-NMR chemical shift at +47.09 ppm for H[**40**] moves to +29.33 ppm for $[NMe_4][$**40**$]$. The $^{11}B\{^1H\}$-NMR for $[NMe_4][$**32**$]$ shows a spectrum with 5 peaks pattern (2:3:2:1:1), as observed for Mg[**40**]$_2$, different of the 6 peaks pattern for H[**40**] and H[**41**], respectively. Also, the apical H shifts from -2.10 ppm in H[**40**], to -1.95 ppm, in $[Me_4N][$**40**$]$.

All these experimental results indicate that the chelated H^+ has significant impact on the electronic communication in the oxidized *nido*-carboranyldiphosphines.

2.1.4.1. Molecular structures of 35, H[41] and Mg[41]$_2$

Compound **35** crystallises as a $B(OH)_3$ adduct (Figure 2.8.). Selected bond parameters are presented in Table 2.3. Individual bonding parameters around P atoms resemble much those in *closo*-carboranylmonophosphine oxides[7] especially those of 1-$OPCy_2$-2-Me-1,2-*closo*-$C_2B_{10}H_{10}$ in which P-O bond is 1.4858(19) Å. In **35**·$B(OH)_3$ P-O bond lengths are 1.4860(12) and 1.4837(13) Å and are almost identical. Also torsion angles P1-C1-C2-P2 [6.3(2)°] and C13-C1-C2-P [6.4(3)°] are same, but C1-C2 distances are different: 1.733 Å in the dioxide compound and 1.687 Å in the mono-oxide compound.

In the adduct there are dimeric H-bonded boric acid units, which form four H-bonds to **35** as presented in Figure 2.9. The dinuclear boric acid unit is also present in bis(triphenylphosphoranediyl)-ammonium chloride : boric acid adduct (1:1).[35]

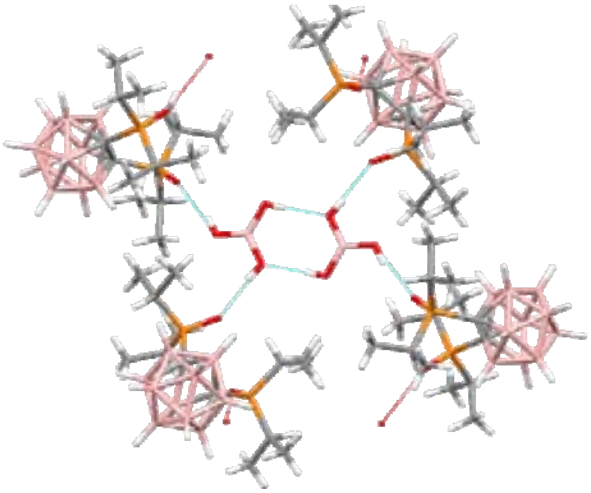

Figure 2.9. Packing view of **35**·$B(OH)_3$.

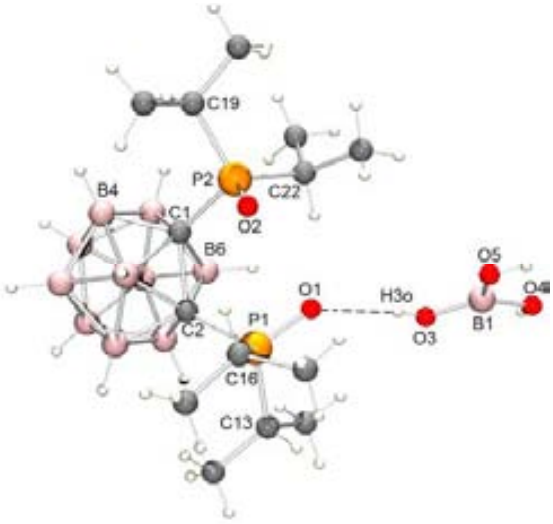

Figure 2.8. Molecular structure of **35**·$B(OH)_3$.

Crystallization of compound H[**41**] from acetone yielded two different needle-shaped crystals, H[**41a**] and H[**41b**], respectively. Compound H[**41a**] crystallizes in the triclinic system while H[**41b**] crystallizes in monoclinic system. Drawings of the molecules are shown in Figures 2.10. For each compound, the X-ray analysis confirmed the expected *nido* structure and the oxidation of both phosphorus atoms. Moreover, the analyses confirmed that the proton sitting between the oxygen atoms balances the negative charge of the *nido* carborane cage in each compound. The short intramolecular O···O distance led to the discovery of this chelated proton, which was located from a difference Fourier map and successfully refined as an independent isotropic atom.[36]

Distances		Angles	
P1–O1	1.486(0)	O1–P1–C2	107.3(7)
P1–C2	1.881(8)	O1–P1–C13	109.7(8)
P1–C13	1.832(4)	O1–P1–C16	111.6(6)
P1–C16	1.816(8)	O2–P2–C1	109.1(9)
P2–O2	1.483(7)	O2–P2–C19	111.3(9)
P2–C1	1.895(0)	O2–P2–C22	113.4(3)
P2–C19	1.829(7)	O3–B1–O5	121.7(8)
P2–C22	1.826(1)	O3–B1–O4	118.2(7)
C1–C2	1.733(2)	O5–B1–O4	119.9(5)
B1–O3	1.355(3)	P1–C1–C2–P2	–6.3(0)
B1–O4	1.373(3)		
B1–O5	1.361(3)		

Table 2.3. Selected interatomic distances [Å], angles [°] and torsion angles [°] for **35**·$(B(OH)_3$

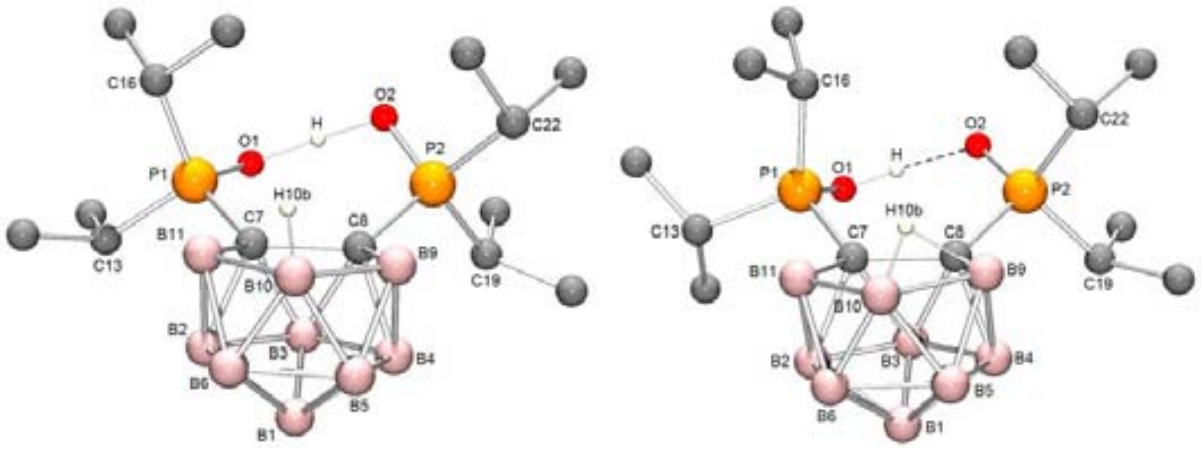

H[**41a**] H[**41b**]

Figure 2.10. Molecular structure of the two polymorphs of H[**41**]. (Hydrogen atoms, except the chelating hydrogen, H and the apical hydrogen, H10b, have been omitted for clarity.)

However, there are noticeable differences between H[**41a**] and H[**41b**]. Mutual orientations of the OP*i*Pr$_2$ substituents are different in H[**41a**] and H[**41b**], but the most striking difference between the molecules concerns the intramolecular O1-H-O2 hydrogen bonding motif (cf. Figures 2.10 and Table 2.4.). In H[**41a**] the short O1···O2 distance of 2.380 Å, the O1-H and O2-H distances of 1.193 and 1.203 Å along with the O1-H-O2 angle of 173° indicate very strong linear and symmetric hydrogen bond between H and both oxygen atoms. In H[**41b**] the short O1···O2 distance of 2.425 Å also indicated strong intramolecular hydrogen bond, but the O1-H and O2···H distances of 0.963 and 1.473 Å, and the O1-H···O2 angle of 171° clearly indicate essentially linear but non-symmetric hydrogen bond between the oxygen atoms. This means that in H[**41b**] the positive charge is meanly localized at P1, while in H[**41a**] the hydrogen between the oxygen atoms possess the most of the positive charge. This different charge distributions most likely causes the structural differences observed between H[**41a**] and H[**41b**].

As far as we know, this observation that two different H-bond systems exist in one compound, H[**33b**], is very rare in chemistry. For H[**41a**] there are several comparable zwitterionic compounds like H[7,8-(OPPh$_2$)$_2$-7,8-*nido*-$C_2B_9H_{10}$], H[**40**] and others,[9a,d,37] where the proton also lies approximately midway between the oxygen atoms and the corresponding hydrogen bond is essentially symmetric and linear. The O1···O2 distance of 2.421 Å in H[**40**] is longer than that in H[**41a**] (2.380 Å), which is most likely due to the different Lewis acidity of the PR$_2$ (R= Ph and *i*Pr) units.

	H[**41a**]	H[**41b**]	H[**40**]
P1 - O1	1.535(9)	1.545(4)	1.523(3)
P2 – O2	1.527(2)	1.517(3)	1.534(3)
P1 – C7	1.830(0)	1.811(6)	1.810(3)
P2 – C8	1.836(0)	1.841(6)	1.808(3)
C7 – C8	1.640(2)	1.624(2)	1.609(5)
O1 – H	1.20(3)	0.96(3)	1.21(5)
O2 – H	1.19(3)	1.47(3)	1.21(5)
O1 – P1 – C7	111.9(6)	112.3(5)	112.1(2)
O2 – P2 – C8	111.6(1)	112.4(7)	112.5(8)
C8 – C7 – P1	124.9(4)	122.0(6)	122.1(2)
C7 – C8 – P2	124.6(6)	125.1(0)	121.4(2)
P1··· P2	3.733(3)	3.646(3)	3.511(3)
O1 ··· O2	2.380(5)	2.425(2)	2.421(4)
O1 – H – O2	173(3)	171(3)	174(4)
C8 – C7 – P1 – O1	23.2(3)	45.6(4)	41.8(3)
C7 – C8 – P2 – O2	10.6(2)	-3.8(4)	-47.7(3)

Table 2.4. Selected interatomic distances [Å], angles [°] and torsion angles [°] for the two polymorphs of H[**41**] and H[**40**].

For H[**41b**], there is no counterpart in the literature. The closest case is found in [P(*i*Pr)$_3$(OH)]I,[37e] that displays a similar P centre but in which there is an OH···I hydrogen bond. The P-O bond length in H[**41b**] is 1.545 Å and in [P(*i*Pr)$_3$(OH)]I it is 1.573 Å. Concerning the different positive charge distribution in H[**41a**] and H[**41b**], clear differences in the P-O and P-C$_c$ distances between the two compounds can be seen (Table 2.4.). Although the differences are relatively small, they support the general observation that distance of the hydrogen atom to the donor and acceptor atoms affects the adjacent bonds: the shorter is the O···H bond the longer is the P=O bond.

Differences in the orientations of P*i*Pr$_2$ groups in H[**41a**] and H[**41b**] can be seen by checking the C8-C7-P1-O1 and C7-C8-P2-O2 torsion angle values that are 23.23° and 10.62° for H[**41a**] and 45.64° and –3.84° for H[**41b**]. These torsion angles indicate different conformations for H[**41a**] and H[**41b**] and influence on the O···O distances and vice versa. Hence, it is difficult to state if the formation of these two crystal forms is due to solid state ordering, conformational effects or possibly of a kinetic origin.

Additional interesting details of the structures are the C$_C$-C$_C$ bond distance. The C7-C8 distances of 1.640, 1.624 and 1.609 Å for H[**41a**], H[**41b**] and H[**40**], respectively, are close to each other. The different orientations of P1 centers in H[**41b**] and H[**41b**] causes the difference of the C$_C$-C$_C$ bond distances in H[**41a**] and H[**41b**], respectively.

Monoanionic [**41**]$^-$ forms complexes with Mg(II) cations, which are of the form [Mg(**41**)$_2$(H$_2$O)]·2CH$_3$CN. The asymmetric unit is shown in Figure 2.11. and selected bond parameters in Table 2.5. In this structure Mg(II) cations have a distorted trigonal bipyramidal coordination sphere, which is made up of four oxide donors from two *nido* cages and of one water molecule. Mg-O bond distances are very similar (about 2.00 Å), but the angles in the trigonal plane are not ideal (120°) as they are 114.98, 118.90 and 126.06°.

As a result of the coordination of [**41**]$^-$ to Mg(II) cation only minor modifications of carborane cage are found if we compare the structural parameters of [**41**]$^-$ in [Mg(**41**)$_2$(H$_2$O)]·2CH$_3$CN to those of H[**41**] in its two crystal forms. The most substantial influence happens to the P-O bonds:

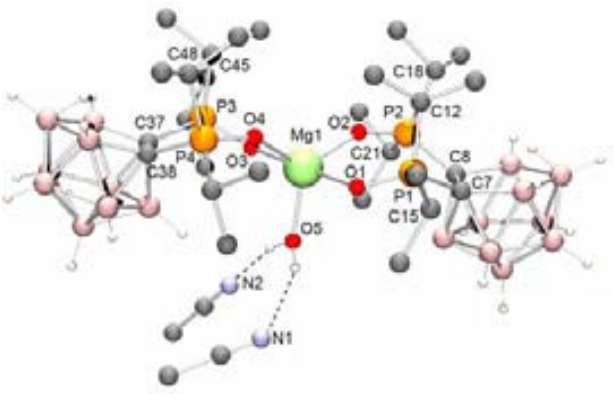

Figure 2.11. Molecular structure of [Mg(**41**)$_2$(H$_2$O)]·2CH$_3$CN. (The CH hydrogen atoms have been omitted for clarity).

Distances		Angles	
Mg1–O1	2.018(1)	O1–Mg1–O2	86.0(2)
Mg1–O2	1.970(1)	O1–Mg1–O3	178.5(0)
Mg1–O3	2.009(9)	O1–Mg1–O4	93.5(6)
Mg1–O4	1.984(6)	O1–Mg1–O5	92.9(0)
Mg1–O5	2.028(5)	O2–Mg1–O3	93.9(7)
P1–O1	1.508(0)	O2–Mg1–O4	126.0(6)
P1–C7	1.827(6)	O2–Mg1–O5	114.9(8)
P1–C12	1.829(4)	O3–Mg1–O4	85.2(3)
P1–C15	1.840(1)	O3–Mg1–O5	88.4(7)
P2–O2	1.505(4)	O4–Mg1–O5	118.9(0)
P2–C8	1.826(8)	O1–P1–C7	115.6(0)
P2–C18	1.847(4)	O2–P2–C8	114.0(4)
P2-C21	1.826(8)	O3–P3–C37	116.3(2)
P3-O3	1.506(9)	O4–P4–C38	113.2(4)
P3-C37	1.827(9)	P1–C7–C8–P2	6.4(4)
P3-C42	1.839(5)	P3–C37–C38–P4	2.3(3)
P3-C45	1.826(7)		
P4-O4	1.506(6)		
P4-C38	1.825(2)		
P4-C48	1.847(7)		
P4-C51	1.824(8)		
C7-C8	1.619(3)		
C37-C38	1.623(7)		

Table 2.5. Selected interatomic distances [Å], angles [°] and torsion angles [°] for [Mg(**41**)$_2$(H$_2$O)]·2CH$_3$CN.

average of four such bonds in Mg complex is 1.507 Å, but in H[**41a**] they are 1.536 and 1.527 and in H[**41b**], 1.545 Å and 1.517 Å. The C7-C8 and P-C bonds are not affected by coordination.

The two *nido* carborane cages are in a *syn* conformation. It has been reported[9d] that *nido*-[7,8-$(OPPh_2)_2$-7,8-$C_2B_9H_{10}]^-$, [**40**]$^-$ forms 1:2 (metal:ligand) complexes with Ni(II), Cu(II) and Zn(II) cations. However in all these complexes the carborane cages are in an *anti* conformation around the metal center.

In solid state the structure of [Mg(**41**)$_2$(H_2O)]·$2CH_3CN$ has been stabilized by two H-bonds, which are formed between the acetonitrile molecules and the protons of the water molecules.

II

2.1.4.2. Mechanistic considerations on the oxidation/deboronation process

The reaction of *closo*-carboranyldiphosphines 1,2-$(PR_2)_2$-1,2-*closo*-$C_2B_{10}H_{10}$ (R= Ph, **9**, ^{i}Pr, **14**) with H_2O_2 in acetone implies two processes: the partial deboronation of the *closo* cluster and the oxidation of the phosphorus atoms. The progress of the reaction has been studied as a function of time to determine which process takes place first. In this sense, the progress of the reaction of both species **9** and **14** with H_2O_2 was monitored by $^{31}P\{^1H\}$ (see Figure 2.12. and Figure 2.14.) and $^{11}B\{^1H\}$-NMR (Figure 2.13.) spectroscopies. The study provides useful information about the structure of the compounds in solution. The resonance at δ 8.22 ppm in the $^{31}P\{^1H\}$-NMR spectrum that corresponds to non-altered 1,2-$(PPh_2)_2$-1,2-*closo*-$C_2B_{10}H_{10}$ decreases with time while a new peak at δ 23.67 ppm increases (Figure 2.12). In four hours there is almost no starting compound left while only the peak at δ 23.67 ppm is observed. The latter resonance also decreases with time while a new one at δ 47.09 ppm emerges. This final resonance persists indefinitely. The $^{11}B\{^1H\}$-NMR spectra also shows the process of conversion of the starting *closo* compound **9** into a *nido* species (Figure 2.13.) but is not as informative as the $^{31}P\{^1H\}$-NMR. The peak at δ 47.09 ppm in the $^{31}P\{^1H\}$-NMR spectrum corresponds to the end species H[7,8-$(OPPh_2)_2$-7,8-*nido*-

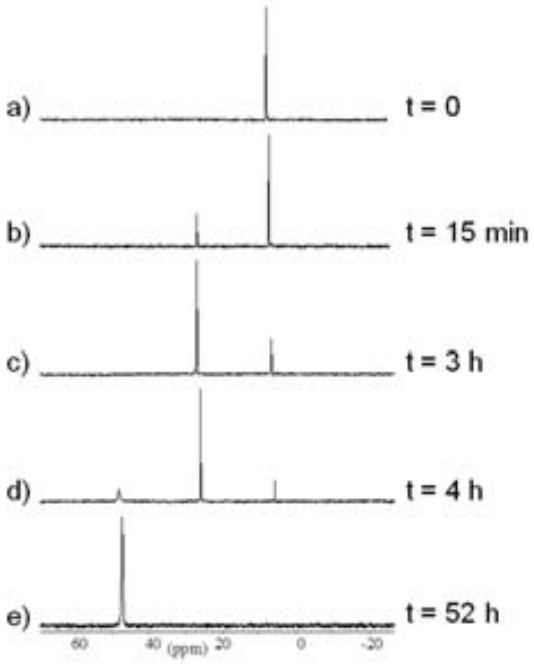

Figure 2.12. $^{31}P\{^1H\}$ spectra (in H_2O_2:acetone) of **9** showing first the oxidation to **34** and later its partial degradation H[**40**].

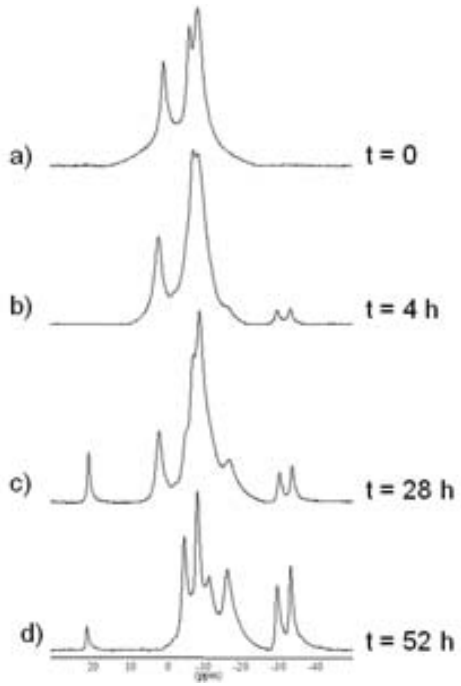

Figure 2.13. $^{11}B\{^1H\}$ spectra (in H_2O_2:acetone) of **9** showing first the oxidation to **34** and later its partial degradation H[**40**].

$C_2B_9H_{10}$].

If the oxidation reaction of **9** is quenched when the peak at δ 23.67 ppm in the $^{31}P\{^1H\}$-NMR is the dominant one, important information about the nature of the intermediate species can be obtained. The $^{11}B\{^1H\}$-NMR spectrum indicates that the cluster is *closo*, which is also supported by the lack of hydrogen bridge in the $^{11}H\{^1B\}$-NMR spectrum. The elemental analysis and FTIR spectroscopy are in agreement with a *closo* species with P=O units. All these data demonstrate that the first step of the reaction is the phosphorus oxidation with cluster preservation and the second one is cluster decapitation as it is shown in Scheme 2.6.

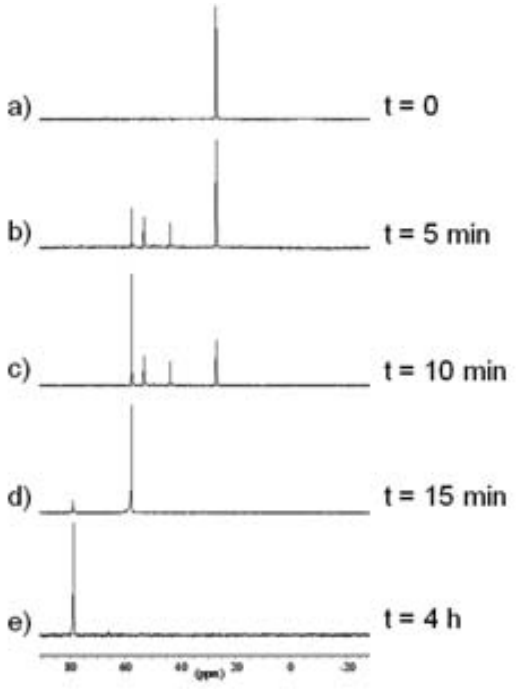

Figure 2.14. $^{31}P\{^1H\}$ spectra (in H_2O_2:acetone) of **14** showing first the oxidation to **35** and latter its partial degradation H[**41**].

This mechanistic study allows accurate determination of the time to complete the two steps of the reaction: phosphorus oxidation and cluster partial deboronation. In the case of 1,2-$(PPh_2)_2$-1,2-*closo*-$C_2B_{10}H_{10}$ 4 hours are necessary to accomplish the formation of both P=O bonds while the cluster partial deboronation of 1,2-$(OPPh_2)_2$-1,2-*closo*-$C_2B_{10}H_{10}$ into H[7,8-$(OPPh_2)_2$-7,8-*nido*-$C_2B_9H_{10}$] is essentially done after 52 hours. It is then clear that the slow step of the total process is the cluster partial deboronation.

When the H_2O_2 reaction study was done on 1,2-$(P^iPr_2)_2$-1,2-*closo*-$C_2B_{10}H_{10}$, resonances at δ 33.27, 47.20, 55.08, 59.08 and 77.26 ppm were observed in the $^{31}P\{^1H\}$-NMR spectra (Figure 2.14.). There were two additional resonances on top of the awaited ones. The resonance at 33.27 corresponds to the starting *closo* compound 1,2-$(P^iPr_2)_2$-1,2-*closo*-$C_2B_{10}H_{10}$, the one at 59.08 corresponds to the *closo* compound **35** and the one at 77.26 to the *nido* compound H[**41**]. Therefore it seems that the extra resonances at δ 47.20 and 55.08 might be attributed to other intermediate species. One interpretation is

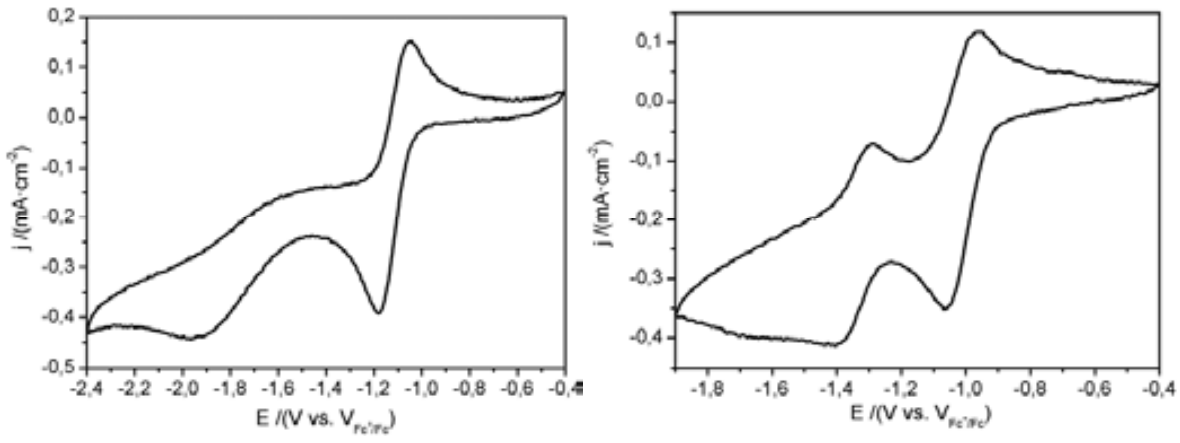

Figure 2.15. Cyclic Voltammograms in acetonitrile for: a) **9** and b) **14**. (solution concentration = 10^{-3} M/[TBA][PF_6] 0.1 M; working electrode = glassy carbon; reference electrode = Ag wire; co-electrode = Pt wire; r_{scan} = 100 mV·s^{-1}).

that the two phosphorus atoms are not oxidized at the same time and a *closo* species containing a P(III) atom and P(V) is obtained which would possibly account for the resonances at δ 55.08 and 47.20 ppm.

The mechanistic study shows that 1,2-(P^iPr_2)$_2$-1,2-*closo*-$C_2B_{10}H_{10}$ is fully oxidized to compound **35** after 15 minutes. So, 1,2-(P^iPr_2)$_2$-1,2-*closo*-$C_2B_{10}H_{10}$ is more susceptible to oxidation than 1,2-(PPh_2)$_2$-1,2-*closo*-$C_2B_{10}H_{10}$ which is *a priori* foreseeable considering the greater donating character of the isopropyl group. Further detail on these processes will be discussed in the computational study section.

The cyclic voltammetry of *closo*-carboranyldiphosphines sustain the above hypothesis since in the case of **9** it shows a reversible curve with one half wave potential: $E_{1/2}$= -1.112 V (*vs.* Fc); whereas for **14** it shows a reversible curve with two half waves potentials: $E_{1/2}^{(1)}$= -1.012 V and $E_{1/2}^{(2)}$= -1.344 V (Figure 2.15.).

2.1.5. Coordination behavior of P(S) and P(Se) units when bonded to carboranyl clusters

The geometrical disposition of the two phosphorus atoms and the two carbon atoms in 1,2-(PPh_2)$_2$-1,2-*closo*-$C_2B_{10}H_{10}$, **9**, is very similar to *cis*-1,2-bis(diphenylphosphine)ethylene, *cis*-Ph_2P-HC=CH-PPh_2, (*cis*-dppen).[38b] Both ligands have a similar orientation of the phosphorus atoms, they are coplanar with the carbon atoms to which they are bonded and with a P···P distance of 3.279 Å in *cis*-dppen and 3.222 Å in 1,2-(PPh_2)$_2$-1,2-*closo*-$C_2B_{10}H_{10}$.[26] Whereas there are over 315 reported crystal structures[39] reported in Cambridge Structural Database (CSD)[8] based on the rigid 1,2-bis(diphenylphosphine)ethylene ligand including *cis* and *trans* isomers, we did not find any example of a monochalcogenide Ph_2P-HC=CH-P(:X)Ph_2 (X = S, Se). Crystal structures of monochalcogenide **26** and **32**, both with one chalcogen, indicated there are two binding sites, each with a distinct chemical nature. A ligand that displays these characteristics is commonly addressed as hemilabile. The potential of these monochalcogenide carboranyl-diphosphines **26** and **32** to behave as asymmetric chelating bidentate ligands for metal coordination has been studied towards different complexes of Ni(II), Pd(II), Au(I) and Ru(II).

The $^{31}P\{^1H\}$-NMR spectrum of the crude reaction of **32** and [$PdCl_2(PPh_3)_2$] displayed three signals at 7.84 ppm, 35.80 ppm and 79.65 ppm after 24 h in CH_2Cl_2 (Figure 2.16.). The peak at 7.84 ppm corresponds to free 1,2-(PPh_2)$_2$-1,2-$C_2B_{10}H_{10}$, the one at 35.80 to Ph_3PSe[23] and the last one to [$PdCl_2${1,2-(PPh_2)$_2$-1,2-$C_2B_{10}H_{10}$}][40] (Figure 2.16). These results prompted us to hypothesise, based on available data in the literature,[41] that the loss of the ligand's chalcogen was a selenium transfer from a weaker phosphine Lewis base, the *closo*-carboranyl-diphenylphosphine, to a more basic one, the triphenylphosphine (Scheme 2.8.a). The kinetics of the

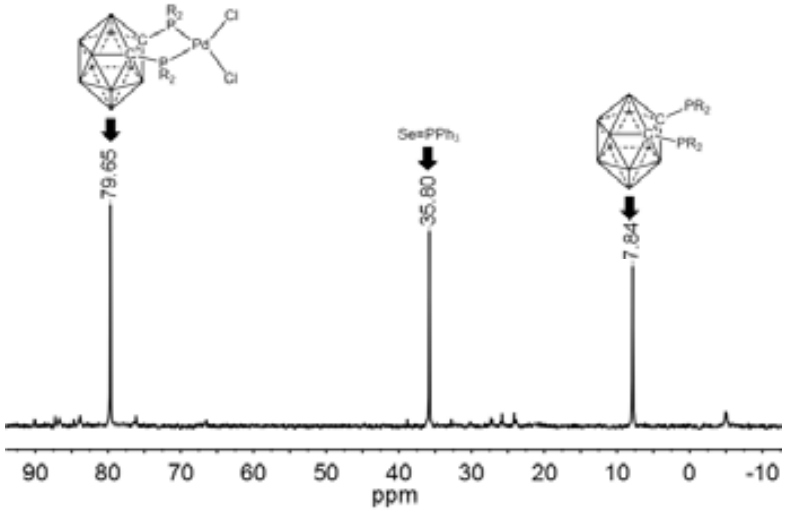

Figure 2.16. $^{31}P\{^1H\}$-NMR spectrum for the crude of reaction of **32** with [$PdCl_2(PPh_3)_2$] in CH_2Cl_2 after 24 h at room temperature.

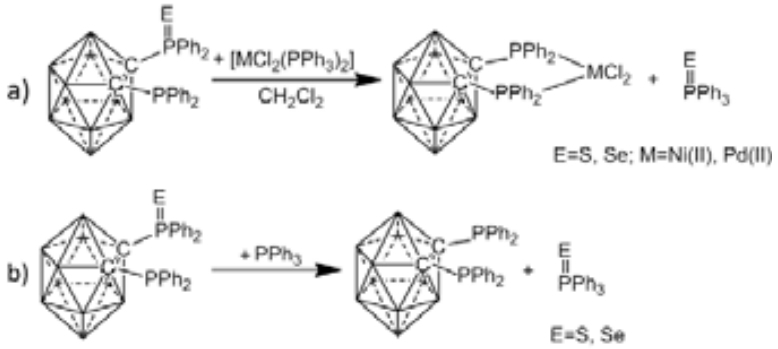

Scheme 2.8. $^{31}P\{^{1}H\}$-NMR spectrum for the crude of reaction of **32** with $[PdCl_2(PPh_3)_2]$ in CH_2Cl_2 after 24 h at room temperature.

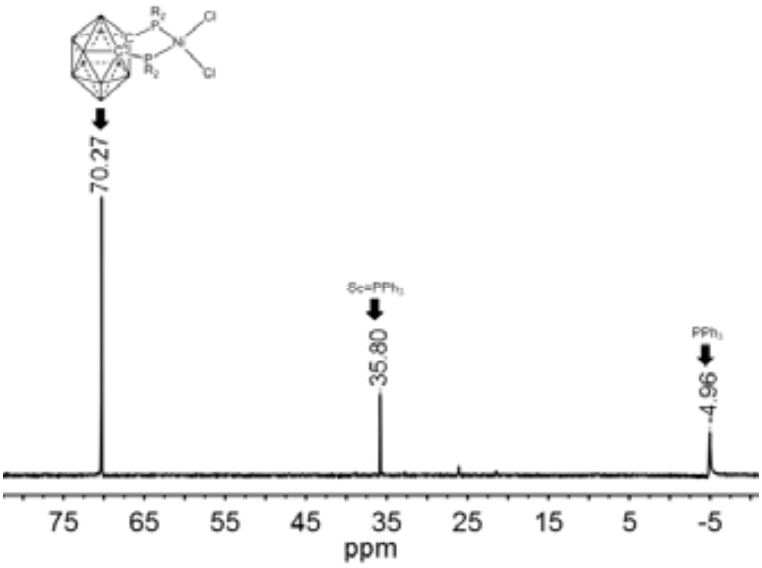

Figure 2.17. $^{31}P\{^{1}H\}$-NMR spectrum for the crude of reaction of **32** with $[NiCl_2(PPh_3)_2]$ in CH_2Cl_2 after 30 minutes at room temperature.

complexation reaction with Pd is slow though, since dechalcogenated, but unreacted, carboranyl-diphosphine is still in the reaction medium after 24 h. The kinetics of the reaction is different though if $[NiCl_2(PPh_3)_2]$, after 30 minutes of reaction only the nickel complex of the dechalcogenated carboranyl-diphosphine, $[NiCl_2\{1,2\text{-}(PPh_2)_2\text{-}1,2\text{-}C_2B_{10}H_{10}\}]$ (**45**), being observed at 70.27 ppm in $^{31}P\{^{1}H\}$-NMR spectrum, together with the signals corresponding to $SePPh_3$ and free PPh_3, at 35.8 ppm and -4.96 ppm, respectively (Figure 2.17). To further verify the hypothesis, the reaction of **32** and $[PdCl_2(cod)]$ was carried out. After 24 h in CH_2Cl_2, the starting yellow solution turned dark-brownish and the $^{31}P\{^{1}H\}$-NMR spectrum of the reaction crude revealed one chemical shift at 79.6 ppm, that was again attributed to the $[PdCl_2\{1,2\text{-}(PPh_2)_2\text{-}1,2\text{-}C_2B_{10}H_{10}\}]$.[40] Upon filtration of the solution a red-grey solid, selenium in the two allotropic forms, was isolated. Starting with the same concentration of **32** in CH_2Cl_2, the reaction with $[PdCl_2(cod)]$ was faster than with $[PdCl_2(PPh_3)_2]$, but the deselenization also took place. Therefore the dechalcogenation was not necessarily concomitant with the presence of a more basic phosphine in the medium.

To verify if the ligand's chalcogen loss was metal/ligand dependent, reactions with, $[NiCl_2(dppe)]$, $[AuCl(PPh_3)]$, $[RuCl_2(PPh_3)_3]$ and anhydrous $NiCl_2$ were performed. Although the loss of ligand's chalcogen was very rapid with $[NiCl_2(PPh_3)_2]$, more than one day was needed with $[NiCl_2(dppe)]$ or $NiCl_2$ to obtain **46**. The deselenation and posterior metal complexation reactions was completed after one day with $[AuCl(PPh_3)]$ and after 5 days with $[RuCl_2(PPh_3)_3]$.

The reaction of **26** and **32** with $[PdCl_2(cod)]$, $[PdCl_2(PPh_3)_2]$ and $[NiCl_2(PPh_3)_2]$ also took place with the loss of the sulphur but at a slower rate than for **32**.

To unambiguously confirm the dechalcogenation process, appropriate crystals of $[NiCl_2\{1,2\text{-}(PPh_2)_2\text{-}1,2\text{-}C_2B_{10}H_{10}\}]$ (**46**) were obtained from the slow evaporation of a CH_2Cl_2/Et_2O solution. The crystal structure (Figure 2.18.) confirmed the spectroscopic data. The structural parameters of **46** are

similar to those of $[NiBr_2\{1,2\text{-}(PPh_2)_2\text{-}1,2\text{-}C_2B_{10}H_{10}\}]\cdot CH_2Cl_2$[42] (the Ni-Cl distances are 0.03 Å shorter than Ni-Br distances).

We also studied the influence of the solvent in the loss of the chalcogen and it was observed that it is independent of the nature and dryness of the solvent. Loss of the chalcogen was attained with dry dichloromethane, toluene, acetonitrile, ethyl acetate, chloroform, 2-propanol or *tert*-butanol. If a nucleophilic solvent was used (e.g., 2-propanol,) the carborane cage was partially deboronated and *nido* complexes were obtained, as previously reported in the literature.[38a,43]

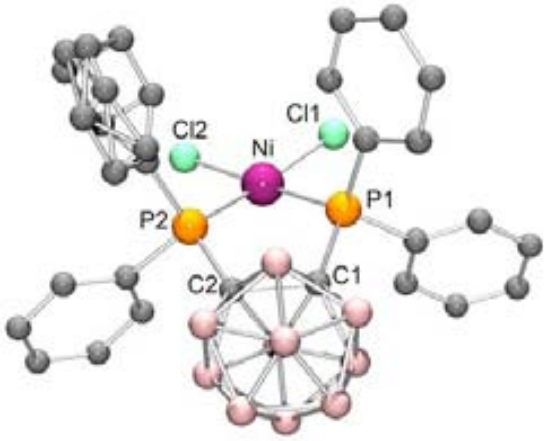

Figure 2.18. Molecular structure of **46**. (The hydrogen atoms are omitted for clarity).

Subsequently, we studied the chalcogen transfer from monochalcogenide carboranyl-diphosphines to triphenylphosphine in the absence of a metal. The transfer was very rapid; the reaction was completed in five minutes (Scheme 2.8.b).

The dechalcogenation of the monochalcogenide carboranyldiphosphines also takes place in solid state, $[NiCl_2\{1,2\text{-}(PPh_2)_2\text{-}1,2\text{-}C_2B_{10}H_{10}\}]$ is obtained when 1 equivalent of **32** was milled with 1 equivalent of $[NiCl_2(PPh_3)_2]$ for an hour in a ball mill.

The experimental coordination chemistry studies presented here show the anomalously high tendency of monochalcogenide carboranyldiphosphines to dechalcogenate. The lability of the chalcogen atom, for these monochalcogenide carboranyldiphosphines, can be associated with steric and electronic effects. In order to test experimentally which of the two effects predominate we tested the less hindered carboranylmonophoshines chacogenides, **24** and **29**. Both **24** and **29** suffered dechalcogenation when reacted with $[PdCl_2(PPh_3)_2]$ and $[NiCl_2(PPh_3)]$ or with PPh_3. The loss of the chalcogen is slower with this chalcogenides and no complexes are formed between the dechalcogenated carboranylmonophospine and the metals, since these phosphines are very poor coordinating ligands.

In order to get further insights on the nature of the chalcogen-phosphorus bond in these compounds was made a computational study using Density Functional Theory (DFT) calculation, Natural Bond Orbital (NBO) analysis and Quantum Theory of Atoms in Molecules (QTAIM), which is presented in Section 2.2.3.

2.2. Computational studies on carboranylphosphines

2.2.1. Contribution of phosphine and oxidized phosphine moieties to the electronic effects on the $C_2B_{10}H_{10}$ cluster

In order to observe the electronic effects on the carborane cluster due to the presence of the phosphine groups, we calculated the charges of the cluster atoms. In a previous work, based on spectroscopic data and DFT calculation, it was observed that the B-iodination and B-methylation induce important electronic effects on the carborane cage, and so, the C_C-H acidic character can be tuned.[44] As measure of the electronic effects that the substituents may exert on the cluster, we defined the cluster-only total charge (CTC), which is obtained summing all calculated individual cluster atoms charges, leaving aside the substituents.[45] NBO calculations[46] were done for the compounds **8**, **9, 14, 34** and **35**

Atom	Compounds					
	1	**8**	**9**	**14**	**34**	**35**
C1	–0.497	-0.644	–0.659	–0.660	–0.715	–0.695
C2	–0.497	-0.514	–0.658	–0.660	–0.715	–0.695
B3	0.159	0.161	0.164	0.167	0.185	0.170
B4	0.000	0.003	0.006	0.000	0.008	–0.001
B5	0.000	0.003	0.002	–0.004	0.014	–0.002
B6	0.159	0.161	0.168	0.167	0.185	0.170
B7	0.000	0.003	0.002	–0.004	0.014	–0.002
B8	–0.165	-0.161	–0.165	–0.172	–0.161	–0.169
B9	–0.139	-0.141	–0.135	–0.136	–0.129	–0.135
B10	–0.165	-0.161	–0.165	–0.171	–0.161	–0.169
B11	0.000	0.003	0.002	0.000	0.008	–0.001
B12	–0.139	-0.136	–0.137	–0.136	–0.129	–0.135
P1		0.923	0.951	0.957	2.034	2.034
P2			0.950	0.957	2.034	2.034
O1					–1.079	–1.099
O2					–1.079	–1.099
CTC[a]	**–1.284**	**-1.423**	**–1.575**	**–1.609**	**–1.596**	**–1.664**

[a] CTC = Σ (C1,C2,B3,B4,B5,B6,B7,B8,B9,B10,B11,B12)

Table 2.6. Computed NPA charges for *closo*-carboranyldiphosphines, their oxides and the parent *o*-carborane.

to determine the charges on the cluster atoms (Table 2.6.).[47] Furthermore, the cluster-only total charge (CTC) of the compounds was calculated and compared with the parent *o*-carborane, **1**.

It is interestingly to observe that the $–PPh_2$ substituents additively influence the CTC charges on the C_2B_{10}. In the monosubstituted phosphine, **8**, the $–PPh_2$ moiety adds $0.139e^-$ to the C_2B_{10} cluster compared with *o*-carborane. Adding the second $–PPh_2$ group, the CTC on C_2B_{10} cluster is increased by $0.152e^-$ for **9** with respect to **8**, summing $0.291e^-$ with respect to **1**. The CTC for **9** and **14** are more negative than **1** (Table 2.6.). This can be explained by the fact that the carboranyl moiety possesses electron withdrawing character and so, the presence of the lone pair on the phosphine moieties, give electronic density to the cluster which contribute to its CTC. It can be observed also that the CTC for **9** is less negative than for **14** due to the presence of the aryl moieties on **9**, which dissipates by delocalization part of the back-donation of the P lone pairs. Important differences are also observed (Table 2.10.) when comparing NPA charges of **34** and **35** with **9**, **14** and **1**. One would expect that the electronic donation to the cluster of the phosphorus oxidized centre in **34** and **35** would be smaller than in **9** and **14** due to the lack of electron lone pairs on the P atoms and consequently, the CTC for **34** and **35** to be less negative than for **9** and **14**. Since the original NPA CTC on *o*-carborane is -1.284 e^-, addition of two $–PR_2$ groups alter the cluster charge with -0.291 e^- if R= Ph and -0.325 e^- for R= ^{i}Pr. While, the $–(O)PR_2$ groups confer an even more negative CTC to the cluster, -0.312 e^- and -0.380 e^- for R= Ph and ^{i}Pr, respectively, contrary to the expected results. In addition, the Hirshfeld[48] method have been used for the computation of the charge (Table 2.7.). The CTC values calculated from Hirshfeld charges go in parallel with the NPA for all the compounds, compared with **1**, but for **34** and **35**, the CTC by Hirshfeld method, are less negative than for **9** and **14**. This come from the fact that the NPA method is based on a representation of the molecular wave function using basis functions, and the charges computed with this method reproduce more or less the difference in electronegativity between the atoms, but it exaggerates bond polarities, displaying large negative or positive charges for covalently bonded atoms. The Hirshfeld method on the other hand is based directly on the electron density as a function of space and is consistent with electronegativity

Atom	Compounds					
	1	8	9	14	34	35
C1	-0.054	-0.020	0.004	0.034	0.009	0.035
C2	-0.054	-0.013	0.005	0.034	0.009	0.035
B3	0.083	0.070	0.015	0.070	0.007	0.077
B4	0.054	0.035	0.036	-0.009	0.030	-0.009
B5	0.054	0.035	0.018	-0.011	0.036	-0.010
B6	0.083	0.070	-0.010	0.070	0.007	0.077
B7	0.054	0.012	0.037	-0.011	0.036	-0.010
B8	-0.008	-0.010	-0.006	-0.006	-0.004	-0.003
B9	0.005	-0.010	-0.017	-0.003	-0.012	-0.020
B10	-0.008	-0.010	-0.015	-0.006	-0.004	-0.003
B11	0.054	0.012	0.013	-0.010	0.030	-0.009
B12	0.005	-0.029	-0.014	-0.004	-0.012	-0.020
P1		0.216	0.176	0.212	0.420	0.464
P2			0.175	0.212	0.420	0.464
O1					-0.360	-0.353
O2					-0.360	-0.353
CTC[a]	**0.268**	**0.142**	**0.066**	**0.058**	**0.132**	**0.140**

[a] CTC = Σ (C1,C2,B3,B4,B5,B6,B7,B8,B9,B10,B11,B12)

Table 2.7. Computed Hirshfeld charges for *closo*-carboranyldiphosphines, their oxides and the parent *o*-carborane.

values of elements. Even so, the carborane cluster withdrawing character is noticeable for both P(III) and P(V) disubstituted derivatives.

2.2.2. Electronic effects in *closo*-carboranylmonophosphines

To further understand the different reactivity of carboranylmonophosphine, 1-PPh_2-1,2-*closo*-1,2-$C_2B_{10}H_{11}$ (**8**), respect to the triphenylphosphine, we undertook a computational study[47] based on NBO analysis.[49]

In Table 2.8. are presented the delocalization energies for the P electron lone pair into the neighbouring NBO antibonds for compound **8** and triphenylphosphine. In 8, the P lone pair delocalizes in the C-C neighbouring bonds from the phenyl ring, but does not interact with the C_C-C_C bonds, communicating with the carborane cage through the tricentric C-B-B bonds. The atoms involved in the interaction presented in Table 2.8. are schematically presented in Figure 2.19.

A further inspection of the Natural Hybrid Orbitals (NHOs) provide information on: i) the withdrawing character of the carborane cluster compared with the phenyl rings and ii) on the availability of the P lone pair to react with sulphur. It was found that in **8** the NHOs for the phosphorus-carbon

Compound	NBO antibond	$\Delta E_{ij}^{(2)}$ [kcal·mol^{-1}]
PPh_3	C1-C2	4.70
	C7-C8	4.83
	C13-C14	4.70
1-PPh_2-1,2-*closo*-$C_2B_{10}H_{11}$	C1-B4-B3	4.10
	C1-B5-B6	4.13
	C13-C14	7.00
	C19-C20	7.00

Table 2.8. Second-order delocalization energies for the phosphorus electron lone pair and the NBO antibonds in triphenylphosphine and carboranyldiphenylphosphine.

bonds have the following composition: $\sigma_{PC(cluster)}$ = $0.5419(sp^{5.26}d^{0.05})_P$ + $0.8405(sp^{2.79})_{C(cluster)}$ and $\sigma_{PC(Ph)}$ = $0.6107(sp^{4.41}d^{0.04})_P$ + $0.7919(sp^{2.56})_{C(Ph)}$ and in PPh_3 the P-C_{Ph} (C_{Ph} = phenyl carbon) have the following composition: $\sigma_{PC(Ph)}$ = $0.6000(sp^{4.92}d^{0.05})_P$ + $0.8000(sp^{2.43})_{C(Ph)}$. It can be observed that the C_C hybrid has a larger polarization coefficient (0.8405) compared with the C_{Ph} hybrid from compound **8** (0.7919) or from PPh_3 (0.8000), which is consequence of the more electron withdrawing character of the carborane cage, compared with the Ph moiety.

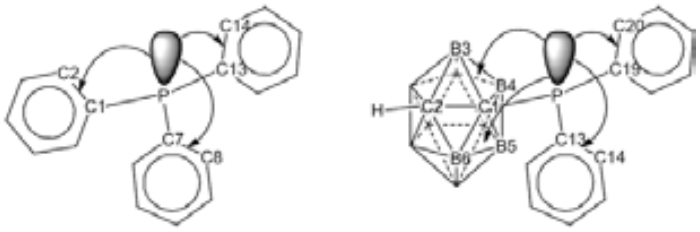

a) b)

Figure 2.19. Schematics of the NBO interaction and the numbering of the atoms involved, for: a) PPh_3 and b) 1-PPh_2-1,2-*closo*-$C_2B_{10}H_{11}$

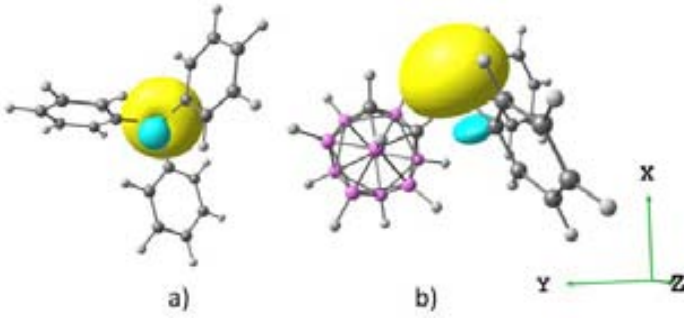

a) b)

Figure 2.20. The NBO hybrid (in PNBO basis) of the phosphorus lone pair for: a) PPh_3 and b) 1-PPh_2-1,2-*closo*-$C_2B_{10}H_{11}$ (yellow stands for negative and light blue stands for positive).

The NHO analysis on the P lone pair showed that it has a *sp* hybrid character in both compounds (in **8** the P lone pair has 47.60% *s* character and 52.39% *p* character and in PPh_3 the P lone pair has a 49.77% *s* character and 50.23% *p* character). The main difference, which stands also for their different reactivity, is the origin of *p* orbital. It was found that the P lone pair in **8** is composed form the hybrid: $h_{lp(P)}$ = $0.6897(3s) + 0.7213(3p_x)$ and in PPh_3 it has the following composition: $h_{lp(P)} = 0.7054(3s) – 0.7074(3p_z)$. The orientation of P lone pair hybrid on the *z* axis (Figure 2.20.a) in PPh_3 favours the orbital overlap needed for bond formation and enhance its nucleophilicity, contrary to the P lone pair hybrid in **8** which is orientated on the *x* axis (Figure 2.20.b). The triphenylphosphine is a notorious ligand in coordination chemistry, forming organometallic complexes with any metal. The carboranyldiphosphine **8** on the other hand, is a very poor ligand, and the origin of this low coordination capacity can be associated with the p_x hybrid type of the P electron lone pair in this compound.

2.2.3. Computational study on the lability of the phosphorus-chalcogen bonds

The nature of P-E (E= O, S, Se, Te) is continuously debated in the literature, the most studied bond being the P-O. For this bond, descriptions as a single σ bond, a single π bond, one σ bond and two π bonds, one σ bond and three π bonds or three Ω bonds (banana bonds) can be found.[50] For P-E (E= S, Se, Te) bonds, three resonance structures (depicted in Figure 2.21.) were proposed. Structure I, that arise from the overlap of phosphorous *3d* and chalcogen *p* orbitals, was discarded by theoretical studies that proved that

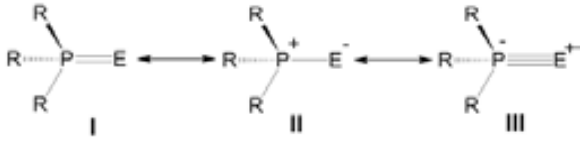

Figure 2.21. Proposed structures for phosphorus-chalcogen bonds (E = S, Se, Te).

the phosphorous *3d* orbitals are unavailable for bonding in this compounds.[51] The structure II is advocated by Burford *et al*. based on NMR studies and crystal structure determinations of a series of triphenylphosphine sulphide and selenide adducts with aluminium trichloride.[23] They classify the coordinative bonding modes of phosphine chalcogenides depending on phosphine-chalcogen-metal angle. Structure III has be proposed to make significant contribution to the P-E bonding mode, containing one σ bond and two π bonds from back donation from chalcogen *p* orbitals to σ^* orbitals on R_3P fragment. The triple nature of this bond was determinate from DFT calculations.[50b]

Although some computational studies on phosphorous-chalcogen bond were found in the literature, no study was encountered on phosphines with such voluminous moieties as carboranyl.

Calculation[47] of the natural hybrid orbitals (NHOs) of the bonds between the phosphorous atom and the chalcogen atoms in compounds **26** and **32** yield the following composition: $\sigma_{PS}=0.7087(sp^{2.49}d^{0.03})_P + 0.7055(sp^{5.01}d^{0.03})_S$ and $\sigma_{PSe}= 0.7433(sp^{2.62}d^{0.02})_P + 0.6690(sp^{7.13}d^{0.02})_{Se}$. As can be seen the phosphorous atom is closer to a sp^3 hybridization in **32** and to a sp^2 in **26**. Also, it can be observed that the contribution to the bonding from the *d* orbitals is negligible. The same analysis of the NHOs revealed that the electron lone pair on the non-oxidized phosphorous atom in both compounds is equally shared between the *s* and *p* orbitals and that the electron lone pairs on the chalcogen atoms have pure *p* character.

Compound	Lone pair[a)]	P-C bond[b)]	$\Delta E_{ij}^{(2)}$ (kcal·mol^{-1})
26	S(1)	P1-C13	12.66
	S(1)	P1-C19	8.43
	S(2)	P1-C1	20.10
	S(2)	P1-C19	6.07
32	Se(1)	P1-C13	9.91
	Se(1)	P1-C19	7.11
	Se(2)	P1-C1	16.91
	Se(2)	P1-C19	4.53

a) The number in parenthesis stands for the first (1) and the second (2) lone pair.
b) The atom numbering is the same as for crystal structure.

Table 2.9. Second order delocalization energies for the electron lone pairs and NBOs antibonding interactions in **26** and **32**.

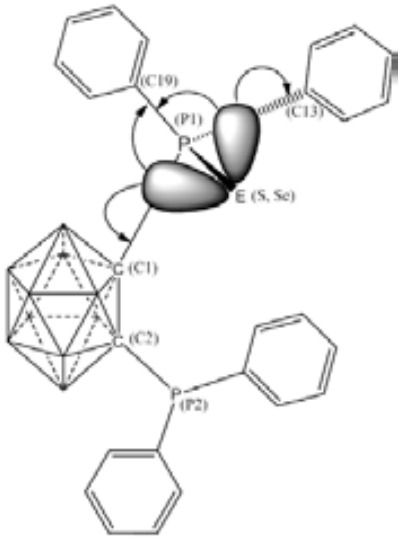

Figure 2.22. Schematic representation for the main interactions between the chalcogen lone pairs and the P-C bonds.

The second order perturbation theory analysis showed that in both compounds, there are significant interactions between the lone pairs on the chalcoge atoms and the P-C_{ipso} and P-C_C NBOs antibonds (Table 2.9.). These interactions (Figure 2.22.) are stronger and more delocalized for **26** than for **32**. The electron lone pairs in **9** occupy the space from the sulphur atom and the phosphorous, meanwhile in **32** the electron lone pairs of the selenium are more localized on the chalcogen. For comparison, we calculated the stabilisation energies for triphenylphosphine sulphide and triphenylphosphine selenide and the same trends were observed, but the magnitude of the stabilization

energies is half of the values obtained for **26** and **32**, due to the stronger electron withdrawing character of the carborane cage.

The calculated NBO interactions are in agreement with the structural features observed from the X-ray structure determination. The distances between the C1 and the oxidized P atom (C1-P1) in **26** and **32**, are 1.902 Å and 1.907 Å, respectively, which are longer than those between C2 and the unoxidized P atom (C2-P2) (1.880 Å for **26** and 1.882 Å for **32**). Also, the distances between the oxidized P atom and the C atom from the phenyl rings, P1-C13 (1.1826 Å for **26** and 1.824 Å for **32**) and P1-C19 (1.817 Å for **26** and 1.817 Å for **32**) are shorter than those between the unoxidized P and the C atoms from the phenyl rings, P2-C25 (1.841 Å for **26** and 1.853 Å for **32**) and P2-C31 (1.856 Å for **26** and 1.855 Å for **32**). As one would expect, the donation of the electrons from the chalcogen lone pairs to the antibonding orbitals of the P-C bonds, should enlarge the P-C distance and diminish the C-P-C angles. As reported, the shortness of the P-C*ipso* bonds has both electronic and steric origins and is typical for a variety of chalcogen phosphines.[23,50b] The peculiarity of compounds **26** and **32** is defined by the presence of the carborane cluster that produces an asymmetry on the P center. Consequently, the effect of multiple lone pairs delocalization in one bond determines three different C-P-C angles. The P1-C19 antibonding orbital receives charge density from both of the lone pairs in the chalcogen atom, opening of the C-P-C angles to 108.18° for C1-P1-C19 and 106.94° for C13-P1-C19 in **26**. This diminishes the C1-P1-C13 angle to 102.85, a value that is typical for C-P-C angles for an unoxidized P center. The P1-C1 bond elongates to meet the steric demands, which are due to the diminishment of the C1-P1-C13 angle and the high interaction energy between the chalcogen's second lone pair and the P-C1 antibonding orbital (Table 2.9.). The same structural features are observed for **32**.

The NBO analysis of **26** and **32** revealed that the chalcogen lone pairs are involved in back donation and in intramolecular interactions, thus they are less available for bonding. The presence of a second phosphine group in **26** and **32** weakens the complexation ability of these ligands due to the steric hindrance of the phenyl groups. This weaking of the P-E bond takes place in at least two ways: the first is due to the strong electronic withdrawing character of the *closo* carborane cluster that tends to polarize the P-E (E=S, Se) bond towards the phosphorus atom. Secondly, the difference in electronegativity between the chalcogen and the phosphorus atoms that tends to polarize the bond towards the chalcogen. The withdrawing character of the carborane cluster is slightly stronger as can be observed from the higher value of the polarization coefficient of the phosphorus atom in the NHOs presented above.

The QTAIM analysis[52] for **26** and **32** revealed intramolecular interactions between the chalcogen and the neighbouring atoms. The electron density value of the P1-S bond (Entry 1 in Table 2.10.) is in the range of the P-S bonds found for compounds like H_3PS or Me_3PS.[50c] For **32** (Entry 6 in Table 2.10.) the electron density for the P1-Se bond is very small and $\nabla^2\rho$ is small but negative indicating that the bond is a weak shared interaction. To our knowledge this is

Entry	Bond	ρ	$\nabla^2\rho$	H
1	S-P1	0.1642	-2.492	-0.1163
2	S-H6	0.0099	0.0297	0.0009
3	S-H18	0.0115	0.0426	0.0017
4	S-H20	0.0127	0.0415	0.0015
5	S-H26	0.0090	0.0235	0.0010
6	Se-P1	0.1296	- 0.0436	-0.0684
7	Se-H6	0.0115	0.0297	0.0009
8	Se-H18	0.0147	0.0109	0.0013
9	Se-H20	0.0148	0.0415	0.0013
10	Se-H26	0.0101	0.0252	0.0010

ρ - electron density, $\nabla^2\rho$ - Laplacian of the electron density, H – total electronic energy density

Table 2.10. Properties of BCP between the chalcogen atoms and their neighboring atoms in **26** (entries 1-5) and **32** (entries 6-10). All the values are in a.u. The numbering is presented in Figure 2.23.

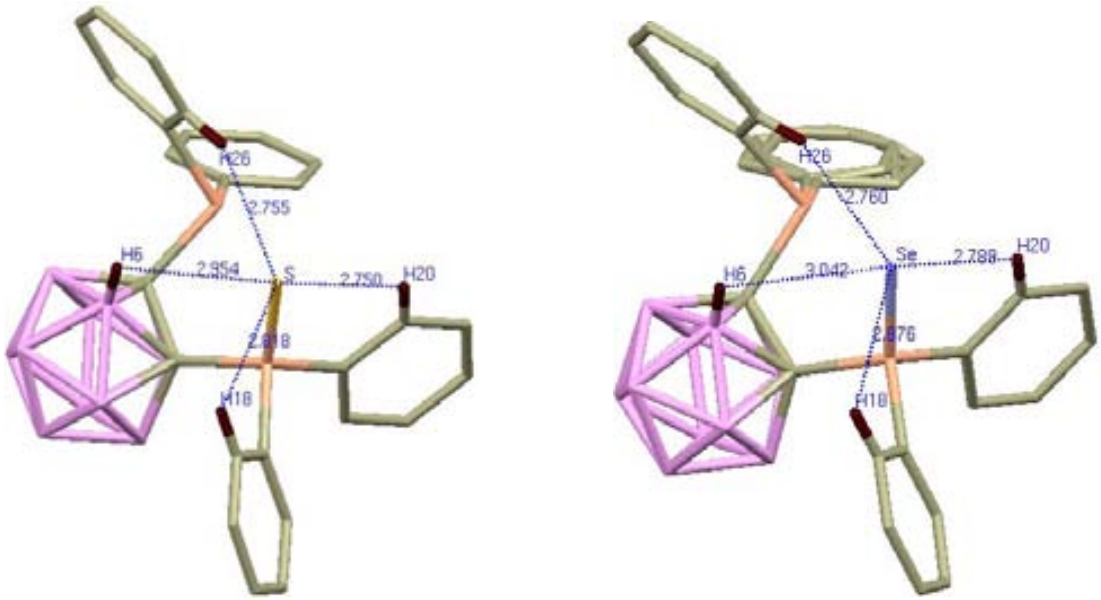

a) b)

Figure 2.23. The distances between the chalcogen and the neighbouring hydrogen atoms in: a) **26** and b) **32**. (Only hydrogen atoms of interest are presented for clarity).

the first time that such studies have been performed on the P-Se bond. Therefore there has been no possibility to compare.

The BCP study reveals that interactions between the chalcogen and its neighbouring hydrogen atoms, either from the phenyl rings or from the carborane cluster (Entries 2-5 and 7-10 in Table 2.10.), fully agree with the X-ray structures (Figure 2.23.). The deshielding of some resonances in the $^{1}H\{^{11}B\}$-NMR spectra for **26** and **32**, compared to the parent 1,2-$(PPh_2)_2$-1,2-*closo*-$C_2B_{10}H_{10}$, indicate that the E ··H interactions are maintained in solution. Two groups of chemical shifts with a ratio of 3:17, corresponding to the hydrogens on the phenyl groups are observed for **26** and **32**, one at 8.43-8.29 ppm (in green in Figure 2.24.) and the second at 7.63-7.27 ppm (in magenta in Figure 2.24.). Even more, the H(6) from the B(6)-H(6) bond of the carborane cluster that interact with the respective chalcogen atom is also deshielded with regard to the parent 1,2-$(PPh_2)_2$-1,2-*closo*-$C_2B_{10}H_{10}$ and appears at 3.06 ppm for **26** and 3.17 ppm for **32** (in black in Figure 2.24).

Recent reports[53] show that the chalcogenides of the carboranylmonophosphines can form complexes with transition metals but an electron rich coordination centre has to be created before on the carborane cage. This can be obtained either by incorporating an anionic group

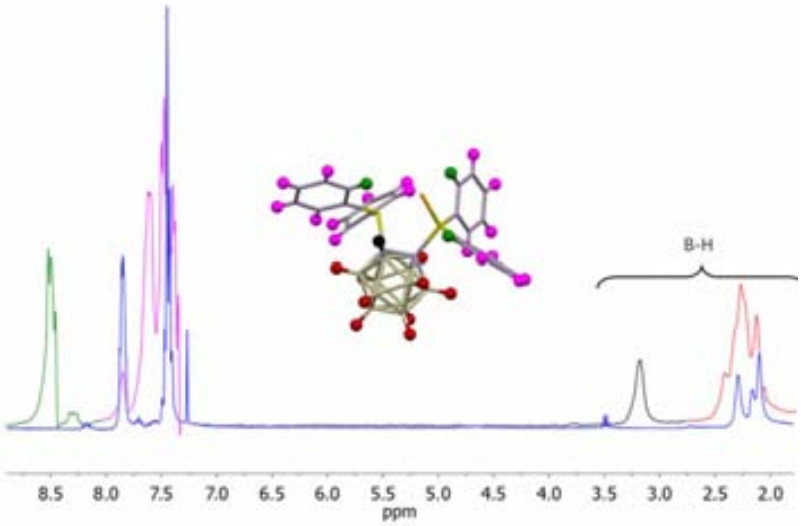

Figure 2.24. $^{11}H\{^{11}B\}$-NMR spectra of compounds **9** (in blue) and **32** (in green the H18, H20 and H26); in pink the other 17 hydrogen atoms of the phenyl groups; in black the H6 and in red the others 9 hydrogen atoms of the cluster vertexes).

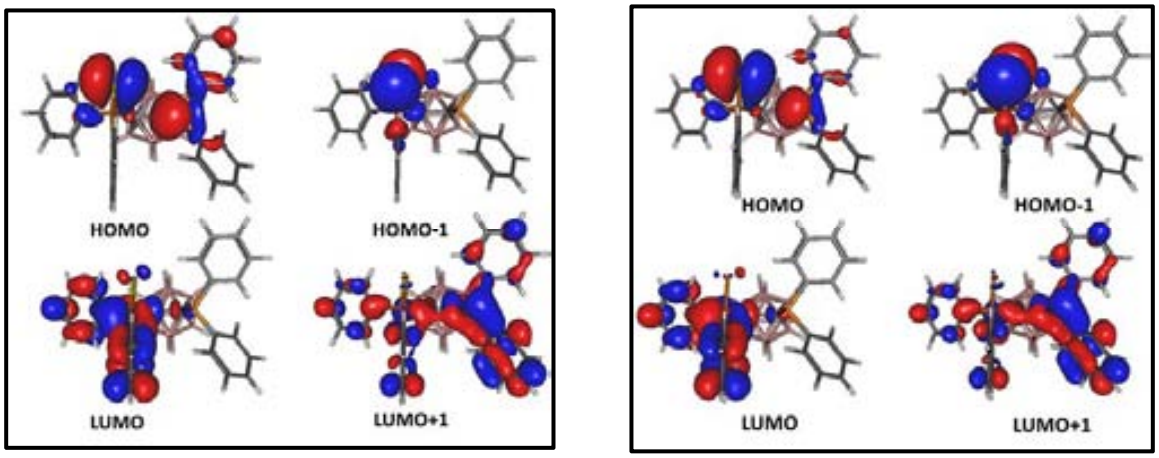

a) b)

Figure 2.25. Frontier molecular orbitals (HOMO and LUMO) and the next occupied (HOMO-1) and unoccupied (LUMO-1) molecular orbitals for: a) **26** and b) **32**.

as is the thiolate grup, or by deprotonation on the C_C-H bond,[53] obtaining thus a bonding anionic bonding centre. The frontier molecular orbitals for **26** and **32** (Figure 2.24.) differ of the ones for the anionic ligands as $[1\text{-}EPPh_2\text{-}2\text{-}S\text{-}1,2\text{-}C_2B_{10}H_{10}]^-$ (E = S, Se) (Figure 2.25.) and $[1\text{-}EPPh_2\text{-}1,2\text{-}C_2B_{10}H_{10}]^-$ (E = S, Se) (Figure 2.26.). In both **26** and **32** the major contribution to HOMO comes from the lone pairs on chalcogen and the unoxidized phosphorus but since the lone pairs have different *s* and *p*-orbital composition they have different symmetry and so, different reactivity. These factors, which are additive to the steric hindrance, makes the P-E bond labile to any reaction, favouring the chalcogen elimination in order to gain symmetrical reactivity sites. On the other hand, the contribution of the lone pairs in anionic carboranylphosphine chacogenides to the frontier orbitals is sequential. In the case of $[1\text{-}EPPh_2\text{-}2\text{-}S\text{-}1,2\text{-}C_2B_{10}H_{10}]^-$ (E = S, Se) first the lone pair of the anionic site contributes to the HOMO, and then, the lone pairs the two chalcogen moieties forms the HOMO-1. In the case of $[1\text{-}EPPh_2\text{-}1,2\text{-}C_2B_{10}H_{10}]^-$ (E = S, Se) the same order is maintained, the HOMO oribital being formed by the lone pair of the unprotonated C_C atom and then, the HOMO-1 is formed by the chalcogen lone pair.

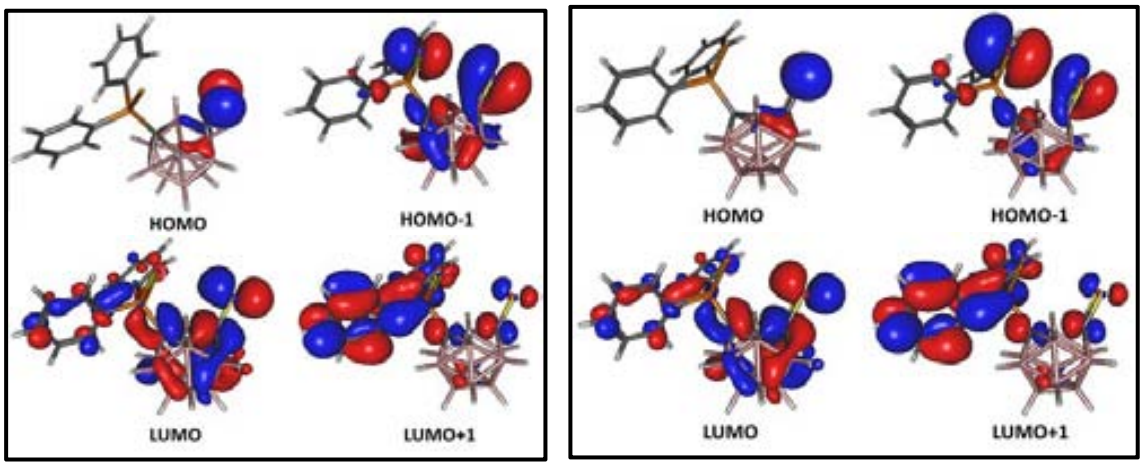

a) b)

Figure 2.26. Frontier molecular orbitals (HOMO and LUMO) and the next occupied (HOMO-1) and unoccupied (LUMO-1) molecular orbitals for: a) $[1\text{-}SPPh_2\text{-}2\text{-}S\text{-}1,2\text{-}C_2B_{10}H_{10}]^-$ and b) $[1\text{-}SePPh_2\text{-}2\text{-}S\text{-}1,2\text{-}C_2B_{10}H_{10}]^-$.

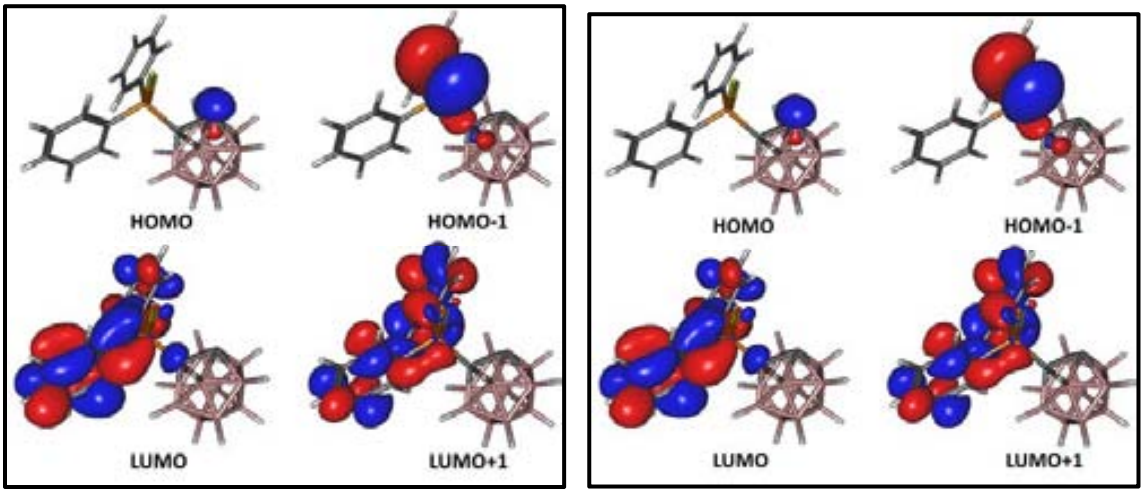

a) b)

Figure 2.27. Frontier molecular orbitals (HOMO and LUMO) and the next occupied (HOMO-1) and unoccupied (LUMO-1) molecular orbitals for: a) $[1\text{-}SPPh_2\text{-}1,2\text{-}C_2B_{10}H_{10}]^-$ and b) $[1\text{-}SePPh_2\text{-}1,2\text{-}C_2B_{10}H_{10}]^-$.

2.2.4. Computational study on the oxidation/degradation processes

Experimental results presented above indicate that H^+ induces the partial deboronation from *closo*-C_2B_{10} to *nido*-$[C_2B_9]^-$ if C_c-di-substituents possess H^+ scavenger elements such oxygen. In order to complement the synthetic studies and get insights into the electronic structures of *o*-carborane derivatives, theoretical calculations based on DFT calculations and natural bond orbitals (NBO) analysis have been performed.[47]

It was shown that the oxidation of phosphines by organic or inorganic peroxides follow a SN2 mechanism,[54] which involves in the rate determining step, a bimolecular nucleophilic displacement of the phosphine on the peroxide molecule (Scheme 2.9.) and the formation of OH^- (a nucleophile) and H^+ (a chelating cation) in the reaction media.

This mechanism implies that the lone pair availability on the phosphorus atom plays a crucial role on the rate of the reaction. The

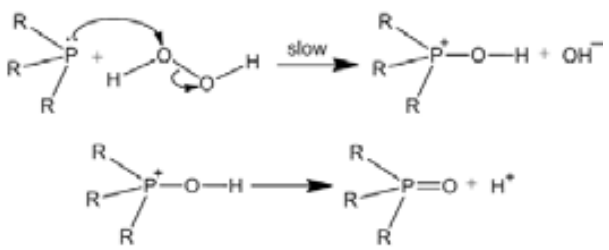

Scheme 2.9. Proposed mechanism for the oxidation of PR_3 (R= alkyl or aryl group) by hydrogen peroxide.

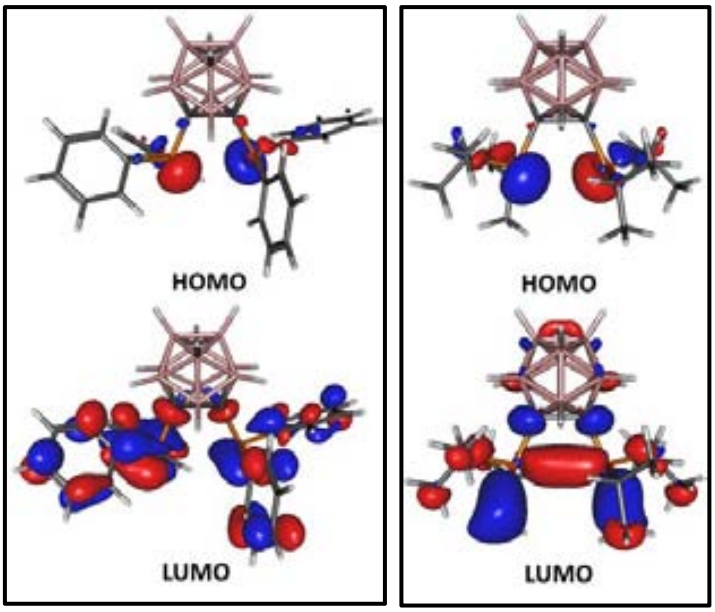

a) b)

Figure 2.28. Frontier orbitals for compounds: a) 1,2-$(PPh_2)_2$-1,2-*closo*-$C_2B_{10}H_{10}$ (**9**) and b) 1,2-$(P^iPr_2)_2$-1,2-*closo*-$C_2B_{10}H_{10}$ (**14**).

contribution of the lone pair of the phosphorus atoms in **9** and **14** to the HOMO orbitals (Figure 2.28.) is significant but cannot explain the different oxidation reaction rates of the two compounds. On the other hand, the LUMO orbitals of the two compounds (Figure 2.28.) are significantly different: there is an important contribution of the phosphorus centres on the LUMO of **14** whereas the LUMO density for **9** is delocalised from the phosphorus centres to the phenyl rings.

The oxidation promptness of the P electron lone pair can also be evaluated based on the natural bond orbital donor-acceptor interactions. In compound **9**, the lone pair delocalizes more in the antibonding orbitals of the neighbouring bonds, than in compound **14** (Table 2.11. and Figure 2.29.), which probably makes it less available for nucleophilic attack on the hydrogen peroxide (the slow first step on Scheme 2.8.). Also, the natural hybrid orbitals (NHOs) of the lone pair on phosphorus atom have a higher *s* character for **14** (52.06% *s* and 47.94% *p*) than for **9** (48.90% *s* and 51.1% *p*) which makes it more nucleophilic.

It should be pointed out that in this first step OH^-, a nucleophile, is slowly produced. The original *closo* backbone structure is not retained in the presence of a nucleophile[29a,30,55] because it attacks the carborane cluster at the boron atom which have less electronic density (namely boron atoms bonded to the both carbon atoms, B3 or B6, see Tables 2.8. and 2.9.) and in the process, a B^+ vertex is removed.[56]

Electronic and steric factors have to be taken into consideration in this partial deboronation process.[57]

Compound	Lone pair[a]	NBO antibond	$E_{ij}^{(2)}$ (Kcal·mol^{-1})
9	P1	C13–C14	5.86
	P1	C19–C20	6.98
	P1	B3–B4–C1	6.21
	P2	C24–C25	6.10
	P2	C29–C30	7.16
	P2	B6–B11–C2	5.91
14	P1	C16–C17	4.45
	P1	B3–B4–C1	5.91
	P2	C22–C23	4.43
	P2	B7–B11–C2	6.87

[a] The numbers in brackets stand for the first (1) and the second (2) lone pairs of the oxygen atoms.

Table 2.11. Second order delocalization energies for the phosphorus electron lone pairs and NBOs antibonding interactions for the *closo*–carboranyldiphosphines.

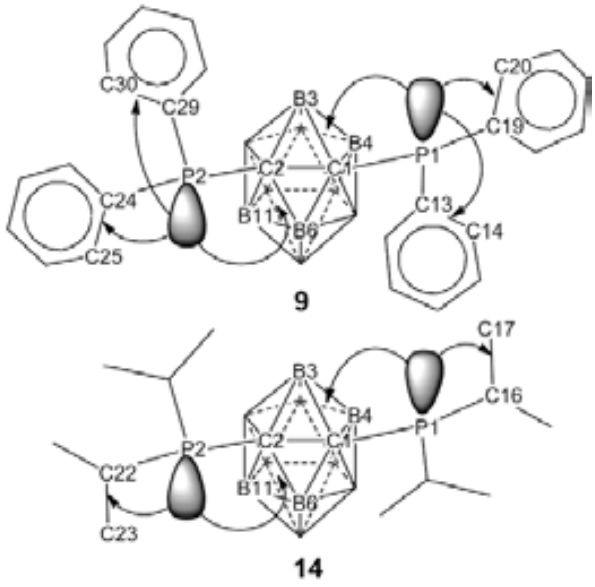

Figure 2.29. Schematic representation of the main donor-acceptor interactions in *closo*-carboranyl-diphosphines **9** and **14**.

The second order perturbation theory analysis showed that there are significant interactions between the electron lone pairs on the oxygen atoms and the P-C_c antibonding orbitals (Table 2.12. and Figure 2.30.) in **34** and **35**. This can be explained by the strong electron-withdrawing character of the *closo* carborane cluster.

As the deboronation process involves the attack of a nucleophile, the distribution of the LUMOs in compounds **34** and **35** is important (Figure 2.31.). For compound **34** the LUMO is again, delocalized on the phenyl rings, and its communication with the cluster is made through the carbon atoms. In compound **35**, on the other hand, the LUMO orbital is on the carborane cage, with significant presence

Compound	Lone pair[a]	NBO antibond	$E_{ij}^{(2)}$ (Kcal·mol^{-1})
34	O1(1)	P1–C13	16.89
	O1(1)	P1–C19	12.84
	O1(2)	P1–C1	24.43
	O1(2)	P1–C19	7.09
	O2(1)	P2–C24	16.89
	O2(1)	P2–C29	12.84
	O2(2)	P2–C2	24.43
	O2(2)	P2–C29	7.09
35	O1(1)	P1–C1	24.97
	O1(1)	P1–C13	14.89
	O1(2)	P1–C16	13.98
	O2(1)	P2–C2	24.97
	O2(1)	P2–C19	14.89
	O2(2)	P2–C22	13.98

[a] The numbers in brackets stand for the first (1) and the second (2) lone pairs of the oxygen atoms.

Table 2.12. Second order delocalization energies for the phosphorus electron lone pairs and NBOs antibonding interactions for the *closo*–carboranyldiphosphines oxides.

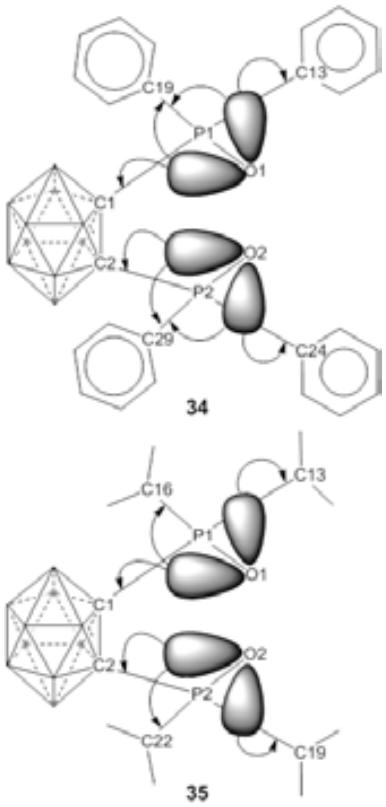

Figure 2.30. Schematic representation of the main donor-acceptor interactions in *closo*-carboranyl-diphosphines oxides **34** and **35**.

on the B3-C1-B6 and B3-C2-B6 bonds. This can account for the readiness for deboronation of **34** with respect to **35**.

Further assessment of the process can be made by looking at the charges on individual atoms. It can be observed from the different charge analysis methods (Tables 2.10. and 2.11.) that the presence of aryl moieties or alkyl moieties bonded to phosphorus atoms, remotely affects the charge density on cluster and on oxygen atoms. The individual charges for B3 and B6 (which are the ones susceptible for the nucleophile attack) are the most positive vertexes in **34** and **35**. In addition, the Hirshfeld method (see Table 2.11.) supports better the fact

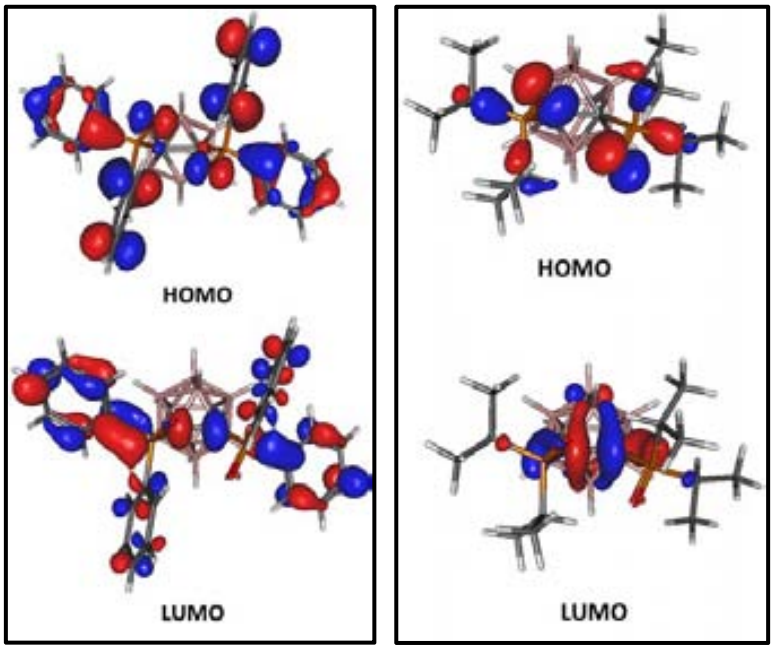

Figure 2.31. Frontier orbitals for compounds: a) 1,2-$(OPPh_2)_2$-1,2-*closo*-$C_2B_{10}H_{10}$ (**34**) and b) 1,2-$(OP^iPr_2)_2$-1,2-*closo*-$C_2B_{10}H_{10}$ (**35**).

that **34** can be more easily attack by a nucleophile than **35**, which is consistent with the experimental results presented.

2.2.5. Intramolecular communication in oxidized anionic carboranyldiphosphines

Hydrogen bonding plays a key role in physical, chemical and biochemical processes [58], being an important interaction in enzymatic catalysis,[59] crystal engineering,[60] and proton transfer reactions.[61] Interest has been directed towards the encapsulation or chelation of the proton,[62] but probably the most important feature of hydrogen bonding is its role in catalysis.[63] For example, organocatalysts as BINOL-based phosphoric acids are able to catalyze Mannich reactions, aza-Friedel-Crafts alkylations, hydrophosphonylation of imines and reduction of imines.[64]

The hydrogen bonds typically imply a transfer of electronic charge from a acceptor to a proton-donating bond, where both of these atoms can be of the same type (homonuclear H-bonds), usually O, N or F atoms; or of different types of atoms (heteronuclear H-bonds) like, N-H···O, O-H···N, O-H···S, S-H···O and N-H···Cl.

The strong intramolecular O-H···O bonds where the O atoms are bonded to atoms other than C and S are not so common. Ten years ago we reported the proton mediated partial degradation of 1,2-$(PPh_2)_2$-*closo*-1,2-$C_2B_{10}H_{10}$ where we demonstrated for the first time that, given the necessary chemical and geometrical conditions to produce proton chelation, the proton can also induce conversion of the *closo*-C_2B_{10} to the *nido*-C_2B_9 species.[9a] The geometrical parameters from the X-ray crystal structure of H[7,8-$(OPPh_2)_2$-*nido*-7,8-$C_2B_9H_{10}$] showed that the oxidized diphosphine fragment does chelate a proton, presenting a strong H-bond, P=O···H···O=P, but at that time no further studies were carried out.

If one searches the Cambridge Structural Database (CSD) for crystal structures having the P=O···H···O=P bond moiety (Chart 2.1), few structures will be found.[65] However, there are different ways how these features D-H···A can be schematically presented. In Chart 1 we propose two ways for performing the search of P=O···H···O=P bonds, which have a remarkable difference concerning the nature of the H-bonds. If mode A is used, no crystal structure can be found whereas using mode B, 139 structures will appear. On the other hand, if P atoms are replaced by C atoms and mode A is used, a large

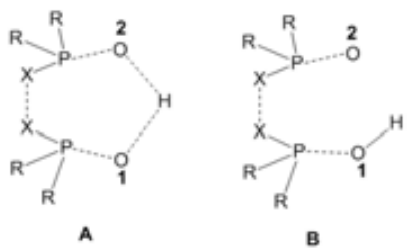

Chart 2.1. Different drawing modes for searching in CSD (X stand for any atom and the dashed line for any kind of bond).any kind of bond).

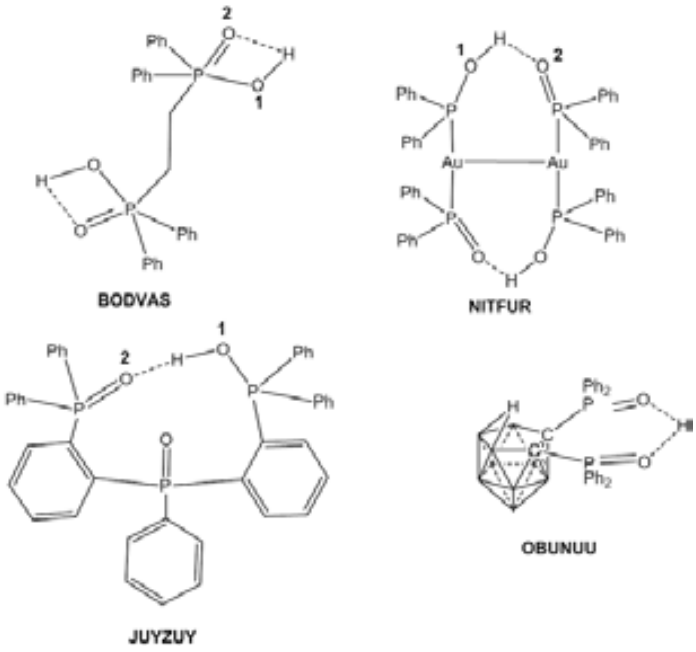

Figure 2.32. Schematic drawing of compounds which present symmetric and asymmetric P=O···H···O=P bonds.

number of crystalline structures are found. This raises questions about the nature of the H-bond in oxidized diphosphine systems.

Using the search mode B one can find structures like BODVAS[66] (Figure 2.32.), where the distance O1-H is 0.820 Å and O2-H is 2.770 Å, whereas the O1-H···O2 angle is 67.9°; there is no symmetric intramolecular H-bond. Another example is the structure NITFUR[67], in which the O1-H distance is 0.978 Å and the O2-H is 1.453 Å; in NITFUR there is an intramolecular H-bond. On the other hand the same search provides results like JUYZUY[68], where the O1-H distance is 1.170 Å and the O2-H is 1.269 Å, being more symmetric, or the structure OBUNUU[9a] in which the H atom bisects the O atoms: O1-H is 1.206 Å and O2-H is 1.218 Å.

As we succeeded to determinate the crystal structures of H[7,8-(OP*i*Pr$_2$)$_2$-7,8-*nido*-$C_2B_9H_{10}$], H[**41**], where two different H-bond systems exist in one compound, we decided to get further insights on the nature of the P=O···H···O=P bonds and to establish the impact of this bonds on the intramolecular electronic communication in this phosphine. To support our experimental results on the nature of the hydrogen bonds and to the underlying reasons for this phenomena, we performed a computational study, based on Natural Bond Orbital (NBO), Quantum Theory of Atoms in Molecules (QTAIM) and Electron Localization Function (ELF) analyses. It is worth mentioning that we did not find in the literature a similar study where the three methods NBO, QTAIM and ELF have been utilized altogether to study the hydrogen bonds on the same structural feature. As recently stated by Fuster and Grabowski,[69] the QTAIM and ELF parameters are useful to categorize and estimate the strength of hydrogen bonds. So, the study of the covalency by computational means is very important for intramolecular hydrogen bonds, as is our case, for which the absence of reference states does not allow to calculate the energy of this interaction.

Compound	δ (ppm)	σ_p (ppm)	σ_d (ppm)
H[**40**] (exp.)	47.09	–	–
Me_4N[**40**] (exp.)	29.33	–	–
H[**40**] (calc.)	29.42	–708.1	975.4
	54.66	–741.6	983.7
[**40**]$^-$ (calc.)	14.93	–689.2	971.0
	14.97	–680.5	962.3
H[**41**] (exp.)	77.26	–	–
Mg[**41**]$_2$ (exp.)	65.48	–	–
H[**41**] (calc.)	76.74	–746.9	967.3
	68.58	–735.9	964.4
[**41**]$^-$ (calc.)	47.96	–715.1	964.2
	43.92	–716.1	964.3

Table 2.13. Experimental and computed ^{31}P–NMR chemical shifts and the computed paramagnetic (σ_p) and diamagnetic (σ_d) contribution terms to the shielding constant.

In order to get a first quantitative picture on the strength of the H bonds, we calculated[70] the stability of the protonated forms, H[**40**] and H[**41**], with respect to the unprotonated [**40**]$^-$ and [**41**]$^-$, by the transference of the H^+ to the amide anion to form ammonia, and it was found that [**40**]$^-$ is enthalpically favoured over H[**40**] by 83.61 kcal·mol^{-1} and [**41**]$^-$ is enthalpically favoured over H[**41**] by 83.76 kcal·mol^{-1}.

As the experimental data shows very distinctive ^{31}P-NMR chemical shifts for protonated or anprotonated forms of [**40**]$^-$ and [**41**]$^-$ which is an indication of the important intramolecular electronic communication in these compounds. In Table 2.13. are presented the experimental and computed

	P1		O1		P2		O2	
	% s	*% p*	*% s*	*% p*	*% s*	*% p*	*% s*	*% p*
H[**40**]	24.29	74.21	33.48	66.44	21.33	77.00	31.48	68.45
[**40**]$^-$	27.16	71.53	34.18	65.71	28.03	70.62	34.59	65.32
H[**41**]	22.24	76.07	32.92	67.01	23.70	74.70	34.08	65.84
[**41**]$^-$	26.73	71.81	35.75	64.15	26.69	71.86	35.64	64.27

Table 2.14. Natural hybrid character of P=O bonds in the studied compounds.

^{31}P-NMR chemical shifts[71] and the computed paramagnetic (σ_p) and diamagnetic (σ_d) contribution terms to the shielding constant. All the compounds are *nido* clusters, that means that on the C_2B_3 open face all the five atoms are non-equivalent. Due to the rapid jumping of the apical H atom on the three boron atoms, in solution, the carbon atoms are equivalent, so the P atoms, bonded to them, are also equivalent, and in consequence, only one chemical shift is displayed in ^{31}P-NMR. As the calculations are performed in gas phase, the two P atoms are non-equivalents and two chemical shifts for the computed ^{31}P-NMR values are obtained. For the H[**41**] the computed chemical shift value fits better to the experimental one than in the case of H[**40**]. Nevertheless, for both couples H[**40**] and [**40**]$^-$ and H[**41**] and [**41**]$^-$, the diamagnetic contribution to the shielding constant is the same, the difference being in the paramagnetic contribution, which is consistent with the general observation for phosphorus compounds.[72] The magnitude of σ_d depends on the density of circulating electrons but since the same moieties are bonded to P atoms in H[**40**] and [**40**]$^-$, and in H[**41**] and [**41**]$^-$, respectively, it is expected that this term to be similar for all the compounds. The σ_p depends on various factors that have to do with the orbitals involved in chemical bonding, mainly the relative electron densities in various *p*- and *d*-orbitals.[73]

In Table 2.14. the percentage of natural orbital hybrid character for the P=O bonds is presented. As can be seen, the P atoms in [**40**]$^-$ have 71.53% and 70.62% *p* character whereas in H[**40**], the P atoms have 74.21% and 77.00%, respectively. The same trends are observed for the couple H[**41**] and [**41**]$^-$. These differences came from the degree of availability of the lone pairs of electrons of O atoms to back-donation. In Table 2.15. are presented the delocalization energies for the lone pairs and NBO antibonding interactions. In H[**40**] and H[**41**] structures, the lone pairs of the O atoms strongly delocalize in O-H antibonds, so are less available to back-donation to the P-C antibonds. On the other hand, in [**40**]$^-$ and [**41**]$^-$ the both O atoms have the lone pairs fully available for back-donation to P-C antibonds.

Compound	Lone pair[a]	NBO antibond	$E_{ij}^{(2)}$ (Kcal·mol^{-1})
H[**40**]	O1(2)	P1–C13	11.67
	O1(2)	P1–C7	5.61
	O2(1)	P2–C24	15.53
	O2(2)	O1–H	60.51
	O2(2)	P2–C8	5.60
	O2(2)	P2–C29	9.60
[**40**]$^-$	O1(1)	P1–C7	10.21
	O1(1)	P1–C19	18.93
	O1(2)	P1–C7	9.55
	O1(2)	P1–C13	18.85
	O2(1)	P2–C8	6.29
	O2(1)	P2–C24	19.44
	O2(2)	P2–C8	15.78
	O2(2)	P2–C29	16.76
H[**41a**]	O1(1)	P1–C7	7.90
	O1(1)	P1–C16	13.30
	O2(1)	P2–C8	5.64
	O2(1)	P2–C19	14.32
	O2(2)	P2–C22	5.01
	O2(2)	O1–H	164.32
H[**41b**]	O1(1)	P1-C7	10.52
	O1(1)	P1-C16	8.48
	O2(1)	P2-C19	15.50
	O2(1)	P2-C22	6.79
	O2(2)	P2-C8	10.16
	O2(2)	P2-C22	8.35
	O2(2)	O1-H	38.52
[**41**]$^-$	O1(1)	P1–C7	5.40
	O1(1)	P1–C13	18.01
	O1(1)	P1–C7	14.06
	O1(1)	P1–C16	16.35
	O2(1)	P2–C19	15.29
	O2(1)	P2–C22	12.11
	O2(2)	P2–C8	18.87
	O2(2)	P2–C22	6.28

[a] The numbers in brackets stand for the first (1) and the second (2) lone pairs of the oxygen atoms

Table 2.15. Second order delocalization energies for the oxygen electron lone pairs and NBOs antibonding interactions for *nido*-carboranyldiphospines (for atom numbering see Figure 2.33.).

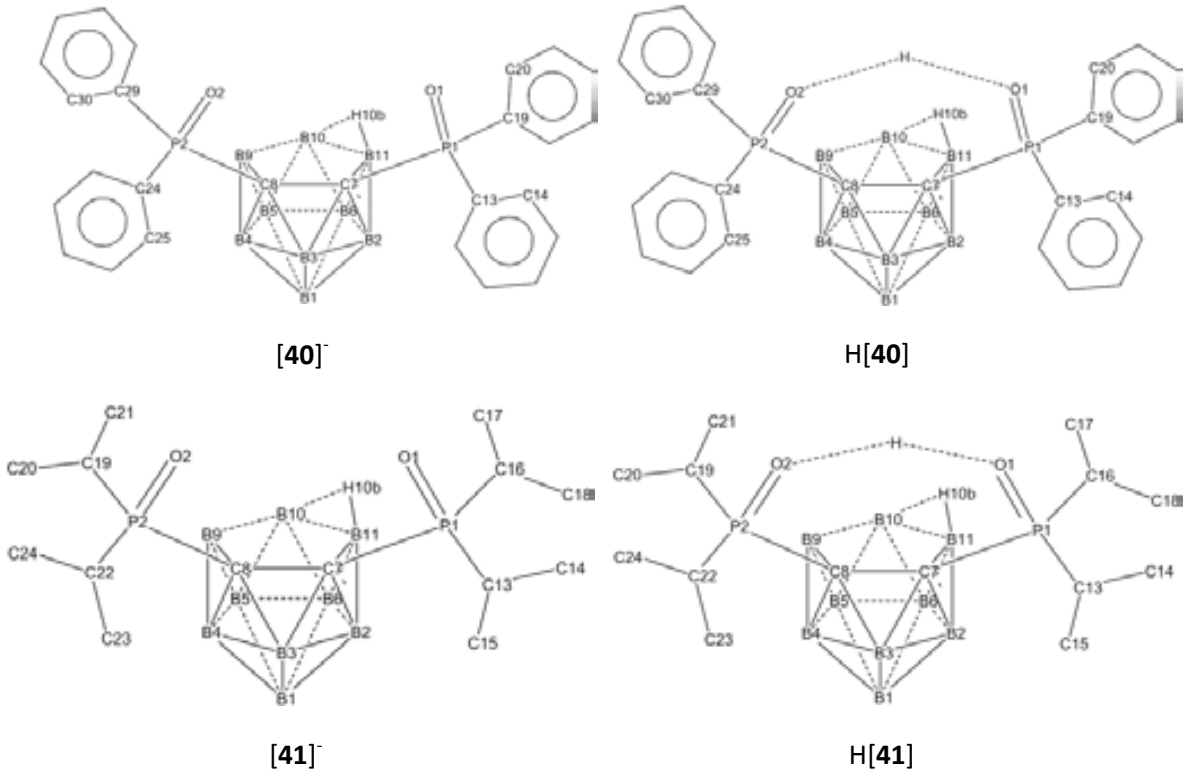

Figure 2.33. Numbering scheme for the compounds presented in Table 2.15.

Different approaches to study the hydrogen bonding can be found in the literature, where the covalency of these bonds is studied.[74] To capture the influence of the H^+ in the crystal structures, we have performed a thorough computational study, based on DFT calculations, by using NBO analysis, and analysis of the topology of the electron density by QTAIM and ELF methods, for the geometries obtained from the X-ray diffraction studies.[75]

The observed delocalizations in H[**40**] and H[**41**] are consistent with the NBO perspective on the hydrogen bonding that is based on the covalent-ionic resonance or charge transfer of the form:[76] A:H :B $\leftrightarrow$ A:⁻ H:B⁺. The charge transfer can be quantified by taking into account the two-electron $n_B \rightarrow \sigma^*_{AH}$ intramolecular donor-acceptor interaction, where electron density from the lone pair n_B of the Lewis base centre B, delocalizes into the unfilled σ^*_{AH} antibonding orbital of the Lewis acid center, AH (which in turn can be seen as bonding between H···B fragment). In H[**41a**], the second lone pair of the O2 atom is strongly delocalized into the antibonding orbital of O1-H bond, the energy for this delocalization (charge transfer energy $\Delta E n_B \rightarrow \sigma^*_{AH}$) being more than four times stronger than the same energy from H[**41b**] and comparable with the values found in the literature[74b,76c] for very strong hydrogen bonded systems like FH···F⁻ (166.2 kcal·mol^{-1}) and $H_2OH^+ \cdots OH_2$ (168.4 kcal·mol^{-1}). The charge transfer energy between the second lone pair of O2 atom and the antibonding orbital of the O1-H bond in compound H[**41b**] is comparable with the one found for complexes like $H_3N \cdots HF$ (34.9 kcal·mol^{-1}), $OH^- \cdots HNH_2$ (31.1 kcal·mol^{-1}) and $H_2O \cdots HNH_3^+$ (30.1 kcal·mol^{-1}). The analysis of the natural hybrid orbitals (NHOs) revealed that the second lone pair of the O2 atoms in compounds H[**41a**] and H[**41b**] gain *s* character, proportional with the quantity of charge transfer from the lone pair to the antibonding orbital. Thus, for H[**41a**], that have the strongest interaction, the σ^*_{O1H} antibonding orbital gain 0.24559 e⁻ and the O2 lone pair have 21.84% *s* character and 78.12% *p* character, whereas in H[**41b**], the σ^*_{O1H} antibonding orbital gain only 0.08932 e⁻, thus the O2 lone pair remains mainly with *p* character, having only 5.07% *s* character.

The QTAIM analysis complements the NBO picture, providing further insight on the nature of H bonds. All the hydrogen bonds fulfill the Koch and Propelier topological criteria for the existence of the hydrogen bonding.[74b,77] In H[**41a**] all three atoms involved in the hydrogen bonding system presents individual negative charge concentrations (Figure 2.34.), with the Bond Critical Point (BCP) being close to the H atom, whereas in H[**41b**] the O1-H fragment form one shared negative charge concentration at O1-H and one individual at O2. From the properties of the BCPs between the O atoms and the H (Table 2.16.), one can evaluate the strength of these bonds.[78] In H[**41a**], the parameters of both BCP found between O atoms and the H indicate that the hydrogen bonds are eminently strong. In H[**41b**] the O1-H bond path parameters indicate a more covalent nature of this bond, comparable with the OH bond in H_2O.[79] The O2-H bond path, on the other hand, is characterized as of moderate strength. All these observations are in agreement with the NBO depiction of these bonds.

The topology of Electron Localization Funcion (ELF) has applied to the study of hydrogen bonding.[80] First designed by Becke and Edecombe, the ELF provides a picture of the electron-pairing regions in molecular space for a given distribution of nuclei and associated electron density, providing an orbital independent description of the electron localization.[81] The ELF in its analytical form is in range from 0 (in those regions where the antiparallel spin pair probability is low) to 1 (in those regions where the antiparallel spin pair probability is high). The topological partition of ELF gradient field (electron density) yield basins, that can be classified as either core or valence

Compound	Bond	ρ	$\nabla^2\rho$	H
H[**41a**]	P1-O1	0.2049	1.0965	-0.8428
	P2-O2	0.2077	1.1593	-0.8731
	O1-H	0.1721	-0.2764	-0.1919
	O2-H	0.1745	-0.2971	-0.1944
H[**41b**]	P1-O1	0.2007	1.0520	-0.8107
	P2-O2	0.2125	1.2102	-0.9119
	O1-H	0.3476	-2.4649	-0.1802
	O2-H	0.0789	0.2017	-0.1463

ρ - electron density, $\nabla^2\rho$ - Laplacian of the electron density, H – total electronic energy density

Table 2.16. Properties of BCP for the studied compounds (all the values are in a.u.).

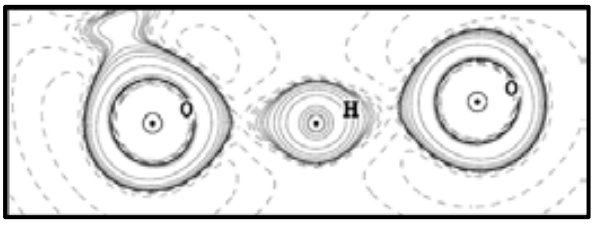

H[**41a**]

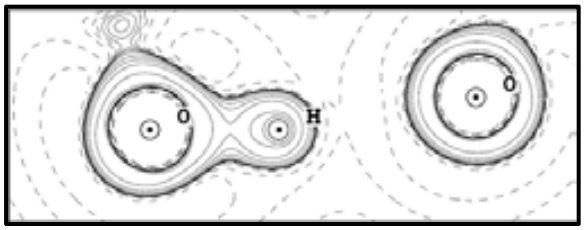

H[**41b**]

Figure 2.34. Contour plots of the Laplacian of the electron density ($\nabla^2\rho$) for H[**41a**] and H[**41b**] (solid lines represent negative values and dashed lines positive values).

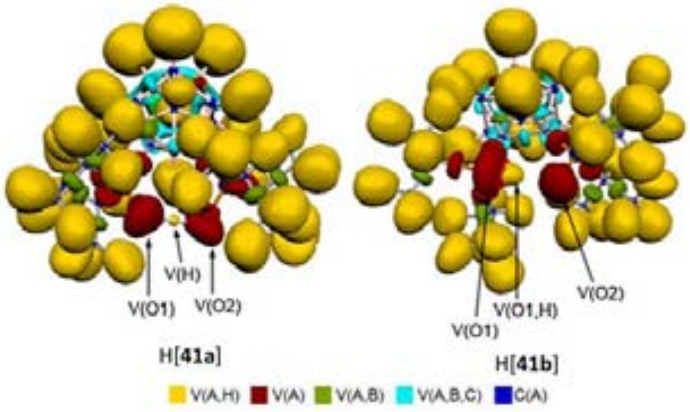

Figure 2.35. ELF localization domains of H[**41a**] and H[**41b**].

basins.[82] The core basins, correspond to the core shells of each atomic species (Z>2) in molecule and are labelled C(A), where A is the atomic symbol of the element. On the other hand are valence basins that can correspond to bonding or non-bonding valence electrons, which can be topologically placed around and/or between core basins. The number of C(A) connected to a given valence basin determinates its synaptic order: there are monosynaptic basins, labelled V(A), that correspond to the lone pairs of the Lewis model, and polysynaptic basins that correspond to the shared pairs of the Lewis model. In particular, there are disynaptic basins, labelled V(A,B), that correspond to two-centre bonds, and trisynaptic basins, labelled V(A,B,C), that correspond to three-centre bonds. A special case of a disynaptic basin is the disynaptic protonated basin, labelled V(A,H), that corresponds to a A-H bond. As hydrogen atoms have no core shell, but have valence shell, they are counted as a formal core in the synaptic order.

The Electron Localization Function (ELF) approach has been applied to further study the intramolecular hydrogen bonding in these compounds. As can be observed from Figure 2.35., for H[**41a**] the ELF gradient field describes two monosynaptic valence basins for the two oxygen atoms and a protonated monosynaptic basin, for the H atom, centered at the O1-O2 midpoint. The appearance of the isolated domain for the hydrogen basin seems to be characteristic for the strong hydrogen bonds, and it was observed for systems like FHF^- $N_2H_7^+$ and $H_5O_5^+$, being also consistent with the formation of the individual negative charge concentration observed in the QTAIM analysis. On the other hand, for H[**41b**] there exists disynaptic valence basins on the O atoms and a protonated disynaptic valence basin

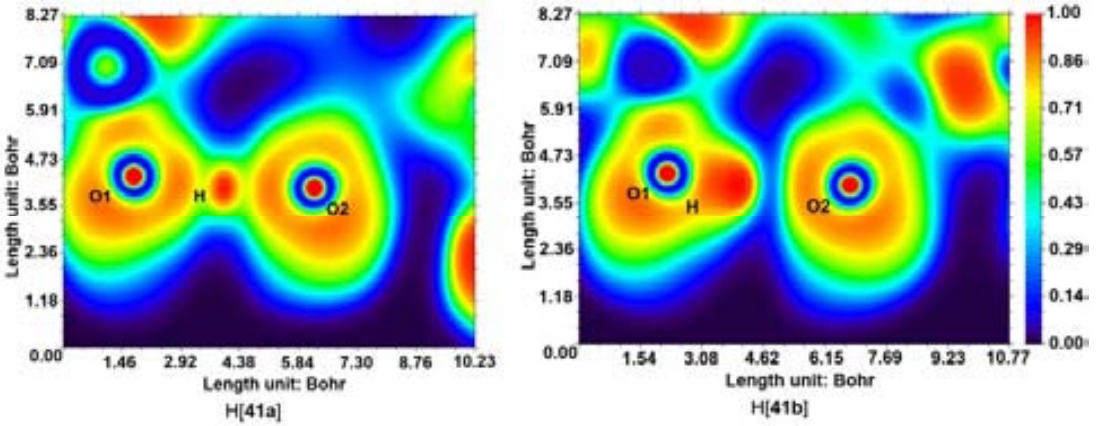

Figure 2.36. 2D representation of the ELF isosurface as cross sections through O1-H-O2 plane for H[**41a**] and H[**41b**].

centered on the O1-H bond. As can be observed from Figure 2.36., the ELF values on H-O2 axis are very low, indicating that the interaction of H with the O2 would be weaker in H[**41b**]. The absence of the monosynaptic basin at attractor H^+ in H[**41b**] is in good agreement with the observed weaker O-H bond in H[**41b**] compared to H[**41a**].

2.3. Base induced *ortho* to *meta* isomerization of anionic *nido*-carboranyldiphosphines

There are different ways to synthesize the *meta*-carborane, 1,7-*closo*-$C_2B_{10}H_{12}$, and its derivatives, though the only practical manner is by thermal isomerisation of *ortho*-carborane, 1,2-*closo*-$C_2B_{10}H_{12}$ and its derivatives.[83]

The correspondent *nido* derivative of 1,7-*closo*-$C_2B_{10}H_{12}$ is [7,9-*nido*-$C_2B_9H_{12}$]$^-$ which is mainly obtained by the base-promoted degradation of 1,7-*closo*-$C_2B_{10}H_{12}$,[29c] though other methods are known starting from the 11-vertex carborane, 2,3-*closo*-$C_2B_9H_{11}$.[84]

There are few examples in the literature where the *ortho* to *meta* isomerisation occurred for open cage systems as are the *nido* derivatives, some reports can be found on the rearrangement upon alkylation at temperatures lower than 0°C of the [7,8-*nido*-$C_2B_9H_{11}]^{2-}$ forming [11-R-2,7-*nido*-$C_2B_9H_{11}]^-$, which left at 20°C isomerizes to [8-R-7,9-*nido*-$C_2B_9H_{11}]^-$.[85]

Due to the peculiarity of these type of reactions, we were surprised to find that the protonated carboranyldiphosphines oxides, H[7,8-$(OPR_2)_2$-7,8-*nido*-$C_2B_9H_{10}$] (R = Ph, **40**, ^{i}Pr, **41**) easily isomerise to [7,9-$(OPR_2)_2$-7,9-*nido*-$C_2B_9H_{10}]^-$ (R = Ph, [**43**]$^-$, ^{i}Pr, [**44**]$^-$) in the presence of NaOH in EtOH at room temperature(Scheme 2.10.). The isomerisation is complete after 2 days for R = ^{i}Pr, whereas for R = Ph several days are needed.

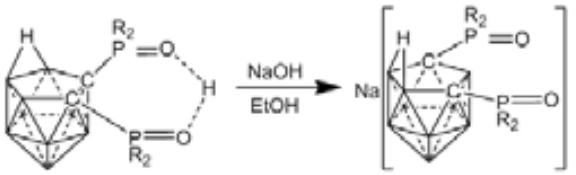

R = Ph, H[**40**]; ^{i}Pr, H[**41**] R = Ph, Na[**43**]; ^{i}Pr, Na[**44**]

Scheme 2.10. Isomerization of *ortho-nido*-carboranylphosphine oxides to *meta-nido*-carboranylphosphine oxides.

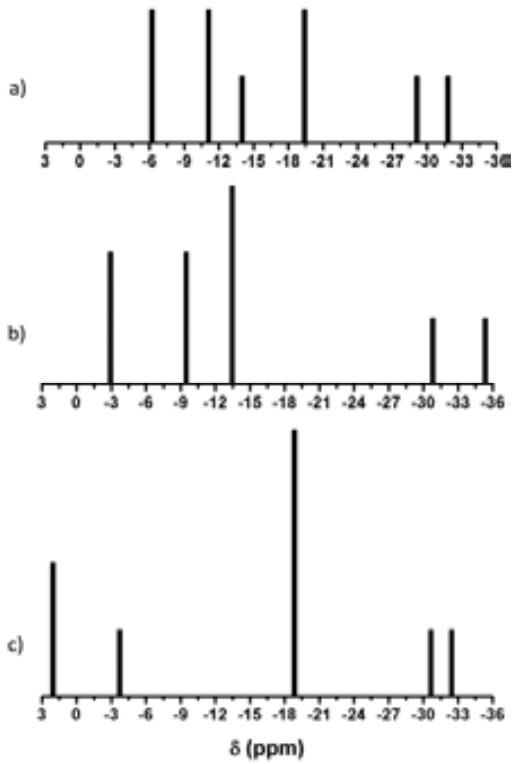

Figure 2.37. Stick representation of the $^{11}B\{^1H\}$-NMR spectra for: a) H[**41**], b) Mg[**41**]$_2$ and c) Na[**44**].

The $^{11}B\{^1H\}$-NMR spectrum for [**44**]$^-$ differs greatly from the one for H[**41**] or Mg[**41**]$_2$, with a five peak pattern (2:1:4:1:1) and a range of chemical shifts from 2.03 ppm to -32.42 ppm (Figure 2.37.). The chemical shift for the P atoms is also different appearing at higher field (δ = 56.33 ppm) comparative with H[**41**] (δ = 77.26 ppm) or Mg[**41**]$_2$ (δ = 65.48 ppm). The ^{1}H-NMR also shows distinctive feature compared with the *ortho* isomers, though the most important feature, characteristic for the [7,9-*nido*-$C_2B_9H_{12}]^-$ derivatives, is the appearance as a triplet for the signal corresponding to the apical H atom in $^1H\{^{11}B\}$-NMR spectrum, at -1.61 ppm (^2J(H,H) = 12 Hz). Definitive proof of the isomerisation process was obtained by X-ray structure determination of the Na[7,9-$(OP^iPr_2)_2$-7,9-*nido*-$C_2B_9H_{10}$] derivative (Figure 2.38.).

The X-ray crystal structure of [**44**]$^-$ showed two crystallographic independent molecules in the asymmetric fraction of the unit cell. The negative charge is balanced by the presence of two sodium ions, which are not coordinated to [**44**]$^-$ molecules but to water molecules, the actual formula of the crystal being [$Na_2(H_2O)_8$(**44**)$_2$], selected bond parameters are presented in Table 2.17. In this structure the Na(I) cations have a distorted square pyramidal coordination sphere, which is made up by five oxide donors coming from water molecules; the oxygen atoms from [**44**]$^-$ are further than the Na-O van der Waals distance and do not coordinate to the Na(I) cations. The Na-O distances for the base of the square pyramide are between 2.288 Å and 2.424 Å and the Na-O distances which form the height are Na1-O6 = 2.517 Å and Na2-O5 = 2.620 Å. The O-Na-O angles in the square plane are very distorted from the ideal (180°), as well as the angles in the triangular faces, though these are closer the ideal value (90°).

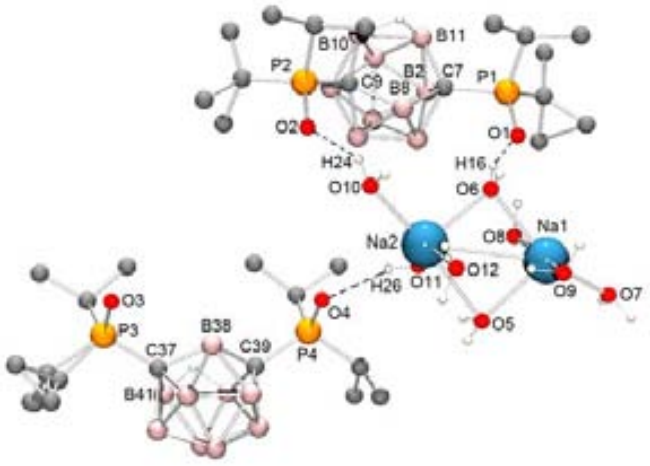

Figure 2.38. Molecular structure of $[Na_2(H_2O)_8(\mathbf{44})_2]$ (The hydrogen atoms, except the ones of the water molecules, are omitted for clarity).

Besides the typical differences due to the isomerization from *ortho* to *meta* for the *nido* cluster, the orientation of the oxidized phosphorus moieties is noteworthy. Though there are not such great differences with respect to the bonds length the angles are very different. The O atoms in the two units are practically perpendicular to the C-C and P-P bonds, with O-P-P angles between 90.4° and 93.6° and O1-C7-C9-O2 and O3-C37-C39-O4 torsion angles of -0.0° and 0.2°, respectively.

Though the oxygen atoms from [**44**]$^-$ are not coordinated to the Na(I) cations, they form strong O···H-O bonds with some water molecules coordinated to Na(I). The strength of the interaction can be deduced from the O···H-O ditances (1.888 Å, 1.933 Å, 2.027 Å) that are very small compared with the O-H van der Waals distance (2.72 Å).

When packing, $[Na_2(H_2O)_8(\mathbf{44})_2]$ forms a layered supramolecular architecture (Figure 2.39.) held together by strong O···O contacts ranging from 2.722 Å to 2.866 Å (O-O van der Waals distance is 3.04 Å). The O···O contacts are formed between the oxygen atoms form [**44**]$^-$ and oxygen atoms of water molecules. The layered structure has one hydrophilic layer formed by sodium ions coordinated to water, that is enclosed by two hydrophobic layers formed by [**44**]$^-$ molecules.

Distances		Angles	
C7-P1	1.801	O1-P1-C7	111.5
C9-P2	1.801	O2-P2-C9	112.3
P1-O1	1.512	O1-P1-P2	91.3
P2-O2	1.512	O2-P2-P1	93.6
P1-P2	5.839	O3-P3-C37	112.0
O1-O2	5.972	O4-P4-C39	112.3
C7-B8	1.655	O3-P3-P4	90.4
C9-B8	1.653	O4-P4-P3	92.0
C37-P3	1.808	P1-C7-B8	119.4
C39-P4	1.800	P2-C9-B8	112.3
P3-O3	1.515	P3-C37-B38	112.0
P4-O4	1.512	P4-C39-B38	112.3
P3-P4	5.817	O5-Na1-O6	93.0
O3-O4	5.883	O5-Na1-O7	167.7
C37-B38	1.646	O5-Na1-O8	92.0
C39-B38	1.647	O5-Na1-O9	85.3
Na1-O1	3.767	O6-Na1-O7	154.7
Na1-O5	2.391	O6-Na1-O8	81.5
Na1-O6	2.517	O6-Na1-O9	85.3
Na1-O7	2.302	O7-Na1-O8	84.3
Na1-O8	2.424	O7-Na1-O9	108.7
Na1-O9	2.333	O8-Na1-O9	166.4
Na2-O2	4.457	O5-Na2-O6	92.8
Na2-O4	3.984	O5-Na2-O10	164.9
Na2-O5	2.620	O5-Na2-O11	69.1
Na2-O6	2.288	O5-Na2-O12	78.1
Na2-O10	2.324	O6-Na2-O10	93.7
Na2-O11	2.336	O6-Na2-O11	100.3
Na2-O12	2.388	O6-Na2-O12	86.6
Na1-Na2	3.378	O10-Na2-O11	122.6
O1-H16	1.888	O10-Na2-O12	88.8
O2-H24	1.933	O11-Na2-O12	146.7
O4-H26	2.027	Na1-O5-Na2	84.6
		Na1-O6-Na2	89.1
		P1-C7-C9-P2	2.6
		P3-C37-C39-P4	-2.6
		O1-C7-C9-O2	-0.0
		O3-C37-C39-O4	0.2

Table 2.17. Selected interatomic distances [Å], angles [°] and torsion angles [°] for $[Na_2(H_2O)_8(\mathbf{44})_2]$.

For the isomerisation process we propose the following mechanism (Scheme2.11.). In the first step the base (EtOH/NaOH couple), abstract the proton from H[**41**] forming [**41**]$^-$. In the second step the

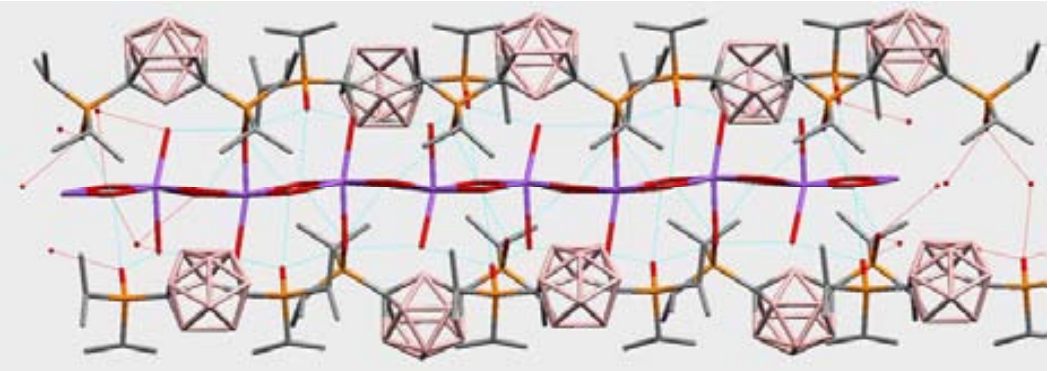

Figure 2.39. Packing view of $[Na_2(H_2O)_8(\mathbf{44})_2]$ (The hydrogen atoms, are omitted for clarity).

nido-carboranyldiphosphine oxide, [**41**]$^-$, is converted into the dicarbollide anion, [**42**]$^{2-}$, by the abstraction of the apical H atom by the base. Then, the dicarbollide anion, isomerizes to the *meta* form, [**45**]$^{2-}$. The dicarbollides anions are known to be very reactives and so, [**45**]$^{2-}$, reacts with the reaction medium forming [**44**]$^-$. In order to verify this mechanism, we inquired thermodynamically the reactions involved in the isomerisation process from H[**41**] to Na[**44**]. Due to the computational cost we did not took into consideration the ethoxide but we considered two bases, which differ in their strength, namely the hydroxide anion (OH^-) and the amide anion (NH_2^-). In Table 2.18. are presented the Gibbs free energy values for the four reactions involved in the isomerisation process. As can be seen the first step that is the deprotonation of H[**41**]$^-$ to [**41**]$^-$ is highly thermodincamically favoured by the action of both bases. The second step is also enthalpically favoured. For the third and the fourth reactions the strength of the bases plays an important role. The hydroxide anion, OH^-, is not strong enough to abstract the apical H atom, which is consistent with experimental requirement that a strong nucleophile as is the ethoxyde is needed. The amide anion though is more nucleophilic and the formation of the dicarbollide anion, [**42**]$^{2-}$ is enthalpically favoured. For the fourth step, as expected, [**45**]$^{2-}$ reacts rather with water than with ammonia to form [**44**]$^-$. The inspection of the total energy of the two isomers reveal that the *ortho* isomer is about 28 kcal·mol^{-1} less stable then the *meta* isomer.

Reaction step	Base (A^-)	
	OH^-	NH_2^-
1	-69.21	-83.76
2	+7.67	-6.87
3	-25.82	-25.82
4	-11.36	+3.18

Table 2.18. Gibbs free energy of reaction (kcal·mol^{-1}) for the reaction steps for the isomerization of H[**41**] to [**44**]$^-$.

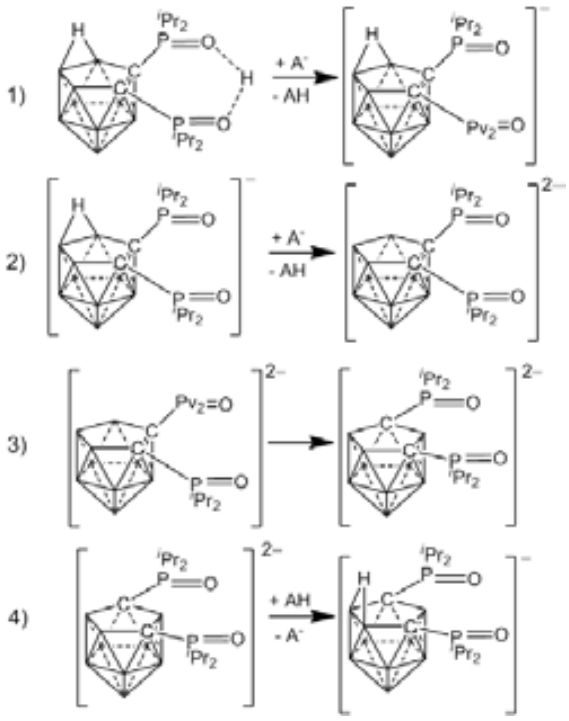

Scheme 2.11. Reaction steps for the isomerization of *ortho-nido*-carboranylphosphine oxides to *meta*-

[1] Berners-Price, S. J.; Norman, R. E.; Sadler, P. J. *J. Inorg. Bioch.*, **1987**, *31*, 197.
[2] Arachchige, I. U.; Brock, S. L.; *Acc. Chem. Res.*, **2007**, *40*, 801.
[3] a) Liaw, B. J.; Lobana, T. S.; Lin, Y. W.; Wang, J. C.; Liu, C. W. *Inorg. Chem.*, **2005**, *44*, 9921. b) Liu, C. W.; Liaw, B. J.; Liou, L. S.; Wang, J. C.; *Chem. Commun.*, **2005**, *15*, 1983. c) Lobana, T. S.; Wang, J.-C.; Liu, C. W. *Coord. Chem. Rev.*, **2007**, *251*, 91.
[4] a) Gray, I. P.; Slawin, A. M. Z.; Woollins, J. D. *Dalton Trans.*, **2005**, 2188. b) Gray, I. P.; Bhattacharyya, P.; Slawin, A. M. Z.; Woollins, J. D. *Chem. Eur. J.*, **2005**, *11*, 6221.
[5] Yu, S.-B.; Papaefthymiou, G. C.; Holm, R. H. *Inorg. Chem.*, **1991**, *30*, 3476.
[6] a) Teixidor, F.; Flores, M. A.; Viñas, C.; Kivekäs, R.; Sillanpää, R. *Angew. Chem. Int. Ed.*, **1996**, *35*, 2251. b) Tutusaus, O.; Viñas, C.; Nuñez, R.; Demonceau, A.; Delfosse, S.; Noels, A. F.; Mata, I.; Molins, E. *J. Am. Chem. Soc.*, **2003**, *125*, 11830. c) Teixidor, F.; Flores, M. A.; Viñas, C.; Sillanpää, R.; Kivekäs, R. *J. Am. Chem. Soc.*, **2000**, *122*, 1963. d) Teixidor, F.; Núñez, R.; Flores, M. A.; Demonceau, A.; Viñas, C. *J. Organomet. Chem.*, **2000**, *614–615*, 48. e) Richel, A.; Delfosse, S.; Demonceau, A.; Noels, A.F.; Paavola, S.; Kivekäs, R.; Sillanpää, R.; Teixidor, F.; Viñas, C. *Abstracts of Papers of the American Chemical Society*, 224: U438-U438 453-POLY Part 2, Aug. 18th, **2002**.
[7] Popescu, A. R.; Laromaine, A.; Teixidor, F.; Sillanpää, R.; Kivekäs, R.; Llambias, J. I.; Viñas, C. *Chem. Eur. J.* **2011**, *17*, 4429.
[8] Bruno, J.; Cole, J. C.; Edgington, P. R.; Kessler, M.; Macrae, C. F.; McCabe, P.; Pearson, J.; Taylor, R. *Acta Crystallogr. B*, **2002**, *58*, 389.
[9] a) Viñas, C.; Núñez, R.; Rojo, I.; Teixidor, F.; Kivekäs, R.; Sillanpää, R. *Inorg. Chem.*, **2001**, *14*, 3259. b) Wang, H.; Chan, H.-S.; Xie, Z. *Organometallics*, **2006**, *25*, 2569. c) Wang, H.; Shen, H.; Chan, H.-S.; Xie, Z. *Organometallics*, **2008**, *27*, 3964. d) Dou, J.; Zhang, D.; Li, D.; Wang, D. *Eur. J. Inorg. Chem.*, **2007**, 53.
[10] Balema, V. P.; Blaurock, S.; Hey-Hawkins, E. *Polyhedron*, **1999**, *18*, 545.
[11] Search performed on October 25th, 2010.
[12] a) Teixidor, F.; Núñez, R.; Viñas, C.; Sillanpää, R.; Kivekäs, R. *Angew. Chem. Int. Ed.*, **2000**, *39*, 4290. b) Nuñez, R.; Farras, P.; Vinñas, C.; Teixidor, F.; Sillanpää, R.; Kivekas, R. *Angew. Chem. Int. Ed.*, **2006**, *45*, 1270. c) Nuñez, R.; Viñas, C.; Teixidor, F.; Sillanpää, R.; Kivekas, R. *J. Organomet. Chem.*, **1999**, *592*, 22.
[13] a) Calhorda, M. J.; Crespo, O.; Gimeno, M. C.; Jones, P. G.; Laguna, A.; López-de-Luzuriaga, J. M.; Perez, J. L.; Ramón, M. A.; Veiros, L. F. *Inorg. Chem.*, **2000**, *39*, 4280. b) Paavola, S.; Kivekäs, R.; Teixidor, F.; Viñas, C. *J. Organomet. Chem.*, **2000**, *606*, 183. c) Paavola, S.; Teixidor, F.; Viñas, C.; Kivekäs, R. *J. Organomet. Chem.*, **2002**, *645*, 39. d) Paavola, S.; Teixidor, F.; Viñas, C.; Kivekäs. R. *J. Organomet. Chem.*, **2002**, *657*, 187. e) Zhang, D. P.; Dou, J. M.; Li, D. C.; Wang, D. Q. *Appl. Organomet. Chem.*, **2006**, *20*, 632.
[14] Greenwood, N. N.; Earnshaw, A. *Chemistry of the Elements*. 2nd Ed., Butterworth-Heinemann, Oxford, **1997**, p751.
[15] Bartlett, P.D., Meguerian, G. *J. Am. Chem. Soc.*, **1956**, *78*, 3710.
[16] Lloyd, J.R.; Lowther, N.; Zsabo, G.; Hall, D. *J. Chem. Soc. Perkin Trans.*, **1985**, 1813.
[17] Greenwood, N. N.; Earnshaw, A. Chemistry of the Elements. 2nd Ed., Butterworth-Heinemann, Oxford, **1997**, p652.
[18] Yao, Z.-J.; Jin, G.-X. *Organometallics*, **2011**, *30*, 5365.
[19] McFarlane, W.; Rycroft, D. S. *J. Chem. Soc., Dalton Trans*. **1973**, *20*, 2162.
[20] Allen, D. W.; Taylor, B. F. *J. Chem. Soc., Dalton Trans*. **1982**, 1, 51.
[21] Jameson, C. J. in *Phosphorous-31 NMR Spectroscopy in Stereochemical Analysis*, L. D Quin, J. G Verkade Eds.; VCH: New York, 1987.
[22] Klapötke, T. M.; Broschag, M. *Compilation of Reported ^{77}Se NMR Chemical Shifts*, Wiley, Chichester, **1996**.
[23] Burford, N.; Royan, B. W.; Spence, R. E. v. H.; Rogers, R. D. *Dalton. Trans.* **1990**, *7*, 2111-2117.
[24] Pyykkö, P.; Atsumi, M. *Chem. Eur. J.*, **2009**, *15*, 12770.

[25] Kivekäs, R.; Sillanpää, R.; Teixidor, F.; Viñas, C.; Núñez, R.; Abad, M. *Acta Cryst.* **1995**, *C51,* 1864-1870.
[26] Sundberg, M. R.; Uggla, R.; Viñas, C.; Teixidor, F.; Paavola, S.; Kivekäs, R. *Inorg. Chem. Commun*. **2007**, *10*, 713.
[27] Steinberger, H. U.; Ziemer, B.; Meisel, M. *Acta Crystallog.* **2001,** *C57,* 835.
[28] a) Stampfl, T.; Gutmann, R.; Czermak, G.; Langes, C.; Dumfort, A.; Kopacka, H.; Ongania, K.-H.; Brüggeller, P. *Dalton Trans.* **2003***,* 3425. b) Stampfl, T.; Czermak, G.; Gutmann, R.; Langes, C.; Kopacka, H.; Ongania, K.-H.; Brüggeller, P. *Inorg. Chem. Commun.* **2002**, *5*, 490. c) Hitchcock, P. B.; Nixon, J. F.; Sakaray, N. *Chem. Commun.* **2000***,* 1745.
[29] a) Wiesboeck, R. A.; Hawthorne, M. F. *J. Am. Chem. Soc.* **1964**, *86*, 164. b) Garret, P. M.; Tebbe, F. N.; Hawthorne, M. F. *J. Am. Chem. Soc.* **1964**, *86*, 5016. c) Hawthorne, M. F.; Young, D. C.; Garret, P. M.; Owen, D. A.; Schwerin, S. G.; Tebbe, F. N.; Wegner, P. M. *J. Am. Chem Soc.* **1968**, *90*, 862.
[30] Zakharkin, L. I.; Kalinin, V. N. *Tetrahedron Lett.* **1965**, 407.
[31] Peymann, T.; Herzog, A.; Knobler, C. B.; Hawthorne, M. F. *Angew. Chem. Int. Ed. Engl.* **1999**, *38*, 1061.
[32] Leites, L. A. *Chem. Rev*., **1992**, *92*, 279.
[33] Wada, M.; Higashizaki, S.; Tsuboi, A. *J. Chem. Res.* **1985**, 38.
[34] a) Dewar, M. J. S.; Jones, R. *J. Am. Chem. Soc.* **1967**, *89*, 4251. b) Nöth, H.; Wrackmeyer, B. *Magnetic Nuclear Resonance Spectroscopy of Boron Compounds*. (Ed. Diehl, P.; Fluck, E.; Kosfeld, R.) Spring-Verlag, Berlin-Heildelberg, **1978**.
[35] Andrews, S. J.; Robb, D. A.; Welch, A. J. *Acta Cryst. C*, **1983**, *39*, 880.
[36] Day, V. W.; Hossain, M. A.; Kang, S. O.; Powell, D.; Lushington, G.; Bowman-James, K. *J. Am. Chem. Soc.*, **2007**, *129*, 8692.
[37] a) Halvorson, K. E.; Willett, R. D.; Massabni, A. C. *J. Chem. Soc, Chem. Commun.* **1990**, *4*, 346. b) Carmalt, C. J.; Norman, N. C.; Farrugia, L. J. *Polyhedron* **1993**, *12*, 2081. c) Lane, H. P.; Godfrey, S. M.; McAuliffe, C. A.; Pritchard, R. G. *J. Chem. Soc., Dalton Trans.* **1994**, *22*, 3249. d) Godfrey, S. M.; Ho, N.; McAuliffe, C. A.; Pritchard, R. G. *Angew. Chem.* **1996**, *108*, 2492. e) Ruthe, F.; Jones, P. G.; Du Mont, W. W.; Deplano, P.; Mercuri, M. L. *Z. Anorg. Allg. Chem.* **2000**, *626*, 1105. f) Boraei, A. A.; Du Mont, W. W.; Ruthe, F.; Jones, P. G. *Acta Crystallog. C* **2002**, *58*, 318.
[38] a) Teixidor, F.; Viñas, C.; Abad, M. M.; Kivekäs, R.; Sillanpää, R. *J. Organomet. Chem*. **1996**, *509*, 139. b) Juanatey, P.; Suárez, A.; López, M.; Vila, J. M.; Ortigueira, J. M.; Fernández, A. *Acta Cryst.* **1999**, *55*, IUC9900062.
[39] Sarch performed on October 26th, 2012.
[40] Dou, J. M.; Zhang, D. P.; Li, D. C.; Wang, D. Q. *Polyhedron*, **2007**, *26*, 719.
[41] a) Bollmark, M.; Stawinski, J. *Chemm. Commun*, **2001**, 771. b) Kullberg, M.; Stawinski, J. *J. Organomet. Chem*, **2005**, *690*, 2571.
[42] Dou, J.; Zhang, D.; Li, D.; Wang, D. *J. Organomet. Chem*., **2006**, *691*, 5673.
[43] a) Teixidor, F.; Viñas, C.; Abad, M. M.; López, M.; Casabó, J. *Organometallics*, **1993**, *12*, 3766. b) Kivekäs, R.; Sillanpää, R.; Teixidor, F.; Viñas, C.; Abad, M. M. *Acta Chim. Scand*, **1996**, *50*, 499. c) Teixidor, F.; Viñas, C.; Abad, M. M.; Whitaker, C.; Rius, J. *Organometallics*, **1996**, *15*, 3154. d) Viñas, C.; Abad, M. M.; Teixidor, F.; Sillanpää, R.; Kivekäs, R. *J. Organomet. Chem.*, **1998**, *555*, 17.
[44] Puga, A. V.; Teixidor, F.; Sillanpää, R.; Kivekäs, R.; Arca, M.; Barberà, G.; Viñas, C. *Chem. Eur. J.*, **2009**, *15*, 9755.
[45] Teixidor, F.; Barberà, G.; Vaca, A.; Kivekäs, R.; Sillanpää, R.; Oliva, J.; Viñas, C. *J. Am. Chem. Soc.*, **2005**, *127*, 10158.
[46] a) Reed, A. E.; Weinhold, F. *J. Chem. Phys.*, **1983**, *78*, 4066. b) Reed, A. E.; Weinstock, R. B.; Weinhold, F. *J. Chem. Phys.*, **1985**, *83*, 735.
[47] Quantum-chemical calculations were performed with the Gaussian 03 and Gaussian 09 commercial suite of programs at DFT level of theory with B3LYP hybrid functional adopting for all the atoms the 6-311+G(d,p) basis set. Geometry optimization was performed from structural data. NBO calculations were done at the optimized geometries.

[48] Hirshfeld, F. L. *Theoret. Chim. Acta*, **1977**, *44*, 129.
[49] Reed, A. E.; Curtiss, L. A.; Weinhold, F. *Chem. Rev.* **1988**, *88*, 899.
[50] a) Gilheany, D. G. *Chem. Rev*,.**1994**, *94*, 1339. b) Sandblom, N.; Ziegler, T.; Chivers, T. *Can. J. Chem.*, **1996**, *74*, 2363. c) Dobado, J. A.; Martínez-García, H.; Molina Molina, J.; Sundberg, M. R. *J. Am. Chem. Soc.*, **1998**, *120*, 8461.
[51] Davies, R. in *Handbook of Chalcogen Chemistry. New Perspectives in Sulfur, Selenium and Tellurium*. (Ed. F. A. De Villanova), The Royal Society of Chemistry, Cambridge, **2007**, pp. 291.
[52] a) Bader, R. F. W. *Atoms in Molecules: A Quantum Theory*. Oxford Univrsity Press. **1994**. b) Matta, F. C.; Boyd, R. J. (Eds). *The Quantum Theory of Atoms in Molecules*. Wiley-VCH. **2007**.
[53] a) Yao, Z.-J.; Jin, G.-X. *Organometallics*, **2011**, *30*, 5365. b) Hu, P.; Yao, Z.-J.; Wang, J.-Q.; Jin, G.-X. *Organometallics*, **2011**, *30*, 4935.
[54] a) Denney, D. B.; Goodyear, W. F.; Goldstein, B. *J. Am. Chem Soc.*, **1960**, *82*, 1393. b) Hiatt, R.; Smythe, R. J.; McColeman, C. *Can. J. Chem.*, **1971**, *49*, 1707. c) Srinivasan, C.; Pitchumani, K. *Int. J. Chem. Kinet.* **1982**, *14*, 1315. d) Srinivasan, C.; Pitchumani, K. *Can. J. Chem.* **1985**, *63*, 2285. e) Chellamani, A.; Suresh, R. *React. Kinet. Catal. Lett.* **1988**, *37*, 501.
[55] a) Fox, M. A.; Gill, W. R.; Herbertson, P. L.; MacBride, J. A. H.; Wade, K. *Polyhedron* **1996**, *15*, 565. b) Davidson, M. G.; Fox, M. A.; Hibbert, T. G.; Howard, J. A. K.; Mackinnon, A.; Neretin, I. S.; Wade, K. *Chem. Commun.* **1999**, 1649.
[56] Grimes. R. N. *Carboranes*. 2nd Ed., Elsevier Inc. **2011**, p197.
[57] Taoda, Y.; Sawabe, T.; Endo, Y.; Yamaguchi, K.; Fujii, S.; Kagechika, H. *Chem. Commun.*, **2008**, 2049.
[58] a) Desiraju, G. R.; Steiner, T.; Eds, *The Weak Hydrogen Bond in Structural Chemistry and Biology*; Oxford University Press Inc., New York, **1999**. b) Prins, L. J.; Reinhoudt, D. N.; Tiemmerman, P. *Agew. Chem. Int. Ed.* **2001**, *40*, 2382.
[59] a) Cleland, W. W. *Biochemistry* **1992**, *31*, 317. b) Gerlt, G. A.; Gassman, P. G. *J. Am. Chem. Soc.* **1993**, *115*, 11552. c) Gerlt, G. A.; Gassman, P. G. *Biochemistry* **1993**, *32*, 11943. d) Cleland, W. W.; Krevoy, M. M. *Science* **1994**, *264*, 1887. f) Frey, P. A.; Whitt, S. A.; Tobin, J. B. *Science* **1994**, *264*, 1927. g) Tong, H.; Davis, L. *Biochemistry* **1995**, *34*, 3362. h) Tobin, J. B.; Whitt, S. A.; Cassidy, C. S.; Frey, P. A. *Biochemistry* **1995**, *34*, 6919. i) Zhao, Q.; Abeygunawardana, C.; Talalay, P.; Mildvan, A. S. *Proc. Natl. Acad. Sci. USA* **1996**, *93*, 8220. j) Hur, O.; Leja, C.; Dun, M. F. *Biochemistry* **1996**, *35*, 7378. k) Cassidy, C. S.; Lin, J.; Frey, P. A. *Biochemistry* **1997**, *36*, 4576. l) Zhao, Q.; Abeygunawardana, C.; Gittis, A. G.; Mildvan, A. S. *Biochemistry* **1997**, *36*, 4616. m) Kahyaoglu, A.; Haghjoo, K.; Guo, F.; Jordan, F.; Kettner, C.; Felföldi, F.; Polgár, L. *J. Biol. Chem.* **1997**, *272,* 25547. n) Cleland, W. W. *The low-barrier hydrogen bond in enzymic catalysis* in *Advances in Physical Organic Chemistry*, Richard, P. J., Ed, **2010**, *44*, 1.
[60] a) Desiraju, G. R. *Crystal Engineering. The Design of Orgainic Solids,* Elsevier; Amsterdam, **1989**. b) Desiraju, G. R. *Acc. Chem. Res.*, **2002**, *35*, 565-573.
[61] Hynes, J. T.; Klinman, J. P.; Limbach, H.-H.; Schowen, R. L. (Eds.), *Hydrogen-Transfer Reactions*, Wiley-VCH Velag CmbH&Co. KGaA, Weinheim, **2007**.
[62] a) Day, V. W.; Hossain, M. A.; Kang, S. O.; Powell, D.; Lushington, G.; Bowman-James, K. *J. Am. Chem. Soc.* **2007**, *129*, 8692. b) Yaghmaei, S.; Khodagholian, S.; Kaiser, J. M.; Tham, F. S.; Mueller, L. J.; Morton, T. H.; *J. Am. Chem. Soc.* **2008**, *130*, 7836.
[63] a) Taylor, M. S.; Jacobsen, E. N.; *Angew. Chem. Int. Ed.*,**2006**, *45*, 1520. b) Doyle, A. G.; Jacobsen, E. N. *Chem. Rev.* **2007**, *107*, 5713.
[64] a) Akiyama, T.; Itoh, J.; Yokota, K.; Fuchibe, K. *Angew. Chem.* **2004**, *116,* 1592. b) Uraguchi, D.; Terada, M. *J. Am. Chem. Soc.* **2004**, *126*, 5356. c) Uraguchi, D.; Sorimachi, K.; Terada, M. *J. Am. Chem. Soc.* **2004**, *126*, 11804. d) Akiyama, T. ; Itoh, J.; Yokota, K.; Fuchibe, K. *Org. Lett.* **2005**, *7*, 2583. e) Rueping, M.; Sugiono, E.; Azap, C.; Theissmann, T.; Bolte, M. *Org. Lett.* **2005**, *7*, 3781.
[65] Search performed in February 22nd, 2012.
[66] Costantino, F.; Ienco, A.; Midollini, S.; Orlandini, A.; Sorace, L.; Vacca, A. *Eur. J. Inorg. Chem.* **2008**, 3046.

[67] Hollatz, C.; Schier, A.; Schmidbaur, H. *J. Am. Chem. Soc.* **1997**, *119*, 8115.

[68] Bigoli, F.; Deplano, P.; Mercuri, M. L.; Pellinghelli, M. A.; Trogu, E. F. *Phosphorus, Sulfur, and Silicon and Related Elements* **1992**, *70*, 145.

[69] Fuster, F.; Grabowski, S. J. *J. Phys. Chem. A*, **2011**, *115*, 10078.

[70] Quantum-chemical calculations were performed with the Gaussian 09 commercial suite of programs at DFT level of theory with B3LYP hybrid functional adopting for all the atoms the 6-311++G(d,p) basis set. Geometry optimization was performed from structural data and all the calculations were done at the optimized geometries.

[71] Magnetic shielding was computed at DFT/B3LYP/6-311+(d,p) level of theory employing gauge-including atomic orbitals (GIAOs). The computed ^{31}P-NMR chemical shift are reported relative to the ^{31}P-NMR chemical shift calculated for PH_3 at the same level of theory and refined to PH_3 to the experimental value in gas phase.

[72] a) Dunn, E. J.; Purdon, J. G.; Bannard, R. A. B.; Albright, K.; Buncel, E. *Can. J. Chem.*, **1988**, *66*, 3137. b) Ruiz-Morales, Y.; Ziegler, T. *J. Chem. Phys. A*, **1998**, *102*, 3970. c) Chesnut, D. B.; Quin, L. D. *Tetrahedron*, **2005**, *61*, 12343. d) Koo, I. S.; Ali, D.; Yang, K.; Park, Y.; Wardlaw, D. M.; Buncel, E. *Bull. Korean Chem. Soc.*, **2008**, *29*, 2252. e) Kühl, O. (Ed.) *Phosphorus-31 NMR Spectroscopy. A Concise Introduction for the Synthetic Organic and Organometallic Chemist*. Springer-Verlag, Berlin Heidelberg, **2008**; f) Farràs, P.; Teixidor, F.; Rojo, I.; Kivekäs, R.; Sillanpää, R.; González-Cardoso, P.; Viñas, C. *J. Am. Chem. Soc.*, **2011**, *133,* 16537.

[73] Akitt, J. W.; Mann, B. E. (Eds.) *NMR and Chemisty. An introduction to modern NMR spectroscopy.* 4th Ed. CRC Taylor & Francis. **2000**.

[74] a) Gilli, P.; Gilli, G. *J. Mol. Struct.* **2010**, *972*, 2. b) Grabowski, S. J. *Chem. Rev.* **2011**, *111*,2597.

[75] The calculation for the geometries obtained from structural data were done with no further optimization at DFT/B3LYP/6-311++(d,p) level of theory. For comparison purposes, we also optimized the structure of H[**33**], for which an intermediate geometry between the structures H[**33a**] and H[**33b**] (determinated from the X-Ray diffraction) has been obtained.

[76] a) Foster, J. P.; Weinhold, F. *J. Am. Chem. Soc.* **1980**, *102*, 7211. b) Weinhold, F. *J. Mol. Struct. (THEOCHEM)* **1999**, *398-399*, 181. c) Weinhold, F.; Landis, C. *Valency and Bonding, A Natural Bond Orbital Donor – Acceptor Perspective*, Cambridge University Press: New York, **2005**.

[77] Koch, U.; Popelier, P. L. A. *J. Phys. Chem.* **1995**, *99*, 9747.

[78] Rozas, I.; Alkorta, I.; Elguero, J. *J. Am. Chem. Soc.* **2000**, *122*, 11154.

[79] Bader, R. F. W.; Essén, H. *J. Chem. Phys.*, **1984**, *80,* 1943.

[80] a) Fuster, F.; Silvi, B. *Theoret. Chem. Acc.*, **2000**, *104*, 13. b) Fuster, F.; Silvi, B. *Chem. Phys.* **2000**, *252*, 279. c) Fuster, F.; Silvi, B.; Berski, S.; Latajka, Z. *J. Mol. Struct.* **2000**, *555*, 75. d) Alikhani, M. E.; Silvi, B.; *Phys. Cehm. Cehm. Phys.* **2003**, *5*, 2494. e) Alikhani, M. E.; Fuster, F.; Silvi, B.; *Struct. Chem.* **2005**, *16*, 203. f) Navarrete-López, A. M.; Garza, J.; Vargas, R. *J. Phys. Chem. A.* **2007**, *111*, 11147. g) Cyranski, M. K.; Jezierska, A.; Klimentowska, P.; Panek, J. J.; Sporzynski, A. *J. Phys. Org. Chem.* **2008**, *21*, 472. h) Drebushchak, I. V.; Kozlova, S. G. *J. Struct. Chem.* **2010**, *51*, 166. i) Chaudret, R.; Cisneros, G. A.; Parsiel, O.; Piquemal, J. P. *Chem.-Eur. J.* **2011**, *17*, 2833.

[81] a) Becke, A. D.; Edgecombe, K. E. *J. Chem. Phys.*, **1990**, *92*, 5397. b) Silvi, B. *Nature*, **1994**, *371*, 683.

[82] Silvi, B. *J. Mol. Struct.*, **2002**, *614*, 3.

[83]Grimes. R. N. *Carboranes*. 2nd Ed., Elsevier Inc. **2011**, p541

[84] a) Plesek, J.; Janousek, Z.; Hermanek, S. *Collect. Czech. Chem. Commun.*, **1978**, *43*, 2862. b) Owen, D. A.; Hawthorne, M. F. *J. Am. Chem. Soc.*, **1969**, *91*, 6002.

[85] Zakharkin, L. I.; Zhigareva, G. G.; Antonovich, V. A.; Yanovskii, A. I.; Struchkov, Yu. T. *Zh. Obshch. Khim.*, **1986**, 56, 2066.

3. Carboranylformaldehyde as platform for new derivatives

3.1. Study on the synthesis of "confined space" multi-cage compounds

As presented in the Introduction, there are several compounds described in the literature which have two or three carborane cages bonded to one or two atoms, forming the so called "star-shape" molecules. The importance of such compounds is yet to be investigated, but due to their elevated number of boron atoms per molecule unit they may be used in BNCT. Derivatives where the central atom is the carbon atom were not reported up to now in the literature. For that, we proposed to study the possibility of synthesizing such compounds. Two possible reactions were tested: i) directly from *o*-carborane and ii) based on the carboranylaldehyde platform.

3.1.1. Studies based on o-carborane as platform for new compounds

The first approach was employing carbon halides and lithiated carborane (Scheme 3.1.). In order to obtain the three-cage derivative, iodoforme was a proper choice for the reaction with $Li[C_2B_{10}H_{11}]$, since it is a solid and can be maintained dry enough to be reacted with an organo-lithium compound. Different reaction conditions were tried changing the solvent, the reaction temperature, the reactants ratio and the addition techniques, but in all the cases we did not succeed to obtain the desired compound. Table 3.1. summarizes the reaction conditions and the resulting compounds identified by NMR. Employing solvents as diethyl-ether or tetrahydrofurane at low temperature (-80°C) or room temperature, the iodine-lithium

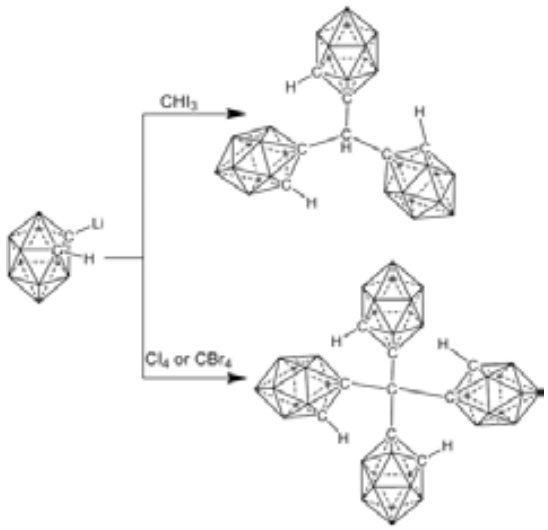

Scheme 3.1. Proposed synthetic route of three-cage and four-cage "confined space" carborane derivatives.

Entry	Reaction mixture	Solvent	T (°C)	Products
1	$Li[C_2B_{10}H_{11}]$:CHI_3 (3:1)	Et_2O	-80[a]	1,2-$C_2B_{10}H_{12}$; 1-I-1,2-$C_2B_{10}H_{11}$
2	$Li[C_2B_{10}H_{11}]$:CHI_3 (6:1)	Et_2O or THF	-80[a]	1,2-$C_2B_{10}H_{12}$; 1-I-1,2-$C_2B_{10}H_{11}$
3	$Li[C_2B_{10}H_{11}]$:CHI_3 (6:1)	THF	65	3-(1-H-$C_2B_{10}H_{10}$)-1,2-$C_2B_{10}H_{12}$
4	$Li[C_2B_{10}H_{11}]$:CHI_3 (10:1)	Solid state	125[b]	1,2-$C_2B_{10}H_{12}$
5	$Li[C_2B_{10}H_{11}]$:CI_4 (4:1)	Et_2O	-80[a]	1,2-$C_2B_{10}H_{12}$; 1-I-1,2-$C_2B_{10}H_{11}$
6	$Li[C_2B_{10}H_{11}]$:CI_4 (8:1)	Et_2O or THF	-80[a]	1,2-$C_2B_{10}H_{12}$; 1-I-1,2-$C_2B_{10}H_{11}$
7	$Li[C_2B_{10}H_{11}]$:CI_4 (10:1)	THF	65	3-(1-H-$C_2B_{10}H_{10}$)-1,2-$C_2B_{10}H_{12}$
8	$Li[C_2B_{10}H_{11}]$:CBr_4 (4:1)	Et_2O	-80[a]	1,2-$C_2B_{10}H_{12}$
9	$Li[C_2B_{10}H_{11}]$:CBr_4 (8:1)	THF	65	3-(1-H-$C_2B_{10}H_{10}$)-1,2-$C_2B_{10}H_{12}$

[a] the reaction mixture was kept 4 h at -80°C and then, 24 h at room temperature.
[b] solid $Li[C_2B_{10}H_{11}]$ was obtained from *o*-carborane and *n*-BuLi in Et_2O at 0°C for 1 h, and then the solvent was evaporated.

Table 3.1. Reaction conditions for the reaction of $Li[C_2B_{10}H_{11}]$ with carbon halides.

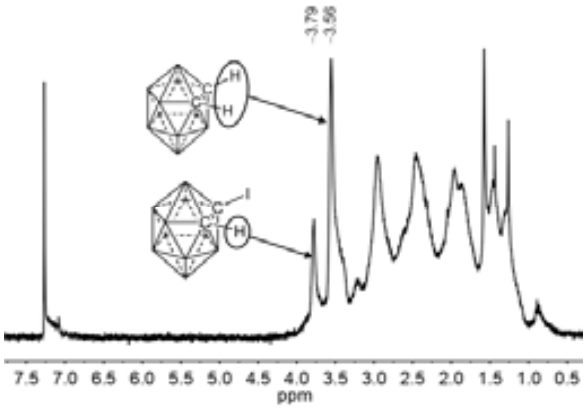

Figure 3.1. ^{1}H-NMR spectrum (in $CDCl_3$) for the reaction products of $Li[C_2B_{10}H_{11}]$ with CHI_3.

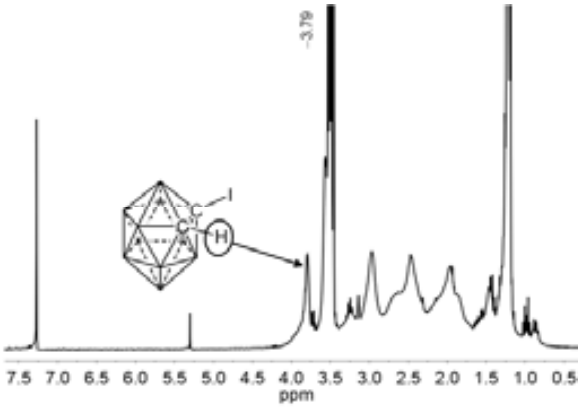

Figure 3.2. ^{1}H-NMR spectrum (in $CDCl_3$) for the reaction products of $Li[C_2B_{10}H_{11}]$ with I_2.

exchange reaction takes place yielding a mixture between unreacted carborane and iodine C-monosubstituted carborane derivative (1-I-1,2-*closo*-$C_2B_{10}H_{11}$), as observed by NMR (Figure 3.1.). In order to confirm that the 1-I-1,2-*closo*-$C_2B_{10}H_{11}$ was indeed formed in the previous reaction, we made the reaction of $Li[C_2B_{10}H_{11}]$ with I_2 in diethyl-ether, and the formation of C-monoidinated carborane was confirmed by NMR analysis (Figure 3.2.). When the reaction was carried in THF at reflux, the B-substituted two-cage compound, 3-(1-H-1,2-$C_2B_{10}H_{10}$)-1,2-$C_2B_{10}H_{12}$, was obtained (Scheme 3.2.).[1] Solvent free condition were also tried, heating a mixture of CHI_3 and $Li[C_2B_{10}H_{11}]$ just above the melting temperature of iodoforme (125°C) for 1 night, but only unreacted carborane was recovered. The low temperature reactions of $Li[C_2B_{10}H_{11}]$ with carbon tetraiodide give the same results as for iodoforme, whereas with carbon tetrabromide only unreacted *o*-carborane was recovered. Both CI_4 and CBr_4 give the same results as CHI_3 if the reactions are carried out at reflux temperature in THF (Scheme 3.2.).

3.1.2. Studies based on carboranylformaldehyde as platform for new compounds

Carboranylformaldehyde or 1-formyl-*o*-carborane, 1-CHO-1,2-*closo*-$C_2B_{10}H_{11}$, is known since several years ago,[2] but a surprisingly lack of studies on its reactivity can be found in the literature. Although there are different methods of synthesis,[2,3] the less laborious and most effective is the one reported by Kahl *et al.*[4] in 2005. Recently, the carboranylaldehyde was used as starting material for the synthesis of BNCT agents[5] and as platform for the synthesis of alkenylcarboranes with fluorophore moieties.[6]

As the first synthetic approach did not yield the desired compounds, we start investigating the possibility to add the cages, in steps, on a ready available platform – the carboranylformaldehyde. The first step was the reaction of 1-CHO-1,2-$C_2B_{10}H_{11}$ with $Li[C_2B_{10}H_{11}]$ (Scheme 3.3). In this way we successfully obtained the two-cages alcohol, namely dicarboranyl-methanol, which was characterized by

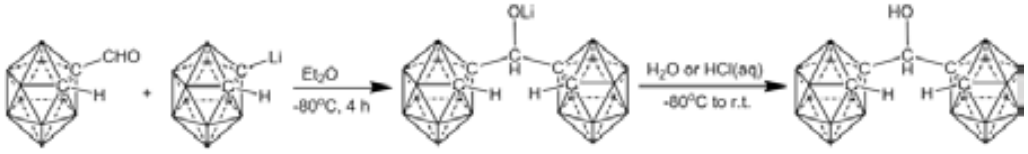

Scheme 3.3. Reaction of carboranylformaldehyde with $Li[C_2B_{10}H_{11}]$.

NMR and mass spectrometry. The reaction conditions are very strict, temperature plays a key role. As it was reported in the literature for alcohol derivatives of carborane,[7] the carbon-carbon bond formed between the carbon atom from the carborane cluster and an *exo*-cluster carbon atom, can be easily cleaved by the action of bases. As in the reaction (Scheme 3.3.) the lithium alkoxide derivative is first formed, this can break the C_C-C bond and yield unreacted carborane, the reaction yield of alcohol derivative being drastically lowered if the temperature is higher than -80°C. Thus, as observed for other carboranylalcohols, keeping the reaction temperature low until quenching or acidolysis is essential to ensure high conversion.[8] The ^{1}H-NMR analysis revealed two resonances at 4.29 ppm and 4.89 ppm, first corresponding to the H bonded to the unsubstituted cluster carbon atom and the second to the H atom bonded to the middle carbon atom (Figure 3.3.). The alcoholic H atom was not observed in the ^{1}H-NMR spectrum. In order to confirm that no Li ions are present, that could interfere in the identification of the –OH resonance, we did ^{7}Li-NMR and no Li signal was observed. The IR analysis, though, was very useful, since the typical –OH stretching frequency was observed at 3560 cm^{-1} (Figure 3.4.). Further analysis by mass spectrometry offered useful information on the nature of the –OH bonds in this alcohol. As can be seen in Figure 3.5., the ESI-MS spectrum shows the mass of the highest intensity at 632.8, which is exactly the double of the mass expected for the alcohol, so it seems that the correspondent dimmer, [1,1-CHOH-(1,2-$C_2B_{10}H_{11}$)$_2$]$_2$, is formed. Another important observation is that this dimmer is so stable that it can be observed even after the electrospray ionization, fact that strongly influences its reactivity, as will be seen further. The theoretical mass spectrum was computed in order to confirm that the isotopic distribution corresponds to the dimmer of the alcohol, and it was found that perfectly mach the experimental one (Figure 3.5.).

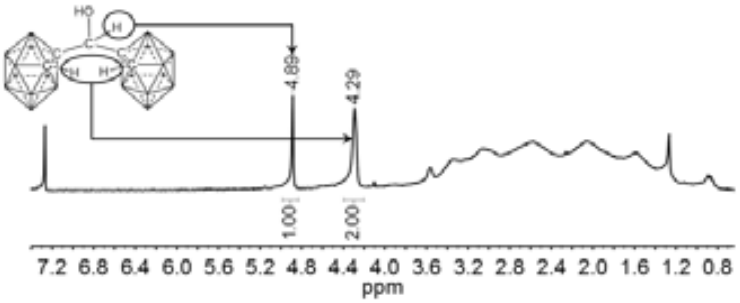

Figure 3.3. ^{1}H-NMR (in $CDCl_3$) spectrum for the product of the reaction of 1-CHO-1,2-$C_2B_{10}H_{11}$ with Li[$C_2B_{10}H_{11}$].

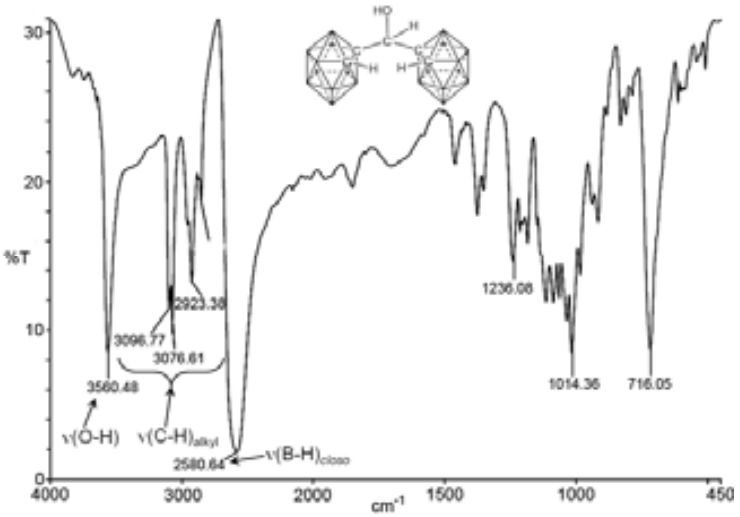

Figure 3.4. FTIR (KBr) spectrum for the product of the reaction of 1-CHO-1,2-$C_2B_{10}H_{11}$ with Li[$C_2B_{10}H_{11}$].

Having ready prepared the two-cage derivative, we proceed to the second step which is the conversion of the alcohol to a ketone, which than, could be reacted with another Li[$C_2B_{10}H_{11}$] and yield the three-cage alcohol. This second step was proved to be the bottle-neck to the synthesis of multi-cage "confined-space" carborane derivatives.

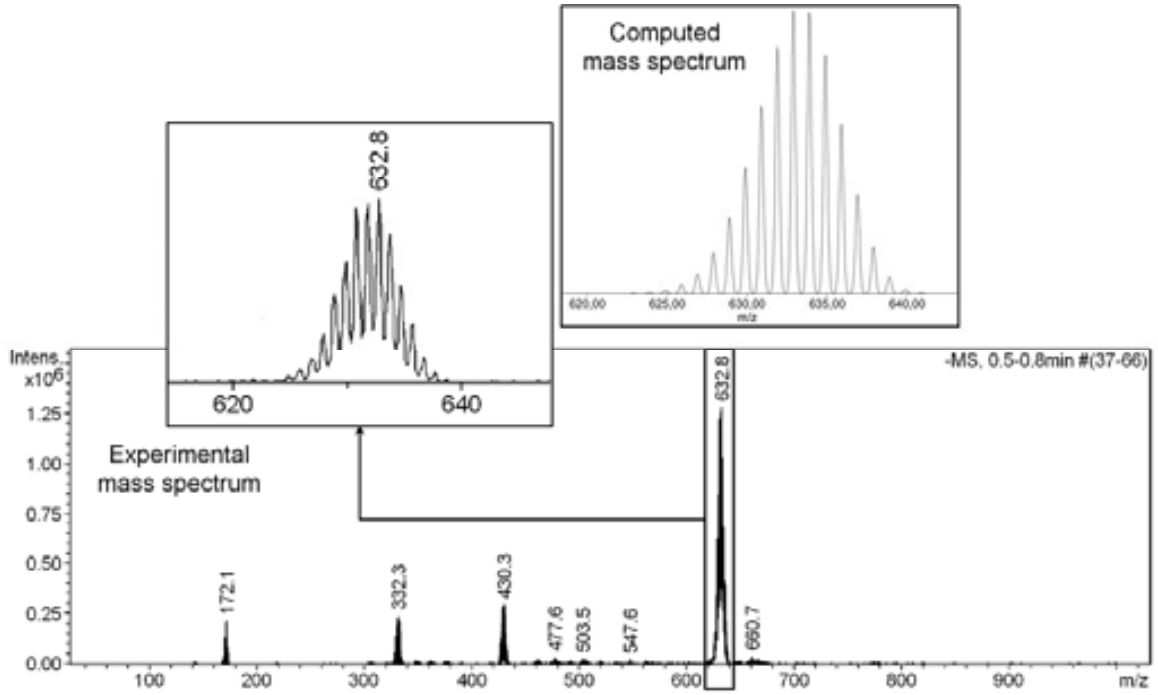

Figure 3.5. ESI-MS spectrum for the compound obtained in the reaction of 1-CHO-1,2-$C_2B_{10}H_{11}$ with Li[$C_2B_{10}H_{11}$] and computed mass spectrum for carboranylmethanol dimmer.

The oxidation of the alcohols can be carried out with a variety of oxidizing agents depending on the nature of the alcohol and desired compound (carbonyl derivative or acid). We tried several methods (Scheme 3.4.) but all were unsuccessful. As the carborane cages are known to be susceptible to bases, yielding the *nido* derivatives, we tried to avoid the use of such. Secondary alcohols can be oxidized with a mild reagent as calcium hypochlorite, $Ca(ClO)_2$, with excellent yield at 0°C in a solvent containing acetic acid. We performed the oxidation of dicarboranyl-methanol with 1 equivalent of $Ca(ClO)_2$ in two different experiments employing first a 3:2 mixture of CH_2Cl_2:CH_3COOH and in the second experiment a 3:2 mixture of CH_3CN:CH_3COOH. [9] Although the oxidation of the alcohol was unsuccesful, interesting results were obtained. It was observed that a part of the alcohol was converted to *o*-carborane in both experiments (observed by the resonance at 3.56 ppm from ^{1}H-NMR in $CDCl_3$), but additional information on the nature of the –OH moiety in dicarboranylmethanol was obtained. If CH_2Cl_2:CH_3COOH mixture is employed as solvent, the ^{1}H-NMR spectrum (Figure 3.6.) shows besides the chemical shifts at 4.29 ppm and 4.89 ppm, as previously observed for the alcohol (Figure 3.3.), another resonance at 3.40. Even more, the resonances at 4.89 ppm and 3.40 ppm are doublets ($^3J_{HH}$ = 6.0 Hz), which indicates H-H coupling between the alcoholic H atom and the H atom bonded to the middle C atom. If CH_3CN:CH_3COOH is employed as solvent, different results are observed in ^{1}H-NMR spectrum (Figure 3.7.). As in previous case two doubles and a singlet were observed but at different chemical shifts. The doublets are observed at 5.47 and 4.82 ($^3J_{HH}$ = 6.0 Hz), and the singlet at 4.22 ppm. Additionally, two other singlets were observed at 2.19 ppm and 2.04

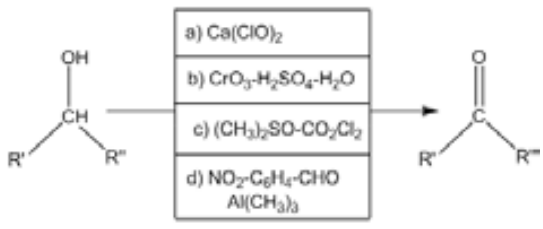

a) Oxidation with calcium hypochlorite
b) Jones oxidation
c) Swern oxidation
d) Oppenauer oxidation

Scheme 3.4. Schematics of the oxidation methods tried for the carboranymethanol.

ppm. The first doublet was assigned to the –OH and the second to the H bonded to the middle C atom. The singlet at 4.22 ppm corresponds to the H atom bonded to the carbon from the cluster. The other two singlets are in a zone where usually methyl H atoms are observed. As the –OH resonance shifts more than 2 ppm, we assume that this is due the interaction with acetonitrile, where –O-H···NC-CH_3 contacts are formed, so the singlet at 2.19 ppm must come from the interacting CH_3CN molecule whereas the one at 2.04 ppm is assigned to the free CH_3CN molecules. The integration of this last to signals is difficult since it overlaps with the BH zone. The ^{11}B-NMR spectra are identical in all the cases, but the ^{1}H{^{11}B}-NMR spectra provide useful information on the complexity of the H···H interaction in this alcohol. The ^{1}H{^{11}B}-NMR spectra for the dimmer and for the alcohol after the reaction with $Ca(ClO)_2$ in CH_2Cl_2:CH_3COOH are similar (Figure 3.8.a and b), so it seems that the CH_2Cl_2:CH_3COOH mixture only breaks the H···H bonds in the dimmer. The ^{1}H{^{11}B}-NMR spectrum for the reaction in CH_3CN:CH_3COOH on the other hand, is different from the previous. Also, the doublet observed at 5.47 ppm in ^{1}H-NMR spectrum is distorted in ^{1}H{^{11}B}-NMR spectrum (Figure 3.8.c). This means that beside –OH···NC-CH_3 interactions other interactions are established, with the H atoms bonded to the boron atoms from the carborane cage. These interactions though are somehow ephemeral since the same samples were analyzed after several months and the ^{1}H-NMR spectrum shows the same singlets at 4.89 ppm and 4.29 ppm. This offers useful information on how the carborane influences the –OH and –CH acidity of dicarboranylmethanol.

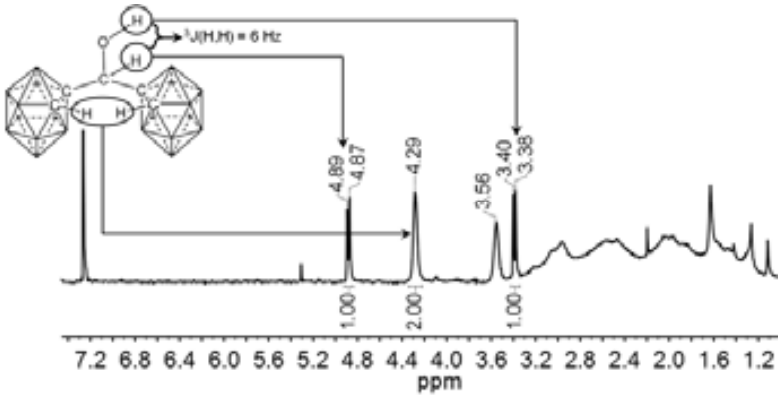

Figure 3.6. ^{1}H-NMR (in $CDCl_3$) spectrum for the product of the reaction of dicarboranylmethanol with $Ca(ClO)_2$ in CH_2Cl_2:CH_3COOH.

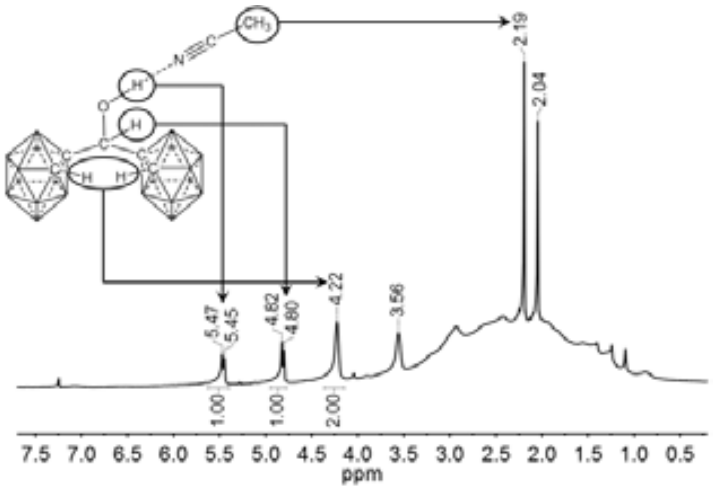

Figure 3.7. ^{1}H-NMR (in $CDCl_3$) spectrum for the product of the reaction of dicarboranylmethanol with $Ca(ClO)_2$ in CH_3CN:CH_3COOH.

As the oxidation with $Ca(ClO)_2$ did not yield the desired compound, several other methods were tried but none was successful. The oxidation with the Jones reagent was carried in the standard conditions: over a mixture of the alcohol in acetone was added an aqueous solution of Jones reagent on an ice bath.[10] The colour changed from orange to green, which indicated that the Cr(VI) specie reduced to Cr(III) specie. The reaction mixture was filtered and the solution was extracted with diethyl-ether. When NMR analysis was done unexpected results were obtained. Different from the previous case, no *o*-carborane was observed as by-product, but neither the formation of the ketone was observed. As previous, in the ^{1}H-NMR was observed that the dimmer was broke and the H atom bonded to the carbon from cluster was observed at 4.27 ppm, and additionally two doublets were observed at 4.74 ppm and

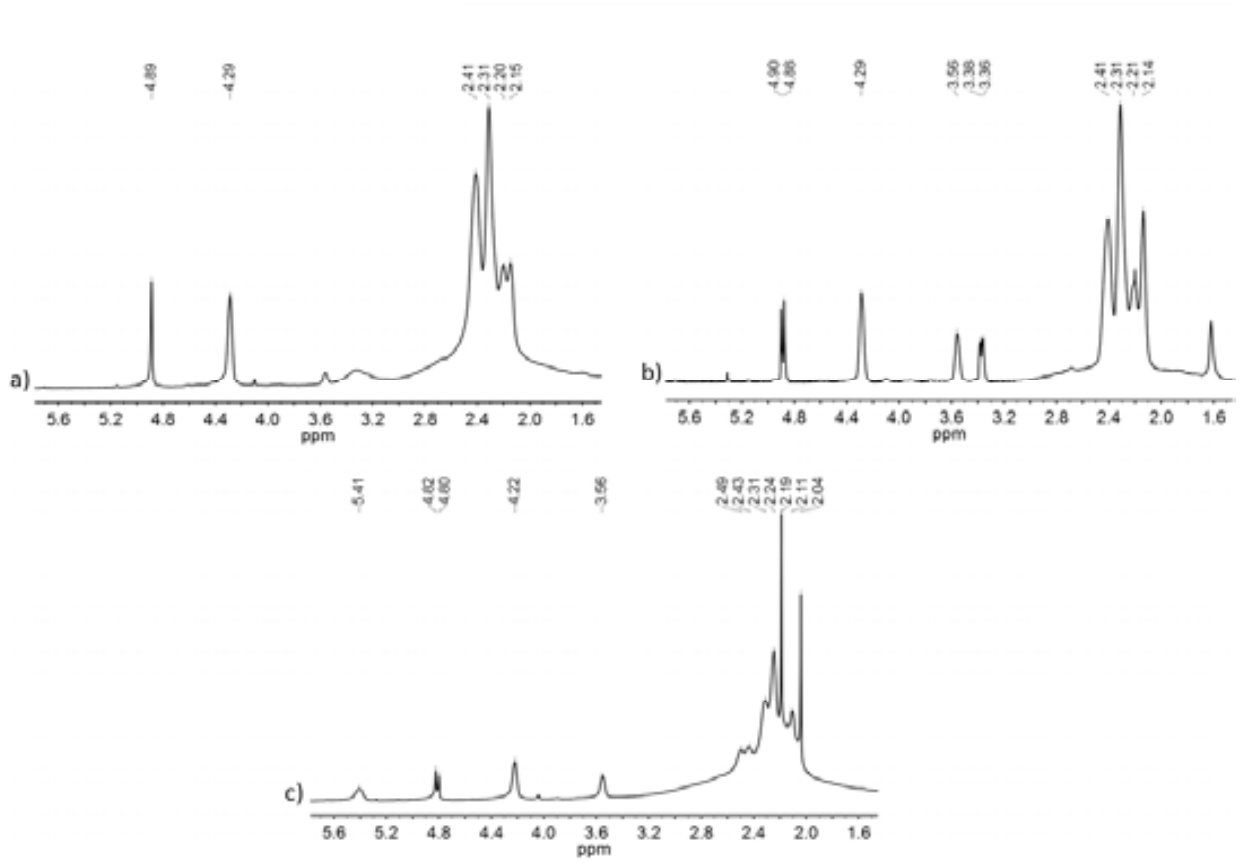

Figure 3.8. $^{1}H\{^{11}B\}$-NMR spectrum (in $CDCl_3$) for the product of the reaction of: a) carboranylformaldehyde with $Li[C_2B_{10}H_{11}]$; b) dicarboranylmethanol with $Ca(ClO)_2$ in CH_2Cl_2:CH_3COOH; c) dicarboranylmethanol with $Ca(ClO)_2$ in CH_3CN:CH_3COOH.

4.88 ppm ($^{3}J_{HH}$ = 6.0 Hz) (Figure 3.9.a). Also, the $^{1}H\{^{11}B\}$-NMR spectrum (Figure 3.9.b) revealed different distribution of the H bonded to the B atoms, and also a distortion of the doublet at 4.74 ppm, which indicate that the –OH moiety is involved in complex interactions with the BH vertices from the carborane cage.

Other methods were tried as the Swern oxidation,[11] that yielded almost all *o*-carborane, whereas the Oppenauer oxidation[12] does not modify at all the carboranylmethanol, though the

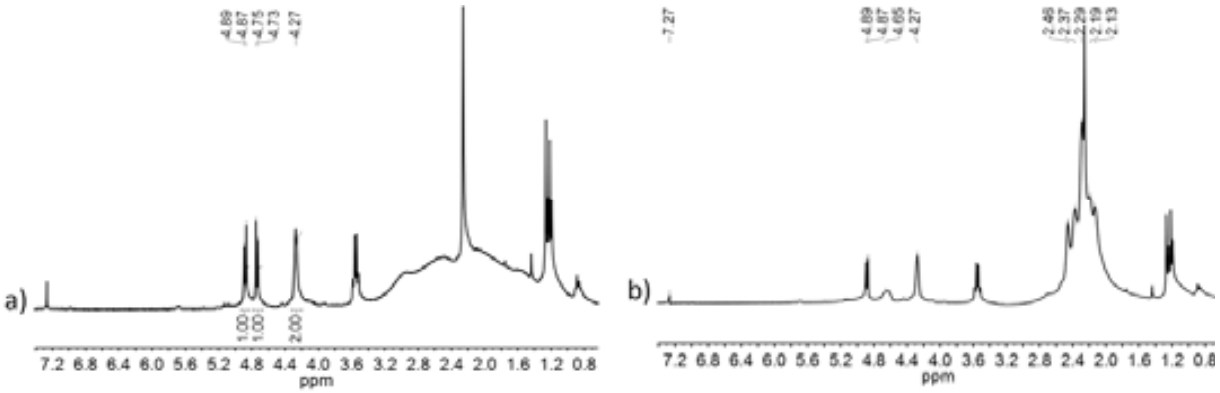

Figure 3.9. a) ^{1}H-NMR spectrum (in $CDCl_3$) and b) $^{1}H\{^{11}B\}$-NMR spectrum (in $CDCl_3$) for the product of the reaction of dicarboranylmethanol with Jones reactive (CrO_3-H_2SO_4-H_2O).

reactions conditions ($Al(CH_3)_3$ and 3-NO_2-C_6H_4-CHO) breaks the dimmer.

Another route to in-corporate the third carborane cluster on the dicarboranylmethanol platform was tried. In order to do so, we needed to convert the –OH moiety to a good leaving group. For that we converted the alcohol to the corresponding mesylate. For that, over o solution of alcohol (1 equiv-alent) in toluene, MsCl (1.5 equivalents), Et_3N (2 equivalents) and $Me_3N{\cdot}HCl$ (0.1 equivalents) were added under nitrogen and on an ice bath. The mixture was kept under stirring for 2 h and water was added, and the mixture was extracted with ethyl acetate. The organic phase was washed with brine and water and dried over $MgSO_4$. The evaporation of the solvent yielded the desired compound with a 100% conversion. The successful conversion was confirmed by ^{1}H-NMR analysis (Figure 3.10.).

Scheme 3.5. Reaction of dicarboranylmethine-mesylate with $Li[C_2B_{10}H_{11}]$.

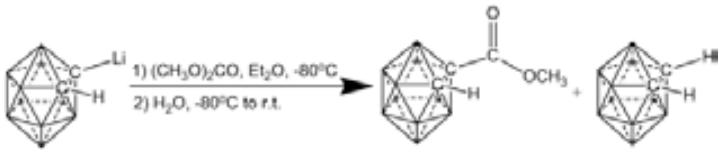

Scheme 3.6. Reaction of $Li[C_2B_{10}H_{11}]$ with dimethylcarbonate

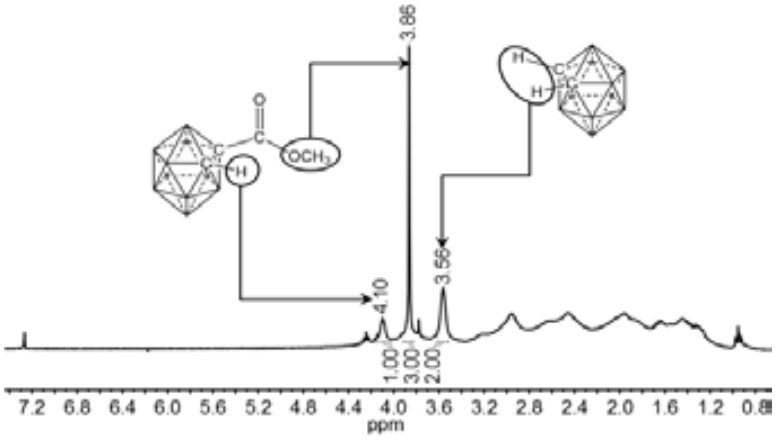

Figure 3.11. ^{1}H-NMR (in $CDCl_3$) spectrum for the reaction of $Li[C_2B_{10}H_{11}]$ with dimethylcarbonate.

The reaction of the mesylate with 1 equivalent of $Li[C_2B_{10}H_{11}]$ yielded only *o*-carborane. Due to the electron with-drawing character of two carborane cages and of the mesylate moiety, carbon-carbon bonds between the cluster and the middle carbon atom are poor in electrons. For this, instead on attacking only the C-O bond, the $Li[C_2B_{10}H_{11}]$ also attack the C-C bonds, yielding *o*-carborane (Scheme 3.5.).

In order to pursue our objective, we tried to obtain the two-cage ketone by other reaction. For that we reacted $Li[C_2B_{10}H_{11}]$ with dimethylcarbonate in 1:1 ratio and 1:2 ratio (Scheme 3.6.), but only a mixture of unreacted *o*-carborane and carborane-containing ester were obtained, as observed by NMR analysis (Figure 3.11.).

The achievement of three-cage or four-cage “space confined” derivatives of *o*-carborane is not a trivial task and further research has to be made. Useful insights were obtained, that can be used as basis for further research.

3.2. Carboranylformaldehyde as platform in electrophilic substitution reactions

It is known that aldehydes and ketones react with aromatic compounds in the presence of Brønsted or Lewis acids.[13] The electrophile is supposed to be the carboxonium ion formed in an

equilibrium reaction by protonation or complexation, respectively (Scheme 3.7.).[14] The formation of carboxonium ion is somewhat debatable, since the carbonylic oxygen atom can also form hydrogen bonds with a Brønsted acid. In order to test if the carboxonium ion (structure **I** in Scheme 3.7.) is really formed in the reaction of carboranylformaldehyde with triflic acid we done ^{1}H-NMR of a mixture of the aldehyde with excess of triflic acid in tetrachloroethylene (C_2Cl_4) using the double tube technique. We did the same mixing carboranyl-formaldehyde with excess of $AlCl_3$, as Lewis acid, which do not give the carboxonium ion (structure **III** in Scheme 3.7.). From the NMR spectra (Figure 3.12.) we observed that the carbonylic hydrogen atom and the H atom bonded to the other carbon from the carborane cage have the same chemical shifts, which indicate that in both cases the same compound is

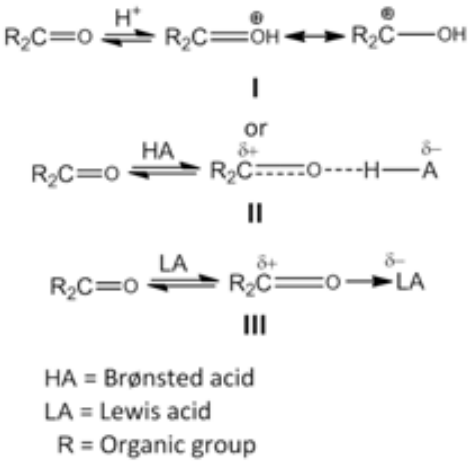

Scheme 3.7. Electrophiles formed by activation of the carbonylic compounds with Brønsted acids (I and II) or Lewis acids (III).

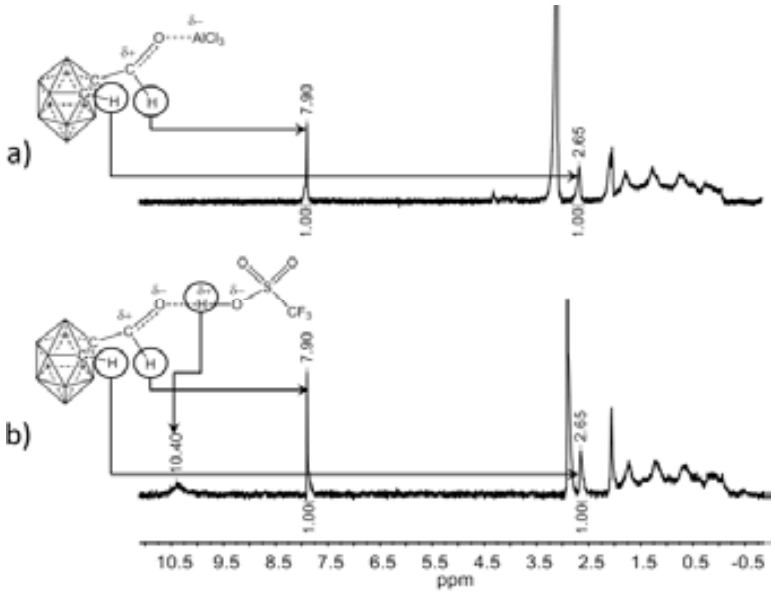

Figure 3.12. ^{1}H-NMR spectra (double tube with CD_3COCD_3) in C_2Cl_4 for the mixture of carboranylformaldehyde with: a) $AlCl_3$ and b) Triflic acid.

formed. This compound is the activated carboranylformaldehyde by the interaction of the O atom either with the H from the Brønsted acid (structure **II** in Schme 3.7.) or with the electron deficient centre of the Lewis acid (structure **III** in Schme 3.7.).

As the above experiments indicate that probably the same active intermediate is formed if the aldehyde is activated by a Brønsted acid or a Lewis acid we started to investigate the reactivity of the carboranylformaldehyde twoards different aromatic substrates taking into consideration: i) the role of the acid, and ii) the temperature of the reaction.

3.2.1. Reactivity of the carboranylformaldehyde activated by Brønsted acids

The choice of the Brønsted acid is important (Scheme 3.8.) since decarbonylation of the aldehyde was observed with H_2SO_4 at room temperature, yielding *o*-carborane. At -80°C the aldehyde is not affected by the sulphuric acid.

The reaction of carboranylformaldehyde with benzene, in the ratio 1:2 (carboranylformaldehyde:benzene) in the presence of excess of triflic acid, on the other hand, yields a compound that has a carborane cage and two benzene moieties (Scheme 3.9.). The intermediate is a substituted alcohol, which, however, is not stable in such acidic media and easily enters in a Friedel-Crafts alkylation with another molecule of benzene (Figure 3.13.).

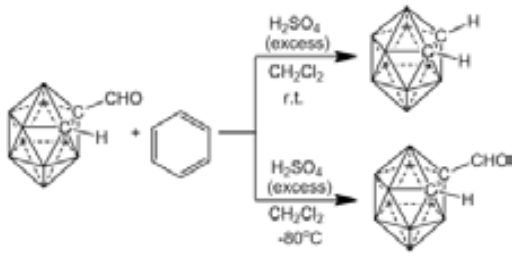

Scheme 3.8. Reaction of carboranylformaldehyde with toluene in presence of sulphuric acid.

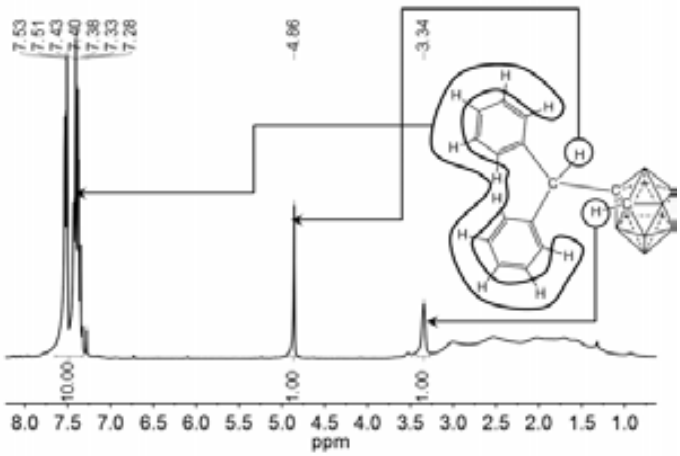

Figure 3.13. ^{1}H-NMR spectra (in $CDCl_3$) for the reaction of carboranylformaldehyde with benzene.

The reactions with polycyclic aromatic compounds as naphthalene, anthracene and fluorine Table 3.2. Entries 2-4) were also performed. With naphthalene and fluorene the same behaviour as for benzene is observed, the derivative with two naphthalene or fluorene moieties, respectively, were obtained, at room temperature in CH_2Cl_2. For the both compounds only one type of derivative is obtained: the electrophilic substitution takes place at α position for naphthalene and at the position 9 for fluorene. The reaction with anthracene is slower than with naphthalene and yield the same type of derivative with two anthracene moieties. Only on type of compound is observed in ^{1}H-NMR, which indicates that only the more favoured derivative of anthracene is obtained, that is the 9-substituted.

With toluene the reaction takes place as with benzene. The reaction is very rapid, at room temperature in CH_2Cl_2, the substitution at the toluene moiety being exclusively in *para* position, as only one type of methyl groups are observed in ^{1}H-NMR spectrum (Figure 3.14.).

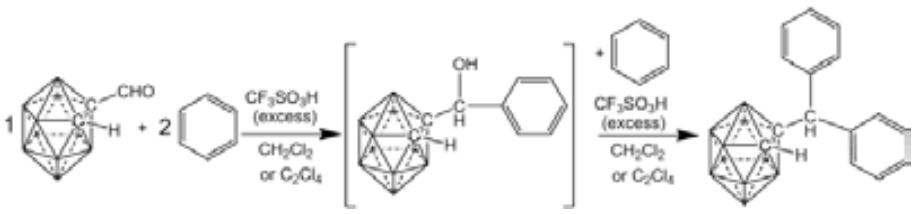

Scheme 3.9. Reaction of carboranylformaldehyde with benzene in presence of triflic acid.

The deactivating substituents on the benzene molecule, as for example the –Cl or $–NO_2$ moieties, difficult the substitution of the aromatic substrate since no reaction was observed in CH_2Cl_2 at room temperature. For that, we changed the solvent to other solvents (as tetrachloroeethylene or mesitylene) that are inert towards electrophilic substitution and have higher boiling point. It was observed for chlorobenzene that only 75% of aromatic substrate is substituted in tetrachloroethylene (C_2Cl_2) at 120°C for 24 h. This proved that the electrophilic substitution on deactivated aromatic substrates with carboranyl-formaldehyde was possible, but the activation energy is higher. For that we searched for another solvent that could reach higher temperature. Mesitylene, which has the boiling point over 160°C, was the next choice as solvent. The reaction yield in mesitylene as solvent is substantially improved, and fully substituted nitrobenzene derivative is obtained in 2 h. The substitution of nitrobenzene yields the derivative which has only one nitrobenzene moiety, substituted in *meta* position, though. On the other hand, the derivative with two chlorobenzene moieties, substituted in *para* position was observed.

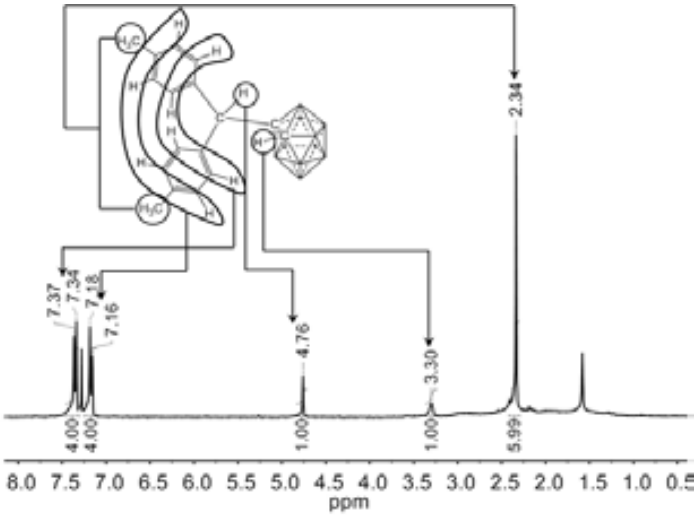

Figure 3.14. ^{1}H-NMR spectra (in $CDCl_3$) for the reaction of carboranylformaldehyde with toluene.

It must be pointed out that regarding anthracene, in CH_2Cl_2 at room temperature for 3 h, only 50% of the conversion is obtained, whereas in C_2Cl_4 at 120°C for 2 h the conversion is almost 100%.

The carboranylformaldehyde reaction with aniline in CH_2Cl_2 at room temperature was performed but no electrophilic substitution was observed. As the aniline is a base, the cleavage the C_C-C bond was produced with the decarbonylation of the –CHO group and the subsequent degradation of the cluster from *closo* to *nido*. This was somehow unespected since the reaction of carborane-aldehydes with aniline was reported to give Schiff bases.[15]

The electrophilic substitutions on heteroarenes give different results. Pyridine produces, as observed with other bases as aniline, the cleavage of C_C-C bond in carboranylformaldehyde and degradation of the carborane cage, whereas quinoline gives a small yield of *nido* compound after 24 h in CH_2Cl_2 in presence of triflic acid, but most probably if the reaction time is prolonged it will yield the same as pyridine. Others diheteroaromatic π-deficient compounds as pyrazine, pyridazine and pyrimidine give no reaction, only pristine carboranylformaldehyde being recovered at the end of the reactions. With π-excessive heteroaromatic compounds the substitution reaction is achieved but in different conditions. It was surprisingly to find that pyrrole do not react with carboranyl-formaldehyde in CH_2Cl_2 at room temperature in presence of triflic acid, although it was reported that trifluoroacetic acid give good results. Others heterocycles polyaromatics as indole give with carboranylformaldehyde in CH_2Cl_2 at room temperature in presence of triflic acid, a mixture of 2-subtituted and 3-substituted derivatives of indole with two moieties of heteroaromatic compound, though more than 1 day is need for the full conversion of the carboranylformaldehyde. With carbazole, on the other hand, it was surprisingly to find that the reaction in CH_2Cl_2 at room temperature do not takes place, although it is generally known that the electrophilic substitutions go faster than with benzene.[16] If CH_2Cl_2 is changed for C_2Cl_4 and the reaction

is carried at 120°C, the electrophilic substitution is achieved, the derivative with two carbazole moieties being obtained. With other heterocycles as imidazole or pyrazole, the reaction does not work. Other π-excessive heteroaromatic compounds as furane or thiophene do not give electrophilic substitution in triflic acid, the furane polymerizes whereas the thiophene gives no reaction.

In order to try the polysubtitution of the aromatic substrate with more carborane moieties, the reaction of carboranylformaldehyde with benzene in 2:1 ratio was performed in CH_2Cl_2 at room temperature for 1 day, but the polysubtitution was unsuccessful. At the end of the reaction the same derivative with one carborane moiety and two benzene rings was observed together with the excess of carboranylformaldehyde (Scheme 3.10.).

Scheme 3.10. Reaction of carboranylformaldehyde with benzene in 2:1 ratio.

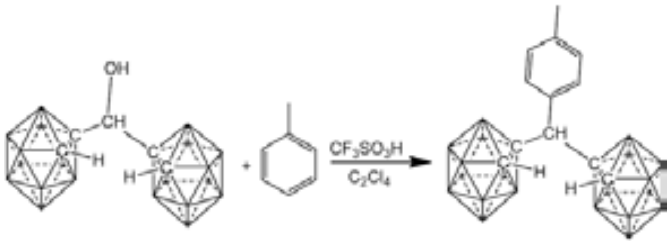

Scheme 3.11. Proposed reaction of dicarboranylmethanol with toluene in the presence of triflic acid.

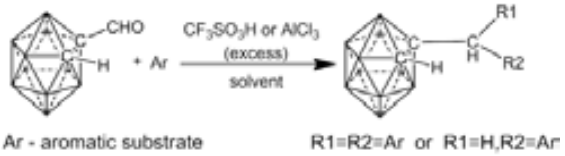

Scheme 3.12. Reaction of carboranylformaldehyde with aromatic substrates.

Also, the alcohol described in the previous section, namely the dicarboranylmethanol, was used for electrophilic substitutions reactions with toluene in tetrachloroethylene at 120°C in presence of triflic acid, but the reaction was unsuccessful, after 1 day only unreacted compounds were observed (Scheme 3.11.).

In all the reactions the synthesized compounds have either two of aromatic substrate (Scheme 3.12.) or one moiety, but in neither the cases is observed the intermediate alcohol. Table 3.2. summarizes the ^{1}H-NMR chemical shifts for synthesized compounds by electrophilic substitution reactions.

Besides, the electrophilic substitution, the aldehydes can be also used in electrophilic additions at the double and triple bonds of alkenes and alkynes in the so-called Prins reaction.[17] The reaction of carboranylformaldehyde with 1-hexene in CH_2Cl_2 at room temperature in presence of triflic acid was unsuccessful, only unreacted compounds being observed. On the other hand, using tetrachloroethylene as solvent at 120°C, in presence of triflic acid, additions of the carboranylformaldehyde to the double bond of 4-Br-1-butene and to the triple bond of 6-Cl-1-hexyne, were achieved. The reactions though are not fully completed after 1 day, in the reaction crude still being observed pristine carboranylformaldehyde. This type of reactions still have to be further studied in order to determine which compounds are formed and also, to try performing the reaction with Lewis acids, since the Prins reaction is strong dependent of the reaction conditions.

Entry	Reaction conditions[a)]	Aromatic substrate	Products	^{1}H-NMR chemical shifts (ppm)			Conversion (%)[b)]
				$\delta(C_C$-**H**)	$\delta(C_C$-C**H**)	δ (organic moiety)	
1	A	Benzene	R1=R2= -C_6H_5 (**52**)	3.34	4.86	7.33-7.53 (H_{arom})	100
2	A	Naphtalene	R1=R2= -α-$C_{10}H_7$ (**53**)	3.35	5.18	7.51-7.94 (H_{arom})	100
3	A	Fluorene	R1=R2= -9-$C_{13}H_9$ (**55**)	3.42	5.03	3.95 (H_{poz-9}), 7.35-7.85 (H_{arom})	100
4	A	Anthracene	R1=R2= -9-$C_{14}H_9$ (**56**)	3.37	4.63	7.50-8.49 (H_{arom})	50[c)]
5	A	Toluene	R1=R2= -*p*-$C_6H_4CH_3$ (**57**)	3.30	4.76	2.34 (-CH_3), 7.16-7.37 (H_{arom})	100
6	A	Chlorobenzene	-	-	-	-	0
7	A	Nitrobenzene	-	-	-	-	0
8	A	Indole	R1=R2= -2-C_8H_5NH (**62**)	3.88	5.64	6.62-7.34 (H_{arom}), 8.17 (NH)	38[c)]
			R1=R2= -3- C_8H_5NH (**63**)	3.96	5.74	6.33-7.89 (H_{arom}), 8.21 (NH)	19[c)]
9	B	Anthracene	R1=R2= -9-$C_{14}H_9$ (**56**)	3.37	4.63	7.50-8.49 (H_{arom})	100
10	B	Carbazole	R1=R2= -3-$C_{12}H_7NH$ (**64**)	3.40	5.17	7.29-8.21 (H_{arom})	100
11	B	Chlorobenzene	R1=R2= -*p*-C_6H_4Cl (**59**)	3.30	4.79	7.38-8.08 (H_{arom})	75[c)]
12	C	Chlorobenzene	R1=R2= -*p*-C_6H_4Cl (**59**)	3.30	4.79	7.38-8.08 (H_{arom})	100
13	C	Nitrobenzene	R1= H; R2= -*m*-$C_6H_4NO_2$ (**60**)	3.49	3.69	6.78-7.03 (H_{arom})	100
14	D	Toluene	R1= -*p*-$C_6H_4CH_3$; R2= -*o*-$C_6H_4CH_3$ (**58**)	3.44	5.26	2.38 (-CH_3 from R1), 2.41 (-CH_3 from R2), 7.20-7.81 (H_{arom})	28[d)]
15	D	Naphtalene	R1=R2= -β-$C_{10}H_7$ (**54**)	3.71	6.32	7.60-8.11 (H_{arom})	40[e)]
16	D	Pyrrole	R1=R2= -2-C_4H_3NH (**61**)	3.24	4.98	6.21-6.25 (H_{poz-3} and H_{poz-4}), 6.76 (H_{poz-5}), 8.23 (NH)	100

a) A – CH_2Cl_2, r.t., CF_3SO_3H;
B – C_2Cl_4, 120°C, CF_3SO_3H,
C – $(CH_3)_3C_6H_3$, 160°C, CF_3SO_3H;
D – CH_2Cl_2, r.t, $AlCl_3$.

b) Calculated from ^{1}H-NMR with respect to carboranylformadehyde.
c) the rest to 100% is unreacted carboranylformaldehyde.
d) the rest to 100% is the derivative from entry 5.
e) the rest to 100% is the derivative from entry 2.

Table 3.2. Yields and ^{1}H-NMR (in $CDCl_3$) chemical shifts for the synthesized compounds from carboranylfromadehyde and aromatic substrates in different reaction conditions (A, B, C and D).

3.2.2. Reactivity of the carboranylformaldehyde activated by $AlCl_3$

As the first reaction tied in the previous section was the reaction of the acid activated carboranylformadehyde with toluene, we first tied this reaction, adding an excess of $AlCl_3$ over a solution of carboranylformadehyde in toluene. The presence of a methyl group in the toluene allows us to discern if the two arenes are bonded at the same position. The reaction went smoothly at room temperature, the reaction products being though different from the ones obtained in the presence of triflic acid (Scheme 3.13.). The compounds obtained in this reaction also have two toluene moieties but a mixture

of disubstituted derivative with the two toluene moieties substituted in *para* (72%) and disubstituted derivative with one toluene moiety substituted in *para* and one in *ortho* (21%) is observed, as identified by ^{1}H-NMR (Figure 3.15.).

Different results were also observed in the reaction of carboranylformaldehyde with naphthalene in presence of $AlCl_3$, with respect to triflic acid. In this case, a mixture between α-subtituted derivative (60%) and β-subtituted derivative (40%) is observed, respectively (Figure 3.16.).

As the reaction with aromatic substrates that give substitution when the carboranylaldehyde is activated by trifilic acid, also work when $AlCl_3$ is used to activate the aldehyde, we tested the reactions that do not give substitution with triflic acid, especially the aromatic heterocycles. The $AlCl_3$ activated carboranylformaldehyde give no substitution reactions when π-deficient heteroaromatics compounds as pyridine, pyrazine, pyridazine and pyrimidine are used as substrates, as observed when triflic acid was used.

The reaction of pyrrole, on the other hand, that did not worked when the carboranyl-formaldehyde was activated by triflic acid, give with $AlCl_3$ the desired results. The reaction goes smoothly in CH_2Cl_2 at room temperature, and the compound

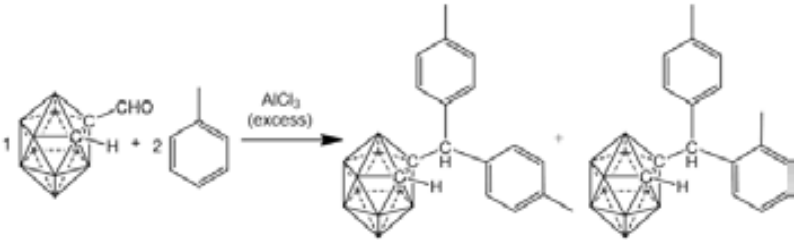

Scheme 3.13. Reaction of carboranylformaldehyde with toluene in presence of $AlCl_3$

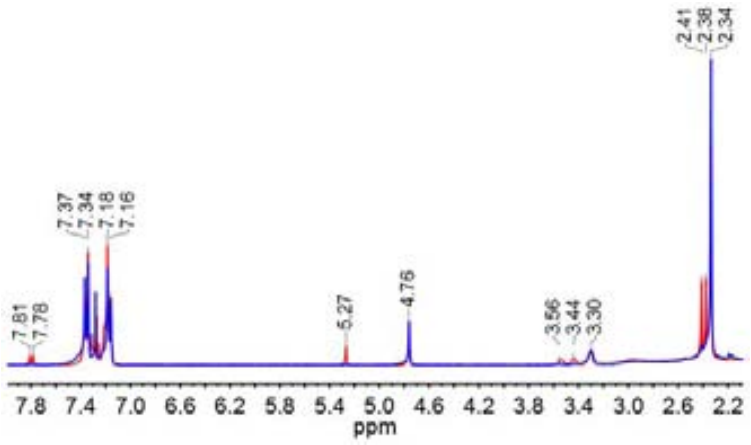

Figure 3.15. ^{1}H-NMR spectra (in $CDCl_3$) for the reaction of carboranylformaldehyde with toluene in the presence of $AlCl_3$ (red) and for the product of reaction of carboranylfromadehyde with toluene in presence of triflic acid (blue) (δ = 3.56 ppm represents impurity of *o*-carborane from the starting aldehyde).

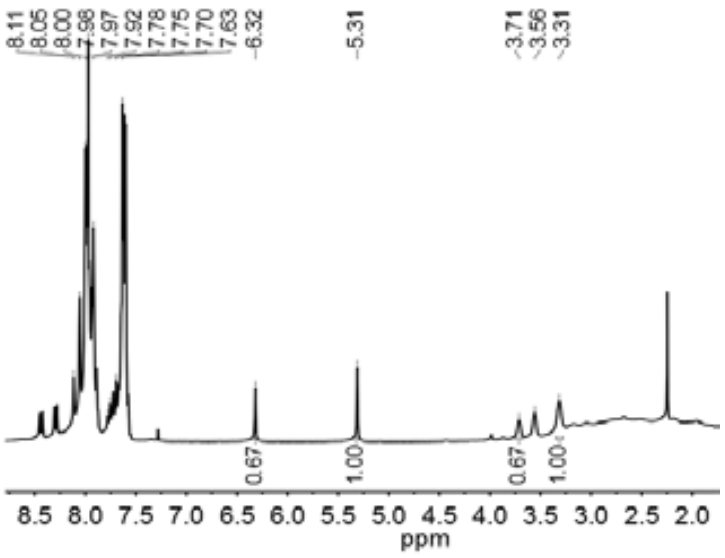

Figure 3.16. ^{1}H-NMR spectra (in $CDCl_3$) for the reaction of carboranylformaldehyde with naphtalene in the presence of $AlCl_3$ (δ = 3.56 ppm represents impurity of *o*-carborane from the starting aldehyde).

with two pyrrole molecules is obtained as observed by ^{1}H-NMR (Figure 3.17.). The behaviour observed by us for carboranyl-formaldehyde is a classical textbook example of how the dipyrromethanes are obtained,[18] and was surprisingly to find in the literature that other behaviour for carboranyl-formaldehyde with other activating agents as trifluoroacetic acid or indium chloride, is observed.[19]

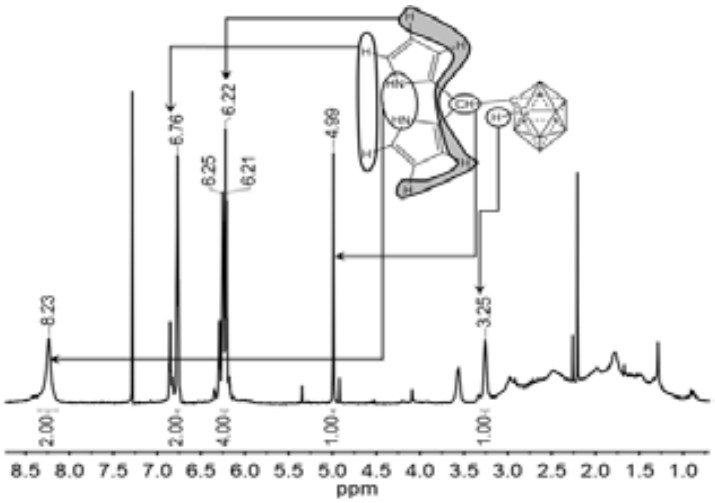

Figure 3.17. ^{1}H-NMR spectra (in $CDCl_3$) for the reaction of carboranylformaldehyde with pyrrole

To summarize the results presented in this section the following observation can be made: 1) the aromatic electrophilic substitution with carboranylformaldehyde, activated by Brønsted or Lewis acids can be smoothly performed for activated aromatic substrates; 2) some deactivated aromatic substrates can react in energetic conditions; 3) the reactions of carboranylformaldehyde give similar compounds as organic aldehydes. Still, the work is not complete and further investigations have to be made, especially substituting the Brønsted acids for Lewis acids, since different results were observed if one or the other are employed.

3.3. Phosphonates and phosphonium salts derivatives of carboranes. First studies on carboranylformaldehyde in Horner-Wadsworth-Emmons and Wittig reactions

In the previous section were presented one class of reactions on carboranylformaldehyde that lead to derivatives of carborane with aromatic molecules that are interesting for their potential spectroscopic properties. Other ways of obtaining compounds capable of absorbing and emit light is by incorporating molecules that have multiple bonds that delocalize electrons by conjugation. The incorporation of such molecules can be done by reactions where C=C double bonds are formed by the reactions of phosphorus derivatives with carbonylic compounds as is the case of the Horner-Wadsworth-Emmons (HWE) or Wittig reactions.

A first approach, for HWE reactions, was trying the direct reaction of carboranylformaldehyde with a highly delocalized phosphonate (Scheme 3.14.) but the results were unexpected and unsuccessful. The HWE reaction begins by the deprotonation of the phosphonate to give the phosphonate carbanion, which produces the nucelophylic addition to the

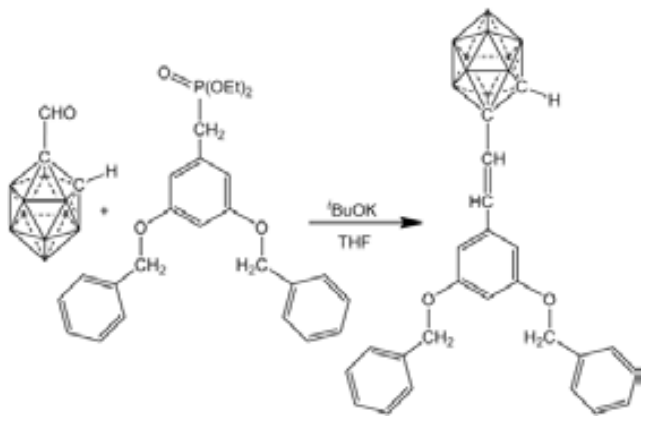

Scheme 3.14. Proposed HWE reaction of carboranylformaldehyde.

carbonyl group (Scheme 3.15.). The main draw-back to this reaction is the formation of this carbanion, which in the case of carboranylformaldehyde, does not give addition, but in change produces the cleavage of the C_C-C bond and CO elimination, giving the parent *o*-carborane. Decarbonylation reaction was observed even at low temperature (-80°C).

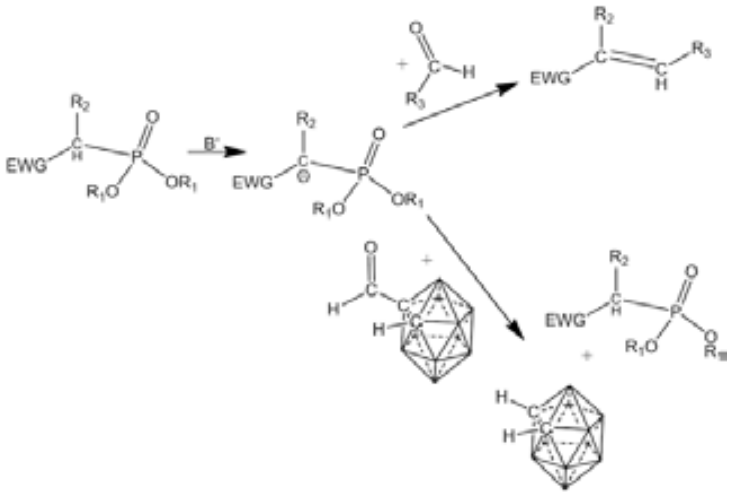

Scheme 3.15. Schematics of the HWE reaction involving organics aldehydes and carboranylformaldehyde

In order to further pursue with our project we change the strategy by trying to incorporate the phosphonate group on the carborane cage and having the carbonyl group on the organic substrate. Phosphonates are generally obtained in the reaction of organic halides with phosphites. For that, first the bromo-derivative of methyl-carborane was obtained from decaborane, $B_{10}H_{14}$ and propargyl bromide (Scheme 3.16.). The phosphonate derivative of carborane was synthetized from bromo-methylcarborane and triethylphosphite (Scheme 3.16.) at 150°C, as identified by NMR and ESI-MS analysis. First studies of the reaction of this phosphonate with aldehydes were though unsuccessful, obtaining methyl-carborane. It is known that the success of the HWE depends of the anion stabilizing character of groups bonded to the nucleophilic carbon, and probably the carborane cage is not so good anion stabilizing. Further studies have to be made though, altering the conditions of the HWE reaction.

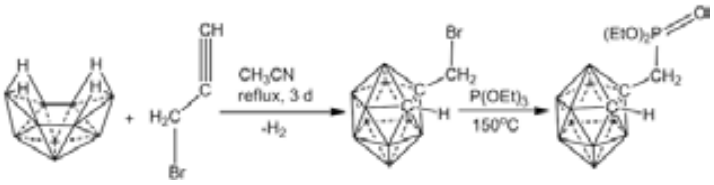

Scheme 3.16. Synthesis of carborane containing phosphonate from bromo-methyl-carborane

Wittig reactions with carboranylformaldehyde and other organic phosphonium salts were already reported by our group,[6] so we tried changing the reaction strategy by incorporating the phosphonium salt on the carborane platform. For that, we tried synthesizing the triphenyl(methylcarborane)phosphonium salt. First we started with the standard conditions, involving triphenylphosphine and bromo-methylcarborane, using aromatic solvents and energetic conditions. We employed solvents as toluene at 110°C, *p*-Xylene at 140°C and mesitylene at 160°C, but all the reactions were unsuccessful. We changed the conditions to a solvent free route of synthesis, using microwave radiation and the synthesis was successful. The reaction goes smoothly by mixing 1 equivalent of bromo-methylcarborane and 1.05 equivalents of triphenylphosphine, in a microwave tube with a pressure-secured lead. The mixture as heated in the microwave oven at 140°C for 1 h and the full

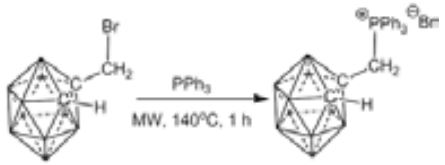

Scheme 3.17. Synthesis of triphenyl(methylenecarboranyl)-phosphonium bromide

conversion of the bromomethylcarborane to the corresponding phosphonium salt was achieved (Scheme 3.17.). Although the synthesis is clean, efficient and can be carried out at grams scale, the formed phosphonium salt is insoluble in the majority of the solvents. It is though, slightly soluble in DMSO, and we could characterized it by NMR. With time, the DMSO solution produce the degradation of the carborane cage, but the phosphonium centre is retained, forming a zwitterion. As the carborane derivative is asymmetric, a mixture of two isomers of the *nido* derivative is formed (Scheme 3.18.) as observed by two signals for the apical H atom in $^{1}H\{^{11}B\}$-NMR spectrum at -3.37 ppm and -3.57 ppm, as well as two chemical shifts for the P centre in $^{31}P\{^{1}H\}$-NMR spectrum (Figure 3.17.). Interestingly, in the $^{1}H\{^{11}B\}$-NMR spectrum two different doublets of doublets can be observed for the two methylene hydrogen atoms, first between 3.59 ppm and 3.68 ppm and the second between 4.15 ppm and 4.24 ppm (Figure 3.17.). First doublet is formed by the coupling of the methylene hydrogen atoms with the P centre ($^{2}J_{P,H}$ = 15.0 Hz) and the second by the coupling between them with ($^{2}J_{H,H}$ = 12.0 Hz).

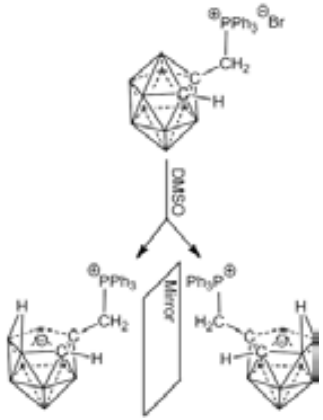

Scheme 3.18. Degradation of carborane-based phosphonium salts in DMSO

Despite its solubility problems we further pursue with the Wittig reactions. A suspension of the phosphonium salt in ethereal solvents (Et_2O or THF) was cooled down on an ice bath and 1 equivalent of ^{t}BuOK was added. The white suspension started to solubilize and in 30 minutes a yellow solution was

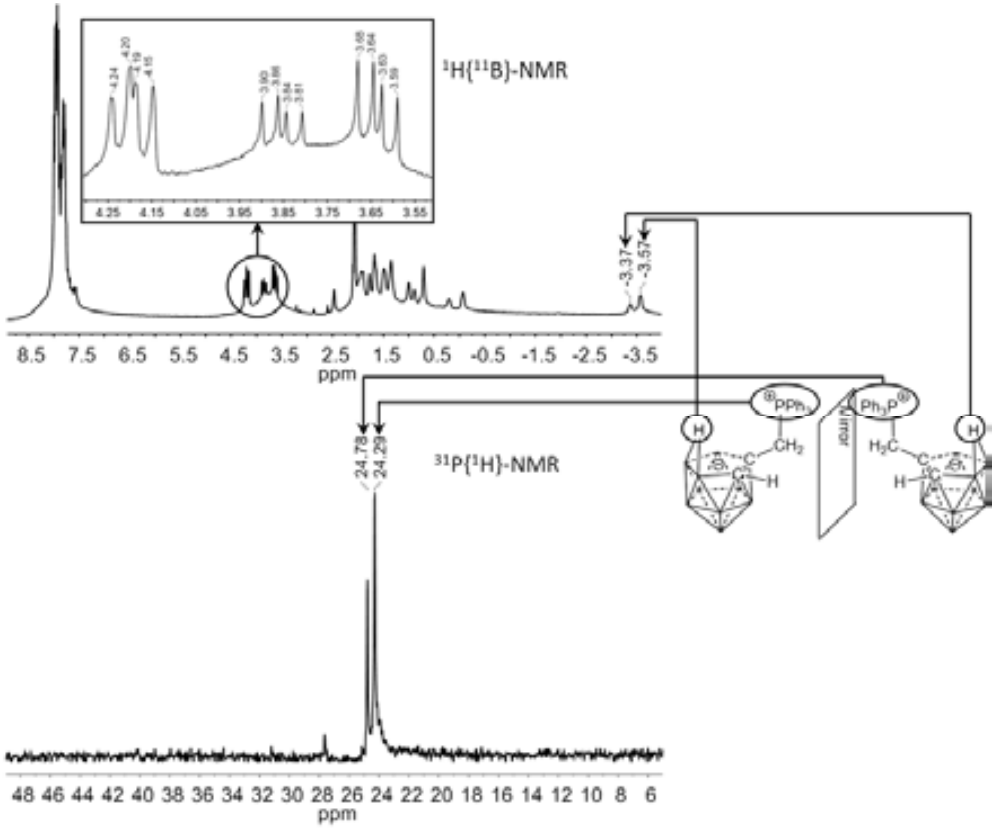

Figure 3.17. $^{1}H\{^{11}B\}$-NMR and $^{31}P\{^{1}H\}$-NMR (in CD_3COCD_3) spectra for the racemic mixture obtained by the deboronation of the carborane-based phosphonum salt in DMSO.

formed. The formation of the ylide was confirmed by $^{31}P\{^1H\}$-NMR, which shifts from 22.65 ppm for the phosphonium salt to 12.94 ppm for the correspondent ylide. The Wittig reaction with benzadehyde and anthracene-9-aldehyde was tried but the reaction was unsuccessful. The reaction with antracene-9-aldehyde was followed by $^{31}P\{^1H\}$-NMR and $^{11}B\{^1H\}$-NMR (Figure 3.18.). It was observed that after 3.5 h the ylide is still present in the reaction mixture and no reaction with the aldehyde is produced. If the reaction time is prolonged, after 22 h, the ylide disproportionate, and methylcarborane and triphenyl-phosphine oxide are formed, as identified by $^{11}B\{^1H\}$-NMR and $^{31}P\{^1H\}$-NMR, respectively. The ^1H-NMR, also confirmed presence at the end of the reaction of the unreacted anthracene-9-aldehyde, identified by the carbonylic H atom and the methylcarborane, identified by the $–CH_3$ moiety and the H atom bonded to the other carbon atom of the carborane cage (Figure 3.19.). The reaction of the phosphonium salt with carboranyl-formaldehyde was also tried and at the end of the reaction only unreacted phosphonium salt and *o*-carborane were observed. As previous observed in HWE reaction, the *o*-carborane is formed by the cleavage of the C_C-C bond of the carboranyl-formaldehyde.

This work is in its first studies and still more is to be done in order to understand how the HWE and Witting reactions take place with these derivatives of

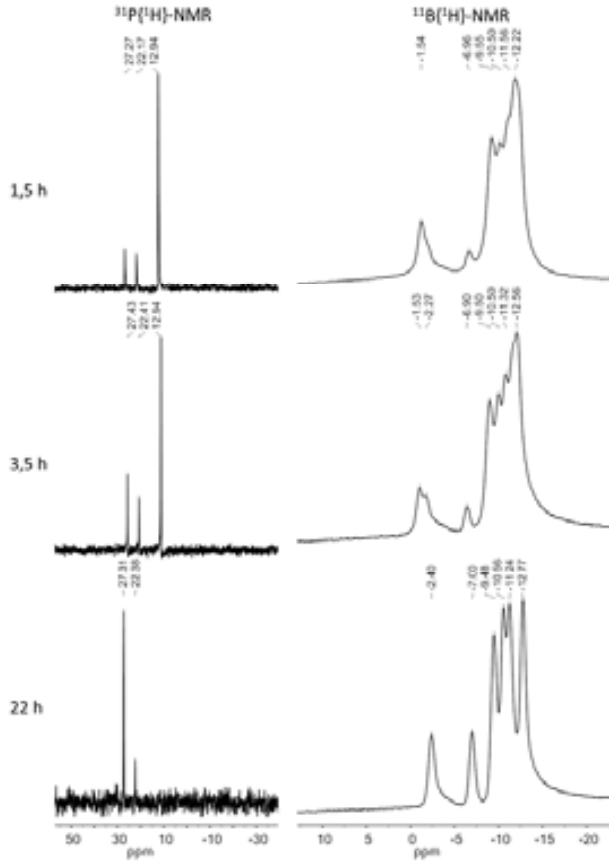

Figure 3.18. $^{31}P\{^1H\}$-NMR and $^{11}B\{^1H\}$-NMR (in Et_2O) spectra for the reaction of triphenyl(methylene-carboranyl)phosphonium bromide with anthracene-9-aldehyde.

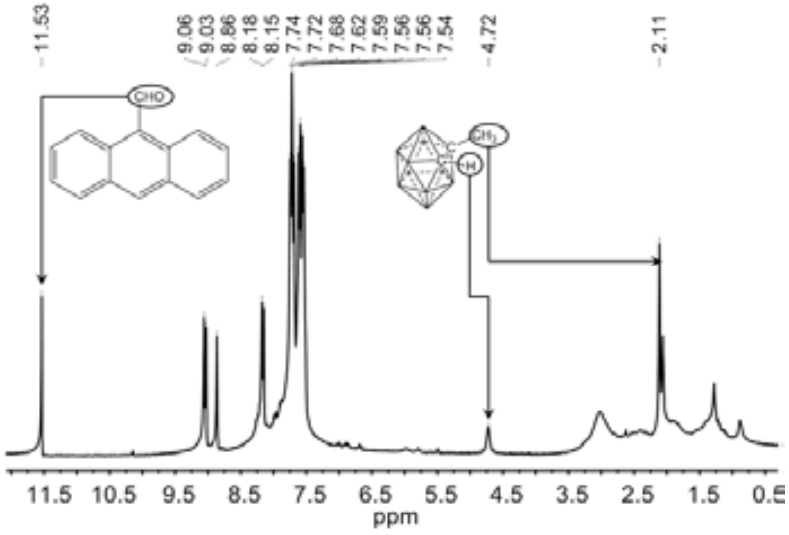

Figure 3.19. ^1H-NMR (in CD_3COCD_3) spectrum for the reaction of triphenyl(methylcarboranyl)phosphonium bromide with anthracene-9-aldehyde.

carborane. Still, the main achievement was the efficient synthesis of the phosphonate and the phosphonium salt derivatives of *o*-carborane, which were previously unknown and offer new insights on how the carborane cage can influence the reactivity of archetypal groups in organic chemistry.

[1] a) Willans, C. E.; Kilner, C. A.; Fox, M. A. *Chem. Eur. J.*, **2010**, *16*,10644. b) Popescu, A. R.; Musteti, A. D.; Ferrer-Ugalde, A.; Viñas, C.; Núñez, R.; Teixidor, F. *Chem. Eur. J.*, **2012**, *18*, 3174.
[2] Stanko, V. I.; Brattsand, Ralph; Al'perovich, N. E.; Titova, N. S. *Zh. Obshch. Khim.*, **1966**, *36*, 1862.
[3] a) Zakharkin, L. I.; L'vov, A. I. *Zh. Obshch. Khim.*, **1967**, *37*, 742. b) Zakharkin, L. I.; Kalinin, V. N. *Synth. Inorg. Met-Org. Chem.*, **1972,** *2*, 113. c) Yang, X.; Hawthorne, M. F. *Inorg. Chem.*, **1993**, *32*, 242.
[4] Dozzo, P.; Kasar, R. A.; Kahl, S. B. *Inorg. Chem.*, **2005**, *44*, 8053.
[5] a) Reddy, V. J.; Roforth, M. M.; Tan, C.; Mereddy, V. R. *Inorg. Chem.*, **2007**, *46*, 381. b) Jonnalagadda, S. C.; Cruz, J. S.; Connell, R. J.; Scott, P. M.; Mereddy, V. R. *Tetrahedron Lett.*, **2009**, *50*, 4314. c) Jonnalagadda, S. C.; Verga, S. R.; Patel, P. D.; Reddy, A. V.; Srinivas, T.; Scott, P. M.; Mereddy, V. R. *Appl. Organomet. Chem.*, **2010**, *24*, 294.
[6] Sousa-Pedrares, A.; Viñas, C.; Teixidor, F. *Chem. Commun.*, **2010**, *46*, 2998.
[7] a) Nakamura, H.; Aoyagi, K.; Yamamoto, Y. *J. Org. Chem.*, **1997**, *62*, 780. b) Nakamura, H.; Aoyagi, K.; Yamamoto, Y. *J. Orgomet. Chem.*, **1999**, *574*, 107.
[8] Terrasson, V.; Planas Giner, J.; Prim, D.; Teixidor, F.; Viñas, C.; Light, M. E.; Hursthouse, M. B. *Chem. Eur. J.*, **2009**, *15*, 12030.
[9] Nwaukwa, S. O.; Keehn, P. M. *Tetrahedron Lett*., **1982**, *23*, 35.
[10]Tojo, G.; Fernández, M. *Oxidation of Alcohols to Aldehydes and Ketones. A Guide to Current Common Practice*. **2006**, Springer. p.1.
[11] a) Omura, K.; Swern, D. *Tetrahedron*, **1978**, *34*, 1651. b) Mancuso, A. J.; Brownfain, D. S.; Swern, D. *J. Org. Chem.*, **1979**, *44*, 4148–4150; c) Mancuso, A. J.; Huang, S.-L.; Swern, D. *J. Org. Chem.*, **1978**, *43*, 2480. c) Tojo, G.; Fernández, M. *Oxidation of Alcohols to Aldehydes and Ketones. A Guide to Current Common Practice*. **2006**, Springer, p.97.
[12] Graves, C. R.; Zeng, B.-S.; Nguyen, S. T. *J. Am. Chem. Soc.*, **2006**, *128*, 12596.
[13] Bruckner, R. *Advanced Organic Chemistry*. *Reaction Mechanisms*. **2002**, Elsevier. p 196.
[14] Sykes, P. *A guidebook to mechanism in organic chemistry*. 6th Ed. John Wiley & Sons. **1996**, p. 204.
[15] Zakharkin, L. I.; L'vov, A. I.; Grebennikov, A. V. *Izv. Akad. Nauk. SSSR, Ser. Khim.*, **1968**, 2157.
[16] Eicher, T.; Hauptmann, S. *The Chemistry of Heterocycles*. 2nd Ed., Wiley-VCH, **2003**.
[17] Carey, F. A.; Sundberg, R. J. *Advanced Organic Chemistry. Part B: Reactions and Synthesis*. 5th Ed. Springer, **2007**, p.864.
[18] a) Laha, J. K.; Dhanalekshmi, S.; Taniguchi, M.; Ambroise, A.; Lindsey, J. S. *Org. Process Res. Dev.*, **2003**, *7*, 799. b) Geier, G. R.; Lindsey, J. S. *Tetrahedron*, **2004**, *60*, 11435. c) Ptaszek, M.; McDowell, B. E.; Lindsey, J. S. *J. Org. Chem.*, **2006**, *71*, 4328. d) Ka, J.-W.; Lee, C.-H. *Tetrahedron Lett.*, **2000**, *41*, 4609. e) Littler, B. J.; Miller, M. A.; Hung, C.-S.; Wagner, R. W.; O'Shea, D. F.; Boyle, P. D.; Lindsay, J. S. *J. Org. Chem.*, **1999**, *64*, 1391. f) Boyle, R. W.; Xie, L. Y.; Dolphin, D., *Tetrahedron Lett.*, **1994**, *35*, 5377.
[19] Satapathy, R.; Dash, B. P.; Zheng, C.; Maguire, J. A.; Hosmane, N. *J. Org. Chem.*, **2011**, *76*, 3562.

4. Carboranylpyridine as platform for new derivatives

4.1. Studies on the improvement of synthesis of carboranylpyridine and cyclometalation reactions of carboranylpyridine

In the first chapter of the Results and Discussion part was presented a detailed study on the reaction of carborane with *n*-BuLi, as is an important intermediate reaction for the synthesis of C-substituted derivatives of carborane. Apart from this route, other manner to synthesise mono- and di-C-substituted *o*-carborane derivatives is the reaction of decaborane (*nido*-$B_{10}H_{14}$) with alkynes either in the presence of a Lewis base,[1] or in an ionic liquid.[2] The reaction with decaborane/Lewis base mixtures precede by the formation of a reactive intermediate, *arachno*-$L_2B_{10}H_{12}$ (e.g. L=SEt_2, CH_3CN), which reacts with alkynes, R-C≡C-R', to give 1-R-2-R'-1,2-*closo*-$C_2B_{10}H_{12}$ (Scheme 4.1.).

Scheme 4.1. General reaction scheme for the synthesis of carboranes from decaborane.

Carboranylpyridine, 1-(2'-C_5H_4N)-1,2-*closo*-$C_2B_{10}H_{11}$ (**69**), was described some time ago,[3] but the synthesis from the decaborane and 2-ethynylpyridine was not so effective. In an attempt to improve the reported yield of 28%, our group made several modifications, such as the use of dimethylaniline, acetonitrile, triethylamine or diethylamine, either as Lewis bases and/or as solvents.[4] Also the reaction time or temperature was altered. A solvent-free procedure was also investigated, which lead to an improvement of the yield of **1** to 45%. The major drawback to the synthesis of this compound was the formation of a very stable adduct between the 2-ethynylpyridine and the borane cluster, namely, 6,9-(2'-(HCC)-$C_5H_4N)_2$-*arachno*-$B_{10}H_{12}$ (Scheme 4.2.). This compound formation was the bottleneck for an efficient achievement of the carboranylpyridine, and was one reason for which the chemistry of this compound was so less studied. In order to extend the study on this compound we had to find an effective route of synthesis. For this we took several approaches.

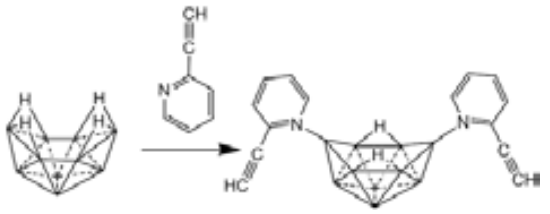

Scheme 4.2. Reaction of decaborane with 2-ethynylpyridine.

Many types of cross-coupling reactions have been known for several decades, and they already become a standard tool for the synthetic chemist.[5] For this, we tied to apply some coupling reaction between a metal derivative of *o*-carborane and a 2-halogenated pyridine derivative (Scheme 4.3.). The Negishi cross-coupling reaction[6]

Scheme 4.3. Proposed cross-coupling reactions of metalated carboranes with halopyridines.

was tried in one pot synthesis. The carborane-zinc derivative was obtained from monolithiated carborane derivative, $Li[C_2B_{10}H_{11}]$, and $ZnCl_2$. Different reaction conditions were tied, for the coupling reactions in THF with 2-bromopyridine, using as catalysts $[PdCl_2(PPh_3)_2]$ and $[NiCl_2(PPh_3)_2]$, but the cross-coupling reaction was unsuccessful, yielding in all the cases unreacted *o*-carborane, upon hydrolysis. The carboranyl-zinc derivative was formed, as identified by $^{11}B\{^1H\}$-NMR (Figure 4.1.) but due to its moisture sensibility it is difficult to separate from the reaction mixture for further characterization.

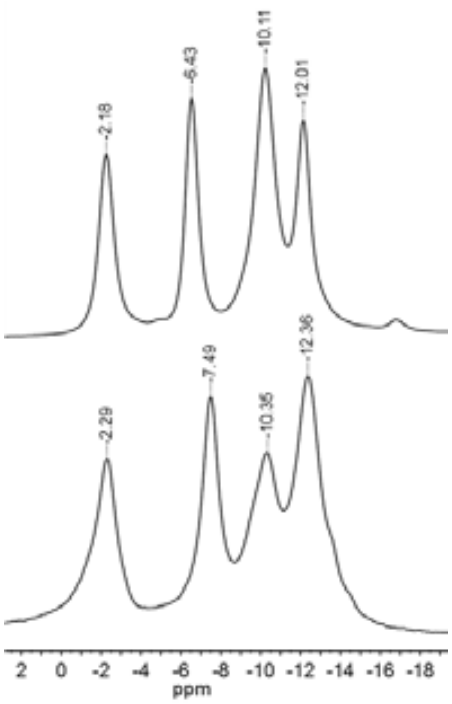

Figure 4.1. $^{11}B\{^1H\}$-NMR spectra (in THF) for $Li[C_2B_{10}H_{11}]$ (up) and $ZnCl[C_2B_{10}H_{11}]$ (down).

Other cross-coupling reaction that we tried was the Stille-Migita reaction[7] with 2-bromopyridine and 2-iodopyridine. The carborane-tin derivative is air and moisture inert, and it was separated from the reaction mixture and fully characterized. The synthesis of carborane-tin derivative was done form the lithiated carborane derivative with tributhyltin chloride, and the product was separated with a 98% yield. The Stille-Migita cross-coupling reaction was unsuccessful, though, even if we tried different reaction conditions described in the literature, involving $Pd(OAc)_2$/Dbaco catalytic system,[8] the unusual PEG400 as solvent and $[Pd(PPh_3)_4]$ or $[PdCl_2(PPh_3)_2]$ as catalyst,[9] or the copper (I) salts and fluoride ion synergic couple.[10] The reaction either yielded *o*-carborane, which indicate that the tin derivative entered in the catalytic cycle but the coupling with the 2-halopyridine did not took place, or *nido*-carborane, due to the degradation of the *closo*-carborane in the presence of bases or protic solvents.

The Hiyama cross-coupling[11] was also tried, for which a carborane-silicon derivative was synthesised from the reaction of $Li[C_2B_{10}H_{11}]$ with chloro(trimethyl)silane, with a 96% yield. The cross-coupling reaction was also unsuccessful, although different conditions described in the literature were tried.[12]

As the above reactions were unsuccessful we used foreword the method proposed by Sneddon *et al.*, using decaborane, 2-ethynylpyridine and ionic liquid. [2]

It was previous showed by our group that **69** react with $[AuCl(PPh_3)]$ to give $[Au\{1\text{-}(2'\text{-}NC_5H_4)\text{-}1,2\text{-}closo\text{-}C_2B_{10}H_{10}\}(PPh_3)]$,[13] in which a C_C-Au bond is formed, so metalation of the unsubstituted carbon atom form the carborane cage is possible. Once synthesized the carboranylpyridine, we tried the possibility to produce cyclometalated complexes. First, we tried the reaction of lithiated carboranylpyridine, Li[**69**], with $[PdCl_2(PPh_3)_2]$ (Scheme 4.4.) and the cyclometalated derivative was successful

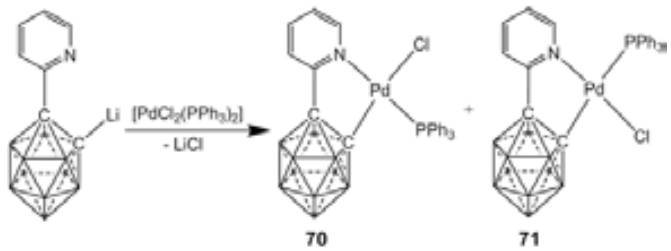

Scheme 4.4. Synthesis of Pd-cyclometalated carboranyl-pyridine derivative.

obtained, as a mixture of two isomers, *cis* and *trans*, with respect to the pyridyl moiety, as indentified by two chemical shifts observed in $^{31}P\{^{1}H\}$-NMR spectrum (Figure 4.2). Although the CN-palladacycles showed interest in catalysis, especially, in Heck and Suzuki reactions,[14] we wanted to extend the application of carboranylpyridine metallacycles, especially in the field of organic-light emitting diodes (OLEDs). For that, we wanted to incorporate metals that are known to induce luminescence properties to N-systems, as are Ir (III), Rh (III), or Ru(II).[15] The desired cyclometallated compounds should contain three carboranylpyridine chelating ligands bonded to the metal centre in an octahedral environment.

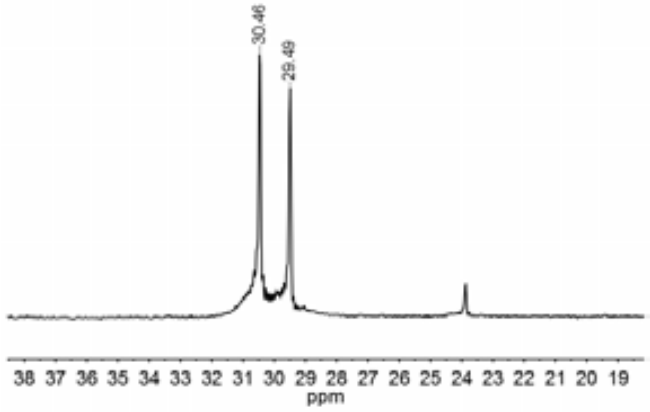

Figure 4.2. $^{31}P\{^{1}H\}$-NMR spectrum (in $CDCl_3$) for the two isomers obtained in the reaction of Li[**1**] with $[PdCl_2(PPh_3)_2]$.

The reactivity of the higher oxidation states metals is generally lower and energetic conditions have to be used, together with protic solvents. The main drawback on using protic solvents and carboranes is the deboronation of the cluster from *closo* to *nido*. For that, first we tried several solvents in which the carborane is maintained in the *closo* form. First we did reactions with the C_C-lithiated carboranylpyridine, in tetrahydrofurane, toluene and diethyl-ether, using different iridium sources as: $IrCl_3$, $[Ir(acac)_3]$, $[IrCl_3(tht)_3]$, $[IrCl(ppy)_2]_2$ but the reactions were unsuccsesfull, at the end only unreacted **69** being recovered. As this results were unsuccessful, we did the reactions with the same iridium sources but in protic solvents as metoxyethanol, ethoxyethanol and glycerol at 130°C with K_2CO_3 as additive, in order to abstract the C_C-H proton, but the reactions were also unsuccessful, and, as expected, deboronated cluster, $[7\text{-}(2'\text{-}C_5H_4N)\text{-}7,8\text{-}nido\text{-}C_2B_9H_{10}]^-$, was obtained. As these reactions were unsuccessful, we changed the strategy looking for a solvent in which the reactants are soluble, that have a high boiling point and which is innocent towards carborane deboronation. The only solvent which fulfils all these criteria is decahydronaphthalene or decalin. The reaction was carried out with four times excess of Li[**69**] with respect to $[IrCl_3(tht)_3]$ at 170°C. After 48 h of reaction a brown solid was separated by filtration. In the organic phase carboranylpyridine was identified by ^{11}B-NMR. The brown solid was tried to be dissolved in different solvents (DMSO, DMF, THF, CH_2Cl_2, toluene, acetone, $CHCl_3$, MeOH, EtOH, CH_3CN, H_2O) but it was proved to be insoluble, so it was impossible to fully characterize it by NMR. The FTIR spectrum though showed no band that could be associated with the B-H stretching so the insoluble brown solid probably contains only inorganic derivatives of Ir and no carboraneylpyridine derivative.

Reaction of the Li[**69**] with $RhCl_3$, $[RhCl_3(tht)_3]$, $[Rh(acac)_3]$ and $RuCl_3$, $[Ru(acac)_3]$, $[RuCl_2(DMSO)_4]$ in THF, toluene and Et_2O were also done, but as for iridium, the reactions were unsuccessful.

The carboranylpyridine is a fragile ligand, due to the susceptibility of the carborane moiety to degradation in energetic conditions, fact which makes it difficult to coordinate to metals in higher oxidation sates.

4.2. Bidentate carboranylpyridine-phosphine hybrid ligands

Hybrid ligands that contain at least two different types of moieties capable of binding to metal centres are of special interest in coordination chemistry due to their potential hemilablity.[16] By combining hard and soft donors in the same molecule, these ligands can be tailored to stabilize metals ions in a variety of oxidation states and geometries, discovering thus a novel and unprecedented chemistry. One class of hemilabile ligands is that combining phosphorus and nitrogen atoms. Coordination compounds bearing P,N functional groups offer the advantage that the π-acceptor phosphorus can stabilize low oxidation state metals, whereas the σ-donor nitrogen stabilizes higher oxidation states and makes the metal more susceptible to oxidative-addition reactions. The chiral and achiral pyridyl phosphanes represent the most studied class among the P,N donor ligands,[17] presenting three different coordination mode to the metals: P-monodentate, P,N-bridge, and P,N-chelate.[18] They found applications in a variety of catalytic processes as: carbonylation of alkynes, oligomerization and polymerization of ethene, and in asymmetric hydrogen transfer.[19]

Just recently, the carboranes were proved versatile moieties for the tuning the properties of various ligand platforms.[20] Our group and others were interested in the exploration of the properties of organometallic complexes derivatives of *o*-carboranes and in this scope a plethora of organometallic compounds were synthesized having on the *o*-carborane platform different homo or hetero coordination centres as: PP;[21] PS;[22] PN;[23] PC;[24] SS;[25] SN;[26] SC;[27] and NC.[28]

As the cyclometallation reactions proved to be troublesome, we wanted to extend the study on this compound and to further found new derivatives. For that we started investigating the possibility to incorporate another type of coordination centre to the ready available carboranylpyridine platform, as is the phosphines moieties. The carboranylpyridine-phosphine hybrid ligands were synthesized from the C_C-lithiated salt of the carboranylpyridine with halophosphines in diethyl ether (Scheme 4.5.). The reaction goes smoothly at room temperature after 2 h, though just a moment after the addition of the $ClPR_2$ (R = Ph, ^{i}Pr, Cy), a white solid started to precipitate. After 2 h, the reaction was quenched with H_2O and extracted 3 times with Et_2O. Organic phase was collected, dried over $MgSO_4$ and evaporated to yield the corresponding carobranylpyridine-phosphines, 1-(2'-C_5H_4N)-2-PR_2-1,2-*closo*-$C_2B_{10}H_{10}$ (R = Ph, ^{i}Pr, Cy), as white solids. All the phosphines were fully characterized by multinuclear NMR (^{1}H, ^{11}B, and ^{31}P) and FTIR spectroscopies and for the ones with phenyl and *iso*-propyl moieties, the structure was determinate by X-ray crystallography.

Scheme 4.5. Synthesis of carboranylpyridine-phosphine hybrid ligands.

4.2.1. Structural aspects

X-ray analysis confirmed the substitution of the C_C carbon with a phosphorus moiety in both 1-(2'-C_5H_4N)-2-PPh_2-1,2-$C_2B_{10}H_{10}$, (**72**), and 1-(2'-C_5H_4N)-2-P^{i}Pr$_2$-1,2-$C_2B_{10}H_{10}$, (**73**). The two compounds though present structural differences. Compound **72** crystallises in P-1 space group, whereas **73** crystallizes in P21/n space group.

The X-ray crystal structure of **72** showed two crystallographic independent molecules in the asymmetric fraction of the unit cell (Figure 4.3.), as observed for the similar phosphine, 1-Ph-2-PPh_2-1,2-*closo*-$C_2B_{10}H_{10}$.[29] The structural parameters of the two monomer units present small differences (Table

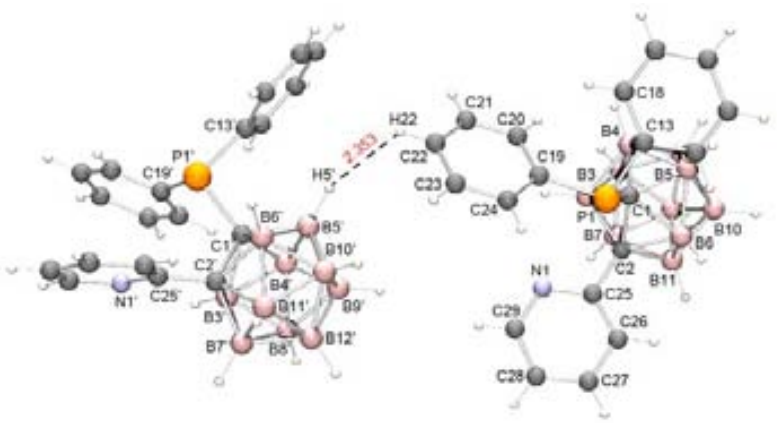

Figure 4.3. Molecular structure of **72**.

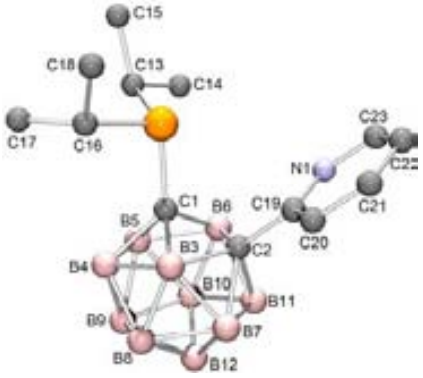

Figure 4.4. Molecular structure of **73** (The hydrogen atoms are omitted for clarity).

4.1.). The monomer units are held together by a intermolecular dihydrogen bond (B5'-H5'···H22-C22 = 2.353 Å) formed between a hydrogen atom from a BH vertex of carborane cage and a hydrogen atom from a phenyl ring of the other molecule. This interaction is so strong that is also observed in solution. The $^{1}H\{^{11}B\}$-NMR spectrum (Figure 4.5.a) shows a displacement of a BH signal from higher field zone of the others BH signals to lower fields. For **73** also can be observed intermolecular –B-H···H-C- contacts (Figure 4.6.), that are even shorter than for **72** (2.286 Å), formed between a H atom from a BH vertex and a H atom bonded to a C atom from the pyridine ring (the C atom orientated in *para* with respect to the N atom). These interactions are strong because, as shown in Figure 4.5., they remain in solution, as observed by the displacement of a BH signal from high field to low field (Figure 4.5b).

The crystal structure of **73** showed important differences respect to **72** (Figure 4.4.). First it showed that **72** in solid state is monomer, as observed for the similar phosphine, 1-Ph-2-P^{i}Pr$_2$-1,2-*closo*-$C_2B_{10}H_{10}$.[30] Other important difference is that the C1-C2 distances in **72** and **73** differ one from each other (Table 4.1.) with more than 0.040 Å. Difference between for the C1-C2 distances in **72** and **73** are expected since the P centres have different substituents, but not by such a large degree, since the C1-C2

72				**73**	
C1-C2	1.697	C1'-C2'	1.704	C1-C2	1.744
C1-P1	1.883	C1'-P1'	1.888	C1-P1	1.886
C2-C25	1.510	C2'-C25'	1.512	C2-C19	1.510
P1-C13	1.839	P1'-C13'	1.839	P1-C13	1.867
P1-C19	1.830	P1'-C19'	1.828	P1-C26	1.878
N1-C25	1.328	N1'-C25'	1.329	N1-C19	1.338
N1-C29	1.337	N1'-C29'	1.344	N1-C23	1.343
N1-P1	3.509	N1'-P1'	3.422	N1-P1	3.540
P1-C1-C2	115.3	P1'-C1'-C2'	114.58	P1-C1-C2	114.23
C25-C2-C1	118.81	C25'-C2'-C1'	118.90	C19-C2-C1	119.27
N1-C25-C2	115.98	N1'-C25'-C2'	116.13	N1-C19-C2	116.36
N1-C2-C1-P1	36.63	N1'-C2'-C1'-P1'	35.03	N1-C2-C1-P1	-32.17
C25-C2-C1-P1	6.02	C25'-C2'-C1'-P1'	7.07	C19-C2-C1-P1	-1.40
H22-H5'	2.353				

Table 4.1. Selected interatomic distances [Å], angles [°] and torsion angles [°] for **72** and **73**.

distances in the similar phosphines, 1-Ph-2-PPh_2-1,2-*closo*-$C_2B_{10}H_{10}$ and 1-Ph-2-P^{i}Pr$_2$-1,2-*closo*-$C_2B_{10}H_{10}$, differ only by 0.015 Å. The pyridine and phosphine substituents in both **72** and **73** are orientated in the planes roughly perpendicular to the C25-C2-C1-P1 plane, and C19-C2-C1-P1, respectively. The difference comes from the B vertex towards which the N atom is pointing. In **72** the N atom is pointing towards the B3, whereas in **73** towards B86. The P1-N1 distance is of 3.466 Å (mean distance) in **72** and 3.540 Å, in **73**, respectively, being higher of the sum of the van der Waals radi (3.35 Å). These geometrical parameters make the two moieties incompatible with any P-N interaction, as for example the pnicogen interaction, which was recently postulated in the literature,[31] and comparable with P-P interactions present in carboranyl-diphosphines.[32]

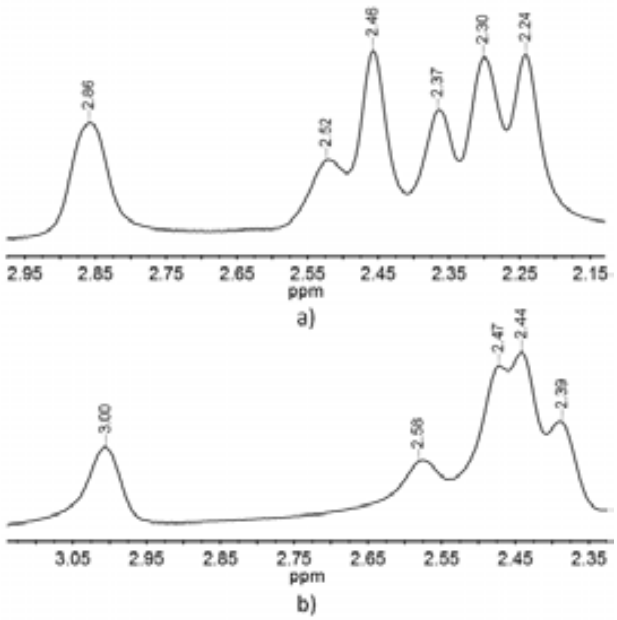

Figure 4.5. BH region in the $^1H\{^{11}B\}$-NMR spectra (in $CDCl_3$) of a) **72** and b) **73** .

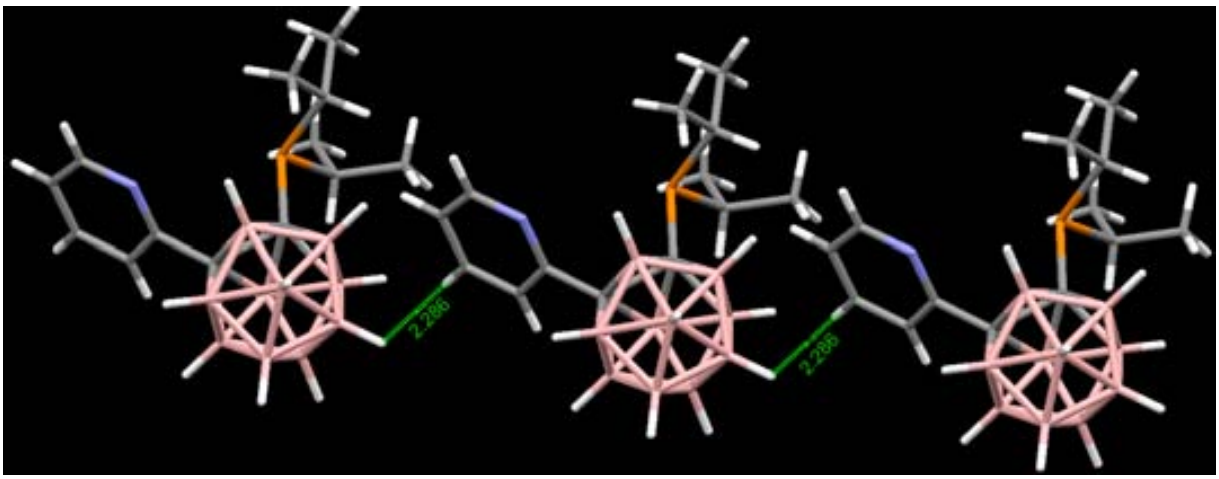

Figure 4.6. Molecular packing for **73** showing the strongest intermolecular interaction.

As some general trends affecting the length of the cluster, C_C-C_C distances have been observed, in Table 4.2. are presented the some carbon-carbon distances in comparison with other derivatives of carboranylpyridine and phenylcarborane-phosphines, 1-X-2-Y-1,2-*closo*-$C_2B_{10}H_{10}$. It was shown in the literature, that the *exo*-dative π-bonding effects, which arise from either electronic charge transfer from the π orbitals of aryl groups[33] or from π-electron back-donation from lone pairs of *exo*-cluster moieties[34] to the C_C-C_C antibonding orbitals, are responsible for the elongation of the C_C-C_C distances. The variation of the C_C-C_C bond length within the monosubstituted derivatives (Entries 1-6 in Table 4.2.) and disubstituted derivatives (Entries 7-8 in Table 4.2.) can be rationalized in the light of this hypothesis, the longer C_C-C_C bond distance among the presented compounds, being for 1-(2'-C_5H_4N)-2-SH-1,2-$C_2B_{10}H_{10}$ due to the higher π-electron back-donation from the sulphur lone pairs. The results are though

Entry	X	Y	*d*(C1-C2)
1	2'-Py	-H	1.632
2	-CH_2-2'-Py	-H	1.622
3	-2'-Py-4'-Br	-H	1.640
4	-3'-Py	-H	1.663
5	-S-2'-Py	-H	1.643
6	-Ph	-H	1.649
7	-Py	-Py	1.689
8	-Py	-SH	1.730
9	-PPh_2	-Py	1.697
10	-P^iPr_2	-Py	1.744
11	-PPh_2	-Ph	1.755
12	-P^iPr_2	-Ph	1.770

Table 4.2. C_C-C_C bond distances [Å] in some *o*-carborane derivatives 1-X-2-Y-$C_2B_{10}H_{10}$.

Compound	Lone pair	NBO antibond[a]	$\Delta E_{ij}^{(2)}$
72	P(1)	C1-B3-B4	6.78
	N(1)	C25-C26	10.33
	N(1)	C28-C29	8.63
73	P(1)	C2-B7-B11	4.2
	N(1)	C13-C14	10.31
	N(1)	C16-C17	8.7

[a] The atom numering is the same as for the crystal structures.

Table 4.3. Second-order delocalization energies [kcal·mol^{-1}] for the electron lone pairs and NBO antibonding interactions in **2** and **3**.

surprising for compounds **72** and **73** which present very different C_C-C_C bond distances when compared with each other (Entries 9 and 10 in Table 4.2.) and when compared with the resembling 1-Ph-2-PR_2-1,2-$C_2B_{10}H_{10}$ (R = Ph, ^{i}Pr) phosphines (Entries 11 and 12 in Table 4.2.).

In order to get further insights on electronic communication in these compounds, which may help us to understand the great difference between the C_C-C_C bonds in compound **72** and **73** we performed the NBO analysis. The stabilization energy for the lone pair → NBO antibonding orbitals interactions are presented in Table 4.3. As can be observed, the lone pair delocalization of the N atom is similar for **72** and **73**. The P lone pair interaction with the carborane cage is different though.

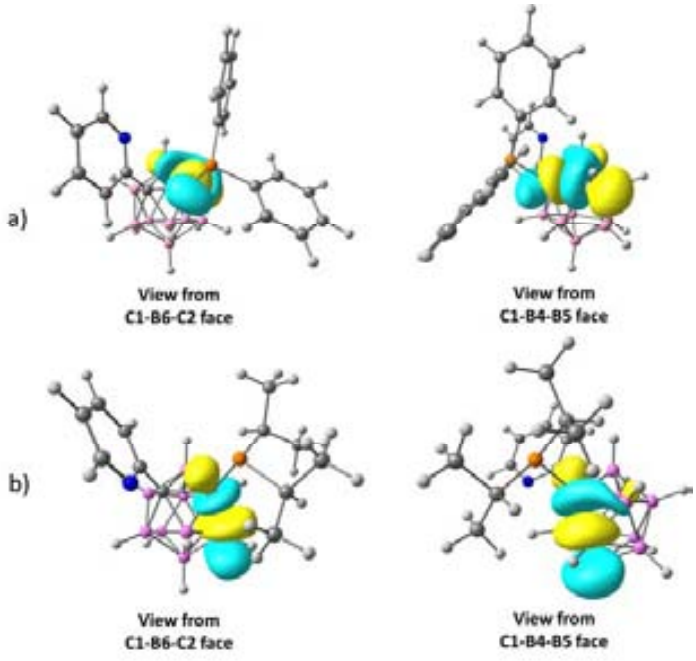

Figure 4.7. NBO antibonding orbitals: a) $\tau^*_{C1-B3-B4}$ for **72** and b) $\tau^*_{C1-B4-B5}$ for **73**. (blue - negative surface and yellow - positive surface).

The nature of the atoms from the cluster with which the lone pair is interacting plays an important role. Based only on structural parameters obtained from the X-ray diffraction, Teixidor and Welch made the hypothesis that in the phosophine 1-Ph-2-P^iPr_2-1,2-$C_2B_{10}H_{10}$[29] the P lone pair lies above the B6-C2 conectivity. The NBO analysis for compound **72** showed that the P lone pair is interacting with a NBO antibonding hybrid formed by the three centre bond C1-B3-B4 (Figure 4.7.a). In compound **73**, the P lone pair interacts also with a three centre hybrid but this is formed by C1-B4-B5 face of the cluster (Figure 4.7.b). The implication of these interactions on the C_C-C_C bond

elongation has to be corroborated with the charge distribution in the two compounds. The NBO charges arising from the NPA population are presented in Table 4.4. As expected, the boron atoms directly bonded to the carbon atoms have the most positive charges, whereas going away from the C atoms the B atoms become more negative. The difference in charges is even better observed when the Hirshfeld charges are taken into consideration. Even so, no matter the charge analysis method, the B3 and B6 vertices are most prone to withdraw electronic density from the C_C atoms then the B4, B5, B7 and B11. As in **72** the delocalization of P lone pair goes on C1-B3-B4, the charge flow is from B4 to C1 to B3 (Figure 4.8.a) and in this manner the gained electrons from B4 are spent by the C1 to B3. In **73**, on the other hand, the charge flow is from both B4 and B5 to C1 (Figure 4.8.b.), so the charge density is maintained by C1. Consequently, this directional charge flow in **73** makes the C_C-C_C to be longer than in **72**. It is interestingly to observe the difference of the charge on N atom in compounds **72** and **73**, with respect to **69**. Though, from the NPA charges the difference is not so great, the Hirshfeld charges, again, offers a better picture. The Hirsfheld charge of the N atom from **69** is more than 3 times greater than for **72** and more than 7 times greater than for **73**. This differences account for the different orientation of the pyridyl ring in these compounds, and is an image of the charge transfer from the pyridyl ring to the carborane cluster. In **69** the pyridyl ring is orientated coplanar on the C_{aryl}-C_C-C_C plane, whereas in **72** and **73** the pyridyl ring is oriented perpendicular on the C_{aryl}-C_C-C_C plane. As observed before,[33b] the orientation of the aromatic rings bonded to carborane cluster directly affect the charge transfer. So, in **69**, the pyridyl orientation does not facilitate the charge transfer, an consequently, the N charge is greater. In **72** and **73**, on the other hand, the orientation of the pyridyl ring totally facilitates the charge transfer and so, the charge on the N atom is smaller.

Atom	NPA charges			Hirshfeld charges		
	69	**72**	**73**	**69**	**72**	**73**
P1		0.945	0.942		0.206	0.203
N1	-0.478	-0.446	-0.443	-0.228	-0.070	-0.029
C1	-0.359	-0.640	-0.644	-0.001	0.030	0.027
C2	-0.500	-0.374	-0.378	-0.020	0.063	0.054
B3	0.180	0.182	0.158	0.085	0.068	0.070
B4	0.011	0.001	0.002	0.028	0.029	-0.011
B5	0.011	0.007	0.001	0.028	-0.024	-0.008
B6	0.180	0.170	0.175	0.085	0.015	0.072
B7	0.000	0.021	0.016	0.062	0.037	0.002
B8	-0.164	-0.168	-0.170	-0.006	-0.017	-0.005
B9	-0.146	-0.138	-0.139	0.001	0.003	-0.011
B10	-0.164	-0.173	-0.168	-0.006	-0.016	-0.005
B11	0.000	0.013	0.025	0.062	-0.022	-0.086
B12	-0.136	-0.135	-0.135	-0.011	0.003	0.004
CTC	-1.087	-1.234	-1.257	0.307	0.169	0.103

Table 4.4. Computed charges for compounds **72** and **73**.

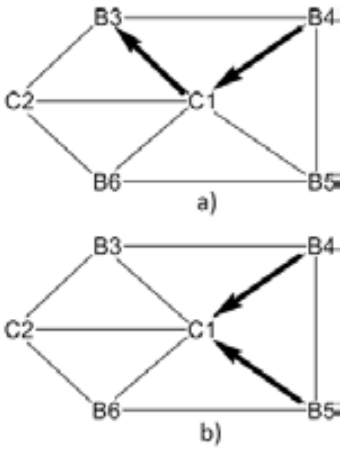

Figure 4.8. Schematics of the electronic density flow in: a) **72** and b) **73**.

4.2.2. Experimental and theoretical spectroscopic and electrochemical studies

Another surprisingly fact about compounds **72** and **73** lies in their properties as material. Whereas the crystal of **72** show no special property, the **73** is fluorescent, when irradiated with UV light of 365 nm, emits orange light (Figure 4.9.). Surprisingly, the fluorescence is given only in crystalline state and not in solution. The UV spectra in solution of acetonitrile of the two compounds (Figure 4.10.) show a wide peak between 262-264 nm, though, for the same concentration, the intensity of the absorbance for compound **72** is higher than for **73**. The spectrum of **72** shows an additional peak at 213 nm, which was discarded as effect of the solvent since for the compound **73** is not present. The spectra of the two compounds is different from the starting carboranylpyridine (Figure 4.10.), although the same peak at 213 nm is observed for both **69** and **72**.

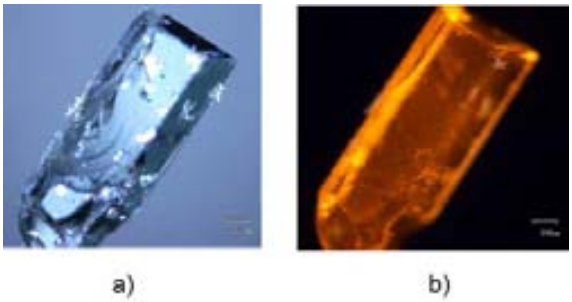

Figure 4.9. Image of crystal of **73**: a) under visible light; b) under UV light.

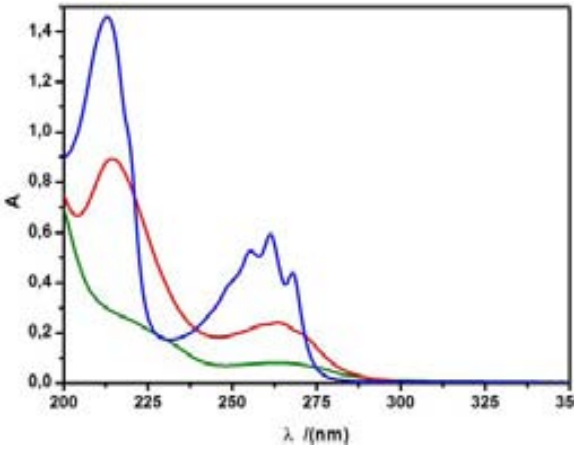

Figure 4.10. Experimental UV spectra in acetonitrile for a concentration of 10^{-5} M for compounds **69** (blue), **72** (red) and **73** (green).

In order to get further insights on the origin of this spectroscopic behaviour we performed a computational study. The computed UV spectra for the two compounds at the TD-DFT/B3LYP/6-31G(d,p) level of theory, including the acetonitrile as solvent, revealed a major peak at around 263 nm for **72** and two peaks at 260 nm and 291 nm, for **73**, respectively (Figure 4.11.). The molecular orbital analysis for **72** showed that the origin of the UV absorption at 263 nm is due to a HOMO→LUMO+1 interaction in proportion of 86%, with minor contribution from HOMO-4→LUMO+1 and HOMO→LUMO+2. In **73** the molecular orbital analysis showed that the absorption at 260 nm is also due to a HOMO→LUMO+1 interaction, in the same proportion of 86%, with minor contributions from HOMO-2→LUMO and HOMO-2→LUMO+1 and the absorption at 291 nm is only due to a LUMO→HOMO interaction. In Figure 4.12. are presented the orbitals involved in interactions in the compound **72** and **73**.

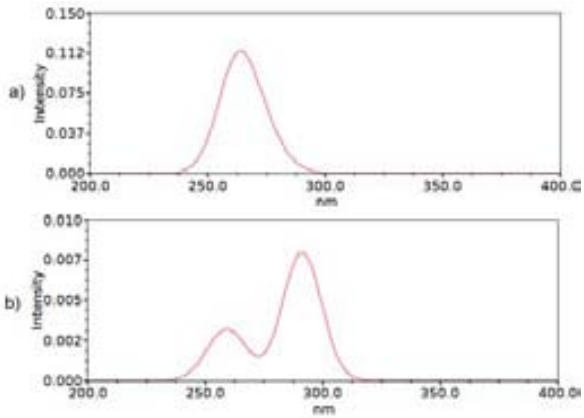

Figure 4.11. Calculated UV spectra in acetonitrile for: a) **72** and b) **73**.

Though the compounds do not present fluorescence in solution, the electrochemical in solution is different. Whereas **72,** as well as the parent compound **69**, show no electrochemical reversibility in the cyclic voltametry measurements, **73** shows a perfect reversible, one electron redox process (Figure 4.13.).

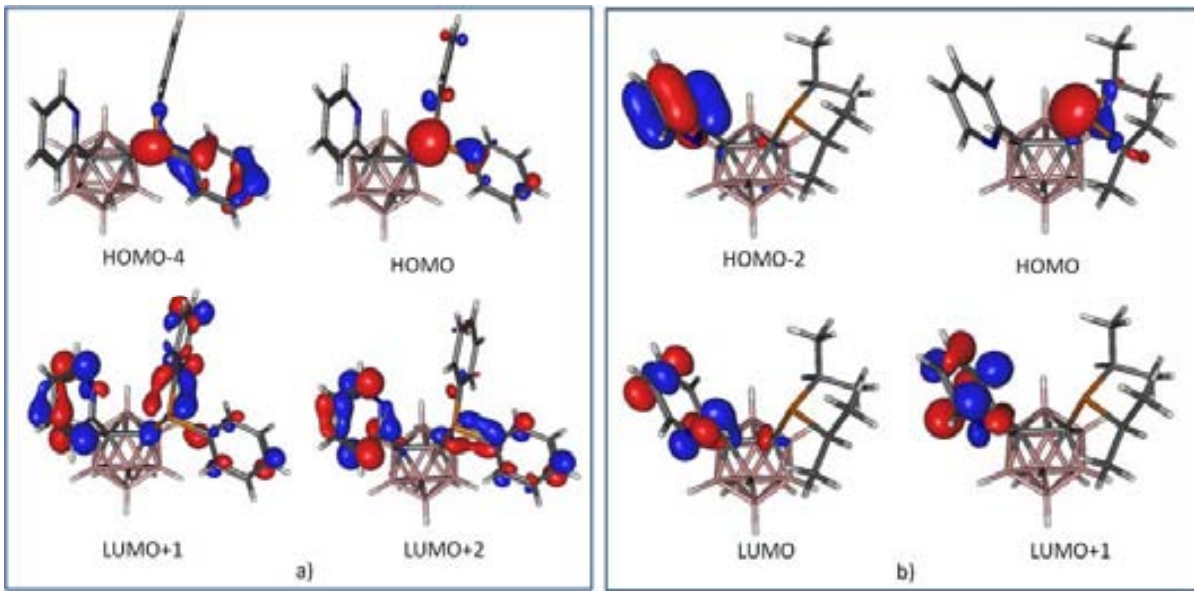

Figure 4.12. Orbitals involved in the interactions that give place to the absorption bands in the computed UV spectra for: a) **72** and b) **73**.

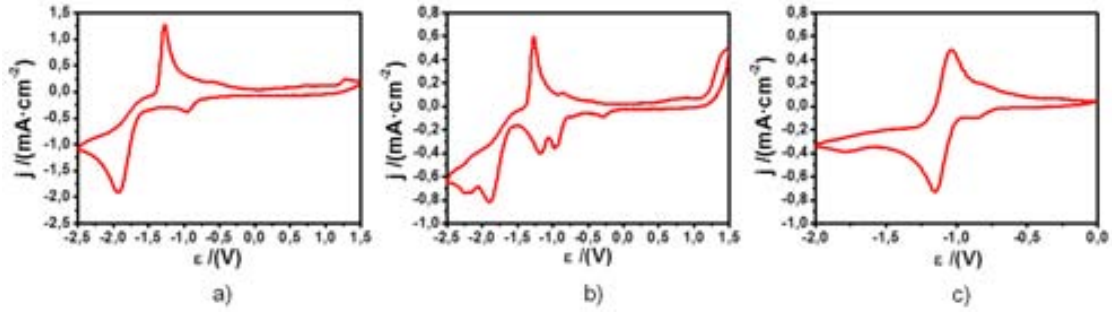

Figure 4.13. Cyclic Voltammograms in acetonitrile for: a) **69**, b) **72** and c) **73**. (solution concentration = 10^{-3} M/[TBA][PF_6] 0.1 M; working electrode = glassy carbon; reference electrode = Ag wire; co-electrode = Pt wire; r_{scan} = 100 mV·s^{-1}).

As the compound **73** do not present fluorescence in solution, but only in the crystalline state, the origin of fluorescence must be searched in the supramolecular assembly in the crystal structure. In **72** the phenyl rings of the diphenylphosphine moiety are the main actor, establishing intermolecular hydrogen bonds with other H atoms from the neighbouring molecules or with the P or N neighbouring centres, in such a manner that the pyridine rings do not play any special role. Except of the strongest contacts presented above, **73** presents other intermolecular interactions, that

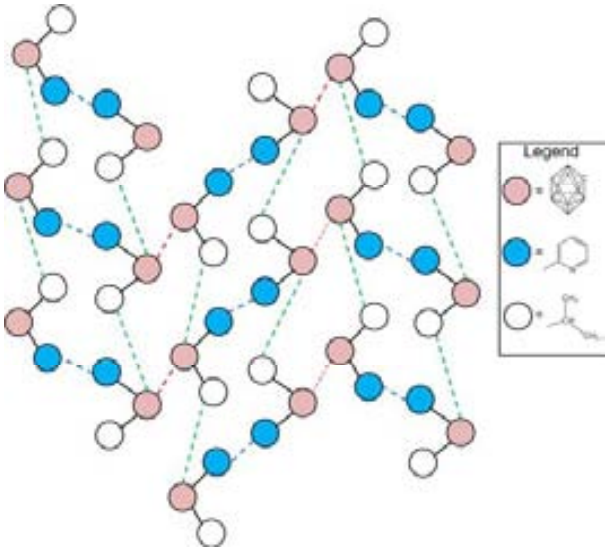

Figure 4.14. Schematics of the crystal packing for **73** and the main intermolecular interactions.

contribute to the building of the supramolecular architecture like a spider web (Figure 4.14). Although compound **73** crystallizes in P21/n space group, the observed optical properties of the crystal and the supramolecular architecture presented above make of compound **73** a candidate for non-linear optical (NLO) properties, which will be studied in the future.

4.2.3. First studies on complexation of carboranylpyridine-phosphines

In order to test the properties of carboranylpyridine-phosphines as ligands we first tried the reaction of **72** with a classical Rh(I) complex, namely $[RhCl(cod)]_2$, in 1:1 ratio. The reaction was monitored by $^{31}P\{^1H\}$-NMR and $^{11}B\{^1H\}$-NMR. The reaction was complete after 1.5 h at reflux in $CHCl_3$, as observed by the disappearance of the signal for compound **72** at 14.98 ppm in the $^{31}P\{^1H\}$-NMR spectrum and appearance of a doublet at 1.23 ppm, characteristic of a Rh-P bond, with the coupling constant, $^1J(P,Rh)$ = 129 Hz (Figure 4.15.). The displacement of the olefinic ligand from the starting Rh(I) complex and the complexation with the N atom of the pyridyl moiety was confirmed by ^1H-NMR spectroscopy, where no signals characteristic of 1,5-cyclooctadiene were observed. Also, the aromatic region in the ^1H-NMR spectrum is different from the starting compound **72**, which indicates that the pyridyl moiety is also involved in the complexation. Although further characterization has to be done for this compound in order to exactly establish its structure, we proposed the reaction scheme presented in Scheme 4.6.

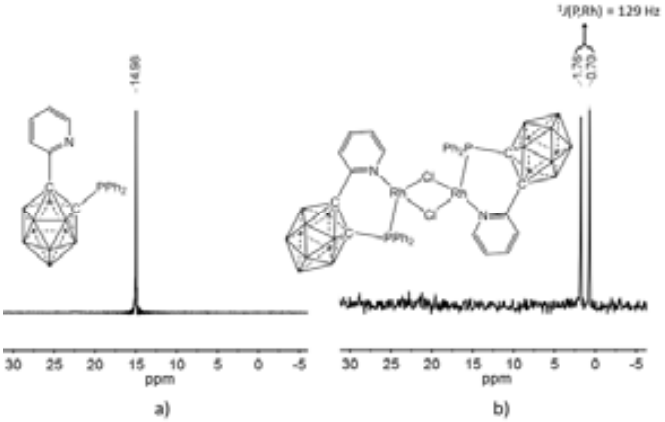

Figure 4.15. $^{31}P\{^1H\}$-NMR spectra (in $CDCl_3$) for: a) **72** and b) $[Rh(\mu\text{-}Cl)(\mathbf{72})]_2$

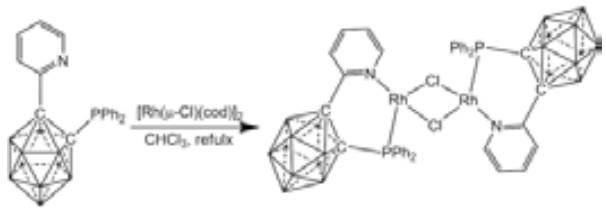

Scheme 4.6. Synthesis of Rh(I) complex of **72**.

The reaction of **72** with $[PdCl_2(cod)]$ in 1:1 ratio in THF at reflux gave, surprisingly, a *nido* derivative (Scheme 4.7.). As in previous case, compound **72** acts as a chelating ligand. The deboronation of the cluster was first observed by $^{11}B\{^1H\}$-NMR from the crude of the reaction, where the typical signal for B1 is observed at high field, around δ = -31 ppm, together with the signal characteristic of the boronic ester formed by the removed B^+ vertex, observed in $^{11}B\{^1H\}$-NMR spectrum around δ = 20 ppm (Figure 4.16.). After extraction with CH_2Cl_2, the $^1H\{^{11}B\}$-NMR spectrum confirmed the *nido* nature of the carborane cage by the presence of the apical H atom at δ = -2.03 ppm (Figure 4.17.).

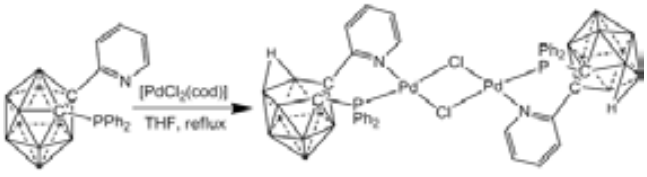

Scheme 4.7. Reaction of **72** with $[PdCl_2(cod)]$ in THF.

The reactions presented above are just the first studies on the coordination ability of compound **72**, but further research has to be done though to better understand the coordination ability of these type of ligands.

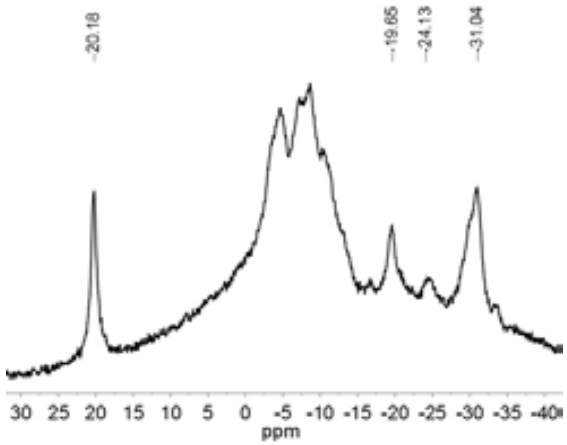

Figure 4.16. $^{11}B\{^{1}H\}$-NMR spectrum for the crude of reaction of **72** with $[PdCl_2(cod)]$ in THF.

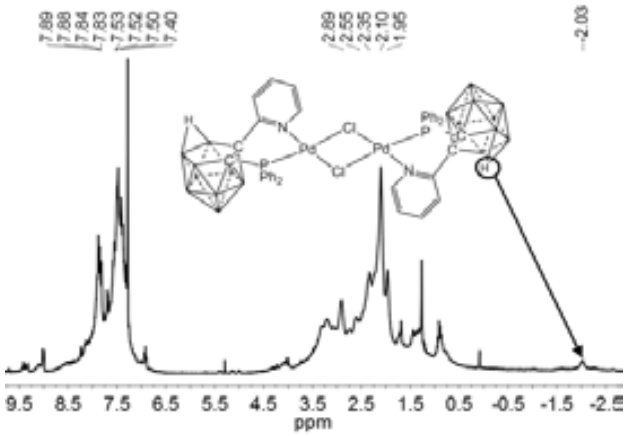

Figure 4.17. $^{1}H\{^{11}B\}$-NMR spectrum for the reaction of **72** with $[PdCl_2(cod)]$ in THF.

4.2.4. First studies on the chalcogen oxidation of carboranylpyridine-phosphines

In Section2 of the Results and Discussion part we presented studies on the oxidation of carboranylmono- and carboranyldiphosphines, where the oxidation process was discussed in detail and interesting results as the dechalcogenation upon complexation were observed. For that, we initiated the first studies on the chalcogen oxidation of compound **72** in order to observe if the pyridine ring plays any role compared with the phenyl ring in 1-PPh_2-2-R-1,2-$C_2B_{10}H_{10}$ (R = Ph, Me).

The oxidation with an excess of S (2 eq.) of compound **72**, in acetone at reflux, was monitored by $^{31}P\{^{1}H\}$-NMR (Figure 4.18.). As can be observed the reaction is slow, after 6 days at reflux only 50% of **72**

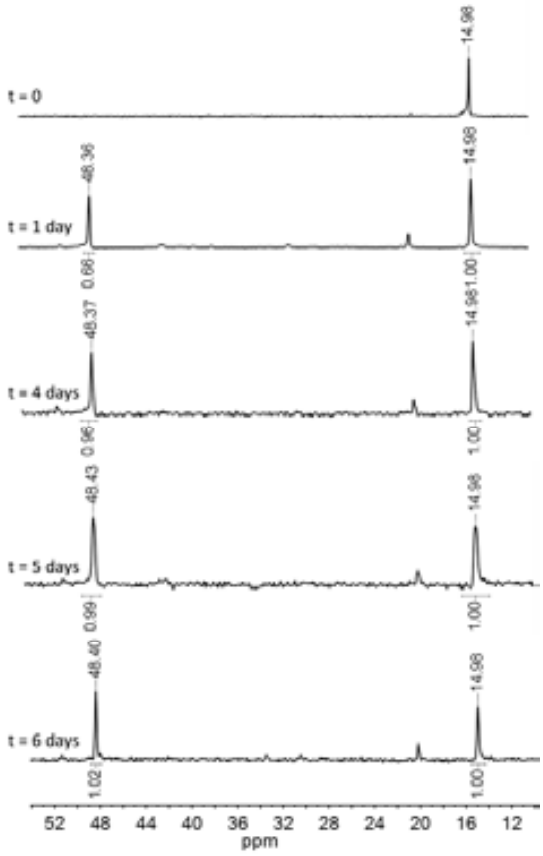

Figure 4.18. Reaction progression measured by $^{31}P\{^{1}H\}$-NMR spectra for the reaction of **72** with S_8 in acetone.

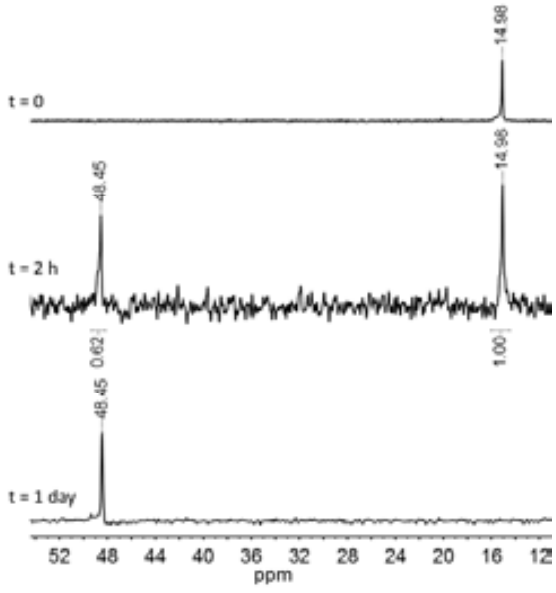

Figure 4.19. Reaction progression measured by $^{31}P\{^{1}H\}$-NMR spectra for the reaction of **72** with S_8 in acetone, using LiCl as additive.

being oxidized. This behaviour is consistent with the behaviour of the analogous carboranylmonophosphines towards oxidation with sulfur. The reaction rate can be enhanced though if LiCl is used as additive, as in the case of carboranylmonophospines. As can be observed from Figure 4.19., the reaction rate grows exponentially, in 2 h at reflux in acetone in the presence of an excess of 10 eq. of LiCl, **72** is oxidized in proportion of 38%; whereas without LiCl it takes about one day to achieve the same grade of conversion. The oxidation with sulphur in presence of LiCl is completed after 1 day at reflux in acetone (Figure 4.19.).

The oxidation for compound **72** with Se follows the same rate of reaction as for carboranylphosphines, the full conversion being achieved after 18 h at reflux in toluene. The Se oxidized carboranylpyridine-diphenylphosphine, 1-$SePPh_2$-2-Py-$C_2B_{10}H_{10}$, **76** was characterized by NMR and X-Ray spectroscopy. It is worth mentioning that the $^{31}P\{^1H\}$-NMR spectrum revealed, beside the signal characteristic of a Se oxidised carborabylphosphine at 46.54 ppm, two satellite lines at 49.90 ppm and 43.19 ppm, characteristic of the coupling between the P and Se (Figure 4.20.). The coupling constant, $^1J(P,Se)$, of 815 Hz, is slightly greater than for other carboranylphosphines as: 1-$SePPh_2$-2-PPh_2-1,2-$C_2B_{10}H_{10}$ ($^1J(P,Se)$=807 Hz), 1-$SePPh_2$-2-Me-1,2-$C_2B_{10}H_{10}$ ($^1J(P,Se)$=804 Hz), and 1-$SePPh_2$-2-Ph-1,2-$C_2B_{10}H_{10}$ ($^1J(P,Se)$=812 Hz).

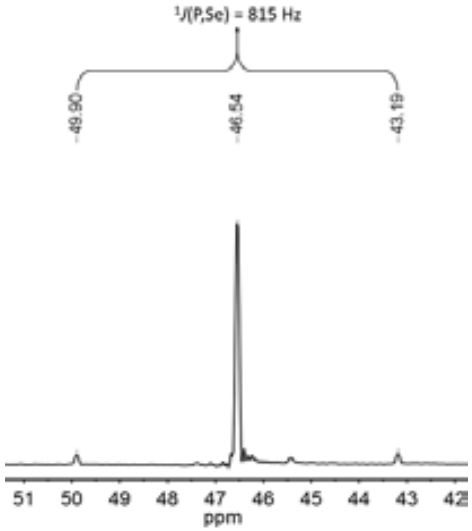

Figure 4.20. $^{31}P\{^1H\}$-NMR spectrum for compound **76**.

The crystal structure of **76** (Figure 4.21.) revealed the Se oxidized P atom in a tetrahedral environment. The P1-Se distance of 2.098 Å is the same as for 1-$SePPh_2$-2-PPh_2-1,2-$C_2B_{10}H_{10}$. The C1-C2 bond of 1.687 Å is smaller than the one in the compound **72** (1.704 Å) and much more smaller than in 1-$SePPh_2$-2-PPh_2-1,2-$C_2B_{10}H_{10}$ (1.733 Å). The

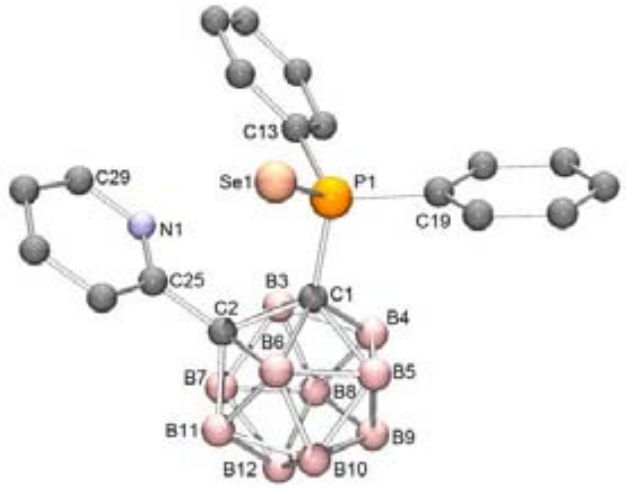

Figure 4.21. Molecular structure of **76** (The hydrogen atoms are omitted for clarity).

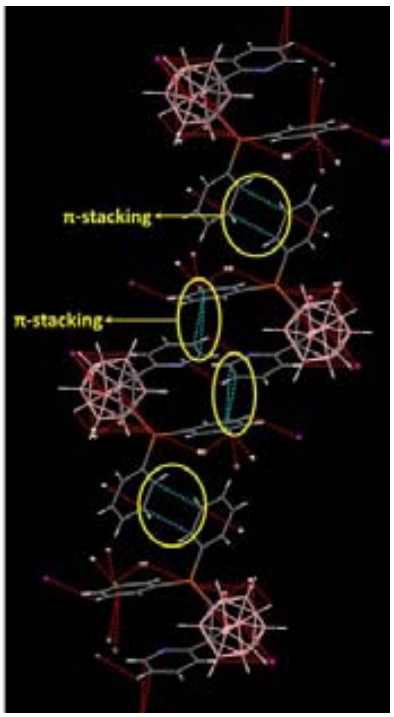

Figure 4.22. Crystal packing for **76**.

N atom is orientated towards B3, whereas the Se atom is orientated towards B6, with the Se-P1-C25-N1 dihedral angle of 115.2(3)°. The pyridyl moiety has the similar geometry as in **72**. The crystal packing of **76** reveals that the pyridine ring of one molecule partially overlaps a phenyl ring of the other molecule, with a distances of 3.274 Å and 3.350 Å, which is consistent with π-stacking interactions (Figure 4.22). Another π-stacking interaction is established between two perfectly overlapped phenyl rings of two neighbouring molecules, with a distance of 3.371 Å (Figure 4.22.).

The reaction of **76** with $[PdCl_2(PPh_3)_2]$ was done and it was observed that it behaves similar with carboranyphosphines towards complexation, giving dechalcogenation.

4.3. First studies on carboranylpyridine-borane Lewis pairs

Aimed by the previous results where unique carboranylpyridine-phosphines were synthesized we went further with the synthesis of new derivatives of carboranylpyrydine, looking now at other type of moieties, as are the so called "electron deficient" borane moieties.

As in previous case, we started from the lithiated derivative of carboranylpyridine, Li[**69**], which was reacted with chloro(dicyclohexyl)borane, $ClBCy_2$. Like the reaction with chlorophosphines, the reaction went smoothly at room temperature in diethyl ether, yielding quantitatively the carboranylpyridine-borane compound, 1-BCy_2-2-(*ortho*-C_6H_4N)-1,2-*closo*-$C_2B_{10}H_{10}$, **77** (Scheme 4.8.). Compound **77** was fully characterized by NMR spectroscopy and X-ray diffraction. The ^{11}B-NMR and $^{11}B\{^1H\}$-NMR revealed a singlet at lower field than the boron atoms from the cluster, characteristic of BR_3 that is bonded *exo*-cluster to C_C atom (Figure 4.23). The X-ray analysis though offered useful information on the structure of compound **77** (Figure 4.24.).

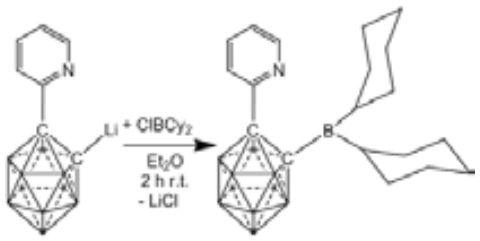

Scheme 4.8. Synthesis of carboranylpyridine-borane compound.

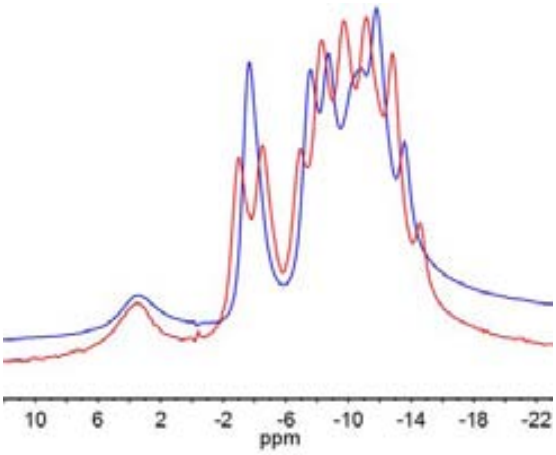

Figure 4.23. $^{11}B\{^1H\}$-NMR (blue) and ^{11}B-NMR (red) spectra for compound **77**.

The structural analysis of **77** confirmed the substitution of the other C_C atom from the carboranylpyrindine with a dicyclohexylborane moiety. Due to the high difference in the Lewis character of the N and B centres, the two centres are in close contact forming a bond of 1.657 Å. The N-B bond distance is characteristic of single N-B bond and is the same as the one found in the pentaphenylborole-lutidine adduct,[35] being though longer than other N-B bond distances found in other B-N adducts.[36] The *exo*-cluster B centre is far from a perfect tetrahedral coordination especially due to the closed N1-B18-C1 angle of 96.4(1)°. Also, the C2-C13 distance of 1.485 Å is smaller than those found for other C_C-disubstituted carborane derivative that have the pyridiyl moiety, as for example compounds **72** and **73**. In Table 4.5. are presented some structural parameters for compound **77**.

C1-C2	1.643
C1-B18	1.693
C1-C13	1.353
N1-C13	1.353
N1-C17	1.349
B18-C19	1.644
B18-C25	1.657
N1-B18	1.657
B18-C1-C2	106.72
C13-C2-C1	107.17

Table 4.5. Selected interatomic distances [Å] and angles [°] for **77**.

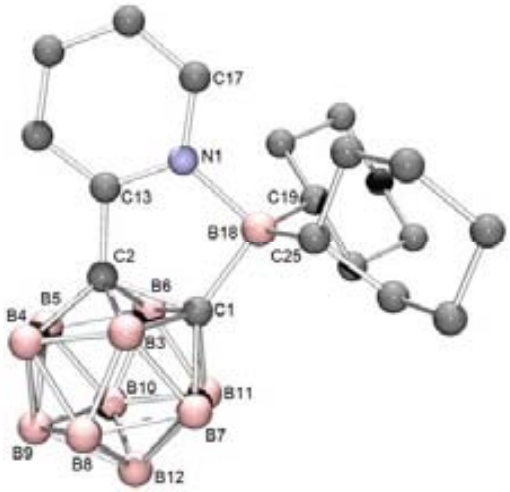

Figure 4.24. Molecular structure of **77** (The hydrogen atoms are omitted for clarity).

The organoboranes cover a wide range of compounds with interesting and unique properties, founding applications in optoelectronics and colorimetric chemosensors.[37] Recently, organoboranes adducts with Lewis bases were investigatited for their properties as frustrated Lewis pairs (FLP).[38] The lower limit for the B-N distance at which an equilibrium between the classical Lewis adducts and the FLP was set to 1.650 Å[39]. For compound **77** the N-B bond distance slightly higher than 1.650 Å, which classify the compound **77** as a candidate to look for its Lewis adduct-FLP equilibrium (Scheme 4.9.). It was observed that though the N-B bond distance may favour the FLP formation for compound **77**, the energy range that allow the equilibrium formation do not enters in the typical range for the FLP formation. The first calculation at the HF level of theory show that the equilibrium energy for B-N bond is of 256 kJ·mol^{-1}, so is very big compared with the range of 60-100 kJ·mol^{-1} established for the formation of FLP.[39] Also, the first calculation at the HF level of theory shows that the sequestration of hydrogen by compound **77** is enthalpycally unfavoured by 35.84 kcal·mol^{-1} (150 kJ·mol^{-1}).

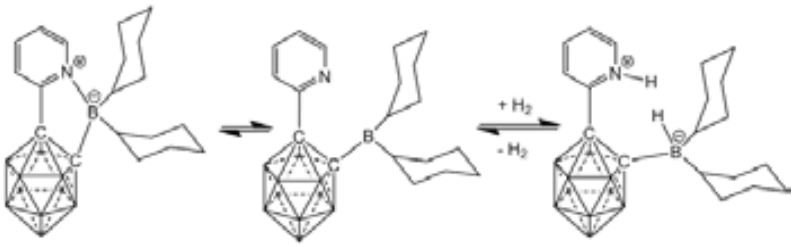

Scheme 4.9. Proposed equilibrium between the classical Lewis addict and FLP, for the sequestration of hydrogen.

With the synthesis of compound **77** we opened the way to a new class of compounds, so the study of carboranylpyridine-borane derivatives is only at its beginnings. Further research has to be done where the substituent of the borane moiety may be tuned to synthesized compounds with target properties. Also, further investigation are being done in the group of on compound **77** both experimentally and computationally to better understand how the structural features may influence in its properties as material and to search for future applications.

4.4. First studies on the synthesis and properties of cobaltocene based on carboranylpyridine platform

In previous sections we explored the possibility of synthesizing new derivatives of carboranylpyridine appealing at the lithiated derivative of this compound, in reactions with electrophiles. In order to extend the study and to explore new compounds we also tried a different approach.

The metalocenes derived from carboranes are obtained from the *nido*-dicarbollide anion and metal salts.[40] The synthesis of such metallocene from the carboranylpyridine (Scheme 4.10.) is done in several steps. First, the *nido*-carboranylpyridine derivative is obtained by the reaction with KOH in EtOH. The *nido*-derivative is obtained as K^+ salt, which is treated to obtain the $HNMe_3^+$ salt that showed to be a better candidate for the complexation reaction. The *nido* derivative is then treated with at least 2 equivalents of another base (*n*-BuLi or *t*-BuOK) in order to obtain the dicarbollide dianion. Then, this is treated with a metal salt (in our case $CoCl_2$) and after 3 days at reflux the corresponding metalocene is obtained. It was surprisingly to find that the $CoCl_2$ is complexed by the dicarbollide anion thorugh the

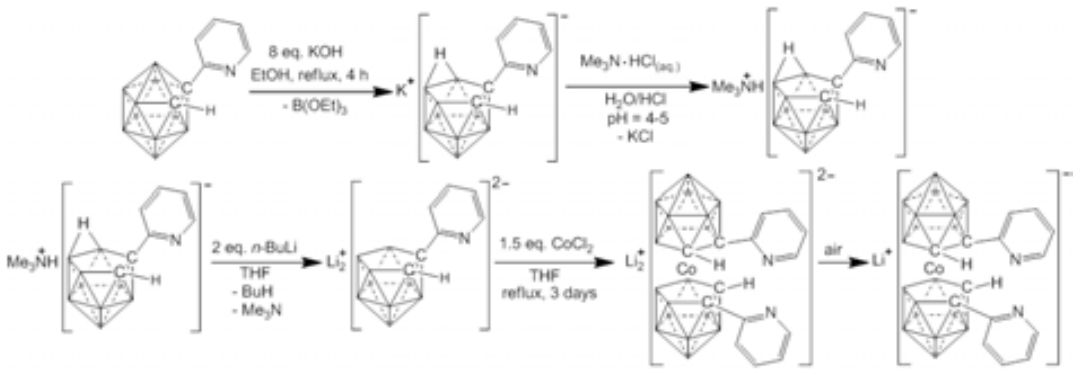

Scheme 4.10. Synthesis of carboranylpyridine based cobaltocene.

open B3C2 face and not through the N atoms of the pyridine. The pyridine-cobaltocene derivative [3,3'-Co(1-(2'-C_5H_4N)-1,2-$C_2B_9H_{10}$)$_2$]$^-$, [**78**]$^-$, was obtained quantitatively.

The $^{11}B\{^1H\}$-NMR spectrum show the typical distribution for a cobaltabisdicarbollide derivative, ranging from δ = +8.67 ppm to -16.54 ppm, which is different from the starting *nido*-carboranylpyridine (Figure 4.25.). The asymmetry of $^{11}B\{^1H\}$-NMR spectrum is consistent with the ^1H-NMR spectrum (Figure 4.26.) where two different chemical shifts are observed for C_C-H and for the H bonded in the pyridine region. This asymmetry of the spectra comes from the presence of various rotational isomers which [**78**]$^-$

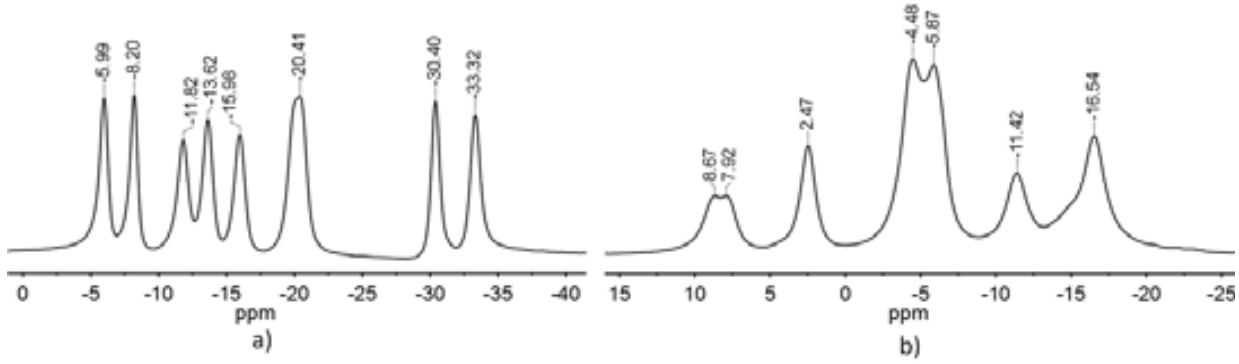

Figure 4.25. $^{11}B\{^1H\}$-NMR spectra (in CD_3COCD_3) for: a) *nido*-carboranylpyridine and b) [Me_4N][**78**]

can adopt (Figure 4.27.). Further studies have to be done though to establish which isomers are obtained.

Cobaltabisdicarbollide are usually stable in highly acidic or basic medium as well as at high temperatures.[41] This made them suitable backbones for different derivatives.[42] The phosphine derivatives of this compound were proved to be good coordinating ligands towards Group 11 elements as Ag(I) and Au(I) or towards catalytically important metals as are Rh(I) and Pd(II), showing a geometrically analogy with the BINAP ligand. The complexation reaction of $[1,1'\text{-}(PPh_2)_2\text{-}3,3'\text{-}(1,2\text{-}C_2B_{10}H_{10})_2]^-$ are usually done in EtOH starting form a metal salt (e.g. $AgClO_4$) or from a metal complex.[43] The reaction goes smoothly either for a short period of time (typically 30 min) at reflux or overnight at room temperature. Based on this previous knowledge developed in our group we tried the same condition for compound [**78**]$^-$ with different metals. The first reaction was carried out starting from $[PdCl_2(cod)]$ as metal source, for half of hour in EtOH. To our surprise, the complexation reaction did not take place, the integrity of the cobaltocene being affected. The $^{11}B\{^1H\}$-NMR spectrum from the crude of the reaction

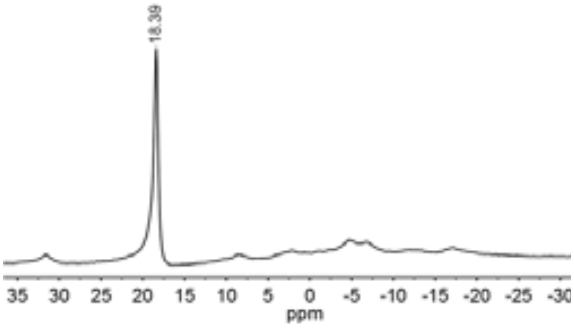

Figure 4.28. $^{11}B\{^1H\}$-NMR spectrum (in EtOH) for the crude of the reaction of Cs[**78**] with $[PdCl_2(cod)]$ in EtOH at reflux.

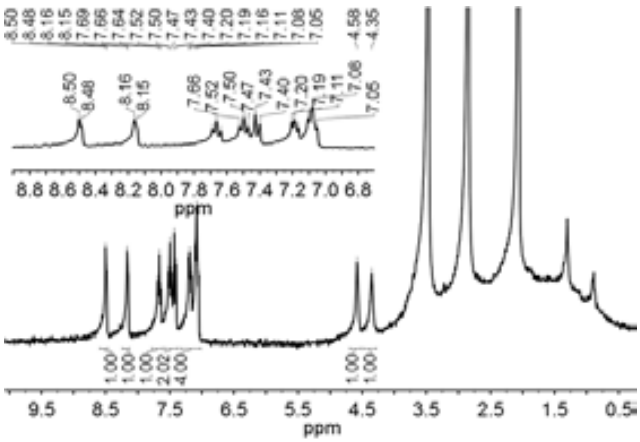

Figure 4.26. ^1H-NMR spectrum (in CD_3COCD_3) for $[Me_4N]$[**78**].

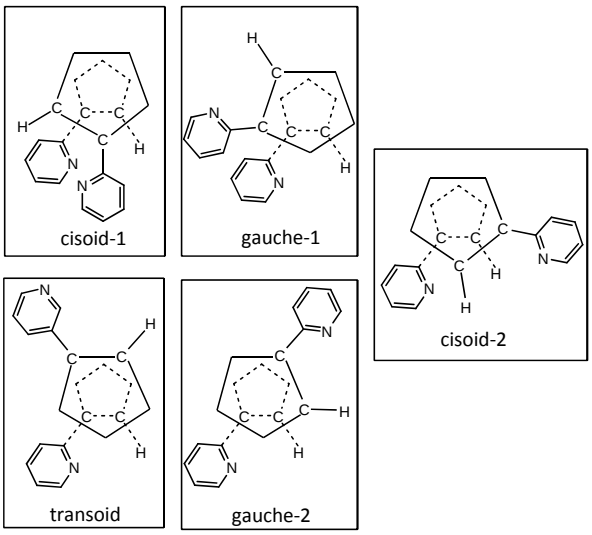

Figure 4.27. Representation of different conformers (rotational isomers) for [**78**]$^-$

revealing a high intensity peak at 18.39 ppm, characteristic of boronic esters (Figure 4.28.). If the reaction is carried out at room temperature, after various days, the cobaltocene is maintained but no complexation occurs. Different reactions were tied at room temperature or reflux in other solvents as MeCN, THF or DME, DMF with different metal sources as $[PdCl_2(cod)]$, $[Ru(acac)_3]$, $RuCl_3$, $NiCl_2$, $[RuCl_3(tht)_3]$ but all were unsuccessful. Further studies have to be done though to better understand the reactivity of this compound.

[1] a) Heying, T. L.; Ager, J. W.; Clark, S. L.; Mangold, D. J.; Goldstein, H. L.; Hillman, M.; Polak, R. J.; Szymanski, J. W. *Inorg. Chem* **1963**,*2*, 1089. b) Fein, M. M.; Bobinski, J.; Mayers, N.; Schwartz, N. N.; Cohen, M. S. *Inorg. Chem.* **1963**, *2*, 1111. c) Potenza, J. A.; Lipscomb, W. N. *Inorg. Chem.* **1966**, *5*, 1471. d) Ott, J. J.; Gimarc, B. M. *J. Am. Chem. Soc.* **1986**, *108*, 4303. e) Vondrak, T.; Plesek, J.; Hermanek, S.; Stibr, B. *Polyhedron* **1989**, *8*, 805. f) Petrov, E. S.; Yakovleva, E. A.; Isaeva, G. G.; Kalinin, V. N.; Zakharkin, L. I.; Shatenshtein, A. I. *Dokl. Akad. Nauk SSSR*, **1970**, *191*, 617. g) Bregadze, V. I. *Chem. Re*v. **1992**, *92*, 209.

[2] Yuqi, L.; Patrick, J. C.; Sneddon, L. G. *Inorg. Chem.*, **2008**, *47*, 9193.

[3] a) Coult, R.; Fox, M. A.; Gill, W. R.; Herbertson, P. L.; MacBride, J. A. H.; Wade, K. *J. Organomet. Chem.*, **1993**, *462*, 19. b) Gill, W. R.; Herbertson, P. L.; MacBride, J. A. H.; Wade, K. *J. Organomet. Chem.*, **1996**, *507*, 249. c) Alekseyeva, E. S.; Batsanov, A. S.; Boyd, L. A.; Fox, M. A.; Hibbert, T. G.; Howard, J. A. K.; MacBride, J. A. H.; Mackinnon, A.; Wade, K. *Dalton Trans.*, **2003**, 475.

[4] Bould, J.; Laromaine, A.; Bullen, N. J.; Viñas, C.; Thornton-Pett, M.; Sillanpää, R.; Kivekäs, R.; Kennedy, J. D.; Teixidor, F. *Dalton Trans.*, **2008**, 1552.

[5] a) Slagt, V. F., de Vries, A. H. M.; de Vries, J. G.; Kellogg, R. M. *Org. Process Res. Dev.*, **2010**, *14*, 30. b) Xue, L; Lin, Z. *Chem. Soc. Rev.*, **2010**, *39*, 1692.

[6] a) King, A. O.; Okukado, N.; Negishi, E. *J. Chem. Soc., Chem. Commun.*, **1977**, 683. b) Negishi, E.; Anastasia, L. *Chem. Rev.*, **2003**, *103*, 1979.

[7] a) Kosugi, M.; Sasazawa, K.; Shimizu, Y.; Migita, T. *Chem.Lett.*, **1977**, 301. b) Milstein, D.; Stille, J. K. *J. Am. Chem. Soc.*, **1978**, *100*, 3636.

[8] Li, J.-H.; Liang, Y.; Wang, D.-P.; Liu, W.-J.; Xie, Y.-X.; Yin, D.-L.; *J. Org. Chem.*, **2005**, *70*, 2832.

[9] Huang, H.; Jiang, H.; Chen, K.; Liu, H.; *J. Org. Chem.*, **2009**, *74*, 5599.

[10] Mee, S. P. H.; Lee, V.; Baldwin, J. E. *Angew. Chem. Int. Ed.,* **2004**, *43*, 1132. b) Mee, S. P. H.; Lee, V.; Baldwin, J. E. *Chem. Eur. J.*, **2005**, *11*, 3294.

[11] Hatanaka, Y.; Hiyama, T. *J. Org. Chem.*, **1988**, *53*, 918.

[12] Denmark, S. E.; Smith, R. C.; Chang, T. W.-T.; Muhuhi, J. M. *J. Am. Chem. Soc.*, **2009**, *131*, 3104.

[13] Batsanov, A. S.; Fox, M. A.; Hibbert, T. G.; Howard, J. A. K.; Kivekäs, R.; Laromaine, A.; Sillanpää, R.; Viñas, C.; Wade, K. *Dalton Trans.*, **2004**, 3822.

[14] Cheprakov, A. V.; Beletskaya, I. P. *J. Organomet. Chem.*, **2004**, *689*, 4055.

[15] a) Elliott, P. I. P. *Annu. Rep. Prog. Chem., Sect. A*, **2010**, *106*, 526. b) Liu, Z.; Bian, Z.; Huang. C. *Top. Organomet. Chem.*, **2010**, *28*, 113. c) Baranoff, E.; Yum, J.-H.; Graetzel, M.; Nazeeruddin, M. K. *J. Organomet. Chem.*, **2009**, *694*, 2661. d) Ulbricht, C.; Beyer, B.; Friebe, C.; Winter, A.; Schubert, U. S. *Adv. Mater.*, **2009**, *21*, 4418. e) Chou, P.-T.; Chi, Y. *Chem. Soc. Rev.*, **2010**, *39*, 638.

[16] a) Slone, C. S.; Weinberger, D. A.; Mirkin, C. A. *Prog. Inorg. Chem.*, **1999**, *48*, 233. b) Braunstein, P.; Naud, F.; *Angew. Chem. Int. Ed.*, **2001**, *40*, 680.

[17] a) Newkome, G. R. *Chem. Rev.* **1993**, *93*, 2067. b) Zhang, Z. Z.; Cheng, H. *Coord. Chem. Rev.* **1996**, *147*, 1. c) Espinet, P.; Soulantica, K. *Chem. Rev.*, **1999**, *193-195*, 499.

[18] a) Anderson, M. P.; Casalnuovo, A. L.; Johnson, B. J.; Mattson, B. M.; Mueting, A. M.; Pignolet, L. H. *Inorg. Chem.* **1988**, *27*, 1649. b) Del Zotto, A.; Mezzetti, A.; Rigo, P. *J. Chem. Soc., Dalton Trans.* **1994**, 2257. c) Flapper, J.; Kooijman, H.; Lutz, M.; Spek, A. L.; Van Leeuwen, P. W. N. M.; Elsevier, C. J.; Kamer, P. C. J. *Organometallics* **2009**, *28*, 1180. d) Flapper, J.; Kooijman, H.; Lutz, M.; Spek, A. L.; Van Leeuwen, P. W. N. M.; Elsevier, C. J.; Kamer, P. C. J. *Organometallics* **2009**, *28*, 3264.

[19] a) Drent, E.; Arnoldy, P.; Budzelaar, P. H. M. *J. Organomet. Chem.* **1993**, *455*, 247. b) Consorti, C. S.; Ebeling, G.; Dupont, *J. Tetrahedron Lett.* **2002**, *43*, 753. c) Drent, E.; Arnoldy, P.; Budzelaar, P. H. M. *J. Organomet. Chem.* **1994**, *475*, 57. d) Speiser, F.; Braunstein, P.; Saussine, L. *Acc. Chem. Res.* **2005**, *38*, 784. f) Flapper, J.; Kooijman, H.; Lutz, M.; Spek, A. L.; van Leeuwen, P. W. N. M.; Elsevier, C. J.; Kamer, P. C. J. *Organometallics*, **2009**, *28*,

3272. g) Ittel, S. D.; Johnson, L. K.; Brookhart, M. *Chem. Rev.* **2000**, *100*, 1169. h) Gibson, V. C.; Spitzmesser, S. K.; *Chem. Rev.* **2003**, *103*, 283. i) Jiang, Q.; Van Plew, D.; Murtuza, S.; Zhang, X. *Tetrahedron Lett.* **1996**, *37*, 797.

[20] Spokyny, A. M.; Machan, C. W.; Clingerman, D. J.; Rosen, M. S.; Wiester, M. J.; Kenedy, R. D.; Stern, C. L.; Sarjeant, A. A.; Mirkin, C. A. *Nature Chemistry*, **2011**, *3*, 590.

[21] a) Alexander, R. P.; Schroder, H. A.; *Inorg. Chem.*, **1963**, *2*, 1107. b) Godovikov, N. N.; Degtyarev, A. N.; Bregadze, V.; Kabachnik, M. I. *Izv. Akad. Nauk SSSR, Ser. Khim.*, **1973**, 2369. c) Rohrsheid, R.; Holm, R. H. *J. Organomet. Chem.*, **1965**, *4*, 335. d) Teixidor, F.; Viñas, C.; Abad, M. M.; Núñez, R.; Kivekäs; R.; Sillanpää, R. *J. Organomet. Chem.*, **1995**, *503*, 193. e) Zakharkin, L. I.; Bregadze, V.; Okhlobystin, O. Y. *Izv. Akad. Nauk SSSR, Ser. Khim.*, **1965**, *4*, 211. f) Zakharkin, L. I.; Bregadze, V. I.; Okhlobystin, O. Y. *Izv. Akad. Nauk SSSR, Ser. Khim.*, **1964**, 1539. g) Balema, V. P.; Blaurock, S.; Hey-Hawkins, E. *Z. Anorg. Allg. Chem.*, **1999**, *625*, 1237. h) Balema, V. P. S.; Blaurock, S.; Hey-Hawkins, E. *Eur. J. Inorg. Chem.*, **1998**, 651.

[22] a) Teixidor, F.; Benakki, R.; Viñas, C.; Kivekäs, R.; Sillanpää, R. *Inorg. Chem.*, **1999**, *38*, 5916. b) Teixidor, F.; Viñas, C.; Benakki, R.; Kivekäs, R.; Sillanpää, R. *Inorg. Chem.*, **1997**, *36*, 1719. c) Huo, X. K.; Su, G.; Jin, G. X. *Dalton Trans*., **2010**, 1954.

[23] Lee, H. S.; Ba, J. Y.; Ko, J.; Kang, Y. S.; Kim, H. S.; Kim, S.-J.; Chung, J.-H.; Kang, S. O. *J. Organomet. Chem.* **2000**, *614-615*, 83.

[24] Lee, T.; Lee, S. W.; Wang, H. G.; Ko, J. S.; Kang, O. *Organometallics*, **2001**, *20*, 741.

[25] a) Teixidor, F.; Romerosa, A. M.; Rius, J.; Miravitlles, C.; Casabó, J.; Viñas, C.; Sanchez, E. *J. Chem. Soc., Dalton Trans.*, **1990**, 525. b) Teixidor, F.; Rudolph, R. W. *J. Organomet. Chem.*, **1983**, *241*, 301. c) Teixidor, F.; Viñas, C.; Rius, J.; Miravitlles, C.; Casabó, J. *Inorg. Chem.*, **1990**, *29*, 149. d) Viñas, C.; Butler, W. M.; Teixidor, F.; Rudolph, R. W. *Inorg. Chem.*, **1986**, *25*, 4369. e) Teixidor, F.; Viñas, C.; Sillanpää, R.; Kivekäs, R.; Casabó, J. *Inorg. Chem.*, **1994**, *33*, 2645. f) Jin, G. X. *Coord. Chem. Re*v. **2004**, *246*, 587. g) Yu, X. Y.; Lu, S. X.; Jin, G. X. *Inorg. Chim. Acta*, **2004**, *357*, 361. h) Yu, X. Y.; Jin, G.-X.; Hu, N. H.; Weng, L. H. *Organometallics* **2002**, *21*, 5540. i) Jin, G. X.; Wang, J. Q.; Zheng, Z.; Weng, L. H.; Herberhold, M. *Angew. Chem., Int. Ed.*, **2005**, *44*, 259. j) Wang, J. Q.; Hou, X. F.; Weng, L. H.; Jin, G. X. *Organometallics* **2005**, *24*, 826. k) Wang, J. Q.; Weng, L. H.; Jin, G. X. *J. Organomet. Chem.* **2005**, *690*, 249. k) Xu, B. H.; Peng, X. Q.; Li, Y. Z.; Yan, H. *Chem. Eur. J.* **2008**, *14*, 9347. l) Zhang, J. S.; Lin, Y. J.; Jin, G. X. *Dalton Trans.* **2009**, 111.

[26] a) Chung, S. W.; Ko, J.; Park, K.; Cho, S.; Kang, S. O. *Collect. Czech. Chem. Commun.* **1999**, *64*, 883. b) Yao, Z. J.; Jin, G. X. *Organometallics*, **2012**, *31*, 1767. c) Teixidor, F.; Laromaine, A.; Kivekäs, R.; Sillanpää, R.; Viñas, C.; Vespalec, R.; Horáková, H. *Dalton Trans.*, **2008**, 345.

[27] a) Yao, Z. J.; Jin, G. X. *Organometallics*, **2011**, *30*, 5365. b) Hu, P.; Yao, Z. J.; Wang, J. Q.; Jin, G. X. *Organometallics*, **2011**, *30*, 4935.

[28] a) Lee, J. D.; Kim, S. J.; Yoo, D.; Ko, J.; Cho, S.; Kong, S. O. *Organometallics* **2000**, *19*, 1695. b) Wang, S.; Li, H. W.; Xie, Z. *Organometallics* **2004**, *23*, 3780. c) Wang, X.; Jin, G.-X. *Chem.Eur. J.* **2005**, *11*, 5758. d) Dröse, P.; Hrib, C. G.; Edelmann, F. T. *J. Am. Chem. Soc.***, 2010**, *132*, 15540. e) Yao, Z. J.; Su, G.; Jin, G. X. *Chem. Eur. J.*, **2011**, *17*, 13298.

[29] McWhannell, M. A.; Rosair, G. M.; Welch, A. J.; Teixidor, F.; Viñas, C. *Acta Crystallogr., Sec. C: Crysta. Struct. Commun.*, **1996**, *52*, 3135.

[30] Sillanpää, R.; Kivekäs, R.; Teixidor, F.; Viñas, C.; Núñez, R. *Acta Crystallogr., Sec. C: Crysta. Struct. Commun.*, **1996**, *52*, 2223.

[31] a) Zahn, S.; Frank, R.; Hey-Hawkins, E.; Kirchner, B. *Chem. Eur. J.*, **2011**, *17*, 6034. b) Scheiner, S. *J. Phys. Chem. A*, **2011**, *115*, 11201. c)) Scheiner, S. *Chem. Phys.*, **2011**, *387*, 79.

[32] a) Sundberg, M. R., Uggla, R.; Viñas, C.; Teixidor, F., Paavola, S.; Kivekäs, R. *Inorg. Chem. Commun.*, **2007**, *10*, 713. b) Bauer, S.; Tschirschwitz, S.; Lönnecke, P., Frank, R.; Kirchner, B.; Clarke, M. L.; Hey-Hawkins, E. *Eur. J. Inorg. Chem.*, **2009**, 2776.

[33] a) Alekseyeva, E. S.; Fox, M. A.; Howard, J. A. K.; MacBride, J. A. H.; Wade, K. *Appl. Organometal. Chem.*, **2003**, *17*, 499. b) Boyd, L. A.; Clegg, W.; Copley, R. C. B.; Davidson, M. G.; Fox, M. A.; Hibbert, T. G.; Howard, J.

A. K.; Mackinnon, A.; Peace, J. R.; Wade, K. *Dalton Trans.*, **2004**, 2786. c) Brain, P. T.; Cowie, J.; Donohoe, D. J.; Hnyk, D.; Rankin, D. W. H.; Reed, D.; Reid, B. D.; Robertson, H. E.; Welch, A. J. *Inorg. Chem.*, **1996**, *35*, 1701.

[34] a) Oliva, J. M.; Viñas, C. *J. Mol. Struct.*, **2000**, *556*, 33. b) Llop, J.; Viñas, C.; Oliva, J. M.; Teixidor, F.; Flores, M. A.; Kivekäs, R.; Sillanpää, R. *J. Organomet. Chem.*, **2002**, *657*, 232. c) Oliva, J. M.; Allan, N. L.; Schleyer, P. v. R.; Viñas, C.; Teixidor, F. *J. Am. Chem. Soc.*, **2005**, *127*, 13538.

[35] Ansorg, K.; Braunschweig, H.; Chiu, C.-W.; Engels, B.; Gamon, D.; Högel, M.; Kupfer, T.; Radacki, K. *Angew. Chem. Int. Ed.*, **2011**, *50*, 2833.

[36] Lesley, M. J. G.; Woodward, A.; Taylor, N. J.; Marder, T. B.: Cazenobe, I.; Ledoux, I.; Thornton, J. Z. A.; Bruce, D. W.; Kakkar, A. K. *Chem. Mater.*, **1998,** *10,* 1355.

[37] a) Yuan, Z.; Taylor, N. J.; Sun, Y.; Marder, T. B.; Williams, J. D.; Cheng, L.-T. *J. Organomet. Chem.*, **1993**, *449*, 27. b) Weber, L.; Werner, V.; Fox, M. A.; Marder, T. B.; Schwedler, S.; Brockhinke, A.; Stammler, H-G.; Neumann, B. *Dalton Trans.*, **2009**, 1339. c) Lorbach, A.; Bolte, M.; Li, H.; Lerner, H-W.; Holthausen, M. C.; Jäkle, F.; Wagner, M. *Angew. Chem. Int. Ed.*, **2009**, 48, 4584. d) Sundararaman, A.; Victor, M.; Varughese, R.; Jäkle, F. *J. Am. Chem. Soc.*, **2005**, *127*, 13748. e) Wade, C. R.; Gabbai, F. P. *Inorg. Chem.*, **2010**, *49*, 714. f) Wade, C. R.; Gabbai, F. P. *Dalton Trans.*, **2009**, 9169. g) Yamaguchi, S.; Akiyama, S.; Tamao, K. *J. Am. Chem. Soc.*, **2001**, *123*, 11372.

[38] a) Welch, G. C.; San Juan, R. R.; Masuda, J. D.; Stephan, D. W. *Science*, **2006**, *314*, 1124. b) Stephan, D. W. *Dalton Trans.*, **2012**, 9015. c) Stephan, D. W. *Org. Biomol. Chem.*, **2008**, *6*, 1535. d) Stephan, D. W. *Org. Biomol. Chem.*, **2012**, *10*, 5740. e) Spies, P.; Schewendemann, S.; Lange, S.; Kehr, G.; Fröhlich, R.; Erker, G. *Angew. Chem., Int. Ed.*, **2008**, *47*, 7543. f) Dureen, M., A.; Lough, A.; Gilbert, T. M.; Stephan, D. W. *Chem. Commun.*, **2008**, 4303. g) McCahill, J. S. J.; Welch, G. C.; Stephan, D. W. *Angew. Chem., Int. Ed.*, **2007**, *46*, 4968. h) Ullrich, M.; Seto, K. S.-H.; Lough, A. J.; Stephan, D. W. *Chem. Commun.*, **2009**, 2335. i) Dureen, M. A.; Stephan, D. W. *J. Am. Chem. Soc.*, **2009**, *131*, 8396. j) Mömming, C. M.; Otten, E.; Kehr, G.; Fröhlich, R.; Grimme, S.; Stephan, D. W.; Erker, G. *Angew. Chem., Int. Ed.*, **2009**, *48*, 6643. k) Otten, E.; Neu, R. C.; Stephan, D. W. *J. Am. Chem. Soc.*, **2009**, 131, 9918. l) Welch, G. C.; Stephan, D. W. *J. Am. Chem. Soc.*, **2007**, *129*, 1880. m) Geier, S. J.; Gilbert, T. M.; Stephan, D. W. *J. Am. Chem. Soc.*, **2008**, 130, 12632. n) Sumerin, V.; Schulz, F.; Atsumi, M.; Wang, C.; Nieger, M.; Leskela, M.; Repo, T.; Pyykkö, P.; Rieger, B. *J. Am. Chem. Soc.*, **2008**, 130, 14117. o) Sumerin, V.; Schulz, F.; Nieger, M.; Leskela, M.; Rieger, B. *Angew. Chem. Int. Ed.*, **2008**, *47*, 6001. p) Caputo, C.B.; Geier, S.J.; Winkelhaus, D.; Mitzel, N.W.; Vukotic, V.N.; Loeb, S. J.; Stephan, D. W. *Dalton Trans.*, **2012**, 2131.

[39] Geier, S. J.; Gille, A. L.; Gilbert, T. M.; Stephan, D. W.; *Inorg. Chem.*, **2009**, *48*, 10466.

[40] a) Hawthorne, M. F.; Young, D. C.; Wegner, P. A., *J. Am. Chem.. Soc.*, **1965**, *87*, 1818. b) Hawthorne, M. F.; Andrews, T. D. *J. Chem. Soc. Chem. Commun.*, **1965**, 443.

[41] Housecroft, C. E. *Encyclopedia of Inorganic Chemistry*, John Wiley & Sons, Ltd, **2008**.

[42]Sivaev, I. B.; Bregadze, V. I. *Collect. Czech. Chem. Commun.*, **1999**, *64*, 783.

[43] Rojo, I.; Teixidor, F.; Viñas, C.; Kivekäs, R.; Sillanpää, R. *Chem. Eur. J.*, **2004**, *10*, 5376.

III. CONCLUSIONS

Get your facts first, and then you can distort them as you please.

Mark Twain

Section 1

1) The disproportionation of Li[1,2-$C_2B_{10}H_{11}$] into Li_2[1,2-$C_2B_{10}H_{10}$] and 1,2-$C_2B_{10}H_{12}$ in ethereal solvents is consequence of the formation of contact ion pair, and in less extent of separated ion pair.
2) In the contact ion pair a large degree of covalent C_c-Li(solvated) bond can be assumed. All ether Et_2O, THF and DME solvents studied generate contact ion pair; however THF and DME tend to produce carboranyllitium ion pair with a slightly higher degree of separated ion pair than Et_2O.
3) In reactions in which a halide is generated (as with $ClPPh_2$ or $BrCH_2CH{=}CH_2$), Et_2O appears to produce the largest degree of monosubstitution. In other situations, such as with S_8, or when no halide is generated, THF or DME facilitate the largest degree of monosubstitution.
4) It has been observed that once Li[1,2-$C_2B_{10}H_{11}$] is obtained, the nucleophilicity of the carboranyllithium is enhanced by synergism with halide salts and Li[1,2-$C_4B_{20}H_{22}$] can be obtained by self-reaction.
5) The mediation of Li^+ in producing isomerizations on allyl has been demonstrated to be dependent on the ether solvent utilized. Et_2O tends to not induce isomerization on allyl substituents; conversely THF or DME produces isomerization.

Section 2

1) A comprehensive study on the oxidation of carboranylmono- phosphines and carboranyldi-phosphines with hydrogen peroxide, sulphur and selenium was presented. The reactivity of the carboranyldiphosphines monochalcogenides is studied and the electronic communication between the different fragments is investigated computationally.
2) Carboranylmono- and carboranyldiphosphines react with H_2O_2, S, and Se to yield the correspondent oxidized carboranylphosphines. The reaction rates can be modulated by changing either the substituent on the P moiety or the substituent on the other C_C atom.
3) When H_2O_2 is added to 1,2-$(PR_2)_2$-1,2-*closo*-$C_2B_{10}H_{10}$ (R= Ph, ^{i}Pr), these oxidize to 1,2-$(OPR_2)_2$-1,2-*closo*-$C_2B_{10}H_{10}$ (R= Ph, ^{i}Pr), though with different reaction rates, only 15 min being necessary to achieve the full oxidation if R = ^{i}Pr, whereas 4 h are needed for R = Ph. Prolonged oxidation of *closo*-carboranyldiphosphines with H_2O_2 yield the *nido* derivatives, where a proton is chelated between the two oxygen atoms.
4) When S and Se are used, a different reactivity is found for 1,2-$(PPh_2)_2$-1,2-*closo*-$C_2B_{10}H_{10}$, and 1,2-$(P^iPr_2)_2$-1,2-*closo*-$C_2B_{10}H_{10}$:
    a) For R= Ph, the reaction with sulfur produces mono- and dioxidation species, thus 1-$SPPh_2$-2-PPh_2-1,2-*closo*-$C_2B_{10}H_{10}$ and 1,2-$(SPPh_2)_2$-1,2-*closo*-$C_2B_{10}H_{10}$ can be isolated. However, when Se is the oxidizing agent, only the mono oxidation species, 1-$SePPh_2$-2-PPh_2-1,2-*closo*-$C_2B_{10}H_{10}$, is obtained.
    b) For R= ^{i}Pr, only mono oxidation takes place with S, and the second C_c-P^iPr_2 bond breaks up to yield 1-SP^iPr_2-1,2-*closo*-$C_2B_{10}H_{11}$ if the reaction time is prolonged. When Se is used on 1,2-$(P^iPr_2)_2$-1,2-*closo*-$C_2B_{10}H_{10}$ only the species with one phosphorus, 1-$SePR_2$-1,2-*closo*-$C_2B_{10}H_{11}$, is found.
    c) It has also been noticed that carboranylmonophosphines oxidation requires longer reaction times than for carboranyldiphosphines.

5) Experimental studies on the coordination ability of the carboranyldiphosphines monochalcogenide have shown that these compounds do not behave as hemilabile ligands because the P-E bond is labile towards metal coordination causing dechalcogenation and P-M bond formation.

6) Computational studies on the carobranyldiphosphine monochalcogenides provide steric and electronic information on the P-E (E= S, Se) bonds. The steric effects block the bonding ability of the P-E bond due to the interactions between the chalcogen and the neighbouring hydrogen atoms. The electronic effects originated by the strong electronic withdrawing character of the *closo* carborane cluster polarize the P-E (E=S, Se) bond towards the phosphorus atom. As a consequence, the E atom is the electron poor site whereas the P atom is the electron rich site in the P-E bond. So, PPh_3 from the starting complex $[ML_x(PPh_3)_y]$, acts as a Lewis base attacking the E side and the metal acts as a Lewis acid coordinating to the P.

7) The electron-donating contribution of the phosphines and oxidized phosphines moieties to the cumulative built-up cluster-only total charge (CTC) were theoretically calculated by NBO studies of the individual charges and cluster total charge (CTC). It was observed that:
   a) CTC for carboranylphosphines are more negative than *o*-carborane and this can be explained by the fact that the carboranyl moiety possesses electron withdrawing character and so, the presence of the lone pair on the phosphine moieties, give electronic density to the cluster which contribute to its CTC.
   b) There are differences in the carboranyldiphosphines bearing Ph or ^{i}Pr moieties due to different degree of the back-donation of the P lone pairs.
   c) Besides the NPA charges calculated from the NBO analysis, the Hirshfeld charges were also calculated and give better results than the NPA charges.

8) The electronic effects on *closo*-carboranylmonophoshines compared with triphenylphosphine revealed important differences. In 1-PPh_2-1,2-*closo*-$C_2B_{10}H_{11}$, the phosphorus lone pair is not delocalized in three C-C neighbouring bonds as in PPh_3 but in two C-C bond from the -PPh_2 moiety and on a tricentric C-B-B bond of the carborane cage. The different reactivity of 1-PPh_2-1,2-*closo*-$C_2B_{10}H_{11}$ compared with PPh_3 arise from the fact that the P lone pair for the first has a p_x composition, whereas in PPh_3 has a p_z composition.

9) Further experimental studies on the oxidation reaction of 1,2-$(PR_2)_2$-1,2-*closo*-$C_2B_{10}H_{10}$ species, established the influence of the R group. In this sense, an electron donating group, ^{i}Pr, facilitates the oxidation reaction more than an electron withdrawing group, Ph. Also, the carboranyldiphosphines oxides bearing alkyls groups are more easily deboronated than the ones bearing aryl groups. The experimental results were well correlated with the DFT calculation.

10) For the *nido*-carboranyldiphosphine oxide, H[1,2-$(OP^{i}Pr_2)_2$-1,2-*nido*-$C_2B_9H_{10}$] it was observed that the proton is chelated by the two O atoms and two polymorphs with different P=O···H^+···O=P distances were observed. One in which the proton is almost in the middle of the O···O distance and other where H^+ is closer to a P=O bond. The strength of these bonds was assessed based on experimental and computational observations:
   a) Experimentally was seen that the presence of these interactions produces a deshielding in the ^{31}P-NMR. This was explained based on DFT calculations, which indicated that the electron lone pairs on the O atoms are less available for back-donation into the P-C antibonds due to the strong O···H···O interaction.

b) By NBO analysis we establish that the structure that have the H atom just in the middle of the distance of the two O atoms, presents very strong P=O···H^+···O=P bonds, whereas the structure, that have one O-H distance shorter than the other, present a covalent O-H bond and a weak O···H interaction.

c) The strength of the P=O···H^+···O=P was also studied by the QTAIM and ELF analysis, and was established that the symmetric P=O···H^+···O=P interaction strength is of the order of the covalent bond, whereas for the unsymmetrical P=O···H^+···O=P interaction is of moderate strength.

11) We also observed that the protonated *nido*-carboranyldiphosphine oxides can be isomerized from *ortho* to *meta* by the simple action of a strong base (NaOH/EtOH), and based on DFT calculations we established thermodynamically the reactions steps, being observed that the isomerization occurs since the *meta* isomer is 28 kcal·mol^{-1} more stable than the *ortho* isomer.

Section 3

1) Synthesis of "space confined" multi-cage carborane derivatives directly from lithiated carborane and carbon halides was unsuccessful.
2) The first step to the achievement to the "space confined" multi-cage carborane derivatives was achieved by the nucleophilic addition of the Li[$C_2B_{10}H_{11}$] to the carboranylformaldehyde, which produces the two-cages alcohol, 1,1-CHOH-(1,2-*closo*-$C_2B_{10}H_{11}$)$_2$.
3) Other star-shape derivatives of carboranylformaldehyde were obtained by the electrophilic substitution of different aromatic substrates with carboranylformaldehyde activated either by $AlCl_3$ or by CF_3SO_3H. In these reactions it was observed that:
   a) The activated aromatic substrates react in softer conditions than the deactivated aromatic.
   b) The π-defficient heterocycles (pyridine, pyrazine, pyridazine, quinoline) does not react with activated carboranylformaldehyde.
   c) The π-excessive heterocycles react with carboranylformaldehyde activated either by CF_3SO_3H or $AlCl_3$.
4) Witting and Horner-Wadsworth-Emmons reactions were tested for carboranylformaldehyde but were unsuccessful. To overcome it, carborane containing phosphorus derivatives as phosphonium salts and phosphonates were synthesized and reacted with aromatic aldehydes but these reactions were also unsuccessful.

Section 4

1) Different cross-coupling reactions between metalated carborane derivatives and pyridine halides were tried in order to improve the synthesis of carboranylpyridine, but all the reactions were unsuccessful.
2) Different metalation reactions of carboranylpyridine with Pd(II), Ir(III), Rh(III) and Ru(II) derivatives were tried but only Pd(II) proved to be successful.
3) Hybrid carboranylpyridine-phosphine ligands were synthesized by the reaction of C_C-lithiated carboranylpyridine with chlorophosphines. The carboranylpyridine-phosphine compound bearing ^{i}Pr groups bonded to phosphorus was proved to be fluorescent in crystalline state but not in solution. The electronic properties of this compound were investigated by DFT calculation.

4) Complexation reactions of carboranylpyridine-phosphine ligands with Pd(II) and Rh(I) were done.
5) A carboranylpyridine-borane compound was successfully synthesized and characterized.
6) The carboranylpyridine was also used as starting compound for the synthesis of a cobalt(bisdicarbollide) derivative with pyridine moieties.

ADDENDUM I

CHEMISTRY
A EUROPEAN JOURNAL

DOI: 10.1002/chem.201102626

Influential Role of Ethereal Solvent on Organolithium Compounds: The Case of Carboranyllithium

Adrian-Radu Popescu,[a, b] Ana Daniela Musteti,[a, b] Albert Ferrer-Ugalde,[a, b] Clara Viñas,[a] Rosario Núñez,[a] and Francesc Teixidor*[a]

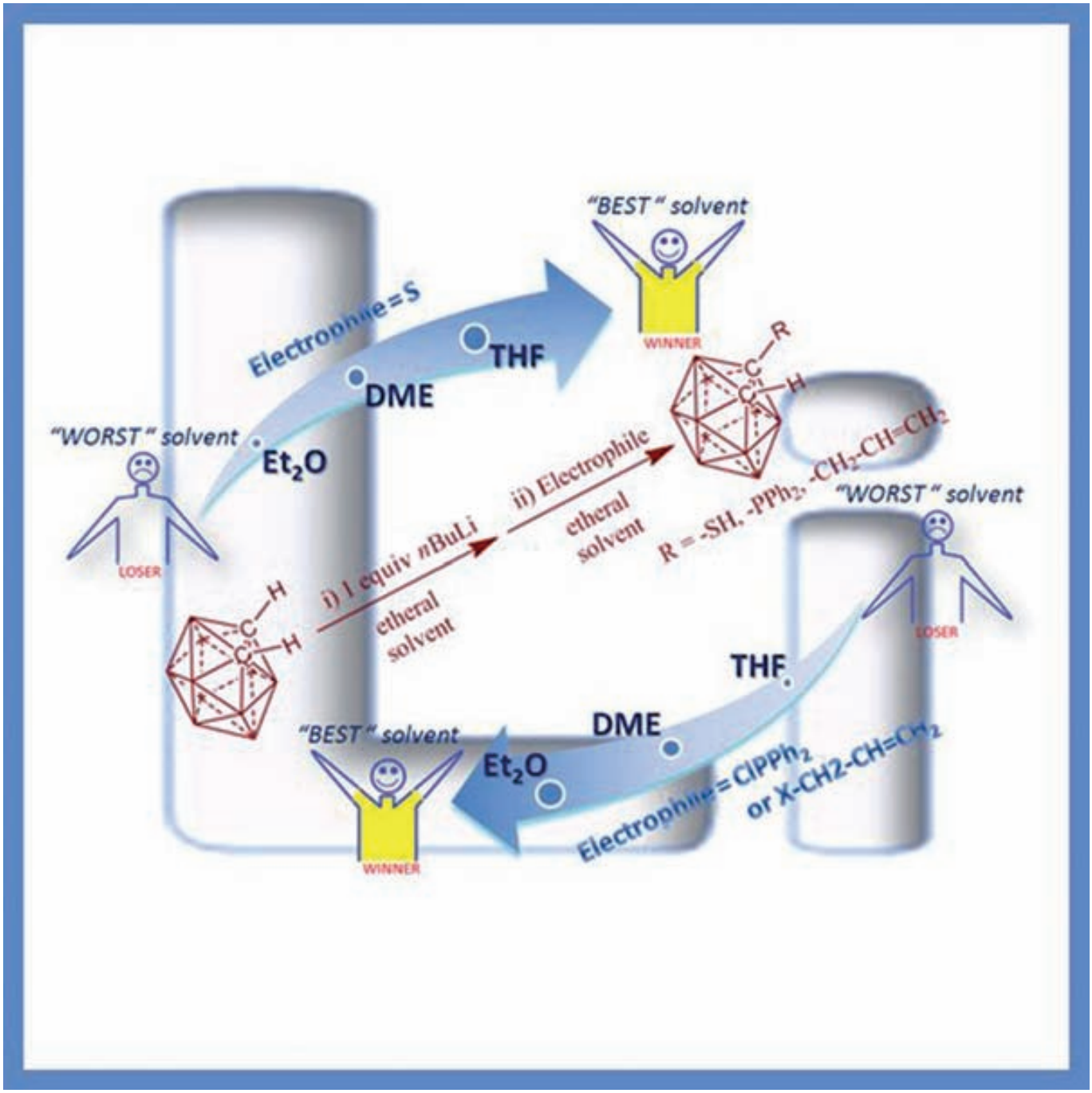

Abstract: The influence of ethereal solvents (diethyl ether (Et_2O), tetrahydrofuran (THF) or dimethoxyethane (DME)) on the formation of organolithiated compounds has been studied on the 1,2-$C_2B_{10}H_{12}$ platform. This platform is very attractive because it contains two C_c–H adjacent units ready to be lithiated. On would expect that the closeness of both C_c–H units would induce a higher resistance of the second C_c–H unit being lithiated following the first lithiation. However, this is not the case, which makes 1,2-$C_2B_{10}H_{12}$ attractive to get a better understanding of the ethereal solvent influence on the lithiation process. The formation of carboranyl disubstituted species has been attributed to the existence of an equilibrium in which the carboranyl monolithiated species disproportionates into dilithium carborane and pristine carborane. The way Li^+ binds to C_c in the carboranyl fragment and how the solvent stabilizes such a binding is paramount to drive the reaction to the generation of mono- and disubstituted carboranes. In fact, the proportion of mono- and disubstituted species is a consequence of the formation of contact ion pairs and, to a lesser extent, of separated ion pairs in ethereal solvents. All ethereal solvents generate contact ion pairs in which a large degree of covalent C_c–Li(solvent) bonding can be assumed, according to experimental and theoretical data. Furthermore, Et_2O tends to produce carboranyllitium ion pairs with a higher degree of contact ion pairs than THF or DME. It has been determined that for a high-yield preparation of monosubstituted 1-R-1,2-$C_2B_{10}H_{11}$, in C_c–R (R = C, S or P) coupling reactions, the reagent type defines which is the most appropriate ethereal solvent. In reactions in which a halide is generated, as with $ClPPh_2$ or $BrCH_2CH{=}CH_2$, Et_2O appears to produce the highest degree of monosubstitution. In other situations, such as with S_8, or when no halide is generated, THF or DME facilitate the largest degree of monosubstitution. It has been shown that upon the self reaction of Li[1,2-$C_2B_{10}H_{11}$] to produce $[LiC_4B_{20}H_{22}]^-$ the nucleophilicity of the carboranyllithium can even be further enhanced, beyond the ethereal solvent, by synergism with halide salts. The mediation of Li^+ in producing isomerizations on allyl substituents has also been demonstrated, as Et_2O does not tend to induce isomerization, whereas THF or DME produces the propenyl isomer. The results presented here most probably can be extended to other molecular types to interpret the Li^+ mediation in C–C or other C–X coupling reactions.

Keywords: cross-coupling · density functional calculations · ion pairs · lithium · organolithium compounds · solvent influence

Introduction

The importance of organolithium compounds has been recognized in all fields of chemistry. Organolithium compounds have long been renowned as highly reactive species and have been frequently used as attractive intermediates in organic chemistry. However, the understanding of the reaction mechanisms in which Li^+ participates is a great challenge and remains a drawback for the development of further applications of the organolithium adducts in synthetic chemistry.[1] Despite many theoretical[2] and experimental[3] studies that have been done on the role of Li^+ in different types of reactions, still a lot of work has to be carried out regarding the use of this light metal as an alternative to the commonly used transition metals, for example, in transition-metal catalysis. To learn more on the mediation of Li^+ to generate C–C, C–S, and C–P bonds, the equilibrium[4] shown in Scheme 1 could be attractive, if somewhat unconventional,

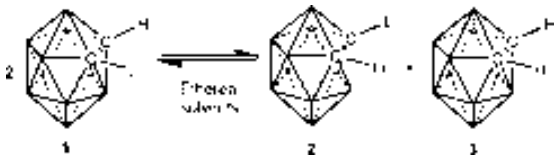

Scheme 1. The equilibrium between the species involved in the reaction of 1,2-$C_2B_{10}H_{12}$ with *n*BuLi.

because it prevents the formation of pure monosubstituted *o*-carborane derivatives. A simple inspection of the Li_2-$[C_2B_{10}H_{10}]$ molecule in Scheme 1 would suggest its improbable existence due to the expected high coulombic repulsion. However, experimental results clearly show that this is not the case. It has been postulated that in the reaction of *o*-carborane, 1,2-$C_2B_{10}H_{12}$, with one equivalent of *n*BuLi, the equilibrium shown in Scheme 1 dominates the formation of mono- and disubstituted derivates.[4] In a reaction aimed at producing monosubstituted 1-R-1,2-$C_2B_{10}H_{11}$, the formation of the disubstituted species 1,2-R_2-1,2-$C_2B_{10}H_{10}$ implies leaving unreacted 1,2-$C_2B_{10}H_{12}$ in the reaction mixture. If the Scheme 1 equilibrium controls the ratio of mono- or disubstituted species, understanding the factors that shift this

[a] A.-R. Popescu, A. D. Musteti, A. Ferrer-Ugalde, Prof. Dr. C. Viñas, Dr. R. Núñez, Prof. Dr. F. Teixidor
Institut de Ciència de Materials de Barcelona (ICMAB-CSIC)
Campus de la U.A.B., 08193 Bellaterra (Spain)
Fax: (+34) 93-580-57-29
E-mail: teixidor@icmab.es

[b] A.-R. Popescu, A. D. Musteti, A. Ferrer-Ugalde
Enrolled in the U.A.B Ph.D. program.

Supporting information for this article is available on the WWW under http://dx.doi.org/10.1002/chem.201102626. It contains ^{11}B NMR spectra of Li[$C_2B_{10}H_{11}$] in ethereal solvents (Et_2O, THF, and DME); ^{11}B-, $^{11}B\{^1H\}$-NMR spectra of Li[1-Me-1,2-$C_2B_{10}H_{10}$] in ethereal solvents (Et_2O, THF and DME); ^{11}B NMR spectra of Li_2[1,2-$C_2B_{10}H_{10}$] in THF; ^7Li-NMR spectra of Li[$C_4B_{20}H_{22}$] and Li_2[1,2-$C_2B_{10}H_{10}$] in THF.

equilibrium to the left or right will contribute to a cleaner and more efficient synthetic procedure and will bring valuable information on the role of the lithium ion.

On the other hand carboranes have raised interest in fields as diverse as catalysis, materials science, supramolecular chemistry, and medicine, among others,[5] therefore the synthesis of monosubstituted derivatives of *o*-carborane in good yields and in as much pure form as possible is very relevant. The first reason is the atom economy,[6] and secondly, but not less important, because the cluster keeps a second position, a $C_{cluster}$–H (C_c–H), for further reaction with a different electrophile. Until now, two strategies have been used to obtain monosubstituted carboranes from 1,2-$C_2B_{10}H_{12}$. The first approach was reported by Hawthorne et al.,[7] in which the *tert*-butyldimethylsilyl (TBDMS) moiety was used as protecting group for a single carbon vertex; the second strategy has been reported by our group,[8] by using a chelating solvent, dimethoxyethane (DME). For the latter method we had hypothesized that the monosubstitution was produced due to steric hindrance with a destabilized disubstituted [Li(DME)$_x$]$_2$[1,2-$C_2B_{10}H_{10}$]. Nevertheless, we could not rule out that it could be due to the influence of the solvent on the monolithiation reaction.

Therefore, in this work we have done further research to understand the role of the Li^+ in C–X (X = C, S or P) coupling reactions. To do so we have used the equilibrium shown in Scheme 1 and studied: 1) the way Li^+ binds to C_c in the carboranyl fragment and how the solvent influences in such a binding to drive the reaction to the generation of mono- and disubstituted carboranes, 2) to determine if the equilibrium shown in Scheme 1 is decisive for the high-yield preparation of monosubstituted 1-R-1,2-$C_2B_{10}H_{11}$, or if there are other factors to be taken into account, and 3) to learn why such an uncommon equilibrium takes place.

Results and Discussion

To learn on the points indicated above, and in particular what factors control the tendency to the left or right of the equilibrium in Scheme 1, we assume that coordinating solvents rarely can be innocent in the presence of Li^+. They can fully or partially solvate the Li^+ ion. In the first situation, a neat negative charge in the cluster is generated, that prevents the formation of a second negative charge, thus leading to monosubstitution. When the solvent partially solvates the Li^+, the C_c–Li bond is largely maintained, in which case it may stabilize the co-existence of two Li atoms on the same carborane, therefore driving to probable disubstitution.

To get experimental evidence on the influence of the solvent in the reaction of 1,2-$C_2B_{10}H_{12}$ with *n*BuLi and to know more on the mechanism of such reaction, we decided to restrict this investigation to only one type of solvent that can coordinate the Li^+, ethereal solvents, and to two different type of reagents S_8 and $ClPPh_2$, which have been previously used by our group.[8,9] Furthermore we investigated how the liberated Li^+ could influence the nature of a newly generated C–X bond (X = C, S or P).

Reaction of carboranyllithium with sulfur: The reaction of 1,2-$C_2B_{10}H_{12}$ with one equivalent of *n*BuLi and 1/8 equiv of S_8 (Scheme 2) was carried out in three different ethereal solvents: diethyl ether (Et_2O), tetrahydrofuran (THF), and dimethoxyethane (DME). To get the maximum information on the solvent influence, the reactions were conducted over a range of temperatures, between −80 and 0 °C, in steps of 20 °C. The concentration dependence of the reaction was also studied, thus two different concentrations 0.07 mol L^{-1} (that is 100 mg of *o*-carborane per 10 mL of solvent) and 0.23 mol L^{-1}(that is 100 mg of *o*-carborane per 3 mL of solvent) were used. Total reaction time was 4 h. The reaction procedure is detailed in the Experimental Section. The percentages in terms of molar fraction of the products separated in the reaction of carboranyllithium with sulfur are presented in Table 1. The reactions in DME were carried out starting at −60 °C due to the melting point of the solvent. To assure the reproducibility of the experimental data the reactions were double or triple checked.

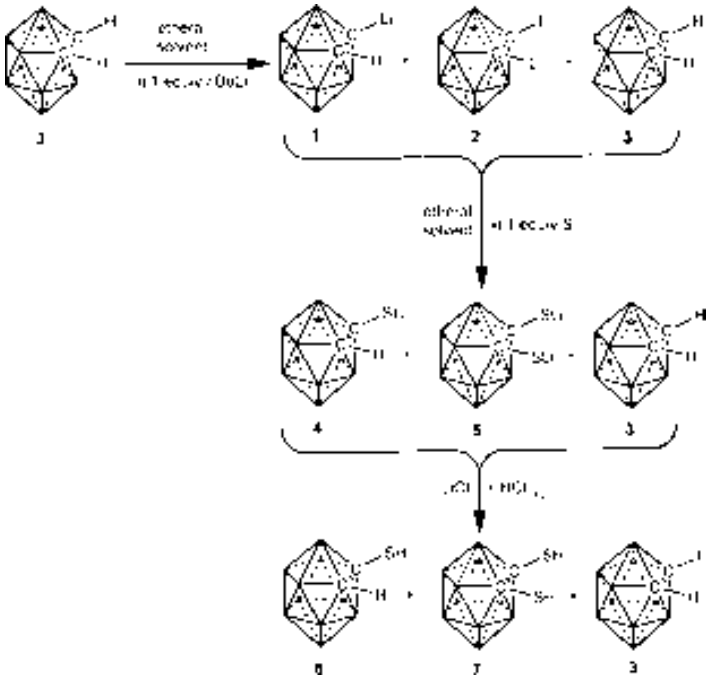

Scheme 2. Reaction of carboranyllithium with sulfur.

As shown in Table 1, the reaction of Li[1,2-$C_2B_{10}H_{11}$] with sulfur gives over 90% of 1-SH-1,2-$C_2B_{10}H_{11}$, peaking up to 98% in both THF and DME and independent of the reaction conditions. The exception was in DME at −60 °C, because the solvent is solid (m.p. −58 °C) at this temperature. When the solvent was Et_2O significantly lower yields of 1-SH-1,2-$C_2B_{10}H_{11}$ were obtained, while that of 1,2-(SH)$_2$-1,2-$C_2B_{10}H_{10}$ increased. The latter eventually exceeded 1-SH-1,2-$C_2B_{10}H_{11}$ at 0 °C. It should be noted that the reaction

Table 1. Percentage (molar fration) of 1-SH-1,2-$C_2B_{10}H_{11}$ in ethereal solvents.

C_{carb}	T	THF			Et_2O			DME		
[mol L^{-1}][a]	[°C]	mono [%]	di [%]	*o*-carborane [%][b]	mono [%]	di [%]	*o*-carborane [%][b]	mono [%]	di [%]	*o*-carborane [%][b]
0.07	−80	91	4	5	56	6	39	–	–	–
0.23	−80	95	0	5	57	9	34	–	–	–
0.07	−60	96	0	4	74	3	23	85	0	14
0.23	−60	98	0	2	53	0	47	81	2	17
0.07	−40	97	0	3	71	16	13	92	1	7
0.23	−40	93	0	7	72	4	24	95	1	4
0.07	−20	97	0	3	80	9	11	95	1	4
0.23	−20	95	0	5	74	12	14	95	1	4
0.07	0	95	0	5	49	13	37	91	1	8
0.23	0	98	0	2	26	38	36	92	3	5

[a] C_{carb} = *o*-carborane concentration. [b] Unreacted *o*-carborane.

was not completed under these conditions, and upon addition of aqueous HCl all lithiated species present in the reaction medium were protonated yielding pristine 1,2-$C_2B_{10}H_{12}$.

Remarkably, the reaction of Li[1,2-$C_2B_{10}H_{11}$] with sulfur in THF is within experimental error independent of the temperature or concentration. This implies that the two steps (Scheme 2): i) the reaction of 1,2-$C_2B_{10}H_{12}$ with *n*BuLi and ii) the nucleophilic attack of the carboranyl on the sulfur, are both temperature independent. The temperature independence of the first of the two steps was confirmed by theoretical calculations using DFT methods. In Figure 1 the variation of the free energy of the reaction of 1,2-$C_2B_{10}H_{12}$ with *n*BuLi versus the temperature is represented, indicating that this energy is not temperature-dependent. This result implies that the kinetics of the global reaction depends on the rate of the second step, that is, the reaction between the carboranyllithium and the electrophile. Thus the mechanism of the reaction between the lithiated species and the electrophile is the relevant one to produce the targeted compound. In fact, sulfur reacts with Li[1,2-$C_2B_{10}H_{11}$] in THF and DME to yield almost exclusively 1-SLi-1,2-$C_2B_{10}H_{11}$, which is subsequently hydrolyzed with aqueous HCl to produce 1-SH-1,2-$C_2B_{10}H_{11}$. This is not the case in Et_2O, in which the proportion of 1,2-$(SH)_2$-1,2-$C_2B_{10}H_{10}$ is even superior to 1-SH-1,2-$C_2B_{10}H_{11}$.

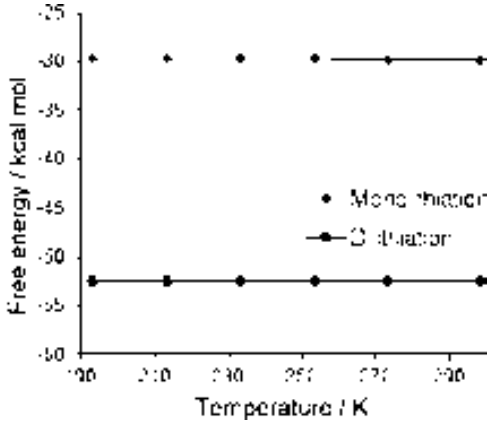

Figure 1. Variation of the free energy of reaction with the temperature in the reaction of 1,2-$C_2B_{10}H_{12}$ with *n*BuLi.

Reaction of carboranyllithium with chlorodiphenylphosphine: The reaction of 1,2-$C_2B_{10}H_{12}$ with one equivalent of *n*BuLi and subsequently one equivalent of $ClPPh_2$ (Scheme 3), under exactly the same conditions as for the above reaction with sulfur, produced lower yields of the monosubstituted 1-PPh_2-1,2-$C_2B_{10}H_{11}$ species in all three solvents (see Table 2). Furthermore, the percentage of unreacted 1,2-$C_2B_{10}H_{12}$ was higher, indicating that the reaction was quenched before being finished. Nevertheless, the highest yields and ratio of monosubstituted 1-PPh_2-1,2-$C_2B_{10}H_{11}$ were obtained in Et_2O. This result is just the opposite to that obtained for the reaction of 1-Li-1,2-$C_2B_{10}H_{11}$ with sulfur, for which the Et_2O was the worst solvent.

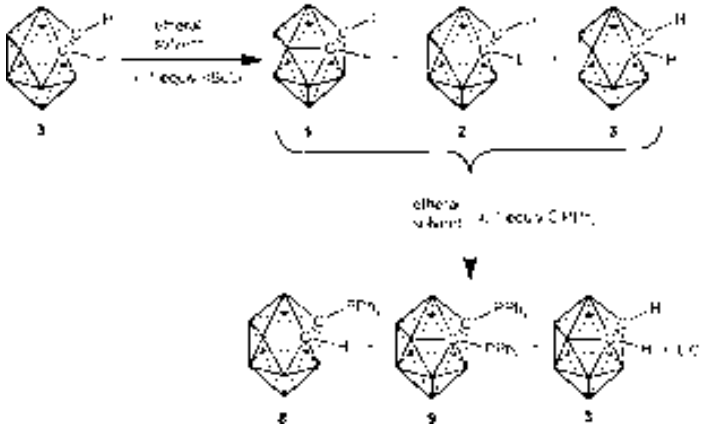

Scheme 3. Reaction of carboranyllithium with chlorodiphenylphosphine.

According to these results, the Et_2O seems to be a suitable solvent for the preparation of 1-PPh_2-1,2-$C_2B_{10}H_{11}$. For that reason, as a complementary task away from the conditions described above and for comparison purposes, we performed the reaction of Li[1,2-$C_2B_{10}H_{11}$] with $ClPPh_2$ at room temperature, and after two hours 1-PPh_2-1,2-$C_2B_{10}H_{11}$ was obtained in over 90% yield.

Table 2. Percentage of 1-PPh_2-1,2-$C_2B_{10}H_{11}$ in ethereal solvents.

C_{carb}	T	THF			Et_2O			DME		
[mol L^{-1}][a]	[°C]	mono [%]	di [%]	*o*-carborane [%][b]	mono [%]	di [%]	*o*-carborane [%][b]	mono [%]	di [%]	*o*-carborane [%][b]
0.07	−80	40	11	49	34	4	62	–	–	–
0.23	−80	16	9	75	28	8	64	–	–	–
0.07	−60	23	6	71	79	8	13	12	21	67
0.23	−60	16	8	76	81	5	14	55	3	42
0.07	−40	16	7	77	55	8	37	28	7	65
0.23	−40	20	6	74	57	6	37	54	10	36
0.07	−20	30	5	65	53	1	46	26	7	67
0.23	−20	26	2	72	41	3	56	57	2	41
0.07	0	5	3	92	57	5	38	35	4	61
0.23	0	15	5	80	60	8	32	32	3	65

[a] C_{carb} = *o*-carborane concentration. [b] Unreacted *o*-carborane.

The reaction of Li[1,2-$C_2B_{10}H_{11}$] with $ClPPh_2$ leads to two main products: 1-PPh_2-1,2-$C_2B_{10}H_{11}$ and LiCl (Scheme 3), whereas in the reaction with sulfur only one product, Li[1-S-1,2-$C_2B_{10}H_{11}$], is obtained (Scheme 2). Thus, the mechanism of the reaction of Li[1,2-$C_2B_{10}H_{11}$] with $ClPPh_2$ is different from that of the reaction with sulfur. Additionally, as different yields and products are obtained in the studied solvents, it is clear that the reactivity of the reagents and the coupling reaction mechanism between the carboranyllithium and the electrophile greatly depend on the interactions with the solvent and the solvation of all involved species.

Solvation capacity of the ethereal solvents: To account for the influence of the reaction solvent, both in the yield and final products, it is necessary to take into consideration the solvation properties of the solvent: the donor (DN) and acceptor (AN) numbers (Table 3).[10] The magnitude of the donor number refers to the ability of a solvent to solvate cations and the magnitude of the acceptor number refers to the ability of a solvent to solvate anions. The three ethers have comparable DNs, but with respect to the acceptor number, both THF and DME have ANs that are at least twice the AN value for Et_2O. Thus, solvation of the carboranyl moiety must be lower in Et_2O than in THF or DME, and therefore the carboranyl in Et_2O should behave as a stronger nucleophile than in THF and DME.

It has been proven that the solvent dramatically influences the aggregation state and consequently the reactivity of organolithium compounds.[11] However, the solvation of organolithium compounds is a complex issue, and no single existing solvation model is appropriate for all such compounds. Although molecular dynamics may ultimately provide the best method to determine average equilibrium solvation numbers,[12] recent studies have modeled the thermodynamics of ethereal solvation of organolithium compounds by locating explicit solvates.[13]

Table 3. Acceptor number (AN) and Donicities (DN) for selected solvents in [kcal mol^{-1}].

	AN	DN
Et_2O	3.9	20.0
THF	8.0	19.2
DME	10.2	24

To know the solvation of the monolithiated Li[1,2-$C_2B_{10}H_{11}$] species in the three different solvents, we have calculated their solvation free energies by using the microsolvation model.[13] This model is the most favorable one to study the solvation of lithiated species in solvents that can form solvated complexes with Li^+. For this, the model structures **I**, **IV**, and **V** (see Figures 2 and 3) were used. When solvation by the explicit solvent molecules is considered, the stabilizing effect of DME, with a solvation energy of −7.87 kcal mol, is twice as large than those of THF

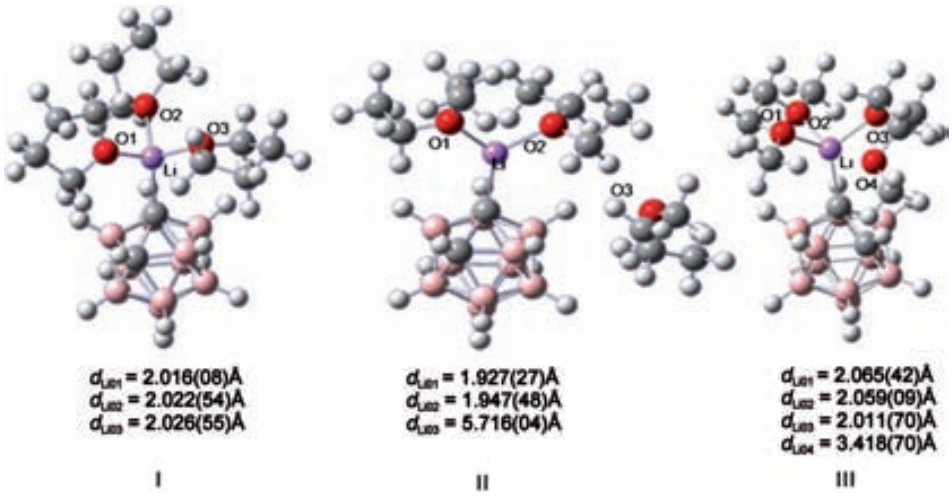

Figure 2. Optimized structures for Li[1,2-$C_2B_{10}H_{11}$] with the explicit coordination solvent molecules: **I** with THF, **II** with Et_2O, **III** with DME.

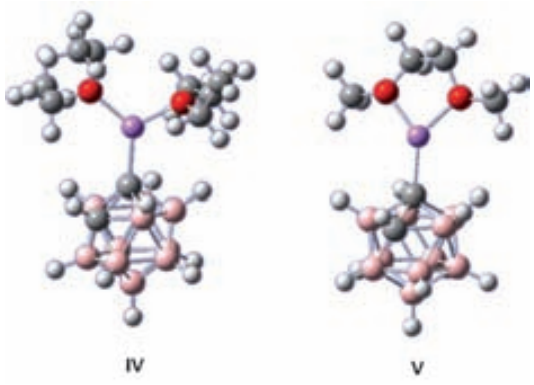

Figure 3. Optimized structures for Li[1,2-$C_2B_{10}H_{11}$] after exclusion of uncoordinated solvent molecules: **IV** with Et_2O and **V** with DME.

(−3.29 kcal mol) or Et_2O (−2.87 kcal mol). These results, however, do not take into consideration the second solvation sphere, because the bulk solvent effects are not adequately represented by microsolvation. These results are in agreement with the qualitative description about the donor and acceptor numbers given at the beginning of the section.

Ethereal solvent impact in the carboranyllithium self-reaction: To learn about the influence of the ethereal solvents in the formation of carboranyllithium species, we used multinuclear NMR spectroscopy to monitor the evolution of carboranyllithium in these solvents. NMR spectroscopy has been a useful tool for the characterization of boranes, carboranes, and metallacarborane clusters over the years.[14] The sensitivity of the electron distribution in carboranes to the presence of substituents has long been apparent[5h,15] and it is manifested in the ^{11}B NMR spectra. Figure 4 displays the differences in the $^{11}B\{^1H\}$-NMR spectra of the three species (1,2-$C_2B_{10}H_{12}$, Li[$C_2B_{10}H_{11}$] and Li_2[$C_2B_{10}H_{10}$]) involved in the equilibrium of Scheme 1.

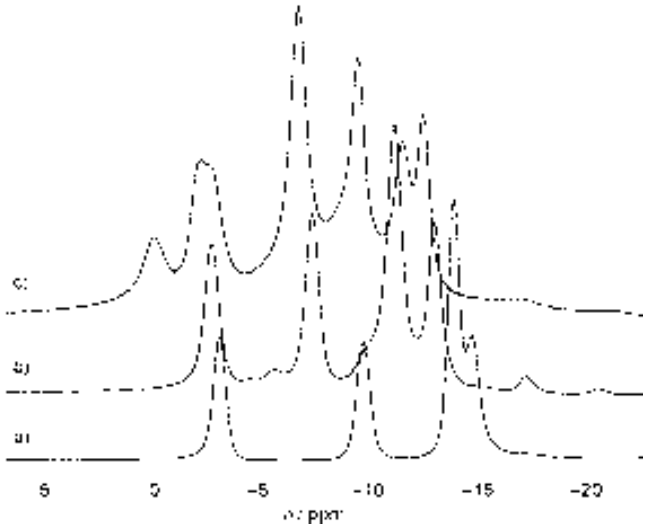

Figure 4. $^{11}B\{^1H\}$-NMR spectra of a) 1,2-$C_2B_{10}H_{12}$, b) Li[1,2-$C_2B_{10}H_{11}$], and c) Li_2[1,2-$C_2B_{10}H_{10}$] in THF.

The ^{7}Li-NMR spectra show a single resonance in the three solvents (Figure 5). A sharp peak appears at −0.40 ppm when using Et_2O as solvent. This moves upfield to −1.32 ppm in both THF and DME. These experimental values fully agree with acceptor and donor numbers of the studied ethereal solvents.

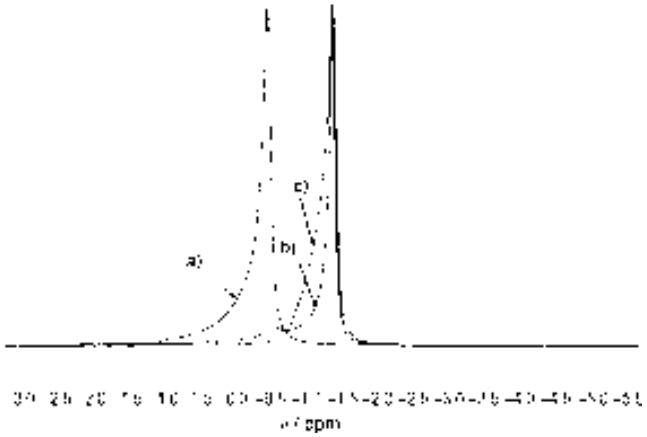

Figure 5. ^{7}Li-NMR spectra of Li[1,2-$C_2B_{10}H_{11}$] in a) Et_2O, b) THF, and c) DME.

Conversely, the $^{11}B\{^1H\}$-NMR spectra show different features in the different ether solvents; in Et_2O, a pattern with five resonances is observed (Figure 6), whereas in THF and

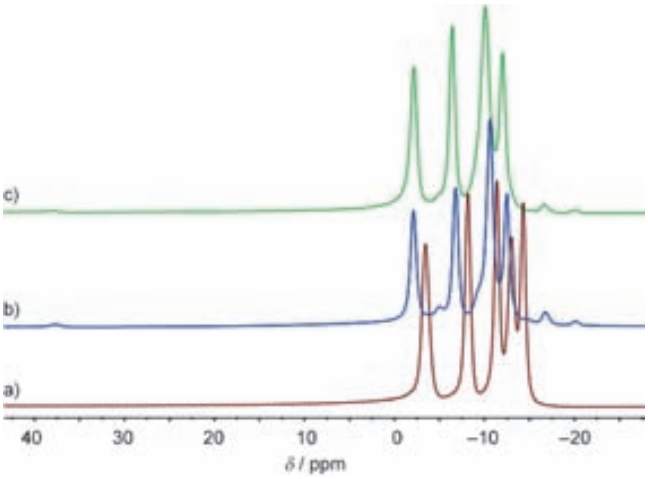

Figure 6. $^{11}B\{^1H\}$-NMR spectra of Li[1,2-$C_2B_{10}H_{11}$] in a) Et_2O, b) THF, and c) DME.

DME, a four-resonance pattern is exhibited. Besides this main pattern, a second set of peaks with lower intensity spread in the interval +37.5 to −20.5 ppm is also found in THF and DME. All peaks of the minor pattern generate doublets in the ^{11}B NMR spectra indicating that every B atom is bonded to one *exo*-cluster hydrogen. Fox et al.[16] have reported a compound with the same pattern, formed

after mixing 1,2-$C_2B_{10}H_{12}$ with N-heterocyclic carbenes. In this case, the carbene removes a proton from a C_c–H bond generating the $[C_2B_{10}H_{11}]^-$ ion; this in turn attacks a second molecule of *o*-carborane at the most positive charged vertex B(3), forming an anion that contains two clusters, $[C_4B_{20}H_{23}]^-$ (Scheme 4). Based on DFT calculations,[16] it

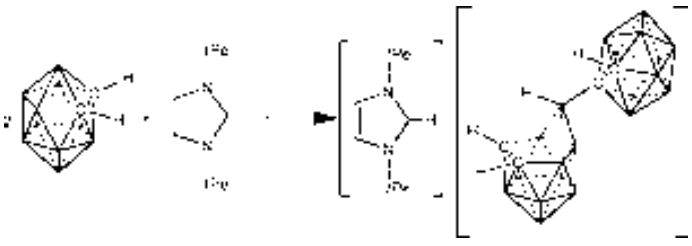

Scheme 4. Carbene-mediated formation of $[C_4B_{20}H_{23}]^-$ as described in reference [16].

was shown there that the imidazolium salt of the discrete $[C_2B_{10}H_{11}]^-$ is less favorable by 13.3 kcal mol^{-1} than the adduct that results between the carbene and the $[C_2B_{10}H_{11}]^-$ ion through the interaction C_c–H···C(carbene). Thus, our interpretation is that in our case the in situ formed $[C_2B_{10}H_{11}]^-$ ion attacks a second carborane molecule. The non-appearance of the minor pattern in Et_2O indicates that a contact ion pair between Li^+ and $[C_2B_{10}H_{11}]^-$ is formed in this solvent, which in the absence of an electrophile in the solution remains without alteration. Et_2O was not good for the reaction with sulfur, and is not good either for the carboranyllithium self-reaction. In the reactions with no halide generation the best solvent was THF or DME; such reactions occur in a similar manner as the carboranyllithium self-reaction. The persistence of a large quantity of unreacted $[C_2B_{10}H_{11}]^-$ upon the monolithiation of the *o*-carborane in THF or DME indicates that even in these solvents, Li[1,2-$C_2B_{10}H_{11}$] is still present mainly as a contact ion pair. We consider that the alternative separated ion pair cannot exist as such in solution, due to its high reactivity; as soon as it would be formed it would attack a second molecule of Li[1,2-$C_2B_{10}H_{11}$] to produce $[LiC_4B_{20}H_{22}]^-$. To support our argumentation and enhance the nucleophilicity of $[C_2B_{10}H_{11}]^-$ we added KBr or KI to the THF solution, and the mixture was heated at reflux overnight. The ^{11}B NMR and $^{11}B\{^1H\}$-NMR analysis (Figure 7) of the crude reaction mixture demonstrated that the equilibrium presented in

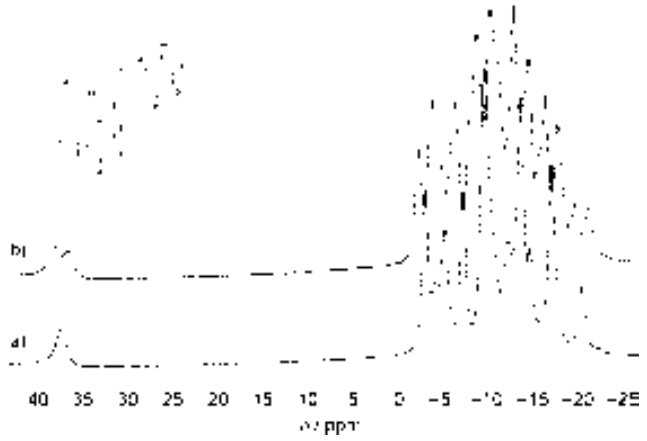

Figure 7. a) $^{11}B\{^1H\}$-NMR and b) ^{11}B NMR spectra of $[LiC_4B_{20}H_{22}]^-$.

Scheme 5 is shifted to the formation of $[LiC_4B_{20}H_{22}]^-$. Furthermore, if a solution of Li[1,2-$C_2B_{10}H_{11}$] in THF is left for 60 h at room temperature in the presence of carbon tetraiodide, $[LiC_4B_{20}H_{22}]^-$ is generated in high yield.

The self-attack of the discrete $[C_2B_{10}H_{11}]^-$ ion was also observed for the reaction of 1-CH_3-1,2-$C_2B_{10}H_{11}$ with *n*BuLi in THF and DME. The $^{11}B\{^1H\}$-NMR spectrum of the lithiated Li[1-CH_3-1,2-$C_2B_{10}H_{11}$] species shows a main pattern of three signals in the region between −1.9 and −8.9 ppm, and a second pattern of six other signals of low intensity in the range +34 to −19 ppm. In the ^{11}B NMR spectrum all these peaks were identified as doublets, indicating the presence of the same type of anion formed by two clusters, $[Li(CH_3)_2C_4B_{20}H_{20}]^-$.

These results evidence that the carboranyllithium species formed after the reaction of carboranyl derivatives with *n*BuLi has a major ratio of contact ion pair over separated ion pair in ethereal solvents, but a larger ratio in Et_2O than in THF or DME. Therefore the nucleophilicity of the carboranyllitium, and most probably of other lithiated compounds, can be tuned by the adequate choice of the ethereal solvent utilized. This nucleophilicity can be further enhanced, at will, by the synergy with potassium salts (KBr or KI), in a manner similar to the LiCl modulation of Grignard reagents successfully achieved by Knochel and co-workers, for example, *i*PrMgCl·LiCl and *s*BuMgCl·LiCl.[17]

Molecular approach to the nucleophilicity of carboranyllithium in ethereal solvents: Understanding the reactivity of organolithium compounds modulated by the solvent is particu-

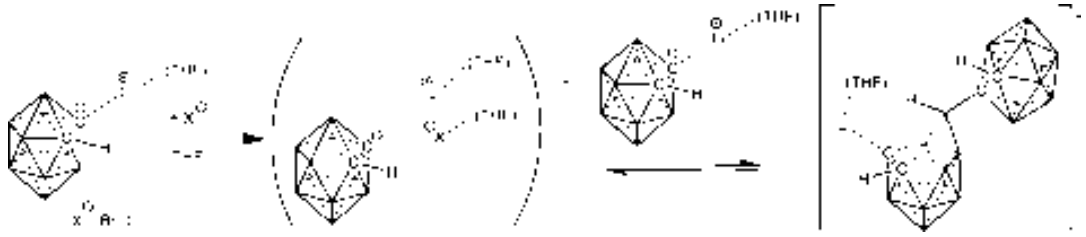

Scheme 5. Reaction of carboranyllithium with halides in THF.

larly difficult because:[18] 1) the solvent has a dual activity as medium and as ligand; 2) lithium compounds may aggregate in solution; 3) lithium can have coordination numbers ranging from 1 to 12; 4) solvent exchange can take place extremely rapidly; 5) competitive and cooperative (mixed) solvation processes occur when solvent mixtures are employed; and 6) the limits of primary and secondary solvation shells are not well defined.

Although the coordination number of Li^+ is very wide, typically a Li^+ ion is surrounded by four coordinating entities as found either in solution or in solid state.[1a,19] Therefore, as a first approach to study the nucleophilicity of carboranyllithium in ethereal solvents by computational methods, we will take a coordination number of four, as this is the most common Li^+ coordination number. In addition, the crystallographic entries in the Cambridge Data Base (CSD)[20] about crystalline structures that contain the $[C_2B_{10}H_{11}]^-$ anion have been explored.[21] Only two crystal structures (CIRFIS and FOFGEM) were found, and in both cases the carborane moiety coordinates to a metal (Li or Mg).

Presumably, Li[1,2-$C_2B_{10}H_{11}$] can be present in solution either as a contact ion pair or as a solvent-separated ion pair. If Li[1,2-$C_2B_{10}H_{11}$] is in solution as contact ion pair, it would be expected that Li was solvated to three solvent molecules according to the more common coordination number of Li^+. This might be the case for mono ethers like THF or Et_2O, but not for DME, which has two oxygen atoms. For DME there would be one or two molecules solvating the Li moiety. Therefore we optimized the structures with three THF, three Et_2O, and two DME molecules. The optimized structures (**I**, **II** and **III**) are shown in Figure 2. We observe that only one structure accommodates three solvent molecules, that is, that with THF (**I**). For Et_2O (**II**) the energy minimum was found for a structure that contains only two ether molecules solvating the lithium. The other molecules are at a distance 1.5 times larger than the sum of the van der Waals radii between Li and O.[22] For DME (**III**), there are three coordinating oxygen atoms, whereas the fourth is at a distance a little bit farther than the sum of the van der Waals radii. These results prompted us to optimize 1-Li(solvent)$_x$-1,2-$C_2B_{10}H_{11}$, for Li coordinated to two molecules of Et_2O (**IV**) and for Li coordinated to one molecule of DME (**V**), respectively (Figure 3). The theoretical O–Li distance in **IV** was 1.924(36) Å. For DME, the O–Li distance was found to be larger, 1.946(09) Å. The C_c–Li distances decreased in the order: **I** (2.133(72)) > **IV** (2.059(44)) > **V**(2.016(66) Å). The experimental C_c–Li distance is 2.176(8) Å in the reported crystal structure for 1-Li-(PMDTA)-2-Me-1,2-$C_2B_{10}H_{10}$.[21a]

To support these computed structures with experimental evidence, the theoretical $^{11}B\{^1H\}$-NMR spectra for the optimized geometries were calculated and compared with the experimental $^{11}B\{^1H\}$-NMR spectra for the carboranyl lithiated compounds in the ethereal solvent (Figure 8). As can be observed from Figure 8b, the computed spectrum for **IV** matches the experimental one very well, displaying five resonances. Conversely, the calculated spectra for **I** and **V** (Figure 8a and c) display some similarities with the experimental ones, but do not match as properly as for **IV**, because in both cases the computed spectra display a different number of peaks (six and five, respectively) to those of the experimental ones (four).

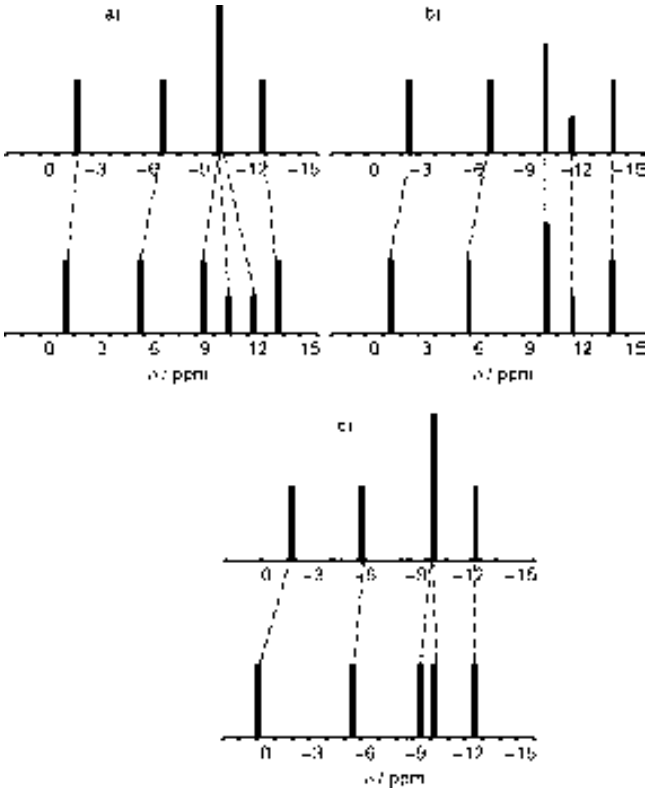

Figure 8. Experimental (upper trace) and computed (lower trace) $^{11}B\{^1H\}$-NMR spectra for Li[1,2-$C_2B_{10}H_{11}$] in a) THF, b) Et_2O, and c) DME.

As a proof of concept the $^{11}B\{^1H\}$-NMR computed spectrum for [Li(Et_2O)$_3$][1,2-$C_2B_{10}H_{11}$] (**II**) was also calculated and compared with that for [Li(Et_2O)$_2$][1,2-$C_2B_{10}H_{11}$] (**IV**), see Figure 9. Despite having the same solvent, the calculated spectra for **II** does not parallel the experimental spectrum of Li[1,2-$C_2B_{10}H_{11}$] in Et_2O (Figure 8b, top), a fact that supports the adequacy of the method.

To our view the good matching of the computed and experimental $^{11}B\{^1H\}$-NMR spectra for [Li(Et_2O)$_2$][1,2-$C_2B_{10}H_{11}$] (**IV**) agrees well with all the previous experimen-

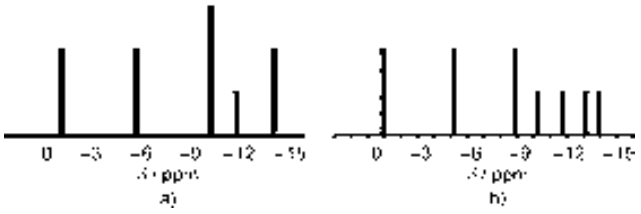

Figure 9. Computed $^{11}B\{^1H\}$-NMR spectra for a) [Li(Et_2O)$_2$][1,2-$C_2B_{10}H_{11}$] (**IV**) and b) [Li(Et_2O)$_3$][1,2-$C_2B_{10}H_{11}$] (**II**).

tal evidence, and confirms that the calculated structure containing a C_c–Li covalent bond is the structure formed in Et_2O. In fact, the Et_2O is the ethereal solvent that has lower AN than THF or DME, and thus is more likely of to support the production of a contact ion pair between Li^+ and $[C_2B_{10}H_{11}]^-$. On the other hand, THF and DME have larger DNs and ANs than Et_2O, and therefore are more suitable to have a larger component of solvent-separated ion pairs. Again, there is a correlation between these experimental values and the acceptor and donor numbers of the studied ethereal solvents. Of the five optimized structures only **IV** meets the experimental criteria discussed, that is, a contact ion pair for the solvent studied; conversely, the structures **I** and **V** do not properly represent the contact/solvent-separated ion-pair concept, and for that reason the calculated and experimental spectra do not match satisfactorily.

Post reaction Li^+ influence—reaction of carboranyllithium with allylbromide: The preceding experimental and theoretical results have led to an understanding of the factors that govern the formation of Li^+ contact or solvent-separated ion pairs. As an application of these considerations, we have studied the reaction of Li[1,2-$C_2B_{10}H_{11}$] with an alkyl halide (RX), capable of producing a C_c–C bond, lithium halide and in addition, for the purpose of this section, susceptible to interactions with the Li^+ polarizing ion. With this aim, we chose CH_2=$CHCH_2Br$ and the three solvents Et_2O, THF, and DME. To confirm the results obtained with Li,[1,2-$C_2B_{10}H_{11}$] we extended the study to other C_c-substituted carboranes, such as Li[2-R-1,2-$C_2B_{10}H_{10}$] (R = Me, Ph). In all reactions the concentration of *o*-carborane was 0.30 mol L^{-1}.

The general procedure for these reactions consists in mixing the corresponding carborane with one equivalent of *n*BuLi at 0 °C, to produce the monolithium salt,[23] and subsequently add the stoichiometric amount of CH_2=$CHCH_2Br$. The reaction was also performed at different temperatures (Table 4). Considering that the expected mechanism for the reaction with CH_2=$CHCH_2Br$ should be basically similar to the reaction of carboranyl lithium with $ClPPh_2$, of the three solvents the best performing should be Et_2O and indeed this is the case. As can be observed in Table 4, from data gathered from ^{1}H NMR spectra, for all carboranes 1-R-1,2-$C_2B_{10}H_{11}$ (R = H, Me, Ph) the reaction in Et_2O led to the C_c–CH_2CH=CH_2-substituted compound as a unique product; no isomerization occurred. Nevertheless, when THF or DME were used as solvents a mixture of isomers was obtained, with either the fragments C_c–CH_2CH=CH_2 (allyl isomer) or C_c–CH=$CHCH_3$ (propenyl isomer), respectively. The ratio of the propenyl versus the allyl isomer depends on the solvent and reaction temperatures, the propenyl isomer being most favored at higher temperatures. For example, in THF at 70 °C the ratio allyl/propenyl is 1:1; at 40 °C the ratio has decreased to 4:1, whereas at room temperature a ratio of 7:1 was obtained according to the ^{1}H NMR spectra. The importance of crowdedness near the reaction site for the isomerization process can be well visualized comparing different 1-R-1,2-$C_2B_{10}H_{11}$carboranes (R = H, Me, Ph). Interestingly, the degree of isomerization allyl/propenyl parallels the bulkiness of the R group. Thus, in the most favorable conditions, the percentage of isomerization is 15, 50, and 60 % for R = H, Me, and Ph, respectively.

Table 4. Reaction of Li[2-Me-1,2-$C_2B_{10}H_{10}$], Li[2-Ph-1,2-$C_2B_{10}H_{10}$], and Li[1,2-$C_2B_{10}H_{10}$] with CH_2=CH-CH_2Br in various solvents.

	T [°C]	Allyl [%][a]
Li[2-Me-1,2-$C_2B_{10}H_{10}$]		
THF	70	50
THF	40	80
THF	25	86
ether/toluene (1:2)	100	100
ether/toluene (1:2)	40	100
ether	40	100
DME	85	66
DME	40	75
Li[2-Ph-1,2-$C_2B_{10}H_{10}$]		
THF	70	40
DME	85	50
ether	40	100
ether/toluene (1:2)	100	100
toluene	110	unknown mixture
Li[1,2-$C_2B_{10}H_{11}$]		
THF	70	95
DME	85	85
ether	40	100
ether/toluene (1:2)	100	100
toluene	110	unknown mixture

[a] Percentage of C–allyl in a 100 % conversion reaction.

To the best of our knowledge this isomerization reaction has not previously been reported mediated by Li^+. This isomerization usually proceeds by acid, base, or organometallic complexes, giving, in general, the thermodynamically stable product.[24] Our view of the phenomenon relates again with the donor and acceptor numbers (DN, AN), characteristics of the solvent, and also to the formation of Li^+ contact ion pair. As for $ClPPh_2$, the substitution of the bromine atom in CH_2=$CHCH_2Br$ by the $[1\text{-R-}C_2B_9H_{10}]^-$ ion most probably follows a S_N2 mechanism (Scheme 6). Our interpretation is that one intermediate similar to that shown in Scheme 6 is formed in which the interactions of the $[1\text{-R-}C_2B_9H_{10}]^-$ and Li^+ ions with CH_2=$CHCH_2Br$ are very relevant. They depend largely on the degree of contact ion pairs formed, which in its turn depends on the solvent. In Et_2O, the solvent with the lowest AN, the carboranyl acts as a stronger nucleophile than in THF, facilitating the interaction with the electrophile to quickly remove the bromine and give the pure allyl–carborane derivative. In contrast, when THF or DME are used, due to a larger degree of solvent-separated ion pairs formed, the Li^+ is more prone to interact with the allyl system, easing the isomerization. The resulting cation interacts subsequently with the carboranyl fragment leading to the formation of the C_c–C bond. We consider that the isomerization and the C_c–C bond formation occur sequentially on the reaction timescale. In favor of this is the fact that the allyl does not isomerize when placed in contact with Li^+, even in DME.

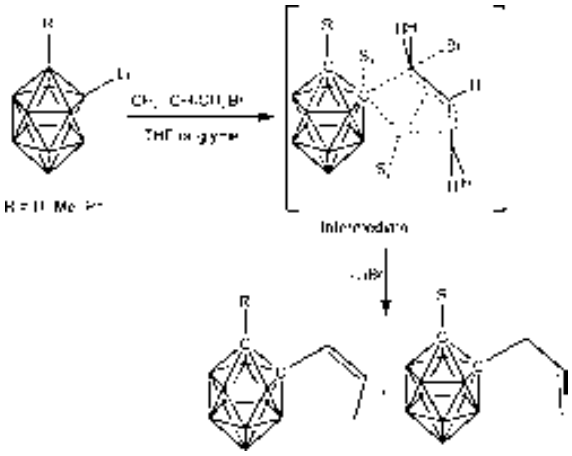

Scheme 6. Reaction of carboranyllithium with CH_2=CH-CH_2Br.

Conclusion

The disproportionation of Li[1,2-$C_2B_{10}H_{11}$] into Li_2[1,2-$C_2B_{10}H_{10}$] and 1,2-$C_2B_{10}H_{12}$ in ethereal solvents is a consequence of the formation of contact ion pairs, and to a lesser extent of solvent-separated ion pairs. In the contact ion pair, a large degree of covalent C_c–Li(solvated) bonding can be assumed. Contact ion pairs are generated in all the solvents studied; however THF and DME tend to produce carboranyllitium ion pair with a slightly higher degree of separated ion pairs than Et_2O. The different degree of contact or separated ion pairs is significant to facilitate mono- or disubstitution, but strongly influenced by the reagent type. In reactions in which a halide is generated as with $ClPPh_2$ or $BrCH_2CH{=}CH_2$, Et_2O appears to produce the largest degree of monosubstitution. In other situations, such as with S_8, or when no halide is generated, THF or DME facilitate the largest degree of monosubstitution. It has been shown upon the self-reaction of Li[1,2-$C_2B_{10}H_{11}$] to produce $[LiC_4B_{20}H_{22}]^-$, the nucleophilicity of the carboranyllithium can even be further enhanced, in addition to the ether solvent used, by synergism with halide salts. The mediation of Li^+ in producing isomerization has also been demonstrated to be dependent on the ether solvent utilized. Et_2O tends to not induce isomerization on allyl substituents; conversely THF or DME produces isomerization. The results presented here most probably can be extended to other molecular types to interpret the Li^+ mediation in C–C or other C–X coupling reactions.

Experimental Section

Instrumentation: The ^{1}H NMR (300.13 MHz), ^{11}B- and ^{11}B{^{1}H}-NMR (96.29 MHz) and ^{7}Li-NMR (116.64 MHz) spectra were recorded on a Bruker ARX 300 instrument equipped with the appropriate decoupling accessories. All NMR spectra were performed at 22 °C. The ^{11}B- and ^{11}B{^{1}H}-NMR spectra were referenced to external $BF_3{\cdot}OEt_2$, while the ^{1}H NMR spectra were referenced to $SiMe_4$ and the ^{7}Li-NMR spectra to 1 M LiCl aqueous solution. Chemical shifts are reported in units of parts per million downfield from reference. The samples were run in deuterated chloroform ($CDCl_3$) or in double tube with $(CD_3)_2CO$ in the inner one.

Materials: All manipulations were carried out under inert atmosphere. THF, EtO_2, and DME were distilled from sodium benzophenone prior to use. Reagents were obtained commercially and used as purchased. 1,2-$C_2B_{10}H_{12}$, 1-Me-1,2-$C_2B_{10}H_{11}$ and 1-Ph-1,2-$C_2B_{10}H_{11}$ were obtained from Katchem.

General procedure for the reaction with S_8 or $ClPPh_2$: A solution of 1,2-$C_2B_{10}H_{12}$ (0.23 mol L^{-1} or 0.07 mol L^{-1}) in ethereal solvent (Et_2O, THF, DME) was cooled at the target temperature for a half an hour. Subsequently, *n*BuLi (1 equiv, 1.6 mol L^{-1} in hexanes) was added dropwise and the mixture was kept at low temperature, with stirring, for two hours. Then, sulfur or chlorodiphenylphosphine (1 equiv) was added and the mixture was further kept at low temperature with stirring. Then the cooling bath was removed and the mixture was stirred for additional 30 min until the room temperature was reached. The solvent was evaporated and diethyl ether was added. Then, the solution was cooled on an ice bath (0 °C) and hydrochloric acid (0.1 M, 5 mL) was added. The two phases were separated. The organic phase was washed three times with water and the acidic phase was washed three times with diethyl ether. The combined organic phases were dried over $MgSO_4$ and filtered, and the solvent was removed under reduced pressure.

General procedure for the reaction with CH_2=$CHCH_2$Br: *n*BuLi (1 equiv, 1.6 mol L^{-1} in hexanes) was added dropwise to a solution of 1,2-$C_2B_{10}H_{12}$, 1-Me-1,2-$C_2B_{10}H_{11}$ or 1-Ph-1,2-$C_2B_{10}H_{11}$ (0.30 mol L^{-1}) in ethereal solvent (Et_2O, THF, DME) at 0 °C. The mixture was kept at low temperature, with stirring, for 1 h. Subsequently, CH_2=$CHCH_2$Br (1 equiv) was added; the mixture was stirred for 1 h at room temperature and heated to reflux overnight. After that, the mixture was cooled down at room temperature, quenched with H_2O (20 mL), transferred to a separating funnel and extracted with Et_2O (4×10 mL). The organic layer was dried over $MgSO_4$ and the volatiles were reduced under vacuum.

Computational details: Quantum-chemical calculations were performed with the Gaussian 03[25] commercial suite of programs at DFT level of theory with B3LYP hybrid functional[26] adopting for all the atoms the 6-31G+(d,p) basis set.[27] The programs Gabedit 2.2.6[28] and GaussView 3.0[29] were used to visualize the optimized structures. All the calculations were performed in computational clusters with workstations with eight processors Intel Xeon Six-Core X5670 of 2.93 GHz and 24 GB of RAM, or with 128 processors Intel Itanium 2 of 1.6 GHz and 512 GB of RAM.

Acknowledgements

This work has been supported by Ministerio de Ciencia e Innovación (CTQ2010-16237) and Generalitat de Catalunya (2009/SGR/00279). A.-R.P. and A.D.M. thank the Ministerio de Ciencia e Innovación for a FPU grant, A.F.-U. thanks the AGAUR (Generalitat de Catalunya) for a FI grant. The access to the computational facilities at the High-Performance Computing Centre of CSIC and Centre de Serveis Científics i Acadèmics de Catalunya (CESCA) is gratefully acknowledged.

[1] a) V. H. Gessner, C. Däschlein, C. Strohmann, *Chem. Eur. J.* **2009**, *15*, 3320–3334; b) C. M. Whisler, S. MacNeil, V. Snieckus, P. Beak, *Angew. Chem.* **2004**, *116*, 2256–2276; *Angew. Chem. Int. Ed.* **2004**, *43*, 2206–2225.

[2] a) A. Abbotto, A. Streitwieser, P. V. R. Schleyer, *J. Am. Chem. Soc.* **1997**, *119*, 11255–11268; b) L. M. Pratt, S. Mogali, K. Glinton, *J. Org. Chem.* **2003**, *68*, 6484–6488; c) L. M. Pratt, S. C. Nguyen, B. T. Thanh, *J. Org. Chem.* **2008**, *73*, 6086–6091; d) A. J. Streitwieser, *J. Mol. Model.* **2006**, *12*, 673–680; e) L. M. Pratt, *THEOCHEM* **2007**, *811*, 191–196; f) N. Deora, P. R. Carlier, *J. Org. Chem.* **2010**, *75*, 1061–1069; g) A. Streitwieser, J. R. Reyes, T. Singhapricha, S. Vu, K. Shah, *J. Org. Chem.* **2010**, *75*, 3821–3830; h) H. K. Khartabil,

P. C. Gros, Y. Fort, M. F. Ruiz-Lopez, *J. Org. Chem.* **2008**, *73*, 9393–9402.

[3] a) H. J. Reich, J. E. Holladay, J. D. Mason, W. H. Sikorski, *J. Am. Chem. Soc.* **1995**, *117*, 12137–12150; b) H. J. Reich, W. H. Sikorski, *J. Org. Chem.* **1999**, *64*, 14–15; c) H. J. Reich, A. W. Sanders, A. T. Fiedler, M. J. Bevan, *J. Am. Chem. Soc.* **2002**, *124*, 13386–13387; d) W. H. Sikorski, H. J. Reich, *J. Am. Chem. Soc.* **2001**, *123*, 6527–6535; e) T. Cohen, W. D. Abraham, M. Myers, *J. Am. Chem. Soc.* **1987**, *109*, 7923–792; f) S. Gronert, A. Streitwieser, *J. Am. Chem. Soc.* **1988**, *110*, 2836–2842; g) E. Buncel, B. Menon, *J. Org. Chem.* **1979**, *44*, 317–320; h) M. Håkansson, C. H. Ottosson, A. Boman, D. Johnels, *Organometallics* **1998**, *17*, 1208–1214; i) S. Neander, J. Kornich, F. Olbrich, *J. Organomet. Chem.* **2002**, *656*, 89–96; j) I. Fernández, E. Matrínez-Vivente, F. Breher, P. S. Pregosin, *Chem. Eur. J.* **2005**, *11*, 1495–1506; k) I. Keresztes, P. G. Williard, *J. Am. Chem. Soc.* **2000**, *122*, 10228–10229; l) H. K. Khartabil, P. C. Gros, Y. Fort, M. F. Ruiz-Lopez, *J. Am. Chem. Soc.* **2010**, *132*, 2410–2416.

[4] L. I. Zakharkin, A. V. Grebennikov, A. V. Kazantzev, *Izv. Akad. Nauk SSSR Ser. Khim.* **1967**, 2077–2078; *Bull. Acad. Sci. USSR Div. Chem. Sci.* **1967**, *16*, 1994–1996.

[5] For reviews see: a) J. Plesek, *Chem. Rev.* **1992**, *92*, 269–278; b) M. F. Hawthorne, A. Maderna, *Chem. Rev.* **1999**, *99*, 3421–3434; c) J. F. Valliant, K. J. Guenther, S. Arienne, S. King, P. Morel, P. Schaffer, O. O. Sogbein, K. A. Stephenson, *Coord. Chem. Rev.* **2002**, *232*, 173–230; d) F. Teixidor, C. Viñas, A. Demonceau, R. Núñez, *Pure Appl. Chem.* **2003**, *75*, 1305; e) I. T. Chizhevsky, *Coord. Chem. Rev.* **2007**, *251*, 1590–1619; f) L. Deng, Z. W. Xie, *Coord. Chem. Rev.* **2007**, *251*, 2452–2476; g) I. B. Sivaev, V. I. Bregadze, *Eur. J. Inorg. Chem.* **2009**, 1433–1450; h) *Carboranes* 2nd ed. (Ed.: R. N. Grimes) Academic Press (Elsevier), London, **2011**; i) *Boron Science: New Technologies and Applications* (Ed.: N. S. Hosmane), CRC, Boca Raton, FL, **2011**.

[6] a) P. A. Wender, B. L. Miller, *Nature* **2009**, *460*, 197–201; b) T. Newhouse, P. S. Baran, R. W. Hoffmann, *Chem. Soc. Rev.* **2009**, *38*, 3010–3021.

[7] F. A. Gomez, M. F. Hawthorne, *J. Org. Chem.* **1992**, *57*, 1384–1390.

[8] C. Viñas, R. Benakki, F. Teixidor, J. Casabo, *Inorg. Chem.* **1995**, *34*, 3844–3845.

[9] a) R. Kivekäs, R. Sillanpää, F. Teixidor, C. Viñas, R. Núñez, *Acta Crystallogr. Sect. C* **1994**, *50*, 2027–2030; b) F. Teixidor, C. Viñas, J. Casabó, A. M. Romerosa, J. Rius, C. Miravitlles, *Organometallics* **1994**, *13*, 914–919; c) R. Kivekäs, F. Teixidor, C. Viñas, R. Nuñez, *Acta Crystallogr. Sect. C* **1995**, *51*, 1868–1870; d) F. Teixidor, C. Viñas, R. Benakki, R. Kivekäs, R. Sillanpää, *Inorg. Chem.* **1997**, *36*, 1719–1723; e) R. Núñez, C. Viñas, F. Teixidor, R. Sillanpää, R. Kivekäs, *J. Organomet. Chem.* **1999**, *592*, 22–28; f) A. S. Batsanov, M. A. Fox, T. G. Hibbert, J. A. K. Howard, R. Kivekäs, A. Laromaine, R. Sillanpää, C. Viñas, K. Wade, *Dalton Trans.* **2004**, 3822–3828; g) A. R. Popescu, A. Laromaine, F. Teixidor, R. Sillanpää, R. Kivekäs, J. I. Llambias, C. Viñas, *Chem. Eur. J.* **2011**, *17*, 4429–4443.

[10] V. Gutmann, *Coord. Chem. Rev.* **1976**, *18*, 225–255.

[11] a) B. Leroy, I. E. Marko, *J. Org. Chem.* **2002**, *67*, 8744–8752; b) A. R. Katritzky, Y.-J. Xu, R. Jian, *J. Org. Chem.* **2002**, *67*, 8234–8236; c) G. Fraenkel, J. H. Duncan, K. Martin, J. Wang, *J. Am. Chem. Soc.* **1999**, *121*, 10538–10544; d) A. Streitwieser, E. Juaristi, Y.-J. Kim, J. Pugh, *Org. Lett.* **2000**, *2*, 3739–3374; e) D. Hoffmann, D. B. Collum, *J. Am. Chem. Soc.* **1998**, *120*, 5810–5811.

[12] a) H. Gérard, A. de La Lande, J. Maddalunu, O. Parisel, M. E. Tuckerman, *J. Phys. Chem. A* **2006**, *110*, 4787–4794; b) R. Declerck, B. De Sterck, T. Verstraelen, G. Verniest, S. Mangelinckx, J. Jacobs, N. De Kimpe, M. Waroquier, V. Van Speybroeck, *Chem. Eur. J.* **2009**, *15*, 580–584.

[13] a) L. M. Pratt, B. Ramachandran, J. D. Xidos, C. J. Cramer, D. G. Truhlar, *J. Org. Chem.* **2002**, *67*, 7607–7761; b) L. M. Pratt, R. Mu, *J. Org. Chem.* **2004**, *69*, 7519–7524; c) L. M. Pratt, R. Mu, D. R. Jones, *J. Org. Chem.* **2005**, *70*, 101–104; d) L. M. Pratt, D. G. Truhlar, C. J. Cramer, S. R. Kass, J. D. Thompson, J. D. Xidos, *J. Org. Chem.* **2007**, *72*, 2962–2966; e) L. M. Pratt, D. Jones, A. Sease, D. Busch, E. Faluade, S. C. Nguyen, B. T. Thanh, *Int. J. Quantum Chem.* **2009**, *109*, 34–42; f) D. D. Dixon, M. A. Tius, L. M. Pratt, *J. Org. Chem.* **2009**, *74*, 5881–5886.

[14] L. J. Todd, A. R. Siedle, *Prog. Nucl. Magn. Reson. Spectrosc.* **1979**, *13*, 87–176.

[15] a) S. Heřmánek, J. Plešek, V. Gregor, B. Štíbr, *J. Chem. Soc. Chem. Commun.* **1977**, 561–563; b) V. I. Stanko, T. A. Babushkina, T. P. Klimova, Y. U. Goltyapin, A. I. Klimova, A. M. Vasilev, A. M. Alymov, V. V. Khrapov, *Zh. Obshch. Khim.* **1976**, *46*, 1071–1079; c) F. Teixidor, C. Viñas, R. W. Rudolph, *Inorg. Chem.* **1986**, *25*, 3339–3345.

[16] C. E. Willans, C. A. Kilner, M. A. Fox, *Chem. Eur. J.* **2010**, *16*, 10644–10648.

[17] a) F. M. Piller, P. Appukkuttan, A. Gavryushin, M. Helm, P. Knochel, *Angew. Chem.* **2008**, *120*, 6907–6911; *Angew. Chem. Int. Ed.* **2008**, *47*, 6802–6806; b) C. J. Rohbogner, G. C. Clososki, P. Knochel, *Angew. Chem.* **2008**, *120*, 1526–1530; *Angew. Chem. Int. Ed.* **2008**, *47*, 1503–1507.

[18] B. L. Lucht, D. B. Collum, *Acc. Chem. Res.* **1999**, *32*, 1035–1042.

[19] a) U. Olsher, R. M. Izatt, J. S. Bradshaw, N. K. Dalley, *Chem. Rev.* **1991**, *91*, 137–164; b) E. Weiss, *Angew. Chem.* **1993**, *105*, 1565–1587; *Angew. Chem. Int. Ed. Engl.* **1993**, *32*, 1501–1523.

[20] F. H. Allen, *Acta Crystallogr. Sect. B* **2002**, *58*, 380–388.

[21] a) W. Clegg, D. A. Brown, S. J. Bryan, K. Wade, *Polyhedron* **1984**, *3*, 307–311; b) W. Clegg, D. A. Brown, S. J. Bryan, K. Wade, *J. Organomet. Chem.* **1987**, *325*, 39–46.

[22] A. Bondi, *J. Phys. Chem.* **1964**, *68*, 441–451.

[23] a) A. González-Campo, C. Viñas, F. Teixidor, R. Núñez, R. Kivekäs, R. Sillanpää, *Macromolecules* **2007**, *40*, 5644–5652; b) A. González-Campo, E. J. Juárez-Pérez, C. Viñas, B. Boury, R. Kivekäs, R. Sillanpää, R. Núñez, *Macromolecules* **2008**, *41*, 8458–8466.

[24] a) E. N. Deryagina, N. A. Korchevin, *Russ. Chem. Bull.* **1996**, *45*, 223–225; b) H. Wakamatsu, M. Nishida, N. Adachi, M. Mori, *J. Org. Chem.* **2000**, *65*, 3966–3970.

[25] Gaussian 03, Revision E.02, M. J. Frisch, G. W. Trucks, H. B. Schlegel, G. E. Scuseria, M. A. Robb, J. R. Cheeseman, J. A. Montgomery, Jr., T. Vreven, K. N. Kudin, J. C. Burant, J. M. Millam, S. S. Iyengar, J. Tomasi, V. Barone, B. Mennucci, M. Cossi, G. Scalmani, N. Rega, G. A. Petersson, H. Nakatsuji, M. Hada, M. Ehara, K. Toyota, R. Fukuda, J. Hasegawa, M. Ishida, T. Nakajima, Y. Honda, O. Kitao, H. Nakai, M. Klene, X. Li, J. E. Knox, H. P. Hratchian, J. B. Cross, V. Bakken, C. Adamo, J. Jaramillo, R. Gomperts, R. E. Stratmann, O. Yazyev, A. J. Austin, R. Cammi, C. Pomelli, J. W. Ochterski, P. Y. Ayala, K. Morokuma, G. A. Voth, P. Salvador, J. J. Dannenberg, V. G. Zakrzewski, S. Dapprich, A. D. Daniels, M. C. Strain, O. Farkas, D. K. Malick, A. D. Rabuck, K. Raghavachari, J. B. Foresman, J. V. Ortiz, Q. Cui, A. G. Baboul, S. Clifford, J. Cioslowski, B. B. Stefanov, G. Liu, A. Liashenko, P. Piskorz, I. Komaromi, R. L. Martin, D. J. Fox, T. Keith, M. A. Al-Laham, C. Y. Peng, A. Nanayakkara, M. Challacombe, P. M. W. Gill, B. Johnson, W. Chen, M. W. Wong, C. Gonzalez, and J. A. Pople, Gaussian, Inc., Wallingford CT, **2004**.

[26] P. J. Stephens, F. J. Devlin, C. F. Chabalowski, M. J. Frisch, *J. Phys. Chem.* **1994**, *98*, 11623–11627.

[27] a) A. D. McLean, G. S. Chandler, *J. Chem. Phys.* **1980**, *72*, 5639–5648; b) R. Krishnan, J. S. Binkley, R. Seeger, J. A. Pople, *J. Chem. Phys.* **1980**, *72*, 650–654; c) J.-P. Blaudeau, M. P. McGrath, L. A. Curtiss, L. Radom, *J. Chem. Phys.* **1997**, *107*, 5016–5021; d) A. J. H. Wachters, *J. Chem. Phys.* **1970**, *52*, 1033–1036; e) P. J. Hay, *J. Chem. Phys.* **1977**, *66*, 4377–4384; f) K. Raghavachari, G. W. Trucks, *J. Chem. Phys.* **1989**, *91*, 1062–1065; g) R. C.Binning Jr., L. A. Curtiss, *J. Comput. Chem.* **1990**, *11*, 1206–1216; h) M. P. McGrath, L. Radom, *J. Chem. Phys.* **1991**, *94*, 511–516; i) L. A. Curtiss, M. P. McGrath, J.-P. Blaudeau, N. E. Davis, R. C. Binning Jr., L. Radom, *J. Chem. Phys.* **1995**, *103*, 6104–6113.

[28] A. R. Allouche, *J. Comput. Chem.* **2011**, *32*, 174–182.

[29] A. Nielsen, A. Holder, *Gauss View 3.0 User's Reference*, Gaussian Inc., Pittsburgh, PA, **2000–2003**.

Received: August 23, 2011
Published online: February 14, 2012

Accepted Manuscript

Chelation of a proton by oxidized diphosphines

Adrian-Radu Popescu, Isabel Rojo, Francesc Teixidor, Reijo Sillanpää, Mikko M. Hänninen, Clara Viñas

PII: S0022-328X(12)00407-X

DOI: 10.1016/j.jorganchem.2012.06.023

Reference: JOM 17599

To appear in: *Journal of Organometallic Chemistry*

Received Date: 29 May 2012

Revised Date: 25 June 2012

Accepted Date: 27 June 2012

Please cite this article as: A.-R. Popescu, I. Rojo, F. Teixidor, R. Sillanpää, M.M. Hänninen, C. Viñas, Chelation of a proton by oxidized diphosphines, *Journal of Organometallic Chemistry* (2012), doi: 10.1016/j.jorganchem.2012.06.023.

Graphical abstract

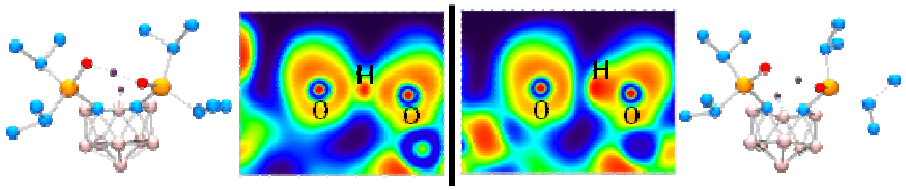

Two polymorphs (H[**1a**] and H[**1b**]) with the formula H[7,8-$(OP^iPr_2)_2$-7,8-*nido*-$C_2B_9H_{10}$] displaying different P=O···H···O=P distances have been structurally characterized. The strength of these bonds has been calculated with DFT protocols.

Graphical abstract

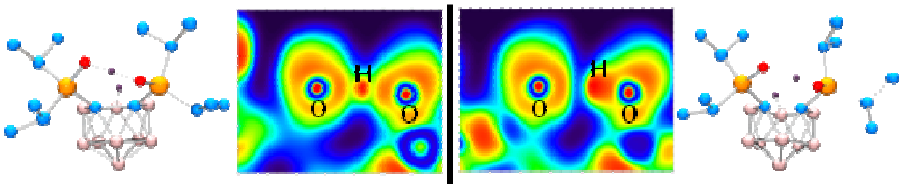

Highlights

Hydrogen bond, symmetrical or not?

Chelation of a Proton by Oxidized Diphosphines†

Adrian-Radu Popescu,[a, #] Isabel Rojo,[a] Francesc Teixidor,[a] Reijo Sillanpää,[b]

Mikko M. Hänninen[b] and Clara Viñas[a,*]

[a] Institut de Ciència de Materials de Barcelona, ICMAB-CSIC, Campus U.A.B. 08193 Bellaterra, Spain.

[b] Department of Chemistry, University of Jyväskylä, FIN-40351, Jyväskylä, Finland.

* clara@icmab.es, Fax: +34 93 580 57 29; Tel: +34 93 580 18 53

[#] enrolled in UAB PhD program.

† Dedicated to Prof. Thomas P. Fehlner on the occasion of his 75th birthday in recognition of his outstanding contributions to Inorganic and Organometallic Chemistry.

Abstract

The chelation of a proton by oxidized diphosphines is studied for the first time both experimentally and theoretically. As a proof of concept the rare case where two different H-bond systems exist in one compound, H[7,8-$(OP^iPr_2)_2$-7,8-*nido*-$C_2B_9H_{10}$] is reported. Based on NBO, QTAIM and ELF calculations, the P-O···H^+···O-P interactions were characterized as strong hydrogen bonds.

Keywords: hydrogen bond, phosphines, carboranes, oxidation, DFT calculations

1. Introducion

Hydrogen bonding plays a key role in physical, chemical and biochemical processes [1], being an important interaction in enzymatic catalysis [2], crystal engineering [3] and proton transfer reactions [4]. Interest has been directed towards the encapsulation or chelation of the proton [5], but probably the most important feature of hydrogen bonding is its role in catalysis [6]. For example, organocatalysts as BINOL-based phosphoric acids are able to catalyze Mannich reactions, aza-Friedel-Crafts alkylations, hydrophosphonylation of imines and reduction of imines [7].

A hydrogen bond is an attractive force interaction between a proton donor atom (D) to an acceptor atom (A), where both of these atoms can be of the same type (homonuclear H-bonds), usually O, N or F atoms; or of different type (heteronuclear H-bonds) like, N-H···O, O-H···N, O-H···S, S-H···O and N-H···Cl. Typically, in strong homonuclear H-bonds, the hydrogen atom resides nearly midway between the two atoms, whereas in the heteronuclear H-bonds the hydrogen atom is positioned closer to the donor than the acceptor, due to the difference in electronegativity of the two.

The strong intramolecular O-H···O bonds where the O atoms are bonded to atoms other than C and S are not so common. Ten years ago we reported the proton mediated partial degradation of 1,2-$(PPh_2)_2$-*closo*-1,2-$C_2B_{10}H_{10}$ where we demonstrated for the first time that, given the necessary chemical and geometrical conditions to produce proton chelation, the proton can also induce conversion of the *closo*-C_2B_{10} to the *nido*-$[C_2B_9]^-$ species [8]. The geometrical parameters from the X-ray crystal structure of H[7,8-$(OPPh_2)_2$-*nido*-7,8-$C_2B_9H_{10}$] showed that the oxidized diphosphine fragment does chelate a proton, presenting a strong H-bond, P=O···H···O=P, but at that time no further studies were carried out.

If one searches the Cambridge Structural Database (CSD) [9] for crystal structures having the P=O···H···O=P bond moiety (Chart 1), few structures will be found [10]. However, there are different ways how these features D-H···A can be schematically presented. In Chart 1 we propose two ways for performing the search of P=O···H···O=P bonds, which have a remarkable difference concerning the nature of the H-bonds. If mode I is used, no crystal structure can be found whereas using mode II, 139 structures will appear. On the other hand, if P atoms are replaced by C atoms and mode I is used, a large number of crystalline structures are found. This raises questions about the nature of the H-bond in oxidized diphosphine systems.

Using the search mode II one can find structures like BODVAS [11] (see S.I.), where the distance O1-H is 0.820 Å and O2-H is 2.770 Å, whereas the O1-H···O2 angle is 67.9º; there is no symmetric intramolecular H-bond. Another example is the structure NITFUR [12], in which the O1-H distance is 0.978 Å and the O2-H is 1.453 Å; in NITFUR there is an intramolecular H-bond. On the other hand the same search provides results like JUYZUY [13], where the O1-H distance is 1.170 Å and the O2-H is 1.269 Å, being more symmetric, or the structure OBUNUU [8] in which the H atom bisects the O atoms: O1-H is 1.206(5) Å and O2-H is 1.218(5) Å.

Can the intramolecular P=O···H···O=P bond be symmetric like C=O···H···O=C or is it so uncommon that it will be hardly accepted as symmetric?

In this communication we wish to make a distinction between the symmetric and asymmetric P=O···H···O=P bonds. As a proof of concept we report a rare case where two different H-bond systems exist in one compound, H[7,8-$(OP^iPr_2)_2$-7,8-*nido*-$C_2B_9H_{10}$], H[**1**]. For that purpose we have determined the X-ray crystal structures of two polymorphs, that have different P=O···H···O=P distances. To support our experimental results on the nature of the hydrogen bonds and to the underlying reasons for this

phenomena, we performed a computational study, based on Natural Bond Orbital (NBO), Quantum Theory of Atoms In Molecules (QTAIM) and Electron Localization Function (ELF) analyses.

2. Experimental Section

2.1. Materials and instrumentation

Reagents were obtained commercially and used as purchased. 1,2-(P^iPr_2)$_2$-1,2-*closo*-$C_2B_{10}H_{10}$ was synthesized as reported [14]. Elemental analyses were performed using a Carlo Erba EA1108 microanalyzer. IR spectra (ν, cm^{-1}; KBr pellets) were obtained on a Shimadzu FTIR-8300 spectrophotometer. The ^1H and $^1H\{^{11}B\}$ NMR (300.13 MHz), $^{13}C\{^1H\}$ NMR (75.47 MHz), ^{11}B and $^{11}B\{^1H\}$ NMR (96.29 MHz) and $^{31}P\{^1H\}$ NMR (121.48 MHz) spectra were recorded on a Bruker ARX 300 instrument equipped with the appropriate decoupling accessories. All NMR spectra were performed in deuterated solvents at 22ºC. The ^{11}B and $^{11}B\{^1H\}$ NMR chemical shifts were referenced to external $BF_3{\cdot}OEt_2$, while the ^1H, $^1H\{^{11}B\}$, and $^{13}C\{^1H\}$ NMR chemical shifts were referenced to $SiMe_4$ and the $^{31}P\{^1H\}$ NMR to external 85% H_3PO_4. Chemical shifts are reported in units of parts per million downfield from reference, and all coupling constants in Hz.

2.2. Synthesis of H[7,8-(OP^{i}Pr$_2$)$_2$-7,8-nido-C$_2$B$_9$H$_{10}$]

Caution!. H_2O_2 in acetone is potential explosive. On this scale and under these conditions no explosions occurred. Nevertheless, this does not preclude such an event when dealing with these species. Extreme precautions should be taken.

To a solution of 1,2-(P^iPr_2)$_2$-1,2-*closo*-$C_2B_{10}H_{10}$ (50 mg, 0.13 mmol) in THF at 0ºC was added 2.0 mL (0.40 mmol) of a solution of 0.2 M H_2O_2. The mixture was stirred for 4 h. Then this was concentrated until a white solid precipitated. The solid was filtered off and dried in vacuum. Yield: 38 mg (71 %). Anal. Calcd for $C_{14}H_{39}B_9O_2P_2$: C: 42.17, H:

9.86 %. Found: C: 41.82, H: 10.04 %. FTIR: 2995, 2973, 2936, 2877 (O-H, C-H_{alkyl}), 2629, 2596, 2587, 2581, 2543, 2552, 2536, 2526, 2608 (B-H), 1073 (P=O). ^{1}H NMR (CD_3COCD_3) δ: 2.82 (m, 2H, CH), 2.59 (m, 2H, CH), 1.47 (dd, ^{3}J(P,H)= 11, ^{3}J(H,H)= 7, 6H, Me), 1.42 (dd, ^{3}J(P,H)= 11, ^{3}J(H,H)= 7, 6H, Me), 1.37 (dd, ^{3}J(P,H)= 16, ^{3}J(H,H)= 7, 6H, Me), 1.31 (dd, ^{3}J(P,H)= 16, ^{3}J(H,H)= 7, 6H, Me), 2.49-0.68 (br s, 9H, B-H), -2.56 (br s, 1H, BHB). ^{1}H{^{11}B} NMR (CD_3COCD_3) δ: 2.82 (m, 2H, CH), 2.59 (m, 2H, CH), 2.49 (br s, 1H, B-H), 2.42 (br s, 1H, B-H), 1.77 (br s, 2H, B-H), 1.61 (br s, 3H, B-H), 1.47 (dd, ^{3}J(P,H)= 11, ^{3}J(H,H)= 7, 6H, Me), 1.42 (dd, ^{3}J(P,H)= 11, ^{3}J(H,H)= 7, 6H, Me), 1.37 (dd, ^{3}J(P,H)= 16, ^{3}J(H,H)= 7, 6H, Me), 1.31 (dd, ^{3}J(P,H)= 16, ^{3}J(H,H)= 7, 6H, Me), 0.68 (br s, 2H, B-H), -2.58 (br s, 1H, BHB). ^{13}C{^{1}H} NMR (CD_3COCD_3) δ: 16.78, 16.71, 16.67, 16.31, 16.21 (s, CH, Me). ^{11}B NMR (CD_3COCD_3): -6.2 (d, ^{1}J(B,H)= 138, 2B, B(9,11)), -11.1 (d, ^{1}J(B,H)= 142, 2B, B(5,6)), -14.0 (d, ^{1}J(B,H)= 169, 1B, B(3)), -19.4 (d, ^{1}J(B,H)= 155, 2B, B(2,4)), -29.1 (dd, ^{1}J(B,H)= 138, ^{1}J(B,H)= 30, 1B, B(10)), -31.8 (d, ^{1}J(B,H)= 143, 1B, B(1)). ^{31}P{^{1}H} NMR (CD_3COCD_3) δ: 77.26 (s, $OP^{i}Pr_2$). Two different types of single crystals were grown by slow evaporation from acetone solution.

2.3. X-Ray Difraction Study

Single-crystal data collections for H[**1a**] and H[**1b**] were performed at –100º with an Enraf Nonius KappaCCD diffractometer and MoKα radiation (λ = 0.71073 Å). The structures for both compounds were solved by direct methods and refined on F2 by the SHELX97 program [15]. Crystallographic data for are presented in Table 1. All non-hydrogen atoms were refined with anisotropic displacement parameters for both compounds. Positional parameters of the hydrogen atoms connected to the boron atoms were refined with fixed isotropic thermal displacement parameters. For both compounds, the chelating hydrogen atom was picked from difference Fourier map, and both coordinates and isotropic thermal displacement parameters of the atom were

refined. Rest of the hydrogen atoms were treated as riding atoms using the SHELX97 default parameters.

2.4. Computational details.

Quantum-chemical calculations were performed with the Gaussian 03 [16] commercial suite of programs at DFT level of theory with B3LYP hybrid functional [17] adopting for all the atoms the 6-311+G(d,p) basis set [18] for the optimization and the NBO analysis. The QTAIM and ELF computation were done at B3LYP/6-311++G(d,p) level of theory. The program Gabedit 2.4.0 [19] was used to prepare and visualize the structures. All the calculations with Gaussian 03 were performed in computational clusters with workstations with eight processors Intel Xeon Six-Core X5670 of 2,93 GHz and 24 GB of RAM, or with 128 processors Intel Itanium 2 of 1,6 GHz and 512 GB of RAM. The NBOView was used on SGI Altix 3700 Bx2 workstation equipped with 128 processors Itanium 2 of 1,6 GHz and 384 GB of RAM. AIMAll program [20] was used to find and characterize all the bond critical points and XAIM program [21] was used to draw the contour maps of the Laplacian of the electron density. The ELF analysis was performed with TopMod suite of programs [22] and the 2D ELF representations were performed with Multiwfn [23].

3. Results and discussion

*3.1. Molecular and crystal structures of two polymorphs of H[**1**]*

Crystallization of compound H[**1**] from acetone yielded two different needle-shaped crystals, H[**1a**] and H[**1b**], respectively. Compound H[**1a**] crystallizes in the triclinic system while H[**1b**] crystallizes in monoclinic system. Drawings of the molecules are shown in Figure 1. For each compound, the X-ray analysis confirmed the expected *nido* structure and the oxidation of both phosphorus atoms. Moreover, the analyses confirmed that the proton sitting between the oxygen atoms balances the negative

charge of the *nido* carborane cage in each compound. The short intramolecular O···O distance is an indication of the presence of the proton between oxygen atoms. In both polymorphs the protons were located from a difference Fourier map and successfully refined as an independent isotropic atom as the hydrogen atom in ref. [5a].

There are noticeable structural differences between H[**1a**] and H[**1b**]. Mutual orientations of the OP^iPr_2 substituents are different in H[**1a**] and H[**1b**], but the most striking difference between the molecules concerns the intramolecular O1-H-O2 hydrogen bonding motif (cf. Figures 1 and Table 1 from S.I.). In H[**1a**] the short O1···O2 distance of 2.3805(15) Å, the O1-H and O2-H distances of 1.20(3) and 1.19(3) Å along with the O1-H-O2 angle of 173(3)º indicate very strong linear and symmetric hydrogen bond between H and both oxygen atoms. In H[**1b**] the short O1···O2 distance of 2.4252(16) Å also indicated strong intramolecular hydrogen bond, but the O1-H and O2···H distances of 0.96(3) and 1.47(3) Å, and the O1-H···O2 angle of 171(3)º clearly indicate essentially linear but non-symmetric hydrogen bond between the oxygen atoms. This means that in H[**1b**] the positive charge is meanly localized at P1, while in H[**1a**] the hydrogen between the oxygen atoms posses the most of the positive charge. This different charge distributions can cause the structural differences observed between H[**1a**] and H[**1b**].

As far as we know, this observation that two different H-bond systems exist in one compound, H[**1**], is very rare in chemistry. For H[**1a**] there are several comparable zwitterionic compounds like H[7,8-$(OPPh_2)_2$-7,8-*nido*-$C_2B_9H_{10}$], H[**2**] [8, 24] and others [25], where the proton also lies approximately midway between the oxygen atoms and the corresponding hydrogen bond is essentially symmetric and linear. The O1···O2

distance of 2.421(4) Å in H[**2**] is longer than that in H[**1a**], 2.3805(15) Å, which is most likely due to the different Lewis acidity of the PR_2 (R= Ph and ^{i}Pr) units.

For H[**1b**], there is no close counterpart in the literature. [P(^{i}Pr)$_3$(OH)]I [25e] displays a similar P center but in which there is an O-H···I hydrogen bond. The P1-O1 bond length in H[**1b**] is 1.5454(12) Å (P2-O2 bond length is 1.5173(12) Å) and in [P(^{i}Pr)$_3$(OH)]I P-O bond length is 1.573(2) Å. Concerning the different positive charge distribution in H[**1a**] and H[**1b**], clear differences in the P-O and P-C_c distances between the two compounds can be seen (see S.I). Although the differences are relatively small, they support the general observation that distance of the hydrogen atom to the donor and acceptor atoms affects the adjacent bonds: the shorter is the O···H bond the longer is the P=O bond.

Differences in the orientations of P^{i}Pr$_2$ groups in H[**1a**] and H[**1b**] can be seen by checking the C8-C7-P1-O1 and C7-C8-P2-O2 torsion angle values that are 23.23(14) and 10.62(14)º for H[**1a**] and 45.64(15) and –3.84(16)º for H[**1b**]. These torsion angles indicate different conformations for H[**1a**] and H[**1b**] and influence on the O···O distances and vice versa. Hence, it is difficult to state if the formation of these two crystal forms is due to solid state ordering, conformational effects or possibly of a kinetic origin.

Additional interesting details of the structures are the C_c-C_c bond distance. The C7-C8 distances of 1.640(2), 1.624(2) and 1.609(5) Å for H[**1a**], H[**1b**] and H[**2**], respectively, are close to each other. The different orientations of P1 centers in H[**1a**] and H[**1b**] causes that the C_c-C_c bond distances are not the same in H[**1a**] and H[**1b**].

3.2. Computational study

Different approaches to study the hydrogen bonding can be found in the literature where the covalency of these bonds is studied [1c, 26]. To capture the influence of the H^+ in the crystal structures, we have performed a thorough computational study, based on DFT calculations, by using NBO analysis, and analysis of the topology of the electron density by QTAIM and ELF methods, for the geometries obtained from the X-ray diffraction studies. For comparison purposes, we also optimized the structure and performed the above mentioned calculations. The optimized structure is referred as H[**1o**]. For the optimized structure an intermediate geometry between the structures obtained from the X-Ray diffraction has been obtained (See S.I.). It is worth mentioning that for the first time in the literature, the three methods NBO, QTAIM and ELF have been utilized altogether to study the hydrogen bonds on the same structural feature. As recently stated by Fuster and Grabowski [27], the QTAIM and ELF parameters are useful to categorize and estimate the strength of hydrogen bonds. So, the study of the covalency by computational means is very important for intramolecular hydrogen bonds, as is our case, for which the absence of reference states does not allow to calculate the energy of this interaction.

3.2.1. NBO analysis.

The NBO analysis gives a clear description of the bonding in these compounds. The delocalization energies for the lone pairs and NBO antibonding interactions are presented in Table 2. In both H[**1**] structures, the lone pairs of the O atoms strongly delocalize in the O-H antibonding orbitals (see also S.I.). This observed delocalization is consistent with the NBO perspective on the hydrogen bonding that is based on the covalent-ionic resonance or charge transfer of the form [28]: $A{:}H\ {:}B \leftrightarrow A{:}^-\ H{:}B^+$

The charge transfer can be quantified by taking into account the two-electron $n_B \rightarrow \sigma^*_{AH}$ intramolecular donor-acceptor interaction, where electron density from the lone pair n_B of the Lewis base centre B, delocalizes into the unfilled σ^*_{AH} antibonding orbital of the Lewis acid center, AH (which in turn can be seen as bonding between H···B fragment). In H[**1a**], the second lone pair of the O2 atom is strongly delocalized into the antibonding orbital of O1-H bond, the energy for this delocalization (charge transfer energy $\Delta E n_B \rightarrow \sigma^*_{AH}$) being more than four times stronger than the same energy from H[**1b**] and comparable with the values found in the literature [26b, 28c] for very strong hydrogen bonded systems like FH···F (166.2 kcal·mol^{-1}) and $H_2OH^+\cdots OH_2$ (168.4 kcal·mol^{-1}). The charge transfer energy between the second lone pair of O2 atom and the antibonding orbital of the O1-H bond in compound H[**1b**] is comparable with the one found for complexes like $H_3N\cdots HF$ (34.9 kcal·mol^{-1}), $OH^-\cdots HNH_2$ (31.1 kcal·mol^{-1}) and $H_2O\cdots HNH_3^+$ (30.1 kcal·mol^{-1}). The analysis of the natural hybrid orbitals (NHOs) revealed that the second lone pair of the O2 atoms in compounds H[**1a**] and H[**1b**] gain *s* character, proportional with the quantity of charge transfer from the lone pair to the antibonding orbital. Thus, for H[**1a**], that have the strongest interaction, the σ^*_{O1H} antibonding orbital gain 0.24559 e$^-$ and the O2 lone pair have 21.84% *s* character and 78.12% *p* character, whereas in H[**1b**], the σ^*_{O1H} antibonding orbital gain only 0.08932 e$^-$, thus the O2 lone pair remains mainly with *p* character, having only 5.07% *s* character.

3.2.2. QTAIM analysis

The QTAIM analysis complements the NBO picture, providing further insight on the nature of H bonds. All the hydrogen bonds fulfill the Koch and Popelier topological criteria for the existence of the hydrogen bonding [26b, 29]. In H[**1a**] all three atoms

involved in the hydrogen bonding system presents individual negative charge concentrations (see S.I.), with the Bond Critical Point (BCP) being close to the H atom, whereas in H[**1b**] the O1-H fragment form one shared negative charge concentration at O1-H and one individual at O2. From the properties of the BCPs between the O atoms and the H (Table 3), one can evaluate the strength of these bonds [30]. In H[**1a**], the parameters of both BCP found between O atoms and the H indicate that the hydrogen bonds are eminently strong. In H[**1b**] the O1-H bond path parameters indicate a more covalent nature of this bond, comparable with the OH bond in H_2O [31]. The O2-H bond path, on the other hand, is characterized as of moderate strength. All these observations are in agreement with the NBO depiction of these bonds.

3.2.3. ELF analysis

The Electron Localization Function (ELF) [32] approach has been applied to further study the intramolecular hydrogen bonding in these compounds. As can be observed from Figure 2, for H[**1a**] the ELF gradient field describes two monosynaptic valence basins for the two oxygen atoms and a protonated monosynaptic basin, for the H atom, centered at the O1-O2 midpoint. The appearance of the isolated domain for the hydrogen basin seems to be characteristic for the strong hydrogen bonds, and it was observed for systems like FHF^-, $N_2H_7^+$ and $H_5O_5^+$ [32], being also consistent with the formation of the individual negative charge concentration observed in the QTAIM analysis. On the other hand, for H[**1b**] there exists disynaptic valence basins on the O atoms and a protonated disynaptic valence basin centered on the O1-H bond. As can be observed from Figure 2, the ELF values on H-O2 axis are very low, indicating that the interaction of H with the O2 would be weaker in H[**1b**]. The absence of the monosynaptic basin at attractor H^+ in H[**1b**] is in good agreement with the observed weaker O-H bond in H[**1b**] compared to H[**1a**].

4. Conclusions

Two polymorphs (H[**1a**] and H[**1b**]) that display different P=O···H···O=P distances have been structurally characterized. The strength of these bonds has been calculated with DFT protocols. Polymorph H[**1a**] has the H atom just in the middle of the two O atoms whereas in H[**1b**] one O-H distance is shorter than the other. Considering that the stabilizing energy of the P=O···H···O=P bond is mainly due to a charge transfer interaction from a lone pair of electrons on one O atom to the antibonding orbital of the O-H bond, and to a covalent O-H bond and weak O···H interaction, it has been established by NBO analysis that structure H[**1a**] presents very strong P=O···H···O=P bonds, whereas the structure H[**1b**] corresponds mostly to the second case with a covalent O-H bond and weak O···H interaction. The symmetry of the P=O···H···O=P interaction in H[**1a**] was also proven by the QTAIM analysis, in which O atoms and the bridging H atom form individual negative Laplacian basins, and by ELF analysis, in which the H atom presents a monosynaptic protonated basin between the two monosynaptic valence basins corresponding to the O atoms. In the H[**1b**], on the other hand, the topological characteristics of the BCP of the shortest O-H bonds corroborate the covalent nature of this bond, whereas for the longer O···H bond, the BCP is characterized as a shared interaction of moderate strength. Also, the ELF analysis yielded a dysinaptic protonated basin for the short O-H bond in H[**1b**].

These results prove that strong P=O···H···O=P interaction do exist, but also, P-O-H···O=P can be formed in the oxidized *nido*-carboranyldiphosphines. Further studies are underway to establish the impact of the presence of these strong H bonds on the intramolecular electronic communication in these compounds and the possible use of

these diphosphines as an alternative to organocatalysts as BINOL-based phosphoric acids.

Acknowledgements

We thank MICINN (CTQ2010-16237), and Generalitat de Catalunya 2009/SGR/00279. A.R.P. thanks to the Spanish Ministry of Education for a FPU grant. The access to the computational facilities of High Performance Computing Centre of CSIC and Centre de Serveis Científics i Acadèmics de Catalunya (CESCA) is gratefully acknowledged.

Appendix A. Supplementary material

CCDC 630895 and 630896 contain the supplementary crystallographic data for H[**1a**] and H[**1b**]. These data can be obtained free of charge from The Cambridge Crystallographic Data Centre via www.ccdc.cam.ac.uk/data_request/cif.

Chart 1. Different drawing modes for searching in CSD (X stand for any atom and the dashed line for any kind of bond).

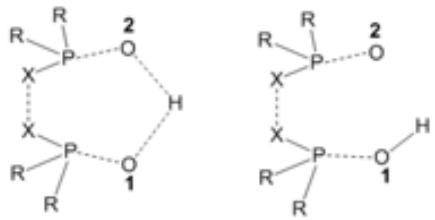

Mode I Mode II

Figure 1. ORTEP drawing of H[**1a**] and H[**1b**]. Thermal displacement ellipsoids are drawn at 30% probability level. Hydrogen atoms, except the chelating hydrogen, H and the apical hydrogen, H10b, have been omitted.

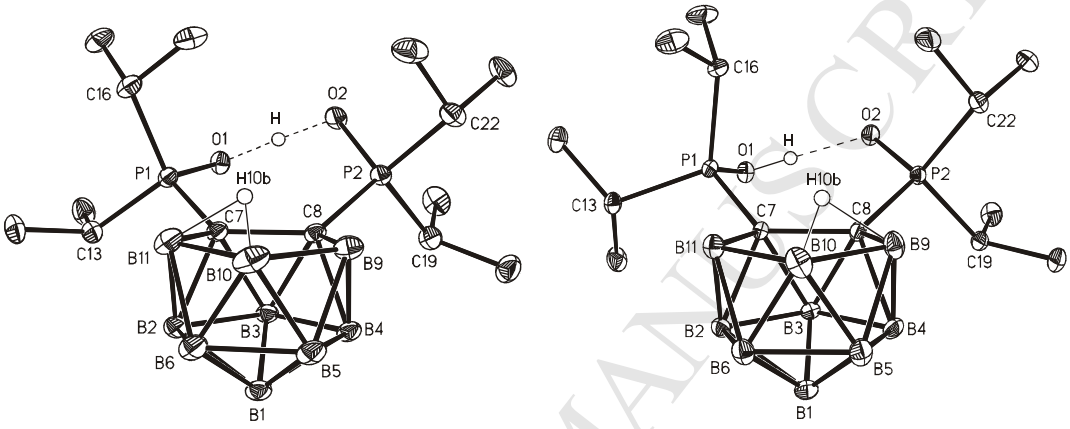

H[**1a**] H[**1b**]

Figure 2. 2D representation of the ELF isosurface as cross sections through O1-H-O2 plane for H[**1a**] and H[**1b**]

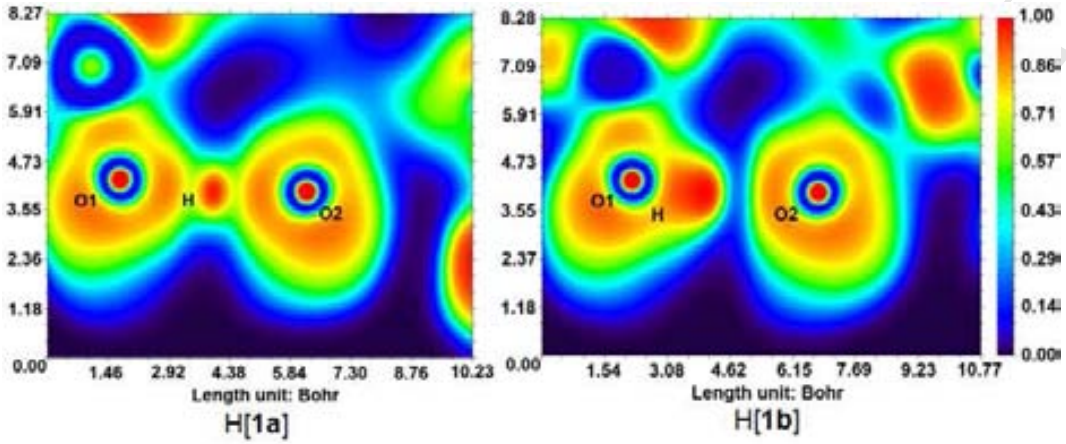

Table 1. Crystal data and structural refinement details for the studied compounds.

	H[**1a**]	H[**1b**]
empirical formula	$C_{14}H_{39}B_9O_2P_2$	$C_{14}H_{39}B_9O_2P_2$
fw	398.68	398.68
cryst syst	triclinic	monoclinic
crystal habit, colour	needle, colourless	needle, colourless
space group	*P*-1 (no. 2)	$P2_1/n$ (no. 14)
a [Å]	8.1964(1)	10.3418(1)
b [Å]	10.2825(1)	17.4103(2)
c [Å]	14.6426(3)	13.3089(2)
α [°]	109.8524(6)	90
β [°]	92.6964(6)	105.876(1)
γ [°]	96.3025(8)	90
V [V^3]	1149.01(3)	2304.91(5)
Z	2	4
ρ [g cm^{-3}]	1.152	1.149
μ [cm^{-1}]	1.97	1.96
goodness-of-fit[b] on F^2	1.047	1.022
R^c [$I > 2\sigma(I)$]	0.0322	0.0347
$R_w{}^d$ [$I > 2\sigma(I)$]	0.0793	0.0820

[b] $S = [\Sigma(w(F_o^2 - F_c^2)^2]/(n-p)^{1/2}$, [c] $R = \Sigma||F_o| - |F_c||/\Sigma|F_o|$, [d] $R_w = [\Sigma w(|F_o^2| - |F_c^2|)^2/\Sigma w|F_o^2|^2]^{1/2}$.

Table 2. NBO second order delocalization energies from the lone pair electrons (n_B; the number in parenthesis stands for the first (1) and the second (2) lone pair) to antibonding orbitals (σ^*).

Compound	n_B	σ*	$E_{ij}^{(2)}$ (Kcal·mol^{-1})
H[**1a**]	O1(1)	P1-C7	7.90
	O1(1)	P1-C16	13.30
	O2(1)	P2-C8	5.64
	O2(1)	P2-C19	14.32
	O2(2)	P2-C22	5.01
	O2(2)	O1-H	164.32
H[**1b**]	O1(1)	P1-C7	10.52
	O1(1)	P1-C16	8.48
	O2(1)	P2-C19	15.50
	O2(1)	P2-C22	6.79
	O2(2)	P2-C8	10.16
	O2(2)	P2-C22	8.35
	O2(2)	O1-H	38.52
H[**1o**]	O1(1)	P1-C7	6.73
	O1(1)	P1-C16	12.26
	O2(1)	P2-C19	14.95
	O2(2)	P2-C8	4.95
	O2(2)	P2-C22	6.83
	O2(2)	O1-H	99.91

Table 3. Properties (ρ - electron density, $\nabla^2\rho$ - Laplacian of the electron density, H – total electronic energy density) of BCP for the studied compounds (all the values are in a.u.).

Compound	Bond	ρ	$\nabla^2\rho$	H
H[**1a**]	P1-O1	0.2049	1.0965	-0.8428
	P2-O2	0.2077	1.1593	-0.8731
	O1-H	0.1721	-0.2764	-0.1919
	O2-H	0.1745	-0.2971	-0.1944
H[**1b**]	P1-O1	0.2007	1.0520	-0.8107
	P2-O2	0.2125	1.2102	-0.9119
	O1-H	0.3476	-2.4649	-0.1802
	O2-H	0.0789	0.2017	-0.1463
H[**1o**]	P1-O1	0.1918	0.8852	-0.7223
	P2-O2	0.2011	1.0270	-0.8061
	O1-H	0.2289	-0.954	-0.1819
	O2-H	0.1265	0.0666	-0.1828

[1] (a) G. R. Desiraju, T. Steiner, Eds, The Weak Hydrogen Bond in Structural Chemistry and Biology; Oxford University Press Inc., New York, 1999.

(b) L. J. Prins, D. N. Reinhoudt, P. Tiemmerman, Agew. Chem. Int. Ed. 40 (2001) 2382-2426.

(c) S. J. Grabowski, (Ed.), Hydrogen Bonding – New Insights, Springer; New York, **2006**.

[2] (a) A. Gerlt, P. G. Gassman, J. Am. Chem. Soc.115 (1993) 11552-11567.

(b) C. L. Perrin, Science 266 (1994) 1665-1668.

(c) W. W. Cleland, M. M. Krevoy, Science 264 (1994) 1887-1890.

(d) P. A. Frey, S. A. Whitt, J. B. Tobin, Science 264 (1994) 1927-1930.

(e) C. L. Perrin, J. B. Nelson, Annu. Rev. Phys. Chem. 48 (1997) 511-544.

(f) H. Tong, L. Davis, Biochemistry 34 (1995) 3362-3367.

(g) Q. Zhao, C. Abeygunawardana, P. Talalay, A. S. Mildvan, Proc. Natl. Acad. Sci. USA, 93 (1996) 8220-8224.

(h) O. Hur, C. Leja, M. F. Dun, Biochemistry 35 (1996) 7378-7386.

(i) C. S. Cassidy, J. Lin, P. A. Frey, Biochemistry 36 (1997) 4576-4584.

(j) W. W. Cleland, P. J. Richard (Ed.) The low-barrier hydrogen bond in enzymic catalysis in Advances in Physical Organic Chemistry, Vol. 44, 2010, p. 1-17.

[3] (a) G. R. Desiraju, Crystal Engineering. The Design of Organic Solids, Elsevier; Amsterdam, 1989.

(b) G. R. Desiraju, Acc. Chem. Res. 35 (2002) 565-573.

[4] J. T. Hynes, J. P. Klinman, H.-H. Limbach, R. L. Schowen (Eds.), Hydrogen-Transfer Reactions, Wiley-VCH Velag CmbH&Co. KGaA, Weinheim, 2007.

[5] (a) V. W. Day, M. A. Hossain, S. O. Kang, D. Powell, G. Lushington, K. Bowman-James, J. Am. Chem. Soc. 129 (2007) 8692-8693.

(b) S. Yaghmaei, S. Khodagholian, J. M. Kaiser, F. S. Tham, L. J. Mueller, T. H. Morton, J. Am. Chem. Soc. 130 (2008) 7836-7838.

[6] (a) M. S. Taylor, E. N. Jacobsen, Angew. Chem. Int. Ed. 45 (2006) 1520-1543.

(b) A. G. Doyle, E. N. Jacobsen, Chem. Rev. 107 (2007) 5713-5743.

[7] (a) T. AKiyama, J. Itoh, K. Yokota, K. Fuchibe, Agew. Chem. Int. Ed. 116 (2004) 1592-1594.

(b) D. Uraguchi, M. Terada, J. Am. Chem. Soc. 126 (2004) 5356-5357.

(c) D. Uraguchi, K. Sorimachi, M. Terada, J. Am. Chem. Soc. 126 (2004) 11804-11805.

(d) T. AKiyama, J. Itoh, K. Yokota, K. Fuchibe, Org. Lett. 7 (2005) 2583-2585.

(e) M. Rueping, E. Sugiono, C. Azap, T. Theissmann, M. Bolte, Org. Lett. 7 (2005) 3781-3783.

[8] C. Viñas, R. Nuñez, I. Rojo, F. Teixidor, R. Kivekäs, R. Sillanpää, Inorg. Chem. 40 (2001) 3259-3260.

[9] Bruno, J.; Cole, J. C.; Edgington, P. R.; Kessler, M.; Macrae, C. F.; McCabe, P.; Pearson, J.; Taylor, R. Acta Crystallogr. B58 (2002) 389-397.

[10] Search performed in February 22nd, 2012.

[11] Costantino, F.; Ienco, A.; Midollini, S.; Orlandini, A.; Sorace, L.; Vacca, A. Eur. J. Inorg. Chem. (2008) 3046-3055.

[12] C. Hollatz, A. Schier, H. Schmidbaur, J. Am. Chem. Soc. 119 (1997) 8115-8116.

[13] F. Bigoli, P. Deplano, M. L. Mercuri, M. A. Pellinghelli, E. F. Trogu, *Phosphorus, Sulfur, and Silicon and Related Elements* 70 (1992) 145-152.

[14] F. Teixidor, C. Viñas, M. Abad, R. Núñez, R. Kivekäs, R. Sillanpää, J. Organomet. Chem. 503 (1995) 193-203.

[15] Sheldrick, G. M.; SHELX-97, University of Göttingen (Germany), 1997.

[16] Gaussian 03, Revision E.02, M. J. Frisch, G. W. Trucks, H. B. Schlegel, G. E. Scuseria, M. A. Robb, J. R. Cheeseman, J. A. Montgomery, Jr., T. Vreven, K. N. Kudin, J. C. Burant, J. M. Millam, S. S. Iyengar, J. Tomasi, V. Barone, B. Mennucci, M. Cossi, G. Scalmani, N. Rega, G. A. Petersson, H. Nakatsuji, M. Hada, M. Ehara, K. Toyota, R. Fukuda, J. Hasegawa, M. Ishida, T. Nakajima, Y. Honda, O. Kitao, H. Nakai, M. Klene, X. Li, J. E. Knox, H. P. Hratchian, J. B. Cross, V. Bakken, C. Adamo, J. Jaramillo, R. Gomperts, R. E. Stratmann, O. Yazyev, A. J. Austin, R. Cammi, C. Pomelli, J. W. Ochterski, P. Y. Ayala, K. Morokuma, G. A. Voth, P. Salvador, J. J. Dannenberg, V. G. Zakrzewski, S. Dapprich, A. D. Daniels, M. C. Strain, O. Farkas, D. K. Malick, A. D. Rabuck, K. Raghavachari, J. B. Foresman, J. V. Ortiz, Q. Cui, A. G. Baboul, S. Clifford, J. Cioslowski, B. B. Stefanov, G. Liu, A. Liashenko, P. Piskorz, I. Komaromi, R. L. Martin, D. J. Fox, T. Keith, M. A. Al-Laham, C. Y. Peng, A. Nanayakkara, M. Challacombe, P. M. W. Gill, B. Johnson, W. Chen, M. W. Wong, C. Gonzalez, and J. A. Pople, Gaussian, Inc., Wallingford CT, 2004.

[17] P. J. Stephens, F. J. Devlin, C. F. Chabalowski, M. J. Frisch, J. Phys. Chem. 98 (1994) 11623-11627.

[18] (a) A. D. McLean, G. S. Chandler, J. Chem. Phys., 72 (1980) 5639.

(b) K. Raghavachari, J. S. Binkley, R. Seeger, J. A. Pople, J. Chem. Phys. 72 (1980) 650.

(c) J. P. Blaudeau, M. P. McGrath, L. A. Curtiss, L. Radom, J. Chem. Phys. 107 (1997) 5016.

(d) A. J. H. Wachters, J. Chem. Phys. 52 (1970) 1033.

(e) P. J. Hay, J. Chem. Phys. 66 (1977) 4377.

(f) K. Raghavachari, G. W. Trucks, J. Chem. Phys. 91 (1989) 1062.

(g) R. C. Binning Jr., L. A. Curtiss, J. Comp. Chem. 11 (1990) 1206.

(h) M. P. McGrath, L. Radom, J. Chem. Phys. 94 (1991) 511.

(i) L. A. Curtiss, M. P. McGrath, J. P. Blaudeau, N. E. Davis, R. C. Binning Jr., L. Radom, Chem. Phys. 103 (1995) 6104.

[19] Allouche, A. R. J. Comput. Chem. 32 (2011) 174-182.

[20] AIMAll (Version 11.12.19), Keith, T. A.; TK Gristmill Software, Overland Park KS, USA, 2011 (aim.tkgristmill.com).

[21] Ortiz Alba, J. C.; Bo Jane, C. *Xaim -- X Atoms in Molecules Interface Version 1.0,* 1998.

[22] (a) S. Noury, X. Krokidis, F. Fuster, B. Silvi, Computers & Chemistry 23 (1999) 597.

(b) The ToPMoD suite of programs can be downloaded free of charge at http://www.lct.jussieu.fr/pagesperso/silvi/.

[23] (a) T. Lu, F. Chen, J. Comput. Chem. 33 (2012) 580.

(b) Multiwfn can be downloaded free of charge at multiwfn.codeplex.com.

[24] J. Dou, D. Zhang, D. Li, D. Wang, Eur. J. Inorg. Chem. 1 (2007) 53-59

[25] (a) K. E. Halvorson, R. D. Willett, A. C. Massabni, J. Chem. Soc, Chem. Commun. 4 (1990) 346-348.

(b) C. J. Carmalt, N. C. Norman, L. J. Farrugia, Polyhedron 12 (1993) 2081-2090.

(c) H. P. Lane, S. M. Godfrey, C. A. McAuliffe, R. G. Pritchard, J. Chem. Soc., Dalton Trans. 22 (1994) 3249-3256.

(d) S. M. Godfrey, N. Ho, C. A. McAuliffe, R. G. Pritchard, Angew. Chem. 108 (1996) 2492-2494; *Angew. Chem. Int. Ed. Engl.*, 35 (1996) 2344-2346.

(e) F. Ruthe, P. G. Jones, W. -W. du Mont, P. Deplano, M. L. Mercuri, Z. Anorg. Allg. Chem. 626 (2000) 1105-1111.

(f) A. A. Boraei, W. W. du Mont, F. Ruthe, P. G. Jones, Acta Crystallog., Sect. C: Cryst. Struct. Commun., 58 (2002) 318-320.

[26] (a) P. Gilli, G. Gilli, J. Mol. Struct. 972 (2010) 2-10.

(b) S. J. Grabowski, Chem. Rev. 111 (2011) 2597-2625

[27] F. Fuster, S. J. Grabowski, J. Phys. Chem. A, 115 (2011) 10078-10086.

[28] (a) A. E. Reed, L. A. Curtiss, F. Weinhold, Chem. Rev. 88 (1988) 899-926.

(b) F. Weinhold, J. Mol. Struct. (THEOCHEM), 398-399 (1997) 181-197.

(c) F. Weinhold, C. Landis, Valency and Bonding, A Natural Bond Orbital Donor – Acceptor Perspective, Cambridge University Press: New York, 2005

[29] U. Koch, P. L. A. Popelier, J. Phys. Chem. 99 (1995) 9747-9754.

[30] I. Rozas, I. Alkorta, J. Elguero, J. Am. Chem. Soc. 122 (2000) 11154-11161.

[31] R. F. W. Bader, H. Essén, J. Chem. Phys. 80 (1984) 1943-1959.

[32] (a) F. Fuster, B. Silvi, Chem. Phys. 252 (2000) 279-287.

(b) M. E. Alikhani, B. Silvi, Phys. Chem. Chem. Phys. 5 (2003) 2494-2498.

(c) A. M. Navarrete- López, J. Garza, R. Vargas, J. Phys. Chem. A. 111 (2007) 11147-11152.

(d) M. K. Cyranski, A. Jezierska, P. Klimentowska, J. J. Panek, A. Sporzynski, J. Phys. Org. Chem. 21 (2008) 472-482.

(e) I. V. Drebushchak, S. G. Kozlova, J. Struct. Chem. 51 (2010) 166-169.

(f) R. Chaudret, G. A. Cisneros, O. Parsiel, J.-P. Piquemal, Chem.-Eur. J. 17 (2011) 2833-2837.

DOI: 10.1002/chem.201003330

Uncommon Coordination Behaviour of P(S) and P(Se) Units when Bonded to Carboranyl Clusters: Experimental and Computational Studies on the Oxidation of Carboranyl Phosphine Ligands

Adrian-Radu Popescu,[a] Anna Laromaine,[a] Francesc Teixidor,[a] Reijo Sillanpää,[b] Raikko Kivekäs,[c] Joan Ignasi Llambias,[a] and Clara Viñas*[a]

Abstract: Oxidation of *closo*-carboranyl diphosphines 1,2-$(PR_2)_2$-1,2-*closo*-$C_2B_{10}H_{10}$ (R = Ph, *i*Pr) and *closo*-carboranyl monophosphines 1-PR_2-2-R′-1,2-*closo*-$C_2B_{10}H_{10}$ (R = Ph, *i*Pr, Cy; R′ = Me, Ph) with hydrogen peroxide, sulfur and elemental black selenium evidences the unique capacity of the *closo*-carborane cluster to produce uncommon or unprecedented P/P(E) (E = S, Se) and P=O/P=S chelating ligands. When H_2O_2 reacts with 1,2-$(PR_2)_2$-1,2-*closo*-$C_2B_{10}H_{10}$ (R = Ph, *i*Pr), they are oxidized to 1,2-$(OPR_2)_2$-1,2-*closo*-$C_2B_{10}H_{10}$ (R = Ph, *i*Pr). However, when S and Se are used, different reactivity is found for 1,2-$(PPh_2)_2$-1,2-*closo*-$C_2B_{10}H_{10}$ and 1,2-$(PiPr_2)_2$-1,2-*closo*-$C_2B_{10}H_{10}$. The reaction with sulfur produces mono- and dioxidation products for R = Ph, whereas Se produces the mono-oxidation product only. For R = *i*Pr, only monooxidation takes place with S, and the second C_c–P*i*Pr_2 bond breaks to yield 1-SP*i*Pr_2-1,2-*closo*-$C_2B_{10}H_{11}$. When Se is used, only 1-SeP*i*Pr_2-1,2-*closo*-$C_2B_{10}H_{11}$ is formed. The potential of the mono-chalcogenide carboranyl diphosphines 1-$EPPh_2$-2-PPh_2-1,2-*closo*-$C_2B_{10}H_{10}$ (E = S, **9**; Se, **15**) to behave as unsymmetric chelating bidentate ligands was studied for different metal complexes, different solvents and in the solid state. Dechalcogenation takes place in each case. Computational studies provided information on the P=E (E = S, Se) bonds. Steric effects block the bonding ability of the P=E group due to interactions between the chalcogen and the neighbouring hydrogen atoms (three from the phenyl rings and one from the carborane cluster). The electronic effects originate from the strongly electron-withdrawing character of the *closo* carborane cluster, which polarizes the P=E (E = S, Se) bond towards the phosphorus atom. As a consequence, the E atom is the electron-poor site and the P atom the electron-rich site in the P=E bond.

Keywords: carboranes · P ligands · phosphorus · selenium · sulfur

Introduction

Since their discovery in 1959,[1] tertiary phosphines have become important ligands. Their electronic and steric properties grant them significant value in coordination chemistry and catalysis.[1a, 2] In general, tertiary phosphines are sensitive species[3] with weakly basic properties; they are easily oxidized to produce more weakly basic compounds such as phosphine chalcogenides. Phosphine oxidation reactions are attractive, as phosphines and their chalcogenides play key roles in catalytic mechanisms.[4] R_3PE, $RP(E)(ESiMe_3)_2$, $\{RP(E)(\mu\text{-}E)\}_2$ (E = S, Se; R = organic group) are useful 1) as starting materials for metal chalcogenide nanoparticles,[5] 2) as synergist agents of CMPO or DTPA to improve An^{III}/Ln^{III} separation in nuclear waste remediation,[6] 3) for preparing molecular complexes with P–chalcogen ligands[7] and 4) in chalcogen-transfer reactions.[8] Different sources of chalcogens are commonly used to obtain soluble chalcogen-containing compounds, although the simplest source is the elemental chalcogen (E = S, Se, Te).[9]

o-Carborane, 1,2-*closo*-$C_2B_{10}H_{12}$, has a cagelike structure with icosahedral faces in which the C and B vertexes can be modified.[10] The C_cH vertices (C_c: cluster carbon atom) are moderately acidic, and can be deprotonated with strong bases; the negatively charged carbon atoms can thus be subsequently functionalized with electrophilic reagents. The electrophilic substitution chemistry of boron-substituted carboranes is in many ways reminiscent of that of arenes.[11]

We are interested in the synthesis of carborane compounds containing exo-cluster substituents with lone pairs

[a] A.-R. Popescu, Dr. A. Laromaine, Prof. Dr. F. Teixidor, J. I. Llambias, Prof. Dr. C. Viñas
Institut de Ciència de Materials de Barcelona (CSIC)
Campus U.A.B. 08193 Bellaterra (Spain)
Fax: (+34) 93-580-57-29
E-mail: clara@icmab.es

[b] Prof. Dr. R. Sillanpää
Department of Chemistry, University of Jyväskylä
40014, Jyväskylä (Finland)

[c] Dr. R. Kivekäs
Department of Chemistry, P.O. Box 55
University of Helsinki, 00014 (Finland)

Supporting information for this article is available on the WWW under http://dx.doi.org/10.1002/chem.201003330. It contains the ^1H NMR spectrum of compound **7**; $^{31}P\{^1H\}$ NMR spectra of compounds **15** and **17**; 3D NBO plots; $^{31}P\{^1H\}$ NMR chemical shifts for 1-PR_2-2-Me-1,2-*closo*-$C_2B_{10}H_{10}$ (R = Ph, Me, Cy), 1-PPh_2-2-R′-1,2-*closo*-$C_2B_{10}H_{10}$ (R = Me, Ph, SBz, H) and their chalcogenides; and optimised geometries in orthogonal format for compounds **9** and **15**.

(e.g., S or P), due to their potential in metal catalysis.[12] Despite the well-known affinity of phosphines towards chalcogens and destruction of the transition metal catalysts through oxidation of the phosphorus-containing ligands, there is a surprising lack of studies on these reactions. Moreover, the Cambridge Crystallographic Database,[13] on October 25th 2010, contained four crystal structures for carboranyl phosphine oxides[14] and only one crystal structure for a carboranyl phosphine sulfide;[15] there are no reported structures for a carboranyl moiety containing a phosphorus–selenium bond.[13] Furthermore, no investigation on the reactivity of *closo* carboranyl phosphine chalcogenides (*closo*-carboranyl)R_2PE (E = S, Se) was found in the literature. A study with (*nido*-carboranyl)R_2PS in which the P=S bond was retained after complexation has been reported.[16]

During our research on (*closo*-carboranyl)R_2P we observed many structural features, as well as reactivity, that contrasts with organic chemical fragments.[17] Here we present the oxidation of *o*-carborane mono- and diphosphine derivatives with hydrogen peroxide, sulfur and selenium. The potential of these mono-chalcogenide carboranyl diphosphines 1-$EPPh_2$-2-PPh_2-1,2-*closo*-$C_2B_{10}H_{10}$ (E = S, Se) to behave as asymmetric chelating bidentate ligands for metal coordination was evaluated for different metal complexes, different solvents and in the solid state. To gain further insight into the nature of the P=E bond in these monochalcogenide carboranyl diphosphines, computational studies were also performed.

Results and Discussion

Oxidation of *closo* carboranyl diphosphines: In contrast to other common phosphines, *closo*-carboranyl mono-phosphines 1-PR_2-2-R′-1,2-*closo*-$C_2B_{10}H_{10}$ showed high stability in the solid state and in solution, under air or in the presence of mild oxidizing agents, alcohols and some acids.[18] The strong electron-acceptor character of the *closo-o*-carborane through the C_c atoms influences the basicity/nucleophilicity of the P atoms. This is evidenced by the resistance of the *closo*-carboranyl di- and *closo*-carboranyl monophosphines towards partial degradation, their high chemical stability and difficult coordination of the P atoms to transition metal ions.[19]

Here we report oxidation of the neutral *closo*-carboranyl diphosphines 1,2-$(PR_2)_2$-1,2-*closo*-$C_2B_{10}H_{10}$ (R = Ph, *i*Pr) and *closo*-carboranyl monophosphines 1-PR_2-2-R′-1,2-*closo*-$C_2B_{10}H_{10}$ (R = Ph, *i*Pr, Cy; R′ = Me, Ph) to their corresponding carboranyl phosphine oxidized species with hydrogen peroxide, sulfur and elemental black selenium (Schemes 1 and 2).

Oxidation of *closo*-carboranyl diphosphines and *closo*-carboranyl monophosphines with hydrogen peroxide in acetone led to two different species: 1,2-$(OPR_2)_2$-1,2-*closo*-$C_2B_{10}H_{10}$ (R = Ph, **1**; *i*Pr, **2**) and 1-OPR_2-2-R′-1,2-*closo*-$C_2B_{10}H_{10}$ (R′ = Me, Ph; R = Ph, *i*Pr, Cy; **3**–**8**).

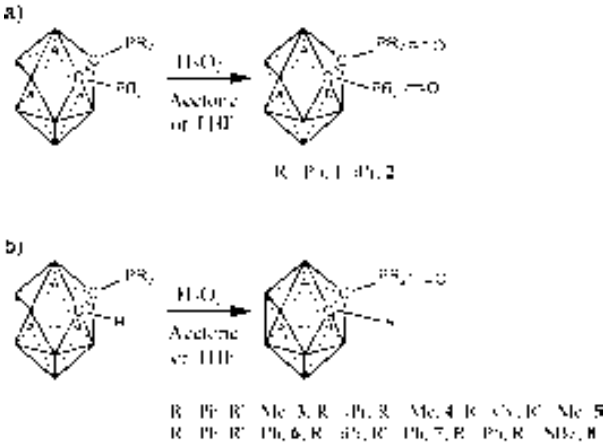

Scheme 1. Reaction of carboranyl phosphines with H_2O_2 in acetone. a) *closo*-Carboranyl diphosphines 1,2-$(PR_2)_2$-1,2-*closo*-$C_2B_{10}H_{10}$ (R = Ph, *i*Pr) and b) *closo*-carboranyl monophosphine 1-PR_2-2-R′-*closo*-$C_2B_{10}H_{10}$ (R′ = H, Me, Ph, SBz; R = Ph, *i*Pr, Cy).

Different behaviour was observed for alkyl and aryl diphosphines in oxidation with sulfur and selenium. Oxidation of 1,2-$(PPh_2)_2$-1,2-*closo*-$C_2B_{10}H_{10}$ with sulfur produced three different species after purification: 1-$SPPh_2$-2-PPh_2-1,2-*closo*-$C_2B_{10}H_{10}$ (**9**), 1,2-$(SPPh_2)_2$-1,2-*closo*-$C_2B_{10}H_{10}$ (**10**) and 1-$SPPh_2$-2-$OPPh_2$-1,2-*closo*-$C_2B_{10}H_{10}$ (**11**). Oxidation of the alkyl species 1,2-(P*i*Pr)$_2$-1,2-*closo*-$C_2B_{10}H_{10}$ produced 1-P*i*Pr_2-2-SP*i*Pr_2-1,2-*closo*-$C_2B_{10}H_{10}$ (**12**), in which only one phosphorus atom was oxidized after 4 h of heating to reflux. The original C_c–P*i*Pr_2 bonds broke yielding 1-SP*i*Pr_2-1,2-*closo*-$C_2B_{10}H_{11}$ (**13**) after 48 h of heating to reflux.

Oxidation of 1,2-$(PPh_2)_2$-1,2-*closo*-$C_2B_{10}H_{10}$ with elemental black selenium powder in refluxing toluene led only to species with one selenophosphine group in which the second group remained intact, 1-$SePPh_2$-2-PPh_2-1,2-*closo*-$C_2B_{10}H_{10}$ (**15**). Longer refluxing periods did not oxidise the second phosphine group. The opposite was observed for sulfur, with which both phosphine groups were oxidized. Oxidation of 1,2-(P*i*Pr$_2$)$_2$-1,2-*closo*-$C_2B_{10}H_{10}$ with selenium splits the second C_c–P bond yielding 1-SeP*i*Pr_2-1,2-*closo*-$C_2B_{10}H_{11}$ (**16**), as was observed with sulfur.

Characterization of oxidized *closo* carboranyl phosphines: *Spectroscopic characterization*: Carboranyl phosphine oxidation products were characterized by IR and ^1H, $^{13}C\{^1H\}$, $^{31}P\{^1H\}$ and ^{11}B NMR spectroscopy. Strong broad absorptions at 2644–2550 cm^{-1}, due to B–H stretching, dominate the IR spectra and support a *closo* cluster structure. P=O, P=S and P=Se stretches are found as strong and sharp absorptions at 1214–1081, 690–652 and 697–687 cm^{-1}, respectively. In addition, the IR spectrum of **13** and **16** exhibited strong ν(C–H) stretching bands at 3029 cm^{-1} confirming the presence of a C_c–H bond. $^{11}B\{^1H\}$ NMR spectroscopy provided information about the symmetry and the cluster structure of the oxidized species. A 2:4:4 or 2:2:6 pattern in the range $\delta = +1.7$ to -12.0 ppm verified a symmetric *closo* structure, whereas a 1:1:8, 1:1:4:4, 1:1:5:3 or 1:1:2:4:2 pattern

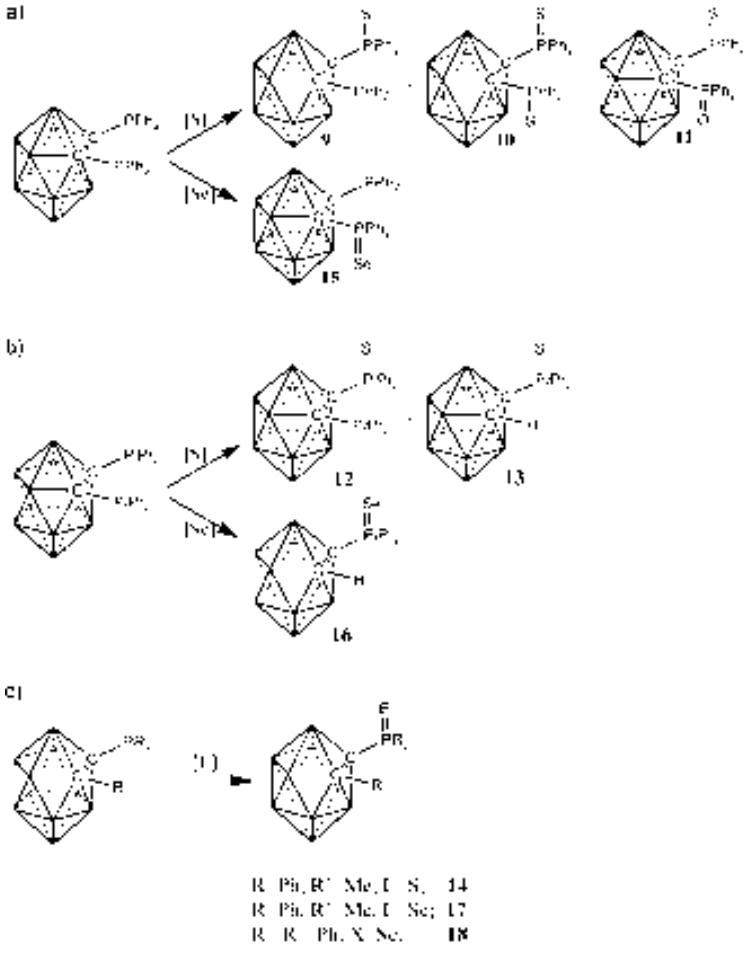

Scheme 2. Oxidation of 1,2-$(PR_2)_2$-1,2-*closo*-$C_2B_{10}H_{10}$ [R = Ph (a), *i*Pr (b)] with chalcogen (S, Se) in acetone/THF and toluene at reflux. c) Oxidation of 1-PPh_2-2-R′-1,2-*closo*-$C_2B_{10}H_{10}$ with S and Se in acetone/THF and toluene at reflux.

in the range $\delta = +3.0$ to -10.4 ppm validated a *closo* cluster with non-symmetric substitution at C_c. Minor differences in the $^{11}B\{^1H\}$ NMR spectra of oxidized carboranyl diphosphine species were detected (Figure 1): The resonance of the antipodal boron atoms (B9 and B12) shifted to lower field from the starting unoxidized species.

^1H NMR spectra of the oxidized carboranyl mono- and diphosphines showed that the two organic substituents at each P atom are non-equivalent. The ^1H NMR spectra of **2** and **7** also evidenced two non-equivalent methyl groups in each isopropyl unit (See Figure S.1, Supporting Information). Their $^{13}C\{^1H\}$ NMR spectra also contained two different resonances, which support different methyl groups in each isopropyl unit. Interaction between the P and C_c nuclei is clearly observed in all $^{13}C\{^1H\}$ NMR spectra with $^1J(^{13}C,^{31}P)$ coupling constants ranging from 19 to 61 Hz.

For each of the oxidized species **1**–**18**, the *closo* cluster structure was preserved despite the change in oxidation state from P^{III} to P^V. Table 1 lists the $^{31}P\{^1H\}$ NMR chemical shifts of the oxidized compounds. Each of the resonances appears at a lower field than that corresponding to the phosphine precursor. The $^{31}P\{^1H\}$ NMR chemical shifts of the carboranyl phosphines followed the trend Ph < Cy < *i*Pr, from upfield to downfield, modulated by the substituent at the second C_c atom (see Tables S.1 and S.2, Supporting Information). The deshielding effect on the $^{31}P\{^1H\}$ chemical shift also followed the trend S > Se > O (Table 1).

$^{31}P\{^1H\}$ NMR spectroscopy corroborated the oxidation state of P, the presence of a P=

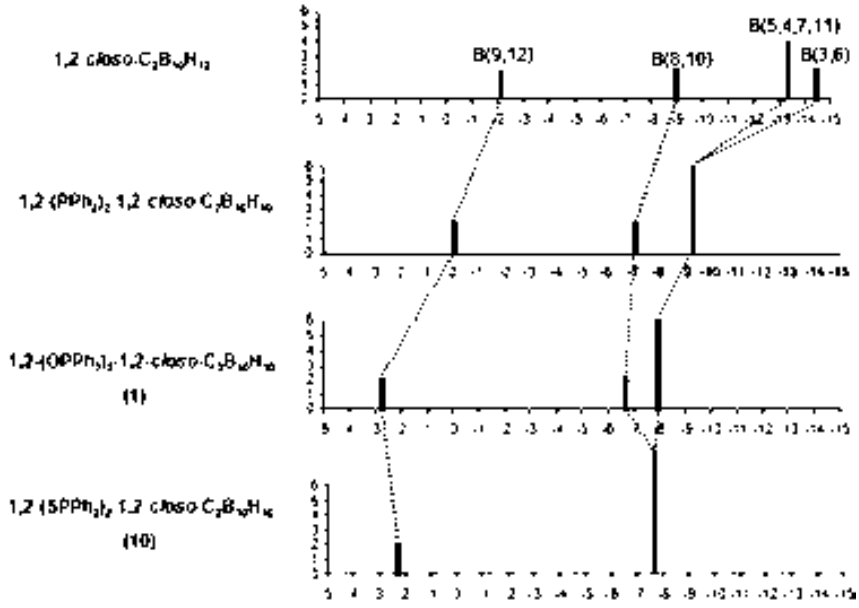

Figure 1. Stick representation of the chemical shifts and relative intensities in the $^{11}B\{^1H\}$ NMR spectra of 1,2-*closo*-$C_2B_{10}H_{12}$ (*o*-carborane), 1,2-$(PPh_2)_2$-1,2-*closo*-$C_2B_{10}H_{10}$, 1,2-$(OPPh_2)_2$-1,2-*closo*-$C_2B_{10}H_{10}$ (**1**) and 1,2-$(SPPh_2)_2$-1,2-*closo*-$C_2B_{10}H_{10}$ (**10**). Lines join equivalent positions in the three compounds.

Table 1. $^{31}P\{^1H\}$ NMR chemical shifts for the *closo*-carboranyl phosphines and their chalcogenides. Positive shifts, according IUPAC convention,[53] are to high frequency.

P^{III} compounds	$\delta(^{31}P)$ [ppm]	P^{V} compounds	$\delta(^{31}P)$ [ppm]	$\Delta\delta$ [ppm]
1,2-$(PPh_2)_2$-1,2-*closo*-$C_2B_{10}H_{10}$	8.22[29a]	1,2-$(OPPh_2)_2$-1,2-*closo*-$C_2B_{10}H_{10}$ (**1**)	23.67	+15.45
		1,2-$(SPPh_2)_2$-1,2-*closo*-$C_2B_{10}H_{10}$ (**10**)	48.65	+40.43
		1-$SPPh_2$-2-PPh_2-1,2-*closo*-$C_2B_{10}H_{10}$ (**9**)	49.16	+40.94
			12.77	+4.43
		1-$SPPh_2$-2-$OPPh_2$-1,2-*closo*-$C_2B_{10}H_{10}$ (**11**)	49.96	+41.74
			21.65	+13.43
		1-$SePPh_2$-2-PPh_2-1,2-*closo*-$C_2B_{10}H_{10}$ (15)	46.48	+38.26
			10.48	+2.26
1,2-$(PiPr_2)_2$-1,2-*closo*-$C_2B_{10}H_{10}$	32.79[54]	1,2-$(OPiPr_2)_2$-1,2-*closo*-$C_2B_{10}H_{10}$ (**2**)	59.08	+26.29
		1-$SPiPr_2$-2-$PiPr_2$-1,2-*closo*-$C_2B_{10}H_{10}$ (**12**)	78.0	+45.21
			35.5	+2.71
1-PPh_2-2-Me-1,2-*closo*-$C_2B_{10}H_{10}$	11.18[55]	1-$OPPh_2$-2-Me-1,2-*closo*-$C_2B_{10}H_{10}$ (**3**)	19.28	+8.10
		1-$SPPh_2$-2-Me-1,2-*closo*-$C_2B_{10}H_{10}$ (**14**)	47.65	+36.85
		1-$SePPh_2$-2-Me-1,2-*closo*-$C_2B_{10}H_{10}$ (**17**)	45.10	+34.3
1-$PiPr_2$-2-Me-1,2-*closo*-$C_2B_{10}H_{10}$	33.82[54]	1-$OPiPr_2$-2-Me-1,2-*closo*-$C_2B_{10}H_{10}$ (**4**)	58.18	+24.36
1-PPh_2-2-Ph-1,2-*closo*-$C_2B_{10}H_{10}$	12.66[56]	1-$OPPh_2$-2-Ph-1,2-*closo*-$C_2B_{10}H_{10}$ (**6**)	19.65	+6.99
		1-$SePPh_2$-2-Ph-1,2-*closo*-$C_2B_{10}H_{10}$ (**18**)	45.06	+32.16
1-$PiPr_2$-2-Ph-1,2-*closo*-$C_2B_{10}H_{10}$	38.50[57]	1-$OPiPr_2$-2-Ph-1,2-*closo*-$C_2B_{10}H_{10}$ (**7**)	53.27	+14.77
1-$PiPr_2$-1,2-*closo*-$C_2B_{10}H_{11}$	54.20[18]	1-$SPiPr_2$-1,2-*closo*-$C_2B_{10}H_{11}$ (**13**)	77.90	+23.74
		1-$SePiPr_2$-1,2-*closo*-$C_2B_{10}H_{11}$ (**16**)	83.67	+29.51
1-PPh_2-2-SBz-1,2-*closo*-$C_2B_{10}H_{10}$	11.17[58]	1-$OPPh_2$-2-SBz-1,2-*closo*-$C_2B_{10}H_{10}$ (**8**)	21.87	+10.70

Se bond and the non-symmetric nature of the oxidized species. For instance, the $^{31}P\{^1H\}$ NMR spectrum of 1-$SePPh_2$-2-PPh_2-1,2-*closo*-$C_2B_{10}H_{10}$ (**15**) showed two doublets, at $\delta = 46.48$ and 10.48 ppm, with a coupling constant of $^3J(^{31}P,^{31}P) = 27$ Hz. The resonance at $\delta = 46.48$ ppm suggests formation of a P=Se bond, whereas the signal at $\delta = 10.48$ ppm corresponds to unoxidized phosphorus. Evidence for the formation of the P=Se bond can be drawn from the $^{31}P\{^1H\}$ NMR spectra of the (*closo*-carboranyl)$SePR_2$ compounds. Upon prolonged recording times, two satellite lines due to $^1J(^{31}P,^{77}Se)$ appeared, indicating the presence of a P=Se bond. According to the literature, coupling constants $^1J(^{31}P,^{77}Se)$ can reach values ranging from 200 to 1100 Hz. A large $^1J(^{31}P,^{77}Se)$ value indicates a strong electron-withdrawing capacity of the substituents attached to the phosphorus atom,[20] increased s character of the phosphorus lone pair[21] and a more positively charged P atom.[22] The ^{77}Se satellites, $^1J(^{31}P,^{77}Se) = 807$ Hz, centered at 46.48 ppm confirmed formation of a P=Se bond (see Figure S.2, Supporting Information), the electron-withdrawing character of the carboranyl moiety and the low coordinating ability of the P atoms in these compounds. The $^{31}P\{^1H\}$ NMR resonances for (*closo*-carboranyl)Ph_2PSe compounds **15** and **17** appeared at higher frequency ($\delta = 46.48$ and 45.06 ppm, respectively) than that of Ph_3PSe ($\delta = 35.8$ ppm).[23] In addition, the coupling constant $^1J(^{31}P,^{77}Se) = 730$ Hz of Ph_3PSe[24] is smaller than those of **15** and **17** ($^1J(^{31}P,^{77}Se) = 807$ and $^1J(^{31}P,^{77}Se) = 812$ Hz, respectively), and this corroborates the stronger electron-acceptor character of *closo* carboranyl groups compared to a phenyl group.[17a,b,18]

Competitive oxidation of S/P, each connected to one of the adjacent cluster carbon atoms, was assessed on 1-PPh_2-2-SBz-1,2-*closo*-$C_2B_{10}H_{10}$. We successfully demonstrated that the P atom at the C_cPPh_2 vertex is more susceptible to oxidation with H_2O_2 than the S atom of the thioether group C_cSBz; the IR and $^{31}P\{^1H\}$ NMR data corroborated our hypothesis.

Crystal structure analyses: X-ray analyses of **3** and **5** confirmed oxidation of the C_cP unit (Figures 2and 3). The structures are similar, diverging from one another in the six-membered ring at the phosphorus atoms: a planar phenyl ring in **3** and cyclohexyl rings with normal chair conformation in **5** (see bond parameters in Table 2). Slight differences in the P–C bonds originate from the aromatic and aliphatic carbon

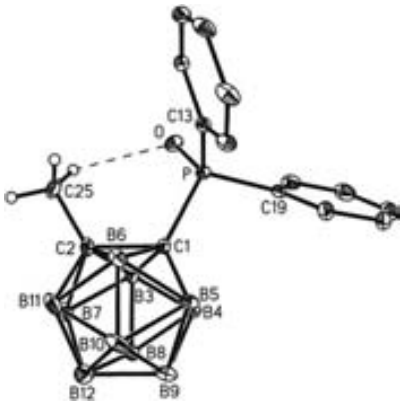

Figure 2. Molecular structure of **3** (ORTEP, thermal displacement ellipsoids are drawn at 20% probability, and hydrogen atoms, except those of the methyl group, are omitted; the intramolecular hydrogen bond is drawn with dashes).

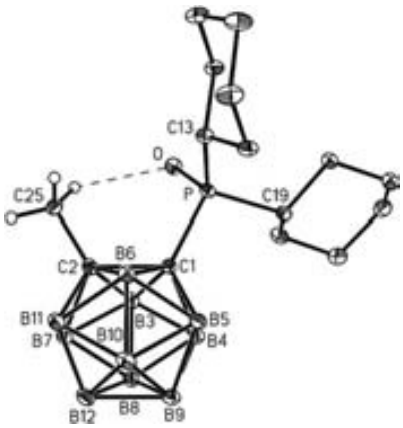

Figure 3. Molecular structure of **5** (ORTEP, thermal displacement ellipsoids are drawn at 20% probability, and hydrogen atoms, except those of the methyl group, are omitted; the intramolecular hydrogen bond is drawn with dashes).

Table 2. Selected interatomic distances [Å], angles [°] and torsion angles [°] for **3** and **5**.

	3	**5**
P–O	1.4759(13)	1.4858(19)
P–C1	1.8715(18)	1.891(2)
P–C13	1.8011(18)	1.821(3)
P–C19	1.7997(19)	1.827(3)
C1–C2	1.677(2)	1.687(3)
C2–C25	1.522(3)	1.505(4)
O-P-C1	110.21(8)	110.05(11)
P-C1-C2	117.47(12)	116.59(16)
C25-C2-C1	120.11(16)	120.5(2)
C2-C1-P-O	39.41(15)	−40.1(2)
P-C1-C2-C25	−4.2(2)	−6.4(3)

atoms connected to the phosphorus atoms. The P–O bond lengths are 1.4759(13) and 1.4858(19) Å for **3** and **5**, respectively. The oxygen atom in each compound points towards the methyl group; the C2-C1-P-C25 torsion angles are −39.41(15)° for **3** and −40.1(2)° for **5**. These conformations arise from the existence of weak intramolecular hydrogen bonds between a methyl hydrogen atom and the oxygen atom in each compound (H···O distances are 2.39 and 2.34 Å for **3** and **5**). In **3** there are also two short H···O distances of 2.51 Å from phenyl hydrogen atoms to the oxygen atom, indicating weak intramolecular H-bonds (the C–H···O angles are 108 and 109°), and in **5** there is also an intramolecular H···O contact (2.60 Å, C–H···O 109°). Weak intermolecular H···O bonds control the crystal packing of **3** and **5** (the shortest intermolecular H···O distances are 2.76 and 2.45 Å, respectively).

The structural analysis of **9** confirmed that only one of the two phosphorus atoms bonded to the *closo* cage was oxidized by sulfur (Figure 4and Table 3). The structure consists

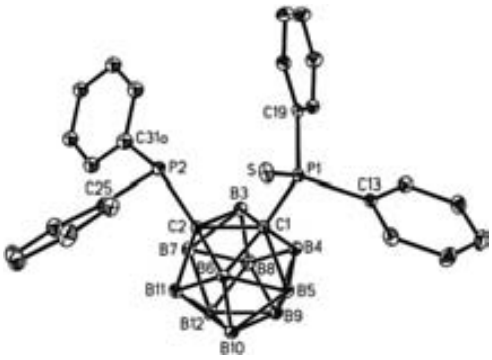

Figure 4. Molecular structure of **9** (ORTEP, thermal displacement ellipsoids are drawn at 30% probability, and hydrogen atoms are omitted and only the major orientation of the disordered phenyl group (C31–C36) is shown).

of well-separated entities with no short contacts between sulfur atoms of neighbouring molecules. Minor differences in the P–C and P–C_c distances between the two phosphorus atoms are due to their different oxidation states. The C1–C2 distance of 1.736(3) Å is close to the values of 1.719(3) and

Table 3. Selected interatomic distances [Å], angles [°] and torsion angles [°] for **9** and **15**. The disordered atoms C31a and C31b have site occupation parameters 0.613(9) and 0.387(9) for **9** and 0.60(3) and 0.40(3) for **15**.

	9	**15**
Se–P1		2.0982(18)
S–P1	1.9423(8)	
P1–C1	1.902(2)	1.906(6)
P1–C13	1.826(2)	1.823(7)
P1–C19	1.817(2)	1.816(6)
P2–C2	1.880(2)	1.881(6)
P2–C25	1.841(2)	1.852(7)
P2–C31a	1.855(6)	1.854(8)
P2–C31b	1.814(8)	1.835(12)
C1–C2	1.736(3)	1.732(9)
Se-P1-C1		114.8(2)
S-P1-C1	113.39(7)	
P1-C1-C2	122.44(14)	122.5(4)
P2-C2-C1	113.25(14)	113.4(4)
C1-P1-C13	102.85(26)	103.01(19)
C1-P1-C19	108.18(65)	108.08(44)
C13-P1-C19	106.94(15)	106.73(46)
C2-P2-C25	102.48(68)	102.60(34)
C2-P2-C31a	104.09(85)	104.60(46)
C25-P2-C31a	104.97(81)	104.15(41)
C2-C1-P2-Se		53.9(5)
C2-C1-P1-S	54.55(18)	
P1-C1-C2-P2	5.8(2)	5.8(6)

1.722(4) Å found for 1,2-($PiPr_2$)$_2$-1,2-*closo*-$C_2B_{10}H_{10}$[25] and 1,2-(PPh_2)$_2$-1,2-*closo*-$C_2B_{10}H_{10}$,[26] respectively. The P1–S distance of 1.9422(7) Å is normal for a P=S bond.[27] In **9** there are four S···H(Ph) contacts from the three ordered phenyl groups shorter than 3.0 Å, three of which (from H18, H20 and H26) are intramolecular (2.76–2.82 Å) and one (from H21) is intermolecular (2.88 Å). Also there is a S···H6B6 contact of 2.95 Å. All these structural features have an important effect on the reactivity of these compounds (see below).

The structural analysis of **11**·CH_2Cl_2 confirmed that both phosphorus atoms were oxidized, although unsymmetrically, that is, one was oxidized by oxygen and the other by sulfur. Spectral data also supported that one of the P atoms is substituted with O and the other with S. The positions of the oxygen and sulfur atoms are disordered such that they are bonded either to P1 or P2 in the crystal, but not to both at the same time (if O is at P1 then S is at P2 and vice versa). Each P atom is bonded to a partially occupied oxygen (SOP = 0.5) and sulfur atom (SOP = 0.5; Figure 5, Table 4). The structural disorder limits detailed discussion, as, for example, P=S bonds in this compound are shorter than 1.95 Å[27] (1.912(6) and 1.908(3) Å). However, there is one remarkable difference between the P-C_c-C_c angles of **9** and **11**. In **9** (with only one oxidized phosphorus atom) P-C_c-C_c angles are 113.25(14) and 122.44(14)°, but in **11** (with two oxidized phosphorus atoms) the P-C_c-C_c angles are 122.1(4) and 121.8(4)°. Therefore, the reason for the opening must be steric interactions.

Structural analysis of **15** confirmed that the *closo* architecture was retained during selenization and only one of the

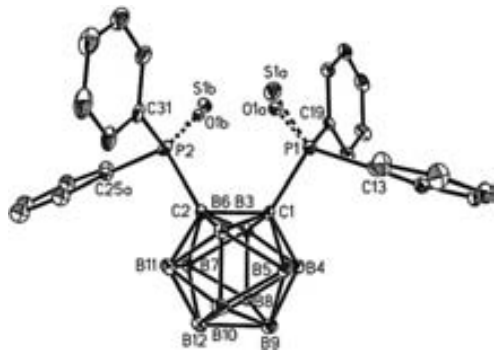

Figure 5. Molecular structure of the carborane moiety of **11**·CH_2Cl_2 (ORTEP, thermal displacement ellipsoids are drawn at 20% probability, and hydrogen atoms are omitted, and only one orientation of the disordered phenyl group (C25–C30) is shown; bonds to disordered atoms S1a, S1b, O1a and O1b (SOP = 0.5) are indicated by dashes).

Table 4. Selected interatomic distances [Å], angles [°] and torsion angles [°] for **11**·CH_2Cl_2. The disordered atoms S1a, S1b, O1a and O1b have occupation parameters of 0.5, and C25a and C25b have values of 0.64(2) and 0.36(2).

S1a–P1	1.912(6)	S1b–P2	1.908(3)
P1–O1a	1.471(11)	P1–C1	1.886(6)
P1–C13	1.811(6)	P1–C19	1.810(6)
P2–O1b	1.495(10)	P2–C2	1.896(6)
P2–C25a	1.839(8)	P2–C25b	1.769(15)
P2–C31	1.814(7)	C1–C2	1.705(8)
S1a-P1-C1	113.9(3)	S1b-P2-C2	113.1(2)
P1-C1-C2	122.1(4)	P2-C2-C1	121.8(4)
C2-C1-P1-S1a	41.8(5)	C1-C2-P2-S1b	42.5(5)
P1-C1-C2-P2	9.8(6)		

phosphorus atoms was oxidized by selenium. This compound is isostructural with **9**. The $SePPh_2$ substituent at C1 is ordered but one of the phenyl groups of the PPh_2 substituent bonded to C2 is disordered and adopts two orientations (Figure 6). There are slight differences in the corresponding P–C and P–C_c distances between the phosphorus atoms having different oxidation states, as seen in Table 3. Also the P-C_c-C_c angles are different; P1-C1-C2 (122.5(4)°) is more obtuse than P2-C2-C1 (113.4(4)°), most likely due to the bulkier substituent at C1. The C1–C2 distance of 1.732(9) Å is, within experimental error, equal to those of 1.719(3) and 1.722(4) Å in the disubstituted *o*-carborane derivatives 1,2-($PiPr_2$)$_2$-1,2-*closo*-$C_2B_{10}H_{10}$[25] and 1,2-(PPh_2)$_2$-1,2-*closo*-$C_2B_{10}H_{10}$.[26] The Se–P1 distance of 2.0982(18) Å is also in the range for comparable Se–P bonds.[28] In the structure of **15** there are four Se···H(Ph) distances, from the three ordered phenyl groups, that are shorter than 3.0 Å, three of which are intramolecular (2.76–2.87 Å) and one (from H21) is intermolecular (2.96 Å). Also there is a Se···H6B6 contact of 3.04 Å. All of these quite long contacts in **9** and **15** gave bond critical points in the QTAIM theoretical calculations (Table 6).

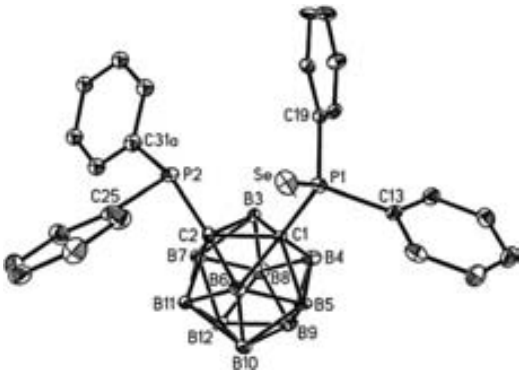

Figure 6. Molecular structure of **15** (ORTEP, thermal displacement ellipsoids are drawn at 30% probability, and hydrogen atoms are omitted, and only the major orientation of the disordered phenyl group (C31-C36) is shown).

Reactivity of monochalcogenide diphosphines: The carboranyl diphosphines reported here should be preferentially compared with *cis*-1,2-bis(diphenylphosphine)ethylene, *cis*-$Ph_2PHC{=}CHPPh_2$ (*cis*-dppen). The geometrical disposition of the two phosphorus atoms and the two cluster carbon atoms in 1,2-(PPh_2)$_2$-1,2-*closo*-$C_2B_{10}H_{10}$ is very similar to that of *cis*-dppen.[29] Both ligands have a similar orientation of the phosphorus atoms; they are coplanar with the carbon atoms to which they are bonded, and the P···P distance is 3.279 Å in *cis*-dppen and 3.2225(12) Å in 1,2-(PPh_2)$_2$-1,2-*closo*-$C_2B_{10}H_{10}$.[26] Whereas there are over 159 reported crystal structures[13] based on the rigid 1,2-bis(diphenylphosphino)ethylene ligand including *cis* and *trans* isomers, we did not find any example of a mono-chalcogenide $Ph_2PHC{=}CHP(X)Ph_2$. Crystal structures of monochalcogenides **9** and **15** indicated that they have two binding sites with a distinct chemical nature. A ligand that displays these characteristics is commonly addressed as hemilabile. The potential of these monochalcogenide carboranyl diphosphines **9** and **15** to behave as asymmetric chelating bidentate ligands for metal coordination was studied with different complexes of Ni^{II}, Pd^{II}, Au^{I} and Ru^{II}.

The $^{31}P\{^1H\}$ NMR spectrum of the crude reaction mixture of **15** and [$PdCl_2(PPh_3)_2$] displayed three signals at $\delta = -5$, +35.8 and +79.6 ppm after 24 h in CH_2Cl_2 (see Scheme 3a). The first peak corresponds to free PPh_3, the second to

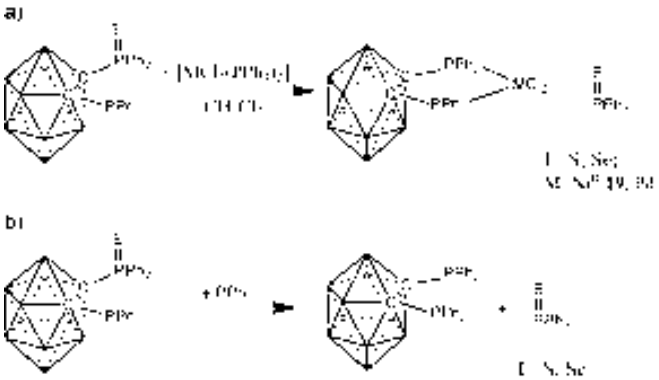

Scheme 3. Dechalcogenation process of the monochalcogenide carboranyl diphosphines.

Ph_3PSe[24] and the third to $[PdCl_2\{1,2\text{-}(PPh_2)_2\text{-}1,2\text{-}C_2B_{10}H_{10}\}]$.[29b] These results prompted us to hypothesise, based on available data in the literature,[30] that the loss of chalcogen from the ligand was a selenium transfer from a weaker phosphine Lewis base, namely, the *closo*-carboranyl diphenylphosphine, to a more basic one, that is, triphenylphosphine. To verify this, the reaction of **15** and $[PdCl_2(cod)]$ (cod = 1,5-cyclooctadiene) was carried out. After 24 h in CH_2Cl_2, the starting yellow solution turned dark brownish and the $^{31}P\{^1H\}$ NMR spectrum of the crude reaction product revealed one resonance at $\delta = +79.6$ ppm, which was again attributed to $[PdCl_2\{1,2\text{-}(PPh_2)_2\text{-}1,2\text{-}C_2B_{10}H_{10}\}]$.[29b] Upon filtration of the solution a red-grey solid, namely, selenium in its two allotropic forms, was isolated. Starting with the same concentration of **15** in CH_2Cl_2, the reaction with $[PdCl_2(cod)]$ was faster than with $[PdCl_2(PPh_3)_2]$, but deselenisation also took place. Therefore, the dechalcogenation was not necessarily concomitant with the presence of a more basic phosphine in the medium.

To verify whether ligand chalcogen loss is metal/ligand-dependent, reactions with $[NiCl_2(PPh_3)_2]$, $[NiCl_2(dppe)]$ (dppe = 1,2-bis(diphenylphosphanyl)ethane), $[AuCl(PPh_3)]$, $[RuCl_2(PPh_3)_3]$ and anhydrous $NiCl_2$ were performed. The loss of ligand chalcogen was very rapid with $[NiCl_2(PPh_3)_2]$. In 30 min 100% conversion to $[NiCl_2\{1,2\text{-}(PPh_2)_2\text{-}1,2\text{-}C_2B_{10}H_{10}\}]$ (**19**) was obtained; conversely, more than one day was needed with $[NiCl_2(dppe)]$ or $NiCl_2$ to obtain **19**. The deselenisation and subsequent metal-complexation reactions were completed after one day with $[AuCl(PPh_3)]$ and after five days with $[RuCl_2(PPh_3)_3]$. The reaction of **9** and **10** with $[PdCl_2(cod)]$, $[PdCl_2(PPh_3)_2]$ and $[NiCl_2(PPh_3)_2]$ also took place with loss of sulfur but at a slower rate than for **15**.

To unambiguously confirm the dechalcogenation process, appropriate crystals of $[NiCl_2\{1,2\text{-}(PPh_2)_2\text{-}1,2\text{-}C_2B_{10}H_{10}\}]$ (**19**) were obtained by slow evaporation of a CH_2Cl_2/Et_2O solution. The crystal structure (Figure 7, Table 5) confirmed the spectroscopic data. The structural parameters of **19** are similar to those of $[NiBr_2\{1,2\text{-}(PPh_2)_2\text{-}1,2\text{-}C_2B_{10}H_{10}\}]\cdot CH_2Cl_2$[31] (the Ni–Cl distances are 0.03 Å shorter than the Ni–Br distances).

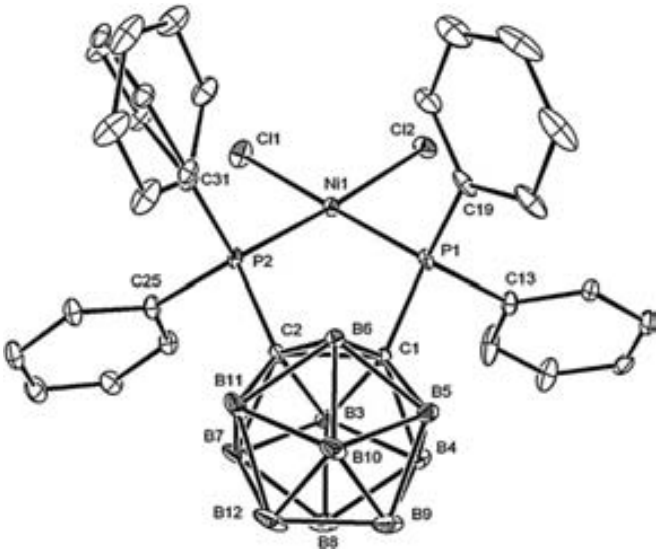

Figure 7. Molecular structure of $[NiCl_2\{1,2\text{-}(PPh_2)_2\text{-}1,2\text{-}C_2B_{10}H_{10}\}]$ (**19**) (ORTEP).

Table 5. Selected interatomic distances [Å], angles [°] and torsion angles [°] for **19**.

Ni1–P1	2.1461(10)	Ni1–P2	2.1500(10)
Ni1–Cl1	2.1831(10)	Ni1–Cl2	2.1861(10)
P1–C1	1.879(4)	P1–C13	1.813(4)
P1–C19	1.809(4)	P2–C2	1.879(4)
P2–C25	1.813(4)	P2–C31	1.811(4)
C1–C2	1.678(4)	P1-Ni1-P2	91.91(4)
P1-Ni1-Cl1	178.31(5)	P2-Ni1-Cl1	87.84(4)
P1-Ni1-Cl2	86.12(4)	P2-Ni1-Cl2	172.79(4)
Cl1-Ni1-Cl2	93.92(5)	Ni1-P1-C1	108.89(10)
Ni1-P2-C2	109.01(11)	P1-C1-C2	111.6(2)
P2-C2-C1	112.4(2)	C2-C1-P1-Ni1	−19.8(2)
C1-C2-P2-Ni	112.9(2)	P1-C1-C2-P2	4.3(3)

We also studied the influence of the solvent on loss of the chalcogen; it is independent of the nature and dryness of the solvent. Loss of chalcogen was attained with dry dichloromethane, toluene, acetonitrile, ethyl acetate, chloroform, 2-propanol or *tert*-butyl alcohol. If a nucleophilic solvent was used (e.g., 2-propanol,) the carborane cage was partially deboronated and *nido* complexes were obtained, as previously reported in the literature.[32]

Subsequently, we studied chalcogen transfer from mono-chalcogenide carboranyl diphosphines to triphenylphosphine in the absence of a metal. Transfer was very rapid; the reaction was completed in five minutes (Scheme 3b). Dechalcogenation of the mono-chalcogenide carboranyl diphosphines also takes place in the solid state; $[NiCl_2\{1,2\text{-}(PPh_2)_2\text{-}1,2\text{-}C_2B_{10}H_{10}\}]$ was obtained when 1 equivalent of **15** was milled with 1 equiv of $[NiCl_2(PPh_3)_2]$ for one hour in a ball mill.

The experimental coordination chemistry studies presented here show an anomalously high tendency of mono-chalcogenide carboranyl diphosphines to undergo dechalcogenation. The lability of the chalcogen atom of these compounds may be associated with steric and electronic effects. The nature of their chalcogen—phosphorus bonds was determined by DFT calculations, natural bond orbital (NBO) analysis and quantum theory of atoms in molecules (QTAIM).

Computational study on monochalcogenide carboranyl diphosphines: Although some computational studies on the phosphorus–chalcogen bond were found in the literature,[33] no study has been done on bulky phosphines or with strongly electron-withdrawing groups bonded to phosphorus. Three P=E bond resonance structures (Figure 8) are proposed in the literature.[24,34,35]

Calculations of the natural hybrid orbitals (NHOs) of the P=E (E = S, Se) bonds in **9** and **15** yielded the following composition: $\sigma_{PS} = 0.7097(sp^{2.54}d^{0.03})_P + 0.7045(sp^{5.12}d^{0.03})_S$ and $\sigma_{PSe} = 0.7426(sp^{2.66}d^{0.02})_P + 0.6697(sp^{7.18}d^{0.07})_{Se}$. Therefore, the phosphorus hybridisation is between sp^2 and sp^3 in both **9** and **15** and the d-orbital contribution to P=E bonding is

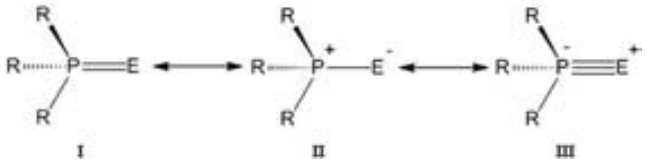

Figure 8. Proposed structures for phosphorus–chalcogen bonds (E = S, Se, Te).

negligible. The same NHO analysis revealed that the electron lone pair on the non-oxidized phosphorus atoms in both compounds is nearly sp in nature and that the electron lone pairs on the chalcogen atoms have almost pure p character.

Analysis by second-order perturbation theory showed significant interactions (Figure 9) between the electron lone pairs on the chalcogen atoms and the P–C_{ipso} and P–C_c anti-

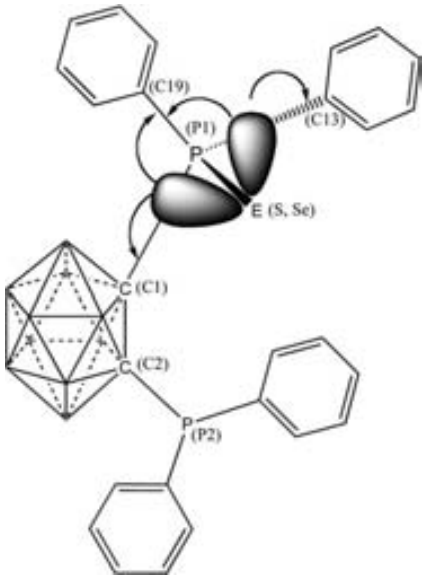

Figure 9. Schematic of the main interactions between the chalcogen lone pairs and the P–C bonds.

bonding orbitals (Table 6) in **9** and **15**. Here, each lone pair interacts with two P–C antibonding orbitals. This interaction is stronger in **9**, as the sulfur lone pairs are more delocalized, whereas in **15** the selenium lone pairs are more localized on the chalcogen. We calculated the stabilization energies for PPh_3S and PPh_3Se, and the same trends were observed, but the energies are half those obtained for **9** and **15**. This can be explained by the stronger electron-withdrawing character of the *closo* carborane cluster compared to the phenyl group.

The calculated NBO interactions are in agreement with the structural features observed in the X-ray structure determination. The distances between the C1 and the oxidized P atom (C1–P1) in **9** and **15** (Table 3) are longer than those between C2 and the unoxidized P atom (C2–P2). Also, the

Table 6. Second-order delocalization energies for the electron lone pairs and NBO antibonding interactions in **9** and **15**.

Compound	Lone pair[a]	P–C bond[b]	$\Delta E_{ij}^{(2)}$ [kcal mol^{-1}]
9	S(1)	P1–C13	12.66
	S(1)	P1–C19	8.43
	S(2)	P1–C1	20.10
	S(2)	P1–C19	6.07
15	Se(1)	P1–C13	9.91
	Se(1)	P1–C19	7.11
	Se(2)	P1–C1	16.91
	Se(2)	P1–C19	4.53

[a] The number in parentheses stands for the first (1) and the second (2) lone pair. [b] The atom numbering is the same as for the crystal structure.

distances between the oxidized P atom and the C atom of the phenyl rings (P1–C13 and P1–C19) are shorter than those between the unoxidized P and the C atoms of the phenyl rings (P2–C25 and P2–C31). As one would expect, donation of electrons from the chalcogen lone pairs to the antibonding orbitals of the P–C bonds should enlarge the P–C distance and diminish the C-P-C angles. As reported, the shortness of the P–C_{ipso} bonds has both electronic and steric origins and is typical of a variety of chalcogen phosphines.[24,34b] The peculiarity of compounds **9** and **15** is determined by the presence of the carborane cluster, which produces an asymmetry on the P center. Consequently, the effect of multiple lone-pair delocalization in one bond results in three different C-P-C angles. The P1–C19 antibonding orbital receives charge density from both of the lone pairs in the chalcogen atom, opening the C-P-C angles to 108.18° for C1-P1-C19 and 106.94° for C13-P1-C19 in **9**. This diminishes the C1-P1-C13 angle to 102.85, a value that is typical for C-P-C angles of an unoxidized P center. The P1–C1 bond elongates to meet the steric demands, which are due to diminishment of the C1-P1-C13 angle and the high interaction energy (Table 6) between the second lone pair of the chalcogen and the P1–C1 antibonding orbital. The same structural features are observed for **15**.

The NBO analysis of **9** and **15** revealed that the chalcogen lone pairs are involved in back-donation and in intramolecular interactions, and thus are less available for bonding. The presence of a second phosphine group in **9** and **15** weakens the complexation ability of these ligands due to the steric hindrance of the phenyl groups. Conversely, the coordination ability of the less hindered anionic ligand [1-S-2-$SP(CH_3)_2$-1,2-$C_2B_{10}H_{10}$]$^-$ is high,[36] as the electronic effects are significant and lower the strength of the P=E bond. This weakening of the P=E bond takes place in at least two ways: the first is due to the strong electron-withdrawing character of the *closo* carborane cluster, which tends to polarize the P=E (E = S, Se) bond towards the phosphorus atom; secondly, the difference in electronegativity between the chalcogen and the phosphorus atoms tends to polarize the bond towards the chalcogen. The electron-withdrawing character of the carborane cluster is slightly stronger as can

be observed from the higher value of the polarization coefficient of the phosphorus atom in the NHOs presented above.

The QTAIM analysis of **9** and **15** revealed intramolecular interactions between the chalcogen and neighbouring atoms. The electron density of the P1–S bond (entry 1 in Table 7) is

Table 7. Properties of the BCP between the chalcogen atoms and their neighbouring atoms in **9** (entries 1–5) and **15** (entries 6–10). All values are in a.u.[a]

Entry	Bond[b]	ρ	$\nabla^2\rho$	ε	H
1	S–P1	0.1642	−2.492	0.0159	−0.1163
2	S–H6	0.0099	0.0297	0.5110	0.0009
3	S–H18	0.0115	0.0426	9.1175	0.0017
4	S–H20	0.0127	0.0415	0.7120	0.0015
5	S–H26	0.0090	0.0235	0.0335	0.0010
6	Se–P1	0.1296	−0.0436	0.0160	−0.0684
7	Se–H6	0.0115	0.0297	0.3101	0.0009
8	Se–H18	0.0147	0.0109	0.3074	0.0013
9	Se–H20	0.0148	0.0415	0.3523	0.0013
10	Se–H26	0.0101	0.0252	0.0432	0.0010

[a] ρ = electron density, $\nabla^2\rho$ = Laplacian of the electron density, ε = ellipticity, H = total electronic energy density. [b] The numbering is presented in Figure S.3 of the Supporting Information.

in the range of those of P=S bonds found for compounds like H_3PS and Me_3PS.[34c] For **15** (entry 6 in Table 7) the electron density for the P1–Se bond is very low, and the small but negative $\nabla^2\rho$ value indicates that the bond is a weak shared interaction. To our knowledge this is the first time that such studies have been performed on the P=Se bond. Therefore, no other data are available for comparison.

The BCP study revealed that interactions between the chalcogen and its neighbouring hydrogen atoms, either from the phenyl rings or from the carborane cluster (entries 2–5 and 7–10 in Table 7), fully agree with the X-ray structures (Table 3, Figure 10). The deshielding of some resonances in the ^{1}H NMR spectra for **9** and **15** compared to the parent 1,2-$(PPh_2)_2$-1,2-*closo*-$C_2B_{10}H_{10}$ indicate that the E···H interactions are maintained in solution. Two groups of chemical shifts with a ratio of 3:17, corresponding to the hydrogen atoms on the phenyl groups, are observed for **9** and **15**, one at $\delta = 8.43$–8.29 ppm and the other at $\delta = 7.63$–7.27 ppm (Figure 11). Moreover, H6 of the carborane cluster, which interacts with the respective chalcogen atom, is also deshielded relative to the parent 1,2-$(PPh_2)_2$-1,2-*closo*-$C_2B_{10}H_{10}$ and appears at $\delta = 3.06$ ppm for **9** and $\delta = 3.17$ ppm for **15** (Figure 11).

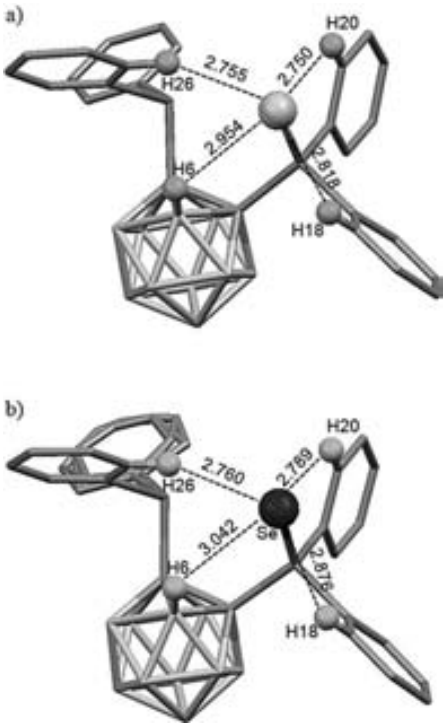

Figure 10. Distances between the chalcogen and the neighbouring hydrogen atoms in **9** (a) and **15** (b). Only the hydrogen atoms of interest are presented for the sake of clarity.

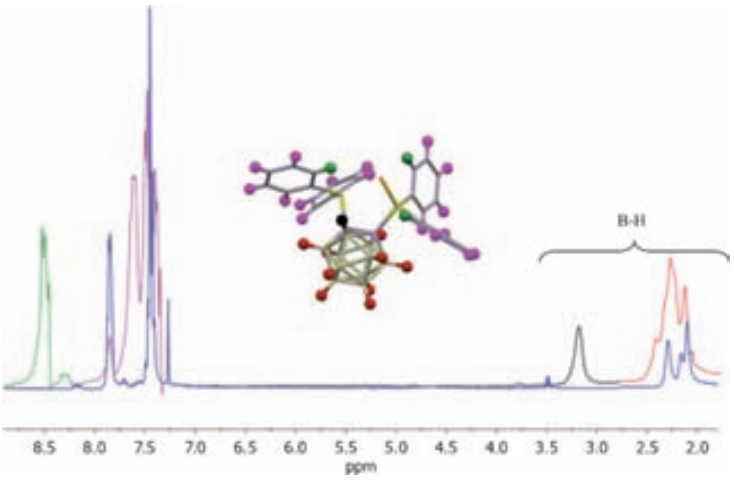

Figure 11. $^{11}H\{^{11}B\}$ NMR spectra of 1,2-$(PPh_2)_2$-*closo*-1,2-$C_2B_{10}H_{10}$ (blue) and 1-$SePPh_2$-2-PPh_2-1,2-*closo*-$C_2B_{10}H_{10}$ (green: H18, H20 and H26; pink: the other 17 hydrogen atoms of the phenyl groups; black: H6; red: the other nine hydrogen atoms of the cluster vertices).

Conclusions

When H_2O_2 is added to 1,2-$(PR_2)_2$-1,2-*closo*-$C_2B_{10}H_{10}$ (R = Ph, *i*Pr), they are oxidized to 1,2-$(OPR_2)_2$-1,2-*closo*-$C_2B_{10}H_{10}$ (R = Ph, *i*Pr). However, when S and Se are used, different reactivity is found for 1,2-$(PPh_2)_2$-1,2-*closo*-$C_2B_{10}H_{10}$ and 1,2-$(PiPr_2)_2$-1,2-*closo*-$C_2B_{10}H_{10}$. For R = Ph, the reaction with sulfur produces mono- and dioxidation species; thus, 1-$SPPh_2$-2-PPh_2-1,2-*closo*-$C_2B_{10}H_{10}$ and 1,2-$(SPPh_2)_2$-1,2-*closo*-$C_2B_{10}H_{10}$ can be isolated. However, when Se is the oxidizing agent, only the monooxidation species 1-$SePPh_2$-2-PPh_2-1,2-*closo*-$C_2B_{10}H_{10}$ is obtained. For R = *i*Pr, only monooxidation takes place with S, and the second C_c–P*i*Pr_2 bond breaks to yield 1-S*i*Pr_2-1,2-*closo*-$C_2B_{10}H_{11}$ if the reaction time is prolonged. When Se is used on 1,2-$(PiPr_2)_2$-1,2-*closo*-$C_2B_{10}H_{10}$ only the species with one phosphorus atom, 1-$SePR_2$-1,2-

closo-$C_2B_{10}H_{11}$, is found. Oxidation of carboranyl monophosphines requires longer reaction times than that of carboranyl diphosphines.

The carboranyl moiety influences the phosphorus atoms bonded to the C_c atoms of the cluster. This is evidenced in the ^{31}P NMR spectra and in the chemical properties. The electron-acceptor character of the carboranyl cluster lowers the charge density on the phosphorus atom, and this results in 1) deshielded P resonances in the ^{31}P NMR spectrum; 2) increased stability of carboranyl diphosphines against oxidation in the solid state and in solution, even under air; and 3) polarisation of the P=E bond towards phosphorus, which weakens this bond. This is relevant to understanding the coordination ability of these ligands. The R group in 1,2-$(PR_2)_2$-1,2-*closo*-$C_2B_{10}H_{10}$ compounds also has an influence, that is, an electron-donating group such *i*Pr facilitates the oxidation reaction better than an electron-withdrawing Ph group.

Experimental studies on the coordination ability of monochalcogenide carboranyl diphosphines (**9** and **15**) have shown that these compounds do not behave as hemilabile ligands because the lability of the P=E bond towards metal coordination results in dechalcogenation and P–M bond formation.

Computational studies provided steric and electronic information on the P=E (E = S, Se) bonds in **9** and **15**. The steric effects block the bonding ability of the P=E bond due to interactions between the chalcogen and the neighbouring hydrogen atoms (H18, H20 and H26 of the phenyl rings and H6 of the carborane cluster). The electronic effects originate in the strongly electron-withdrawing character of the *closo* carborane cluster, which polarizes the P=E (E = S, Se) bond towards the phosphorus atom. As a consequence, the E atom is the electron-poor site and the P atom is the electron-rich site in the P=E bond. Hence, PPh_3 as a Lewis base attacks the E side, and the metal as a Lewis acid the P side. Computational studies fully agree with the experimental observations reported in this paper.

Experimental Section

Caution! H_2O_2 in acetone is potential explosive. On this scale and under these conditions no explosions occurred. Nevertheless, this does not preclude such an event when dealing with these species. Extreme precautions should be taken.

Instrumentation: Elemental analyses were performed with a Carlo Erba EA1108 microanalyzer. IR spectra ($\tilde{\nu}$/cm^{-1}; KBr pellets) were obtained on a Shimadzu FTIR-8300 spectrophotometer. The ^1H and $^1H\{^{11}B\}$ (300.13 MHz), $^{13}C\{^1H\}$ (75.47 MHz), ^{11}B and $^{11}B\{^1H\}$ (96.29 MHz) and $^{31}P\{^1H\}$ (121.48 MHz) NMR spectra were recorded on a Bruker ARX 300 instrument equipped with the appropriate decoupling accessories. All NMR spectra were performed in deuterated solvents at 22 °C. The ^{11}B and $^{11}B\{^1H\}$ NMR shifts were referenced to external $BF_3{\cdot}OEt_2$, the ^1H, $^1H\{^{11}B\}$ and $^{13}C\{^1H\}$ NMR shifts to $SiMe_4$ and the $^{31}P\{^1H\}$ NMR shifts to external 85% H_3PO_4. Chemical shifts are reported in units of parts per million downfield from reference, and all coupling constants in hertz. The mass spectra were recorded in negative-ion mode on a Bruker Biflex MALDI-TOF-MS [N_2 laser; λ_{exc} = 337 nm (0.5 ns pulses); voltage ion source 20.00 kV (U_{is1}) and 17.50 kV (U_{is2})].

Materials: All manipulations were carried out under inert atmosphere. THF, 1,2-dimethoxyethane (DME) and toluene were distilled from sodium benzophenone prior to use. EtOH was dried over molecular sieves and deoxygenated prior to use. Reagents were obtained commercially and used as purchased. 1,2-*closo*-$C_2B_{10}H_{12}$, 1-Me-1,2-*closo*-$C_2B_{10}H_{11}$, 1-Ph-1,2-*closo*-$C_2B_{10}H_{11}$ were from Katchem. 1,2-$(PPh_2)_2$-1,2-*closo*-$C_2B_{10}H_{10}$,[37] 1,2-$(P^iPr_2)_2$-1,2-*closo*-$C_2B_{10}H_{10}$, $[NMe_4][7,8\text{-}(PR_2)_2\text{-}7,8\text{-}nido\text{-}C_2B_9H_{10}]$, 1-$PR'_2$-2-R-1,2-*closo*-$C_2B_{10}H_{10}$ (R = Me, Ph and R′ = Ph, ^{i}Pr) were prepared from *o*-carborane according to the literature. [$PdCl_2$(cod)],[38] [$PdCl_2(PPh_3)_2$],[39] [$NiCl_2(PPh_3)_2$],[40] [$NiCl_2$(dppe)],[41] [AuCl(PPh_3)][42] and [$RuCl_2(PPh_3)_3$][43] were synthesized as described elsewhere. Anhydrous $NiCl_2$ was purchased from Aldrich.

General procedure for preparation of carboranyl phosphine oxides: Carboranyl phosphines were oxidized with a 0.2 M solution of H_2O_2 in acetone or THF at 0 °C. In the following preparations only the reagents are indicated.

Synthesis of 1,2-$(OPPh_2)_2$-1,2-*closo*-$C_2B_{10}H_{10}$ (1): 1,2-$(PPh_2)_2$-1,2-*closo*-$C_2B_{10}H_{10}$ (50 mg, 0.10 mmol), H_2O_2 (1.5 mL, 0.40 mmol), THF (5 mL) produced 1,2-$(OPPh_2)_2$-1,2-*closo*-$C_2B_{10}H_{10}$ (48 mg, 98%) as a white solid after stirring for 4 h. Elemental analysis (%) calcd for $C_{26}H_{30}B_{10}O_2P_2$: C 57.34, H 5.55; found: C 57.12, H 5.80; FTIR: $\tilde{\nu}$ = 3048, 2962 (CH_{aryl}); 2555 (BH); 1214, 1191 cm^{-1} (P=O); ^1H NMR ($CDCl_3$): δ = 8.03 (m, 10H, Ph), 7.52 (m, 10H, Ph), 2.68–2.09 ppm (br m, 10H, BH); $^1H\{^{11}B\}$ NMR ($CDCl_3$): δ = 8.03 (m, 10H, Ph), 7.52 (m, 10H, Ph), 2.68 (br s, 2H, BH), 2.49 (br s, 1H, BH), 2.35 (br s, 2H, BH), 2.30 (br s, 3H, BH), 2.09 ppm (br s, 2H, BH); $^{13}C\{^1H\}$ NMR ($CDCl_3$): δ = 132.58 (d, ^2J(C,P) = 8 Hz, Ph), 132.27, 130.80, 129.33 (s, Ph), 128.25 ppm (d, ^2J(C,P) = 14 Hz, Ph); ^{11}B NMR ($CDCl_3$): δ = 2.8 (d, ^1J(B,H) = 88 Hz, 2B), −6.7 (4B), −7.9 ppm (4B); $^{31}P\{^1H\}$ NMR ($CDCl_3$): δ = 23.67 ppm (s, $OPPh_2$).

Synthesis of 1,2-$(OPiPr_2)_2$-1,2-*closo*-$C_2B_{10}H_{10}$ (2): 1,2-$(PiPr_2)_2$-1,2-*closo*-$C_2B_{10}H_{10}$ (50 mg, 0.13 mmol), H_2O_2 (2.0 mL, 0.40 mmol), THF (5 mL) afforded 1,2-$(OPiPr_2)_2$-1,2-*closo*-$C_2B_{10}H_{10}$ (54 mg, 99%) as a white solid after stirring for 40 min. Elemental analysis (%) calcd for $C_{14}H_{38}B_{10}O_2P_2$: C 41.16, H 9.38; found: C 41.04, H 9.25; FTIR: $\tilde{\nu}$ = 2996, 2970, 2933, 2878 (CH_{alkyl}); 2644, 2622, 2596, 2575, 2550 (BH); 1192 cm^{-1} (P=O); ^1H NMR ($CDCl_3$): δ = 2.02 (m, 4H, CH), 1.41 (dd, ^3J(P,H) = 11 Hz, ^3J(H,H) = 7 Hz, 12H, Me), 1.35 ppm (dd, ^3J(P,H) = 13 Hz, ^3J(H,H) = 7 Hz, 12H, Me); $^{13}C\{^1H\}$ NMR ($CDCl_3$): δ = 81.61 (d, ^1J(C,P) = 19 Hz, C_c), 30.53 (d, ^1J(C,P) = 61 Hz, CH), 17.4 (s, Me), 18.4 ppm (s, Me); ^{11}B NMR ($CDCl_3$): δ = 2.8 (d, ^1J(B,H) = 140 Hz, 2B, B(9,12)), −6.5 (d, ^1J(B,H) = 211 Hz, 2B, B(8,10)), −9.1 ppm (d, ^1J(B,H) = 138 Hz, 6B, B(3,4,5,6,7,11)); ^{31}P NMR ($CDCl_3$): δ = 59.08 ppm (d, ^2J(P,H) = 16 Hz, $OPiPr_2$).

Synthesis of 1-$OPPh_2$-2-Me-1,2-*closo*-$C_2B_{10}H_{10}$ (3): 1-PPh_2-2-Me-1,2-*closo*-$C_2B_{10}H_{10}$ (500 mg, 1.46 mmol), H_2O_2 (7.13 mL, 1.46 mmol), acetone (10 mL) afforded 1-$OPPh_2$-2-Me-1,2-*closo*-$C_2B_{10}H_{10}$ (500 mg, 96.5%) as a white solid after stirring overnight. Elemental analysis (%) calcd for $C_{15}H_{23}B_{10}OP$: C 50.30, H 6.40; found: C 50.05, H 6.89; FTIR: $\tilde{\nu}$ = 3061 (CH_{aryl}); 2962, 2933, 2872 (CH_{alkyl}); 2631, 2594, 2575, 2556 (BH); 1967, 1909, 1819 (C=C); 1437 (PPh); 1213 cm^{-1} (P=O); ^1H NMR (CD_3COCD_3): δ = 8.27 (d, ^3J(H,H) = 6.5 Hz, 2H, Ph), 8.23 (d, ^3J(H,H) = 6.9 Hz, 2H, Ph), 7.69 (m, 6H, Ph), 2.25 (s, 3H, Me), 2.53–2.11 (br m, 10H, BH); $^1H\{^{11}B\}$ NMR (CD_3COCD_3): δ = 8.27 (d, ^3J(H,H) = 6.5 Hz, 2H, Ph), 8.23 (d, ^3J(H,H) = 6.9 Hz, 2H, Ph), 7.69 (m, 6H, Ph), 2.53 (br s, 1H, BH), 2.41 (br s, 1H, BH), 2.25 (s, 3H, Me), 2.11 ppm (br s, 8H, BH); $^{13}C\{^1H\}$ NMR (CD_3COCD_3): δ = 133.50 (s, Ph), 132.44 (d, ^3J(C,P) = 9.6 Hz, Ph), 128.90 (d, ^2J(C,P) = 12.4 Hz, Ph), 24.25 (s, Me); ^{11}B NMR (CD_3COCD_3): δ = 0.4 (d, ^1J(B,H) = 141 Hz, 1B), −4.7 (d, ^1J(B,H) = 148 Hz, 1B), −8.2 (d, ^1J(B,H) = 123 Hz, 2B), −9.3 (d, ^1J(B,H) = 164 Hz, (2+2)B), −10.4 ppm (d, ^1J(B,H) = 154, 2B); $^{31}P\{^1H\}$ NMR (CD_3COCD_3): δ = 19.28 ppm (s, $OPPh_2$). Single crystals were grown by slow evaporation from diethyl ether solution.

Synthesis of 1-$OPiPr_2$-2-Me-1,2-*closo*-$C_2B_{10}H_{10}$ (4): 1-$PiPr_2$-2-Me-1,2-*closo*-$C_2B_{10}H_{10}$ (1.1 g, 4.0 mmol), H_2O_2 (24 mL, 4.7 mmol), acetone (50 mL) afforded 1-$OPiPr_2$-2-Me-1,2-*closo*-$C_2B_{10}H_{10}$ (957 mg, 82%) as a yellow oil after stirring for 90 min. FTIR: $\tilde{\nu}$ = 2974, 2930, 2878 (CH_{alkyl}); 2627, 2576 (BH); 1941, 1845 (C=C); 1174 cm^{-1} (P=O); ^1H NMR (CD_3COCD_3): δ = 2.60 (sept., ^3J(H,H) = 7.2 Hz, 2H, CH), 2.37 (s, 3H, Me), 1.42 (d, ^3J(H,H) = 7.2 Hz, 6H, Me), 1.36 (d, ^3J(H,H) = 7.2 Hz, 6H,

Me), 2.71–2.27 ppm (brm, 10H, BH); $^{1}H\{^{11}B\}$ NMR (CD_3COCD_3): $\delta =$ 2.71 (brs, 1H, BH), 2.60 (s, $^{3}J(H,H) = 7.2$ Hz, 2H, CH), 2.46 (brs, 1H, BH), 2.37 (s, 3H, Me), 2.27 (brs, 8H, BH), 1.42 (d, $^{3}J(H,H) = 7.2$ Hz, 6H, Me), 1.36 ppm (d, $^{3}J(H,H) = 7.2$ Hz, 6H, Me); $^{13}C\{^{1}H\}$ NMR (CD_3COCD_3): $\delta = 80.73$ (s, C_c), 73.23 (d, $^{1}J(C,P) = 22$ Hz, C_c), 30.28 (d, $^{1}J(C,P) = 63$ Hz, CH), 24.47 (s, Me), 16.63 ppm (d, $^{2}J(C,P) = 40$ Hz, Me); ^{11}B NMR (CD_3COCD_3): $\delta = 1.6$ (d, $^{1}J(B,H) = 145$ Hz, 1B), -4.6 (d, $^{1}J(B,H) = 153$ Hz, 1B), -8.2 ppm (m, 8B); $^{31}P\{^{1}H\}$ NMR (CD_3COCD_3): $\delta =$ 58.18 ppm (s, OP*i*Pr$_2$).

Synthesis of 1-OPCy$_2$-2-Me-1,2-*closo*-C$_2$B$_{10}$H$_{10}$ (5): 1-PCy$_2$-2-Me-1,2-*closo*-$C_2B_{10}H_{10}$ (950 mg, 2.7 mmol), H_2O_2 (18.4 mL, 3.7 mmol), THF (30 mL) afforded 1-OPCy$_2$-2-Me-1,2-*closo*-$C_2B_{10}H_{10}$ (670 mg, 67.2%) as a white solid after stirring for 90 min. Elemental analysis (%) calcd for $C_{15}H_{35}B_{10}OP$: C 48.60, H 9.40; found: C 48.86, H 9.75; FTIR: $\tilde{\nu} = 2934$, 2856 (CH_{alkyl}); 2635, 2615, 2579, 2561 (BH); 1186 cm^{-1} (P=O); ^{1}H NMR ($CDCl_3$): $\delta = 2.33$ (s, 3H, Me), 1.36–1.28 (m, 22H, Cy); $^{13}C\{^{1}H\}$ NMR ($CDCl_3$): $\delta = 80.31$ (s, C_c), 72.19 (d, $^{1}J(P,C) = 26.2$ Hz, C_c), 41.63 (d, $^{1}J(P,C) = 62.0$ Hz, Cy), 27.11, 26.88, 26.71 (s, Cy), 25.88 ppm (s, Me); ^{11}B NMR ($CDCl_3$): $\delta = 2.9$ (d, $^{1}J(B,H) = 140$ Hz, 1B), -3.6 (d, $^{1}J(B,H) = 155$ Hz, 1B), -7.1 (d, $^{1}J(B,H) = 160$ Hz, 4B), -9.1 ppm (d, $^{1}J(B,H) = 160$ Hz, 4B); $^{31}P\{^{1}H\}$ NMR ($CDCl_3$): $\delta = 48.84$ ppm (s, $OPCy_2$). Single crystals were grown by slow evaporation from a hexane/acetone solution.

Synthesis of 1-OPPh$_2$-2-Ph-1,2-*closo*-C$_2$B$_{10}$H$_{10}$ (6): 1-PPh$_2$-2-Ph-1,2-*closo*-$C_2B_{10}H_{10}$ (2.2 g, 5.4 mmol), H_2O_2 (27.6 mL, 5.4 mmol), acetone (30 mL) afforded 1-OPPh$_2$-2-Ph-1,2-*closo*-$C_2B_{10}H_{10}$ (2.1 g, 92%) as a white solid after stirring overnight. Elemental analysis (%) calcd for $C_{20}H_{25}B_{10}OP$: C 57.10, H 5.90; found: C 56.44, H 5.95; FTIR: $\tilde{\nu} = 3061$ (CH_{aryl}); 2594, 2575, 2557 (BH); 1965, 1894, 1817 (C=C); 1437 (PPh); 1211 cm^{-1} (P=O); ^{1}H NMR (CD_3COCD_3): $\delta = 7.95$ (d, $^{3}J(H,H) = 7.5$ Hz, 2H, Ph), 7.91 (d, $^{3}J(H,H) = 7.5$ Hz, 2H, Ph), 7.64 (d, $^{3}J(H,H) = 7.2$ Hz, 2H, Ph), 7.53 (m, 6H, Ph), 7.40 (d, $^{3}J(H,H) = 7.5$ Hz, 2H, Ph), 7.20 (t, $^{3}J(H,H) = 8.2$ Hz, 1H, Ph), 3.25–2.23 ppm (brm, 10H, BH); $^{1}H\{^{11}B\}$ NMR (CD_3COCD_3): $\delta = 7.95$ (d, $^{3}J(H,H) = 7.5$ Hz, 2H, Ph), 7.91 (d, $^{3}J(H,H) = 7.5$ Hz, 2H, Ph), 7.64 (d, $^{3}J(H,H) = 7.2$ Hz, 2H, Ph), 7.53 (m, 6H, Ph), 7.40 (d, $^{3}J(H,H) = 7.5$ Hz, 2H, Ph), 7.20 (t, $^{3}J(H,H) = 8.2$ Hz, 1H, Ph), 3.25 (brs, 1H, BH), 2.53 (brs, 1H, BH), 2.31 (brs, 2H, BH), 2.23 ppm (brs, 6H, BH); $^{13}C\{^{1}H\}$ NMR (CD_3COCD_3): $\delta = 133.08$ (s, Ph), 132.50 (d, $^{3}J(P,C) = 8.3$ Hz, Ph), 131.81 (s, Ph), 130.60 (s, Ph), 130.03 (d, $^{1}J(P,C) = 12.4$ Hz, Ph), 128.40 (d, $^{2}J(P,C) = 12.4$ Hz, Ph), 127.93 (s, Ph), 126.35 (s, Ph), 85.66 (s, C_c), 79.70 ppm (d, $^{1}J(C,P) = 51$ Hz, C_c); ^{11}B NMR (CD_3COCD_3): $\delta = 1.9$ (d, $^{1}J(B,H) = 150$ Hz, 1B), -1.6 (d, $^{1}J(B,H) = 150$ Hz, 1B), -6.6 (d, $^{1}J(B,H) = 165$ Hz, 2B), -8.6 (d, $^{1}J(B,H) = 170$ Hz, (2+2)B), -9.6 ppm (d, $^{1}J(B,H) = 121$ Hz, 2B); $^{31}P\{^{1}H\}$ NMR (CD_3COCD_3): $\delta = 19.65$ ppm (s, $OPPh_2$).

Synthesis of 1-OP*i*Pr$_2$-2-Ph-1,2-*closo*-C$_2$B$_{10}$H$_{10}$ (7): 1-P*i*Pr$_2$-2-Ph-1,2-*closo*-$C_2B_{10}H_{10}$ (900 mg, 2.7 mmol), H_2O_2 (15.6 mL, 3.1 mmol), THF (20 mL) afforded 1-OP*i*Pr$_2$-2-Ph-1,2-*closo*-$C_2B_{10}H_{10}$ (540 mg, 57.4%) as a white solid after stirring for 90 min. Elemental analysis (%) calcd for $C_{14}H_{29}B_{10}OP$: C 47.70, H 8.20; found: C 47.15, H 8.71; FTIR: $\tilde{\nu} = 3070$ (CH_{aryl}); 2972, 2939, 2878 (CH_{alkyl}); 2575 (BH); 1201 cm^{-1} (P=O); ^{1}H NMR ($CDCl_3$): $\delta = 7.70$ (d, $^{3}J(H,H) = 7.3$ Hz, 2H, Ph), 7.35 (m, 3H, Ph), 2.28 (sept., $^{3}J(H,H) = 7.3$ Hz, 2H, CH), 1.28 (dd, $^{3}J(H,P) = 16$ Hz, $^{3}J(H,H) = 7.3$ Hz, 6H, Me), 1.21 (dd, $^{3}J(H,P) = 16$ Hz, $^{3}J(H,H) = 7.3$ Hz, 6H, Me), 3.25–2.43 ppm (brm, 10H, BH); $^{1}H\{^{11}B\}$ NMR ($CDCl_3$): $\delta =$ 7.70 (d, $^{3}J(H,H) = 7.3$ Hz, 2H, Ph), 7.35 (m, 3H, Ph), 3.25 (brs, 1H, BH), 2.69 (brs, 1H, BH), 2.43 (brs, 8H, BH), 2.28 (sept., $^{3}J(H,H) = 7.3$ Hz, 2H, CH), 1.28 (dd, $^{3}J(H,P) = 16$ Hz, $^{3}J(H,H) = 7.3$ Hz, 6H, Me), 1.21 ppm (dd, $^{3}J(H,P) = 16$ Hz, $^{3}J(H,H) = 7.3$ Hz, 6H, Me); $^{13}C\{^{1}H\}$ NMR ($CDCl_3$): $\delta = 131.88$, 130.51, 127.86 (s, Ph), 87.50 (s, C_c), 82.66 (s, C_c), 30.35 (d, $^{1}J(P,C) = 63.4$ Hz, CH), 17.32 ppm (d, $^{2}J(P,C) = 19.3$ Hz, Me); ^{11}B NMR ($CDCl_3$): $\delta = 3.0$ (d, $^{1}J(B,H) = 156$ Hz, 1B), -1.8 (d, $^{1}J(B,H) = 152$ Hz, 1B), -7.6 (d, $^{1}J(B,H) = 146$ Hz, (2+2)B), -9.6 ppm (d, $^{1}J(B,H) = 150$ Hz, (2+2)B); $^{31}P\{^{1}H\}$ NMR ($CDCl_3$): $\delta = 53.27$ ppm (s, OP*i*Pr$_2$).

Synthesis of 1-OPPh$_2$-2-SBz-1,2-*closo*-C$_2$B$_{10}$H$_{10}$ (8): 1-PPh$_2$-2-SBz-1,2-*closo*-$C_2B_{10}H_{10}$ (5.0 mg, 0.011 mmol), H_2O_2 (0.1 mL, 0.2 mmol), acetone (1 mL) afforded 1-OPPh$_2$-2-SBz-1,2-*closo*-$C_2B_{10}H_{10}$ (4.2 mg, 79.5%) after stirring for 25 min. FTIR: $\tilde{\nu} = 3061$ (CH_{aryl}); 2926, 2854 (CH_{alkyl}); 2569 (BH); 1437 (PPh); 1211 cm^{-1} (P=O); ^{1}H NMR ($CDCl_3$): $\delta = 8.17$ (d, $^{3}J(H,H) = 6.9$ Hz, 2H, Ph), 8.13 (d, $^{3}J(H,H) = 6.9$ Hz, 2H, Ph), 7.63–7.32 (m, 11H, Ph), 4.44 ppm (s, 2H, CH_2); $^{1}H\{^{11}B\}$ NMR ($CDCl_3$): $\delta = 8.17$ (d, $^{3}J(H,H) = 6.9$ Hz, 2H, Ph), 8.13 (d, $^{3}J(H,H) = 6.9$ Hz, 2H, Ph), 7.63–7.32 (m, 11H, Ph), 4.44 (s, 2H, CH_2), 2.84 (brs, 1H, BH), 2.55 (brs, 3H, BH), 2.23 ppm (brs, 6H, BH); $^{13}C\{^{1}H\}$ NMR ($CDCl_3$): $\delta = 133.61$, 133.01, 132.80, 132.68, 129.88, 128.70, 128.56, 128.39, 128.02 (s, Ph), 85.66 (s, C_c), 80.67 (d, $^{1}J(C,P) = 56$ Hz, C_c), 42.32 ppm (s, CH_2); ^{11}B NMR ($CDCl_3$): $\delta =$ 0.8 (d, $^{1}J(B,H) = 131$ Hz, 1B), -3.1 (d, $^{1}J(B,H) = 149$ Hz, 1B), -9.4 ppm (d, $^{1}J(B,H) = 142$ Hz, 8B); $^{31}P\{^{1}H\}$ NMR ($CDCl_3$): $\delta = 21.87$ ppm (s, $OPPh_2$).

General procedure for preparation of carboranyl phosphine sulfides: Carboranyl phosphines were oxidized with sulfur powder in acetone, THF or toluene under reflux. For the following preparations, only the reagents are indicated.

Oxidation of 1,2-(PPh$_2$)$_2$-1,2-*closo*-C$_2$B$_{10}$H$_{10}$ with S: Acetone (4 mL) and THF (1 mL) were added to [1,2-(PPh$_2$)$_2$-1,2-*closo*-$C_2B_{10}H_{10}$] (100 mg, 0.20 mmol). Then, S powder (13 mg, 0.40 mmol) was added to the solution and the mixture was heated to reflux for two days. After evaporation of the solvent a white solid appeared, which was extracted with diethyl ether (10 mL). From the suspension solid **9** was filtered (yield: 33 mg, 31%). Purification of the ether phase by preparative thin-layer chromatography (silica G, CH_2Cl_2/hexane 4/1) yielded **10** ($R_f = 0.56$, 22 mg, 20%) and **16** ($R_f = 0.3125$, 23 mg, 20%).

1-SPPh$_2$-2-PPh$_2$-1,2-*closo*-C$_2$B$_{10}$H$_{10}$ (9): Elemental analysis (%) calcd for $C_{26}H_{30}B_{10}SP_2 \cdot 0.3\,CH_2Cl_2$: C 55.20, H 5.39, S 5.60; found: C 55.24, H 5.66, S 5.94; FTIR: $\tilde{\nu} = 3053$ (CH_{aryl}); 2574 (BH); 652 cm^{-1} (P=S); ^{1}H NMR ($CDCl_3$): $\delta = 8.43$ (d, $^{3}J(H,H) = 7$ Hz, 2H, Ph), 8.39 (d, $^{3}J(H,H) = 7$ Hz, 2H, Ph), 7.63–7.27 (m, 16H, Ph), 3.1–2.00 (brm, BH); $^{1}H\{^{11}B\}$ NMR ($CDCl_3$): 8.43 (d, $^{3}J(H,H) = 7$ Hz, 2H, Ph), 8.39 (d, $^{3}J(H,H) = 7$ Hz, 2H, Ph), 7.63–7.27 (m, 16H, Ph), 3.06 (brs, 1H, BH), 2.32 (brs, 4H, BH), 2.23 (s, 4H, BH), 1.63 ppm (brs, 1H, BH); $^{13}C\{^{1}H\}$ NMR ($CDCl_3$): $\delta =$ 135.8 (d, $J(C,P) = 10$ Hz, Ph), 135.1 (d, $J(C,P) = 23$ Hz, Ph), 134.6 (d, $J(C,P) = 10$ Hz, Ph), 133.9 (d, $J(C,P) = 18$ Hz, Ph), 132.5 (s, Ph), 130.2 (s, Ph), 128.2 (d, $J(C,P) = 8$ Hz, Ph), 127.8 (d, $J(C,P) = 12$ Hz, Ph), 85.5 (d, $^{1}J(C,P) = 87$ Hz, C_c), 82.5 ppm (dd, $^{3}J(C,P) = 15$ Hz, $^{1}J(C,P) = 32$ Hz, C_c); ^{11}B NMR ($CDCl_3$): $\delta = 2.15$ (d, $^{1}J(B,H) = 151$ Hz, 1B), 1.05 (d, $^{1}J(B,H) = 140$ Hz, 1B), -6.83 (d, $^{1}J(B,H) = 135$ Hz, 5B), -9.11 ppm (d, $^{1}J(B,H) = 153$ Hz, 3B); $^{31}P\{^{1}H\}$ NMR ($CDCl_3$): $\delta = 49.16$ (d, $^{3}J(P,P) = 21$ Hz, $SPPh_2$), 12.77 ppm (d, $^{3}J(P,P) = 21$ Hz, PPh_2). Single crystals were grown by slow evaporation from a chloroform/dichloromethane solution.

1,2-(SPPh$_2$)$_2$-1,2-*closo*-C$_2$B$_{10}$H$_{10}$ (10): Elemental analysis (%) calcd for $C_{26}H_{30}B_{10}S_2P_2 \cdot 2\,CH_2Cl_2$: C 45.05, H, 4.59, S, 8.59; found: C 44.56, H, 4.85, S, 8.98; FTIR: $\tilde{\nu} = 3058$ (CH_{aryl}); 2632, 2603, 2574, 2557 (BH); 652 cm^{-1} (P=S); ^{1}H NMR (CD_3COCD_3): $\delta = 8.26$ (m, 8H, Ph), 7.60 (m, 12H, Ph), 3.7–0.80 ppm (brm, BH); $^{1}H\{^{11}B\}$ NMR (CD_3COCD_3): 8.26 (m, 8H, Ph), 7.60 (m, 12H, Ph), 3.61, 2.34, 2.20, 1.28, 0.86 ppm (brs, BH); $^{13}C\{^{1}H\}$ NMR (CD_3COCD_3): $\delta = 133.7$ (d, $J(C,P) = 10$ Hz, Ph), 132.3 (s, Ph), 130.5 (s, Ph), 127.9 (d, $J(C,P) = 14$ Hz, Ph), 87.7 ppm (d, $^{1}J(C,P) = 21$ Hz, C_c); ^{11}B NMR (CD_3COCD_3): $\delta = 2.59$ (d, $^{1}J(B,H) = 140$ Hz, 2B), -7.70 ppm (d, $^{1}J(B,H) = 134$ Hz, 8B); $^{31}P\{^{1}H\}$ NMR (CD_3COCD_3): $\delta = 48.65$ ppm (s, $SPPh_2$).

1-SPPh$_2$-2-OPPh$_2$-1,2-*closo*-C$_2$B$_{10}$H$_{10}$ (11): Elemental analysis (%) calcd for $C_{26}H_{30}B_{10}SP_2O \cdot CHCl_3$: C 47.69, H 4.59, S 4.72; found: C 47.78, H 5.04, S 4.98; FTIR: $\tilde{\nu} = 3060$ (CH_{aryl}); 2572, 2621 (BH); 1186, 1215 (P=O); 652, 690 cm^{-1} (P=S); ^{1}H NMR (CD_3COCD_3): $\delta = 8.37$ (q, $^{2}J(H,H) =$ 7 Hz, 5H, Ph), 7.96 (q, $^{2}J(H,H) = 8$ Hz, 5H, Ph), 7.63–7.54 (m, 10H, Ph), 3.1–2.00 ppm (brm, BH); $^{1}H\{^{11}B\}$ NMR (CD_3COCD_3): 8.37. (q, $^{2}J(H,H) = 7$ Hz, 5H, Ph), 7.96 (q, $^{2}J(H,H) = 8$ Hz, 5H, Ph), 7.63–7.54 (m, 10H), 3.33 (brs, 1H, BH), 2.36 (brs, 1H, BH), 2.25 (brs, 4H, BH), 2.04 ppm (brs, 4H, BH); $^{13}C\{^{1}H\}$ NMR (CD_3COCD_3): $\delta = 134.16$ (d, $J(C,P) = 11$ Hz, Ph), 132.62 (d, $J(C,P) = 3$ Hz, Ph), 132.29–132.18, 131.37 (s, Ph), 130.91 (s, Ph), 128.31 (d, $J(C,P) = 12$, Ph), 121.55 (d, $J(C,P) = 12$ Hz, Ph), 86.47 (d, $^{1}J(C,P) = 19$ Hz, C_c), 82.26 ppm (d, $^{1}J(C,P) = 28$ Hz, C_c); ^{11}B NMR (CD_3COCD_3): $\delta = 2.98$ (d, $^{1}J(B,H) = 146$ Hz, 1B), 1.40 (d, $^{1}J(B,H) = 138$ Hz, 1B), -7.52 ppm (8B); $^{31}P\{^{1}H\}$ NMR (CD_3COCD_3): $\delta =$ 49.96 (s, $SPPh_2$), 21.65 ppm (s, $OPPh_2$). Single crystals were grown by slow evaporation from dichloromethane/acetone solution.

Synthesis of 1-SP*i*Pr$_2$-2-P*i*Pr$_2$-1,2-*closo*-$C_2B_{10}H_{10}$ (12): 1,2-(P*i*Pr$_2$)$_2$-1,2-*closo*-$C_2B_{10}H_{10}$ (102 mg, 0.27 mmol), acetone (4 mL), THF (1 mL) and S powder (17 mg, 0.54 mmol). The mixture was heated to reflux for 4 h. Evaporation of the solvent yielded a yellow oil. Diethyl ether (10 mL) and water (10 mL) were added and the mixture was thoroughly shaken. The organic layer was dried with $MgSO_4$, filtered and evaporated. Compound **12** was isolated. Yield: 31 mg (23%). FTIR: $\tilde{\nu}$ = 3058 (CH_{aryl}); 2633, 2629, 2570 (BH); 655 cm^{-1} (P=S); ^{11}B NMR ($CDCl_3$): δ = 1.7 (d, ^1J(B,H) = 132 Hz, 1B), 0.8 (d, ^1J(B,H) = 153 Hz, 1B), −6.2 (d, ^1J(B,H) = 151 Hz, 3B), −9.2 ppm (d, ^1J(B,H) = 145 Hz, 5B); ^{31}P{^{1}H} NMR ($CDCl_3$): δ = 78.0 (d, ^3J(P,P) = 20 Hz, SP*i*Pr$_2$), 35.5 ppm (d, ^3J(P,P) = 20 Hz, P*i*Pr$_2$).

Synthesis of 1-SP*i*Pr$_2$-1,2-*closo*-$C_2B_{10}H_{11}$ (13): 1,2-(P*i*Pr$_2$)$_2$-1,2-*closo*-$C_2B_{10}H_{10}$ (102 mg, 0.27 mmol), acetone (4 mL), THF (1 mL) and S powder (17 mg, 0.54 mmol). The mixture was heated to reflux for two days. The oily residue was purified by preparative thin-layer chromatography with CH_2Cl_2/hexane (4/1). Compound **13** (R_f = 0.71, 55 mg, 22%) was isolated. Elemental analysis (%) calcd for $C_8H_{24}B_{10}SP{\cdot}0.4\,CH_3COCH_3$: C 35.12, H, 8.46, S, 10.19; found: C 34.96, H 9.04, S, 11.03; FTIR: $\tilde{\nu}$ = 3029 (C_cH); 2999, 2972, 2875 (CH_{alkyl}); 2621, 2574 (BH); 655 cm^{-1} (P=S); ^{1}H NMR ($CDCl_3$): δ = 2.63 (h, ^3J(H,H) = 7 Hz, 2H, CH), 1.42 (t, ^3J(H,H) = 7 Hz, 6H, Me), 1.33 (t, ^3J(H,H) = 7 Hz, 6H, Me), 2.5–2.00 ppm (brm, BH); ^{1}H{^{11}B} NMR ($CDCl_3$): 2.63 (h, ^3J(H,H) = 7 Hz, 2H, CH), 1.42 (t, ^3J(H,H) = 7 Hz, 6H, Me), 1.33 (t, ^3J(H,H) = 7 Hz, 6H, Me), 2.42 (brs, BH), 2.27 (brs, BH), 2.12 ppm (brs, BH); ^{13}C{^{1}H} NMR ($CDCl_3$): δ = 71 (s, C_c), 31.16 (d, ^1J(C,P) = 47 Hz, CH), 18.73 (d, ^2J(C,P) = 28 Hz, Me).^{11}B NMR ($CDCl_3$): δ = 0.77 (d, ^1J(B,H) = 152 Hz, 1B), −1.97 (d, ^1J(B,H) = 152 Hz, 1B), −6.42 (d, ^1J(B,H) = 151 Hz, 2B), −10.84 (d, ^1J(B,H) = 160 Hz, 2B), −11.98 ppm (d, ^1J(B,H) = 160 Hz, 4B); ^{31}P{^{1}H} NMR ($CDCl_3$): δ = 77.96 ppm (s, SP*i*Pr$_2$).

Synthesis of 1-SPPh$_2$-2-Me-1,2-*closo*-$C_2B_{10}H_{10}$ (14): 1-PPh$_2$-2-Me-1,2-*closo*-$C_2B_{10}H_{10}$ (22 mg, 0.06 mmol), toluene (8 mL), S powder (5 mg, 0.16 mmol). The mixture was heated to reflux for four days. The white solid was washed with hexane to give 10.2 mg of **14** (Yield 42.5%). FTIR: $\tilde{\nu}$ = 3055 (CH_{aryl}); 2960, 2925, 2856 (CH_{alkyl}); 2638, 2621, 2572, 2555 (BH); 690, 653 cm^{-1} (P=S); ^{1}H NMR ($CDCl_3$): δ = 8.39 (d, ^3J(H,H) = 7.3 Hz, 2H, Ph), 8.35 (d, ^3J(H,H) = 7.3 Hz, 2H, Ph), 7.66–7.56 (m, 6H, Ph), 2.11 ppm (s, 3H, Me); ^{1}H{^{11}B} NMR ($CDCl_3$): δ = 8.39 (d, ^3J(H,H) = 7.3 Hz, 2H, Ph), 8.35 (d, ^3J(H,H) = 7.3 Hz, 2H, Ph), 7.66–7.56 (m, 6H, Ph), 2.81 (brs, 1H, BH), 2.45 (brs, 1H, BH), 2.23 (brs, 8H, BH), 2.11 ppm (s, 3H, Me); ^{13}C{^{1}H} NMR ($CDCl_3$): δ = 134.16, 134.04, 132.90, 128.30, 128.14 (s, Ph), 24.76 ppm (s, Me); ^{11}B NMR ($CDCl_3$): δ = 0.1 (d, ^1J(B,H) = 132 Hz, 1B), −3.8 (d, ^1J(B,H) = 152 Hz, 1B), −7.9 (d, ^1J(B,H) = 138 Hz, 2B), −10.2 ppm (d, ^1J(B,H) = 140 Hz, 6B); ^{31}P{^{1}H} NMR ($CDCl_3$): δ = 47.65 ppm (s, SPPh$_2$).

General procedure for preparation of carboranyl phosphine selenides: Carboranyl phosphines were oxidized with black selenium powder in acetone, THF or toluene at reflux.

Synthesis of 1-SePPh$_2$-2-PPh$_2$-1,2-*closo*-$C_2B_{10}H_{10}$ (15): 1,2-(PPh$_2$)$_2$-1,2-*closo*-$C_2B_{10}H_{10}$ (35 mg, 0.068 mmol), toluene (8 mL) and Se powder (11 mg, 0.14 mmol). The mixture was heated to reflux overnight. The excess selenium was filtered off. Evaporation of the solvent yielded a yellow solid. Yield: 24 mg (0.041 mmol, 61%). Elemental analysis (%) calcd for $C_{26}H_{30}B_{10}P_2Se$: C 52.79, H, 5.11; found: C 52.59, H 4.98; FTIR: $\tilde{\nu}$ = 3049, 2927 (CH_{aryl}); 2532 (BH); 692 cm^{-1} (P=Se); ^{1}H NMR ($CDCl_3$: δ = 8.49–8.41 (m, 4H, Ph), 7.61–7.30 (m, 16H, Ph), 3.1–2.00 ppm (brm, BH); ^{1}H{^{11}B} NMR ($CDCl_3$): 8.49–8.41 (m, 4H, Ph), 7.61–7.30 (m, 16H, Ph), 3.17 (brs, 1H, BH), 2.27–2.01 ppm (brs, 9H, BH); ^{13}C{^{1}H} NMR ($CDCl_3$: δ = 135.79 (d, J(C,P) = 10 Hz, Ph), 135.11 (d, J(C,P) = 23 Hz, Ph), 134.58 (d, J(C,P) = 10 Hz, Ph), 133.95 (d, J(C,P) = 18 Hz, Ph), 132.49 (s, Ph), 130.17 (s, Ph), 128.19 (d, J(C,P) = 8 Hz, Ph), 127.83 (d, J(C,P) = 12 Hz, Ph), 86.21 (s, C_c), 79.81 ppm (s, C_c); ^{11}B NMR ($CDCl_3$: δ = 1.26 (d, ^1J(B,H) = 149 Hz, 1B), −0.34 (d, ^1J(B,H) = 134 Hz, 1B), −7.89 ppm (d, ^1J(B,H) = 140 Hz, 8B); ^{31}P{^{1}H} NMR ($CDCl_3$: δ = 46.48 (d, ^3J(P,P) = 27 Hz, ^1J(P,Se) = 807 Hz, SePPh$_2$), 10.48 ppm (d, ^3J(P,P) = 27 Hz, PPh$_2$). Single crystals were grown by slow evaporation from acetone solution.

Synthesis of 1-SeP*i*Pr$_2$-1,2-*closo*-$C_2B_{10}H_{11}$ (16): 1,2-(P*i*Pr$_2$)$_2$-1,2-*closo*-$C_2B_{10}H_{10}$ (82 mg, 0.22 mmol), toluene 5 mL and Se powder (35 mg, 0.44 mmol). The mixture was heated to reflux for five days and cooled to room temperature. Evaporation of the solvent yielded a yellow oil. Purification by preparative thin-layer chromatography (hexane) gave compound **16** (R_f = 0.79, 25 mg, 11%). FTIR: $\tilde{\nu}$ = 2989, 2872 (CH_{alkyl}); 2550 (BH); 697 cm^{-1} (P=Se); ^{1}H NMR ($CDCl_3$): δ = 2.69 (m, 2H, CH), 1.37 (d, ^3J(H,H) = 2 Hz, 6H, Me), 1.35 (d, ^3J(H,H) = 2 Hz, 6H, Me), 2.7–1.5 ppm (brm, BH); ^{1}H{^{11}B} NMR ($CDCl_3$): 2.69 (m, 2H, CH), 1.37 (d, ^3J(H,H) = 2 Hz, 6H, Me), 1.35 (d, ^3J(H,H) = 2 Hz, 6H, Me), 2.48, 2.29, 2.20 ppm (brs, BH); ^{13}C{^{1}H} NMR ($CDCl_3$: δ = 66.29 (s, C_c), 21.18 (s, CH), 20.19 (s, Me), 18.92 ppm (s, Me); ^{11}B NMR ($CDCl_3$: δ = 0.5 (d, ^1J(B,H) = 147 Hz, 1B), −2.1 (d, ^1J(B,H) = 151 Hz, 1B), −6.8 (d, ^1J(B,H) = 150 Hz, 2B), −10.6 (d, ^1J(B,H) = 166 Hz, 2B), −11.8 ppm (d, ^1J(B,H) = 175 Hz, 4B); ^{31}P{^{1}H} NMR ($CDCl_3$: δ = 83.67 ppm (s, SeP*i*Pr$_2$).

Synthesis of 1-SePPh$_2$-2-Me-1,2-*closo*-$C_2B_{10}H_{10}$ (17): 1-PPh$_2$-2-Me-1,2-*closo*-$C_2B_{10}H_{10}$ (22 mg, 0.06 mmol), toluene (7 mL) and Se powder (30 mg, 0.38 mmol). The mixture was heated to reflux for 23 h. The excess selenium was filtered off. Evaporation of the solvent gave a yellow oil. Yield: 19 mg (0.044 mmol, 71%). Elemental analysis (%) calcd for $C_{15}H_{23}B_{10}PSe$: C 42.80, H, 5.50; found: C 44.21, H 5.81; FTIR: $\tilde{\nu}$ = 3051 (CH_{aryl}); 2925, 2854 (CH_{alkyl}); 2621, 2586, 2567 (BH); 694 cm^{-1} ν-(P=Se); ^{1}H NMR ($CDCl_3$): δ = 8.44 (d, ^3J(H,H) = 8.2 Hz, 2H, Ph), 8.40 (d, ^3J(H,H) = 7.7 Hz, 2H, Ph), 7.59 (m, 6H, Ph), 2.09 (s, 3H, Me), 2.89–2.15 ppm (brm, 10H, BH); ^{1}H{^{11}B} NMR (CD_3COCD_3): δ = 8.44 (d, ^3J(H,H) = 8.2 Hz, 2H, Ph), 8.40 (d, ^3J(H,H) = 7.7 Hz, 2H, Ph), 7.59 (m, 6H, Ph), 2.89 (brs, 2H, BH), 2.43 (brs, 2H, BH), 2.16 (brs, 8H, BH), 2.09 ppm (s, 3H, Me); ^{13}C{^{1}H} NMR ($CDCl_3$): δ = 135.10 (d, ^3J(C,P) = 11.0 Hz, Ph), 132.97 (s, Ph), 128.16 (d, ^2J(C,P) = 12.4 Hz, Ph), 78.76 (s, C_c), 72.50 (d, ^1J(C,P) = 16.5 Hz, C_c), 24.56 ppm (s, Me); ^{11}B NMR ($CDCl_3$): δ = −0.06 (d, ^1J(B,H) = 144 Hz, 1B), −3.60 (d, ^1J(B,H) = 149 Hz, 1B), −7.82 (d, ^1J(B,H) = 161 Hz, 3B), −10.35 ppm (d, ^1J(B,H) = 142 Hz, 5B); ^{31}P{^{1}H} NMR ($CDCl_3$): δ = 45.10 ppm (s, ^1J(P,Se) = 804 Hz, SePPh$_2$).

Synthesis of 1-SePPh$_2$-2-Ph-1,2-*closo*-$C_2B_{10}H_{10}$ (18): 1-PPh$_2$-2-Ph-1,2-*closo*-$C_2B_{10}H_{10}$ (17.5 mg, 0.04 mmol), toluene (7 mL) and Se powder (24 mg, 0.30 mmol). The mixture was heated to reflux for 23 h. The excess selenium was filtered off. Evaporation of the solvent gave a white solid. Yield: 17 mg (0.035 mmol, 82%). Elemental analysis (%) calcd for $C_{20}H_{25}B_{10}PSe$: C 49.70, H, 5.20; found: C 51.57, H 5.59; FTIR: $\tilde{\nu}$ = 3057, 2922, 2852 (CH_{aryl}); 2573 (BH); 687 cm^{-1} (P=Se); ^{1}H NMR ($CDCl_3$): δ = 8.15 (d, ^3J(H,H) = 8.1 Hz, 2H, Ph), 8.10 (d, ^3J(H,H) = 7.5 Hz, 2H, Ph), 7.29 (m, 11H, Ph), 3.50–2.35 ppm (brm, 10H, BH); ^{1}H{^{11}B} NMR (CD_3COCD_3): δ = 8.15 (d, ^3J(H,H) = 8.1 Hz, 2H, Ph), 8.10 (d, ^3J(H,H) = 7.5 Hz, 2H, Ph), 7.29 (m, 11H, Ph), 3.50 (brs, 1H, BH), 2.60 (brs, 2H, BH), 2.37 ppm (brs, 7H, BH); ^{13}C{^{1}H} NMR ($CDCl_3$): δ = 134.86, 132.55, 132.00, 130.58, 128.21, 127.86 (s, Ph), 86.85 ppm (s, C_c); ^{11}B NMR ($CDCl_3$): δ = 0.69 (d, ^1J(B,H) = 151 Hz, 1B), −1.87 (d, ^1J(B,H) = 150 Hz, 1B), −7.36 (d, ^1J(B,H) = 162 Hz, 2B), −9.90 ppm (d, ^1J(B,H) = 129 Hz, 6B); ^{31}P{^{1}H} NMR ($CDCl_3$): δ = 45.09 ppm (s, ^1J(P,Se) = 812 Hz, SePPh$_2$).

General procedure for reactions of monochalcogenide carboranyl diphosphines with organometallic compounds: One equivalent of the organometallic compound or transition-metal salt was added to a solution of one equivalent of monochalcogenide carboranyl diphosphine in 5 mL of solvent (dichloromethane, chloroform, toluene, acetonitrile, ethyl acetate, 2-propanol or *tert*-butyl alcohol). The mixture was kept at room temperature for between one and five days, depending on the metal. The reactions were monitored by ^{31}P NMR and ^{11}B NMR spectroscopy, and the data were compared with literature values. Single crystals suitable for X ray diffraction were grown by slow evaporation from dichloromethane/diethyl ether solution.

Characterization of [NiCl$_2${1,2-(PPh$_2$)$_2$-1,2-*closo*-$C_2B_{10}H_{10}$}] (19): FTIR: $\tilde{\nu}$ = 3060 (CH_{aryl}); 2568 (BH); 1431, 1090, 687 (phosphino groups); ^{1}H NMR ($CDCl_3$): δ = 8.52–8.45 (m, 8H, Ph), 7.68–7.56 (m, 12H, Ph), 2.98–1.15 ppm (brm, 10H, BH); ^{1}H{^{11}B} NMR ($CDCl_3$): δ = 8.52–8.45 (m, 8H, Ph), 7.68–7.56 (m, 12H, Ph), 2.63 (brs, 2H, BH), 2.40 (brs, 2H, BH), 2.23 (brs, 2H, BH), 1.99 ppm (brs, 4H, BH); ^{11}B NMR ($CDCl_3$): δ = −0.95 (d, ^1J(B,H) = 153 Hz, 2B), −3.1 (d, ^1J(B,H) = 149 Hz, 3B), −9.46 ppm (5B); ^{31}P{^{1}H} NMR ($CDCl_3$): δ = 72.41 ppm (s, PPh$_2$). Single crystals of **19** suitable for X-ray diffraction were grown by slow evaporation from dichloromethane/diethyl ether solution.

Table 8. Crystal data and structural refinement details for **3**, **5**, **9**, **11**·CH_2Cl_2 and **15**.

	3	**5**	**9**	**11**·CH_2Cl_2	**15**	**19**
empirical formula	$C_{15}H_{23}B_{10}OP$	$C_{15}H_{35}B_{10}OP$	$C_{26}H_{30}B_{10}P_2S$	$C_{27}H_{32}B_{10}Cl_2OP_2S_2$	$C_{26}H_{30}B_{10}P_2Se$	$C_{26}H_{30}B_{10}Cl_2NiP_2$
FW	358.40	370.50	544.60	645.53	591.50	642.15
crystal system	monoclinic	orthorhombic	orthorhombic	monoclinic	orthorhombic	triclinic
crystal habit, colour	needle, colourless	block, colourless	plate, colourless	prism, colourless	plate, colourless	bar, red
space group	$P2_1/c$ (no. 14)	*Pbna* (no. 60)	*Pbca* (no. 61)	$P2_1/n$ (no. 14)	*Pbca* (no. 61)	$P\bar{1}$ (no. 2)
a [Å]	10.1769(4)	8.3453(3)	19.7179(5)	10.0767(3)	19.9127(12)	8.2083(4)
b [Å]	13.3211(4)	20.1739(5)	10.0751(2)	27.5776(11)	10.0226(4)	10.8612(4)
c [Å]	14.4605(5)	24.9904(9)	28.5189(8)	12.1741(5)	28.6778(16)	17.2008(8)
α [°]	90	90	90	90	90	89.066(3)
β [°]	90.860(2)	90	90	109.017(2)	90	83.827(2)
γ [°]	90	90	90	90	90	76.467(2)
V [Å^3]	1960.15(12)	4207.3(2)	5665.6(2)	3198.4(2)	5723.4(5)	1482.20(11)
Z	4	8	8	4	8	2
ρ [g cm^{-3}]	1.214	1.170	1.277	1.341	1.373	1.439
μ [cm^{-1}]	1.42	1.34	2.45	3.92	14.42	9.62
GOF[a] on F^2	1.032	1.033	1.030	1.046	1.019	1.035
R[b] [$I>2\sigma(I)$]	0.0451	0.0505	0.0415	0.0686	0.0745	0.0570
R_w[c] [$I>2\sigma(I)$]	0.1049	0.1102	0.0889	0.1700	0.1457	0.1454

[a] $S=[\Sigma\{w(F_o^2-F_c^2)^2\}/(n-p)]^{1/2}$. [b] $R=\Sigma||F_o|-|F_c||/\Sigma|F_o|$. [c] $R_w=[\Sigma w(|F_o^2|-|F_c^2|)^2/\Sigma w|F_o^2|^2]^{1/2}$.

X-ray structure determination: Crystallographic data for compound **3** **5**, **9**, **11**, **15** and **19** were collected at 173 K on a Nonius-Kappa CCD area-detector diffractometer by using graphite-monochromatized $Mo_{K\alpha}$ radiation ($\lambda=0.71073$ Å). The data sets for **15** and **19** were corrected for absorption using SADABS.[44a] The structures were solved by direct methods by means of the SHELXS-97 program.[44b] The full-matrix, least-squares refinements on F^2 were performed with SHELXL-97 program.[44b] Crystal data and structural refinement details for **3**, **5**, **9**, **11**·CH_2Cl_2 and **15** are listed in Table 8.

For compounds **9, 15** and **19** one of the phenyl groups of each compound is disordered over two orientations. For **9**, and **15**, the disordered group was refined isotropically as a rigid group, but the rest of the non-hydrogen atoms were refined with anisotropic thermal displacement parameters, and those of **19** anisotropically. Hydrogen atoms were treated as riding atoms by using the SHELX97 default parameters.

In the structure of **11**·CH_2Cl_2 partially occupied oxygen and sulfur atoms are bonded to each phosphorus atom. Refinement of site occupation parameters of the disordered O and S atoms revealed values very near to 0.5, and therefore the parameters were fixed to 0.5. Moreover, one of the phenyl groups is disordered over two orientations. The disordered group was refined isotropically as a rigid group, but the rest of the non-hydrogen atoms, except the disordered oxygen atom, were refined with anisotropic thermal displacement parameters. Hydrogen atoms were treated as riding atoms by using the SHELX97 default parameters.

CCDC-630889 (**3**), CCDC-630890 (**5**), CCDC-630892 (**9**), CCDC-630893 (**11**·CH_2Cl_2) CCDC-630894 (**15**) and CCDC-800463 (**19**) contain the supplementary crystallographic data for this paper. These data can be obtained free of charge from The Cambridge Crystallographic Data Centre via www.ccdc.cam.ac.uk/data_request/cif.

Computational details: Quantum-chemical calculations were performed with the Gaussian 03[45] commercial suite of programs at the DFT level of theory with B3LYP hybrid functional[46] and the 6-311G+(d,p) basis set for all atoms.[47] Geometry optimisation was performed from structural data. NBO calculations were done at the optimised geometries. The programs Gabedit 2.2.6[48] and Chemcraft 1.6[49] were used to visualise the optimised structures. Molekel 4.3[50] program was used to visualise the NBO orbitals. The 3D NBO plots were done with NBOView 1.0. The bond critical point parameters were calculated with AIMAll[51] from the electronic wave function obtained with Gaussian 03. All calculations with Gaussian 03 were performed in computational clusters with workstations with eight Intel Xeon Six-Core X5670 processors with 2.93 GHz and 24 GB of RAM, or with 128 Intel Itanium 2 processors with 1.6 GHz and 512 GB of RAM. NBOView was used on SGI Altix 3700 Bx2 workstation equipped with 128 Itanium 2 processors with 1.6 GHz and 384 GB of RAM.

Acknowledgements

We thank Generalitat de Catalunya 2009/SGR/279 and Spanish Ministry of Education CTQ2010-16237. A.R.P. thanks the Spanish Ministry of Education for the FPU grant. The access to the computational facilities of High Performance Computing Centre of CSIC and Centre de Supercomputació de Catalunya (CESCA) is gratefully acknowledged.

[1] a) P. W. N. M. Van Leeuwen, P. C. J. Kamer, J. N. H. Reek, P. Dierkes, *Chem. Rev.* **2000**, *100*, 2741–2769; b) S. D. Ittel, L. K. Johnson, M. Brookhart, *Chem. Rev.* **2000**, *100*, 1169–1203; c) *Applied Homogeneous Catalysis with Organometallic Complexes, Vols. 1 & 2* (Eds.: B. Cornils, W. A. Herrmann), Wiley-VCH, Weinheim, **2002**.

[2] D. S. Glueck, *Chem. Eur. J.* **2008**, *14*, 7108–7117.

[3] *Organic Phosphorus Compounds* (Eds.: D. M. Kosolapoff, L. Maier), Wiley, New York, **1973**.

[4] S. J. Berners-Price, R. E. Norman, P. J. Sadler, *J. Inorg. Biochem.* **1987**, *31*, 197–209.

[5] I. U. Arachchige, S. L. Brock, *Acc. Chem. Res.* **2007**, *40*, 801–809.

[6] a) F. Sansone, M. Fontanella, A. Casnati, R. Ungaro, V. Boehmer, M. Saadioui, K. Liger, J-F. Dozol, *Tetrahedron* **2006**, *62*, 6749–6753; b) C. Lamouroux, S. Rateau, C. Moulin, *Rapid Commun. Mass Spectrom.* **2006**, *20*, 2041–2052; c) Y. Sasaki, S. Umetani, *J. Nucl. Sci. Technol.* **2006**, *43*, 794–797; d) A. Y. Zhang, E. Kuraoka, M. Kumagai, *Sep. Purif. Technol.* **2006**, *50*, 35–44; e) B. Grüner, J. Plešek, J. Báča, I. Císařová, J.-F. Dozol, H. Rouquette, C. Viñas, P. Selucký, J. Rais, *New J. Chem.* **2002**, *26*, 1519–1527; f) M. M. Reinoso-García, D. Janczewski, D. N. Reinhoudt, W. Verboom, E. Malinowska, M. Pietrzak, C. Hill, J. Baca, B. Gruner, P. Selucky, C. Grüttner, *New J. Chem.* **2006**, *30*, 1480–1492; g) H. Naganawa, H. Suzuki, S. Tachimori, A. Nasu, T. Sekine, *Phys. Chem. Chem. Phys.* **2001**, *3*, 2509–2517; h) J. F. Malone, D. J. Marrs, M. A. Mckervey, P. O'Hagan, N. Thompson, A. Walker, F. Arnaud-Neu, O. Mauprivez, M. J. Schwing-Weill, J. F. Dozol, H. Rouquette, N. Simon, *J. Chem. Soc. Chem. Commun.* **1995**, 2151–2153.

[7] a) B. J. Liaw, T. S. Lobana, Y. W. Lin, J. C. Wang, C. W. Liu, *Inorg. Chem.* **2005**, *44*, 9921–9929; b) C. W. Liu, B. J. Liaw, L. S. Liou, J. C.

Wang, *Chem. Commun.* **2005**, 1983–1985; c) T. S. Lobana, J.-C. Wang, C. W. Liu, *Coord. Chem. Rev.* **2007**, *251*, 91–110.
[8] a) I. P. Gray, A. M. Z. Slawin, J. D. Woollins, *Dalton Trans.* **2005**, 2188–2194; b) I. P. Gray, P. Bhattacharyya, A. M. Z. Slawin, J. D. Woollins, *Chem. Eur. J.* **2005**, *11*, 6221–6227.
[9] S.-B. Yu, G. C. Papaefthymiou, R. H. Holm, *Inorg. Chem.* **1991**, *30*, 3476–3485.
[10] F. Teixidor, C. Viñas in *Science of Synthesis: Boron Compounds, Vol. 6* (Eds.: D. E. Kaufmann, D. S. Matteson), Thieme, Stuttgart, **2005**, pp. 1235–1275, and references therein.
[11] H. D. Smith, T. A. Knowles, H. Schroeder, *Inorg. Chem.* **1965**, *4*, 107–111.
[12] a) F. Teixidor, J. Casabó, A. M. Romerosa, C. Viñas, J. Rius, C. Miravitlles, *J. Am. Chem. Soc.* **1991**, *113*, 9895–9896; b) F. Teixidor, M. A. Flores, C. Viñas, R. Kivekas, R. Sillanpää, *Angew. Chem.* **1996**, *108*, 2388–2391; *Angew. Chem. Int. Ed. Engl.* **1996**, *35*, 2251–2253; c) F. Teixidor, M. A. Flores, C. Viñas, R. Kivekäs, R. Sillanpää, *J. Am. Chem. Soc.* **2000**, *122*, 1963–1973; d) O. Tutusaus, C. Viñas, R. Núñez, F. Teixidor, A. Demonceau, S. Delfosse, A. F. Noels, I. Mata, E. Molins, *J. Am. Chem. Soc.* **2003**, *125*, 11830–11831; e) A. Richel, S. Delfosse, A. Demonceau, A. F. Noels, S. Paavola, R. Kivekäs, R. Sillanpää, F. Teixidor, C. Viñas, abstracts of papers of the American Chemical Society 224: U438–U438 453-POLY, Part 2, August 18, **2002**.
[13] J. Bruno, J. C. Cole, P. R. Edgington, M. Kessler, C. F. Macrae, P. McCabe, J. Pearson, R. Taylor, *Acta Crystallogr. Sect. B: Struct. Sci* **2002**, *58*, 389–397.
[14] a) C. Viñas, R. Núñez, I. Rojo, F. Teixidor, R. Kivekäs, R. Sillanpää, *Inorg. Chem.* **2001**, *40*, 3259–3260; b) H. Wang, H.-S. Chan, Z. Xie, *Organometallics* **2006**, *25*, 2569–2573; c) H. Wang, H. Shen, H.-S. Chan, Z. Xie, *Organometallics* **2008**, *27*, 3964–3970; d) J. Dou, D. Zhang, D. Li, D. Wang, *Eur. J. Inorg. Chem.* **2007**, 53–59.
[15] V. P. Balema, S. Blaurock, E. Hey-Hawkins, *Polyhedron* **1998**, *18*, 545–552.
[16] X. K. Huo, G. Su, G. X. Jin, *Chem. Eur. J.* **2010**, *16*, 12017–12027.
[17] a) F. Teixidor, R. Núñez, C. Viñas, R. Sillanpää, R. Kivekäs, *Angew. Chem.* **2000**, *112*, 4460–4462; *Angew. Chem. Int. Ed.* **2000**, *39*, 4290–4292; b) R. Núñez, P. Farras, C. Viñas, F. Teixidor, R. Sillanpää, R. Kivekäs, *Angew. Chem.* **2006**, *118*, 1292–1294; *Angew. Chem. Int. Ed.* **2006**, *45*, 1270–1272; c) F. Teixidor, G. Barbera, A. Vaca, R. Kivekäs, R. Sillanpää, J. Oliva, C. Viñas, *J. Am. Chem. Soc.* **2005**, *127*, 10158–10159.
[18] R. Nuñez, C. Viñas, F. Teixidor, R. Sillanpää, R. Kivekas, *J. Organomet. Chem.* **1999**, *592*, 22–28.
[19] a) M. J. Calhorda, O. Crespo, M. C. Gimeno, P. G. Jones, A. Laguna, J. M. López-de-Luzuriaga, J. L. Perez, M. A. Ramón, L. F. Veiros, *Inorg. Chem.* **2000**, *39*, 4280–4285; b) S. Paavola, R. Kivekäs, F. Teixidor, C. Viñas, *J. Organomet. Chem.* **2000**, *606*, 183–187; c) S. Paavola, F. Teixidor, C. Viñas, R. Kivekäs, *J. Organomet. Chem.* **2002**, *645*, 39–46; d) S. Paavola, F. Teixidor, C. Viñas, R. Kivekäs, *J. Organomet. Chem.* **2002**, *657*, 187–193; e) D. P. Zhang, J. M. Dou, D. C. Li, D. Q. Wang, *Appl. Organomet. Chem.* **2006**, *20*, 632–637.
[20] W. McFarlane, D. S. Rycroft, *J. Chem. Soc. Dalton Trans.* **1973**, 2162–2166.
[21] D. W. Allen, B. F. Taylor, *J. Chem. Soc. Dalton Trans.* **1982**, 51–54.
[22] C. J. Jameson in *Phosphorus-31 NMR Spectroscopy in Stereochemical Analysis* (Eds. J. G Verkade, L. D Quin), Wiley, New York, **1987**.
[23] T. M. Klapötke, M. Broschag, *Compilation of Reported ^{77}Se NMR Chemical Shifts*, Wiley, Chichester, **1996**.
[24] N. Burford, B. W. Royan, R. E. v. H. Spence, R. D. Rogers, *J. Chem. Soc Dalton Trans.* **1990**, 2111–2117.
[25] R. Kivekäs, R. Sillanpää, F. Teixidor, C. Viñas, R. Núñez, M. Abad, *Acta Crystallogr. Sect. C: Cryst. Struct. Commun.* **1995**, *51*, 1864–1870.
[26] M. R. Sundberg R. Uggla, C. Viñas, F. Teixidor, S. Paavola, R. Kivekäs, *Inorg. Chem. Commun.* **2007**, *10*, 713–716.
[27] H. U. Steinberger, B. Ziemer, M. Meisel, *Acta Crystallog. Sect. C: Cryst. Struct. Commun.* **2001**, *57*, 835–837.
[28] a) T. Stampfl, R. Gutmann, G. Czermak, C. Langes, A. Dumfort, H. Kopacka, K.-H. Ongania, P. Brüggeller, *Dalton Trans.* **2003**, *3425*–3435; b) T. Stampfl, G. Czermak, R. Gutmann, C. Langes, H. Kopacka, K.-H. Ongania, P. Brüggeller, *Inorg. Chem. Commun.* **2002**, *5*, 490–495; c) P. B. Hitchcock, J. F. Nixon, N. Sakaray, *Chem. Commun.* **2000**, 1745–1746.
[29] a) F. Teixidor, C. Viñas, M. M. Abad, R. Kivekäs, R. Sillanpää, *J. Organomet. Chem.* **1996**, *509*, 139–150; b) P. Juanatey, A. Suárez, M. López, J. M. Vila, J. M. Ortigueira, A. Fernández, *Acta Crystallogr. Sect. C: Cryst. Strct. Commun.* **1999**, *55*, IUC9900062.
[30] a) M. Bollmark, J. Stawinski, *Chemm. Commun.* **2001**, 771–772; b) M. Kullberg, J. Stawinski, *J. Organomet. Chem.* **2005**, *690*, 2571–2576.
[31] J. Dou, D. Zhang, D. Li, D. Wang, *J. Organomet. Chem.* **2006**, *691*, 5673–5679.
[32] a) F. Teixidor, C. Viñas, M. M. Abad, M. López, J. Casabó, *Organometallics* **1993**, *12*, 3766–3768; b) F. Teixidor, C. Viñas, M. M. Abad, R. Kivekäs, R. Sillanpää, *J. Organomet. Chem.* **1996**, *509*, 139–150; c) R. Kivekäs, R. Sillanpää, F. Teixidor, C. Viñas, M. M. Abad, *Acta Chim. Scand.* **1996**, *50*, 499–504; d) F. Teixidor, C. Viñas, M. M. Abad, C. Whitaker, J. Rius, *Organometallics* **1996**, *15*, 3154–3160; e) C. Viñas, M. M. Abad, F. Teixidor, R. Sillanpää, R. Kivekäs, *J. Organomet. Chem.* **1998**, *555*, 17–23.
[33] J. B. Cook, B. K. Nicholson, D. W. Smith, *J. Organomet. Chem.* **2004**, *689*, 860–869, and references therein.
[34] a) D. G. Gilheany, *Chem. Rev.* **1994**, *94*, 1339–1374; b) N. Sandblom, T. Ziegler, T. Chivers, *Can. J. Chem.* **1996**, *74*, 2363–2371; c) J. A. Dobado, H. Martínez-García, J. Molina Molina, M. R. Sundberg, *J. Am. Chem. Soc.* **1998**, *120*, 8461–8471.
[35] R. Davies in *Handbook of Chalcogen Chemistry: New Perspectives in Sulfur Selenium and Tellurium* (Ed.: F. A. De Villanova), RSC, Cambridge, **2007**, pp. 291–292.
[36] J.-D. Lee, B.-Y. Kim, C. Lee, Y.-J. Lee, J. Jo, S.-O. Kang, *Bull. Korean Chem. Soc.* **2004**, *25*, 1012–1018.
[37] R. P. Alexander, H. A. Schroeder, *Inorg. Chem.* **1963**, *2*, 1107–1110.
[38] D. Drew, J. R. Doyle, *Inorg. Synth.* **1990**, *28*, 346–349.
[39] J. R. Doyle, P. E. Slade, H. B. Jonassen, *Inorg. Synth.* **1960**, *6*, 216–220.
[40] J. R. Blackburn, R. Nordberg, F. Stevie, R. G. Albridge, M. M. Jones, *Inorg. Chem.* **1970**, *9*, 2374–2376.
[41] G. Booth, J. Chatt, *J. Chem. Soc.* **1965**, 3238–3241.
[42] M. I. Bruce, B. K. Nicholson, O. Bin Shawkataly, *Inorg. Synth.* **1989**, *26*, 324–328.
[43] a) T. A. Stephenson, G. Wilkinson, *J. Inorg. Nucl. Chem.* **1966**, *28*, 945–956; b) P. S. Hallman, T. A. Stephenson, G. Wilkinson, *Inorg. Synth.* **1970**, *12*, 237–240.
[44] a) G. M. Sheldrick, SADABS. University of Göttingen, Germany, **2002**; b) G. M. Sheldrick, *Acta. Crystallogr. Sect. A*, **2007**, *64*, 112–122.
[45] Gaussian 03, Revision E.02, M. J. Frisch, G. W. Trucks, H. B. Schlegel, G. E. Scuseria, M. A. Robb, J. R. Cheeseman, J. A. Montgomery, Jr., T. Vreven, K. N. Kudin, J. C. Burant, J. M. Millam, S. S. Iyengar, J. Tomasi, V. Barone, B. Mennucci, M. Cossi, G. Scalmani, N. Rega, G. A. Petersson, H. Nakatsuji, M. Hada, M. Ehara, K. Toyota, R. Fukuda, J. Hasegawa, M. Ishida, T. Nakajima, Y. Honda, O. Kitao, H. Nakai, M. Klene, X. Li, J. E. Knox, H. P. Hratchian, J. B. Cross, V. Bakken, C. Adamo, J. Jaramillo, R. Gomperts, R. E. Stratmann, O. Yazyev, A. J. Austin, R. Cammi, C. Pomelli, J. W. Ochterski, P. Y. Ayala, K. Morokuma, G. A. Voth, P. Salvador, J. J. Dannenberg, V. G. Zakrzewski, S. Dapprich, A. D. Daniels, M. C. Strain, O. Farkas, D. K. Malick, A. D. Rabuck, K. Raghavachari, J. B. Foresman, J. V. Ortiz, Q. Cui, A. G. Baboul, S. Clifford, J. Cioslowski, B. B. Stefanov, G. Liu, A. Liashenko, P. Piskorz, I. Komaromi, R. L. Martin, D. J. Fox, T. Keith, M. A. Al-Laham, C. Y. Peng, A. Nanayakkara, M. Challacombe, P. M. W. Gill, B. Johnson, W. Chen, M. W. Wong, C. Gonzalez, and J. A. Pople, Gaussian, Inc., Wallingford, CT, **2004**.
[46] P. J. Stephens, F. J. Devlin, C. F. Chabalowski, M. J. Frisch, *J. Phys. Chem.* **1994**, *98*, 11623–11627.

[47] a) A. D. McLean, G. S. Chandler, *J. Chem. Phys.* **1980**, *72*, 5639–5648; b) K. Raghavachari, J. S. Binkley, R. Seeger, J. A. Pople, *J. Chem. Phys.* **1980**, *72*, 650–654; c) J.-P. Blaudeau, M. P. McGrath, L. A. Curtiss, L. Radom, *J. Chem. Phys.* **1997**, *107*, 5016–5021; d) A. J. H. Wachters, *J. Chem. Phys.* **1970**, *52*, 1033–1036; e) P. J. Hay, *J. Chem. Phys.* **1977**, *66*, 4377–4384; f) K. Raghavachari, G. W. Trucks, *J. Chem. Phys.* **1989**, *91*, 1062–1065; g) R. C. Binning Jr. , L. A. Curtiss, *J. Comput. Chem.* **1990**, *11*, 1206–1216; h) M. P. McGrath, L. Radom, *J. Chem. Phys.* **1991**, *94*, 511–516; i) L. A. Curtiss, M. P. McGrath, J.-P. Blaudeau, N. E. Davis, R. C. Binning Jr., L. Radom, *Chem. Phys.* **1995**, *190–201*, 6104–6113.

[48] A. R. Allouche, *J. Comput. Chem.* **2011**, *32*, 174–182.

[49] http://www.chemcraftprog.com

[50] MOLEKEL, Version 4.3.linux, 11.Nov.02, by Stefan Portmann, Copyright © 2002, CSCS/ETHZ.

[51] AIMAll (Version 10.03.25), T. A. Keith, 2010.

[52] International Union of Pure and Applied Chemistry, *Pure Appl. Chem.* **1976**, *45*, 217–219.

[53] F. Teixidor, C. Viñas, R. Nuñez, R. Kivekäs, R. Sillanpää, *J. Organomet. Chem.* **1995**, *503*, 193–203.

[54] R. Kivekäs, R. Sillanpää, F. Teixidor, C. Viñas, R. Nuñez, *Acta Crystallogr. Sect. C: Cryst. Struct. Commun.* **1994**, *50*, 2027–2030.

[55] M. A. McWhannell, G. M. Rosair, A. J. Welch, F. Teixidor, C. Viñas, *Acta Crystallogr. Sect. C: Cryst. Struct. Commun.* **1996**, *52*, 3135–3138.

[56] R. Sillanpää, R. Kivekäs, F. Teixidor, C. Viñas, R. Nuñez, *Acta Crystallogr. Sect. C: Cryst. Struct. Commun.* **1996**, *52*, 2223–2225.

[57] F. Teixidor, C. Viñas, R. Benakki, R. Kivekäs, R. Sillanpää, *Inorg. Chem.* **1997**, *36*, 1719–1723.

Received: November 18, 2010
Published online: March 8, 2011

